National Institute of Environmental Health Sciences

NIEHS Report on the In Vivo Repeat Dose Biological Potency Studies of 1,4-Dichlorobenzene (CASRN 106-46-7) in Female Sprague Dawley (Hsd:Sprague Dawley® SD®) Rats and B6D2F1/Crl Mice (Whole-body Inhalation Studies)

NIEHS 13

April 2026

NIEHS Report on the In Vivo Repeat Dose Biological Potency Studies of 1,4-Dichlorobenzene (CASRN 106-46-7) in Female Sprague Dawley (Hsd:Sprague Dawley® SD®) Rats and B6D2F1/Crl Mice (Whole-body Inhalation Studies)

NIEHS Report 13

April 2026

National Institute of Environmental Health Sciences
Public Health Service
U.S. Department of Health and Human Services
ISSN: 2768-5632

Research Triangle Park, North Carolina, USA

Foreword

The National Institute of Environmental Health Sciences (NIEHS) is one of 27 institutes and centers of the National Institutes of Health, part of the U.S. Department of Health and Human Services. The NIEHS mission is to discover how the environment affects people to promote healthier lives. NIEHS works to accomplish its mission by conducting and funding research on human health effects of environmental exposures, developing the next generation of environmental health scientists, and providing critical research, knowledge, and information to citizens and policymakers to help in their efforts to prevent hazardous exposures and reduce the risk of preventable disease and disorders connected to the environment. NIEHS is a foundational leader in environmental health sciences and committed to ensuring that its research is directed toward a healthier environment and healthier lives for all people.

The environmental health sciences research described in this series is conducted primarily by the Division of Translational Toxicology (DTT) at NIEHS. NIEHS/DTT scientists conduct innovative toxicology research that aligns with real-world public health needs and translates scientific evidence into knowledge that can inform individual and public health decision-making.

This report is available free of charge on the NIEHS website and cataloged in PubMed, a free resource developed and maintained by the National Library of Medicine (part of the National Institutes of Health).

Table of Contents

Tables

About This Report

Authors

Scott S. Auerbach[a], Michelle C. Cora[a], Ying F. Liu[a], Jeanne Luh[b], Lisa M. Prince[b], Georgia K. Roberts[a], Kelly A. Shipkowski[a], Suramya Waidyanatha[a]

[a]Division of Translational Toxicology, National Institute of Environmental Health Sciences, Research Triangle Park, North Carolina, USA

[b]ICF, Reston, Virginia, USA

Division of Translational Toxicology, National Institute of Environmental Health Sciences, Research Triangle Park, North Carolina, USA
Scott S. Auerbach, Ph.D., Lead Toxicologist[1,9,10]
Michelle C. Cora, D.V.M.[1,9,10]
Ying F. Liu, Ph.D.[2,5,10]
Georgia K. Roberts, Ph.D.[1,5,10]
Kelly A. Shipkowski, Ph.D.[1,5,10]
Suramya Waidyanatha, Ph.D.[1,5,9,10]

ICF, Reston, Virginia, USA
Contracts 75N96025C00003 and GS00Q14OADU417 (Order No. HHSN273201600015U)
Jeanne Luh, Ph.D.[9,10]
Lisa M. Prince, Ph.D.[9,10]

Contributors

Division of Translational Toxicology, National Institute of Environmental Health Sciences, Research Triangle Park, North Carolina, USA
Danica Andrews, B.S.[5]
John R. Bucher, Ph.D. (Retired)[1]
Warren Casey, Ph.D.[1]
Helen C. Cunny, Ph.D.[5]
Michael J. DeVito, Ph.D. (currently at U.S. Environmental Protection Agency)[1]
Jennifer M. Fostel, Ph.D.[1]
Michelle F. Fyle, Ph.D. (currently at Procter & Gamble)[10]
William M. Gwinn, Ph.D.[1]
Alison H. Harrill, Ph.D. (currently at Corteva Agriscience)[1]
Ronald A. Herbert, D.V.M., Ph.D.[5]
Scott A. Masten, Ph.D.[1]
Cynthia V. Rider, Ph.D.[1]
Kristen R. Ryan, Ph.D.[10]
Keith R. Shockley, Ph.D.[5]
John T. Sloop, Ph.D.[5]
Jason P. Stanko, Ph.D.[5]
Matthew D. Stout, Ph.D.[1,5]
Gregory S. Travlos, D.V.M. (Retired)[1]
Mary S. Wolfe, Ph.D. (Retired)[1,12]

Pei-Li Yao, Ph.D.[10]

Battelle, Columbus, Ohio, USA
Contracts 75N96024C00005 and HHSN273201400015C
Dawn M. Fallacara, Ph.D., Principal Investigator[5,6]
Katherine A.B. Knostman, D.V.M., Ph.D.[3]
Jamie S. Richey, M.S.[3]
Anthony J. Skowronek, D.V.M., Ph.D.[3]

Contract HHSN273201400027C
Jessica Pierfelice, B.S., Principal Investigator[5,6]
Timothy A. Cristy, B.A.[3]
Jayda Meisel, Ph.D.[3]
John Taylor, Ph.D.[3]

AmplifyBio, West Jefferson, Ohio, USA
Subcontract to 75N96024C00005 and HHSN273201400015C
Mark R. Perry, M.S.[3]

CSS Corporation, Research Triangle Park, North Carolina, USA
Contracts 75N94025C00006 and HHSN273201500006C
Steven Brecher, Ph.D., Principal Investigator[5,6,11]
Daniel Brown, Ph.D., Principal Investigator[5,6,11]
Sudha Iyer, B.S.[11]
Varghese S. Tharakan, D.V.M.[11]

Experimental Pathology Laboratories, Inc., Research Triangle Park, North Carolina, USA
Contract 75N96024C00002
Emily Singletary, B.S., Manager[5,6]
Leslie C. Couch, B.S.[3]

Social & Scientific Systems, a DLH Holdings Corp Company, Research Triangle Park, North Carolina, USA
Contract GS-00F-173CA/75N96022F00055
Katherine N. Allen, Ph.D., Principal Investigator[2,5,6]
Laura J. Betz, M.S.[2]
Shawn F. Harris, M.S.[2]
Angela Jeffers, B.S.[2]
Guanhua Xie, Ph.D.[2]

Instem, Staffordshire, United Kingdom
Contract 75N96023D00001
Mark Handley, Computing H.N.C., Program Manager[2,5,6]
Pam Reese, B.S.[2]
Martin Tyszka, M.S.[2]

ASRC Federal Data Solutions, Beltsville, Maryland, USA
Contract 75N96023A00001
Julie Berke, B.S.[2]
Elizabeth V. Black, M.S.[2]
Phyllis B. Brown, B.S.[2]
Karen S. Gilbert, B.S.[2]
Courtney R. Goslowsky, B.S.[2]
Marcus A. Jackson, B.S.[2]
Kelsey J. Oeler, Ph.D.[2]
Satya S. Uppuganti, M.S.[2]

ICF, Reston, Virginia, USA
Contracts 75N96025C00003 and GS00Q14OADU417 (Order No. HHSN273201600015U)
David Burch, M.E.M., Principal Investigator[5,6]
Katherine S. Duke, Ph.D.[10]
Tara Hamilton, M.S.[10]
Cary E. Haver, M.P.H.[5]
Courtney D. Rosenthal, M.S.[10]
Jenna L.N. Sprowles, Ph.D.[10]
Nkoli Ukpabi, M.S.[10]
Janielle S. Vidal, Ph.D.[10]
Jessica A. Wignall, M.S.P.H.[5,6]

Author and Contributor Roles and Definitions[a]

No.	Role	Definition
1	Conceptualization	Ideas; formulation or evolution of overarching research goals and aims
2	Data Curation, Formal Analysis, and Software	Management activities to annotate (produce metadata), scrub, and maintain research data (including software code, when it is necessary for interpreting the data) for initial use and later reuse or Application of statistical, mathematical, computational, or other formal techniques to analyze or synthesize study data or Programming and software development; design of computer programs; implementation of computer code and supporting algorithms; testing of existing code components
3	Investigation	Conduct of the research/investigation process, specifically the performance of experiments or the collection of data/evidence
4	Methodology	Development or design of methodology; creation of models
5	Project Administration	Management and coordination responsibility for research planning and execution
6	Resources for Study Conduct	Provision of study materials, reagents, patients, laboratory samples, animals, instrumentation, computing resources, or other analysis tools
7	Validation	Verification, whether as a part of the activity or separately, of the overall replication/reproducibility of results/experiments and other research outputs
8	Visualization	Preparation, creation, and/or presentation of the published work, specifically visualization/data presentation
9	Writing: Original	Preparation, creation, and/or presentation of the published work, specifically the writing of the initial draft (including substantive translation)
10	Writing: Review and Editing	Preparation, creation, and/or presentation of the published work by those from the original research group, specifically provision of substantive critical review, commentary, or revision—including pre- or post-publication stages
11	Quality Assessment	Conduct of independent assessments of accuracy, consistency, and completeness of various aspects of research products and their components, including data; identification of areas in the conduct and documentation of studies that merit correction or improvement of the description of methodologies
12	Peer Review and Production	Coordination and management of external peer review and publication, including identification of experts, conflict-of-interest screening, correspondence with reviewers, preparation of review documents, and publication activities

[a]Developed using the Contributor Roles Taxonomy (CRediT) framework.[1]

Peer Review

This report was modeled after the *NTP Research Report on In Vivo Repeat Dose Biological Potency Study of Triphenyl Phosphate (CAS No. 115-86-6) in Male Sprague Dawley Rats (Hsd:Sprague Dawley SD) (Gavage Studies)* (https://doi.org/10.22427/NTP-RR-8), which was reviewed internally at the National Institute of Environmental Health Sciences and peer reviewed by external experts. Importantly, these reports employ mathematical model-based approaches to identify and report potency of dose-responsive effects and do not attempt more subjective interpretation (i.e., make calls or reach conclusions on hazard). The peer reviewers of the initial 5-day research report determined that the study design, analysis methods, and results presentation were appropriate. The study design, analysis methods, and results presentation employed for this study are identical to those previously reviewed, approved, and reported; therefore, following internal review, the *NIEHS Report on the In Vivo Repeat Dose Biological Potency Studies of 1,4-Dichlorobenzene (CASRN 106-46-7) in Female Sprague Dawley (Hsd:Sprague Dawley® SD®) Rats and B6D2F1/Crl Mice (Whole-body Inhalation Studies)* was not subjected to further external peer review.

Publication Details

Publisher: National Institute of Environmental Health Sciences

Publishing Location: Research Triangle Park, NC

ISSN: 2768-5632

DOI: https://doi.org/10.22427/NIEHS-13

Report Series: NIEHS Report Series

Report Series Number: 13

Official citation: Auerbach SS, Cora MC, Liu YF, Luh J, Prince LM, Roberts GK, Shipkowski KA, Waidyanatha S. 2026. NIEHS report on the in vivo repeat dose biological potency studies of 1,4-dichlorobenzene (CASRN 106-46-7) in female Sprague Dawley (Hsd:Sprague Dawley® SD®) rats and B6D2F1/Crl mice (whole-body inhalation studies). Research Triangle Park, NC: National Institute of Environmental Health Sciences. NIEHS Report 13.

Acknowledgments

This work was supported by the Intramural Research Program (ES103374 and ES103380) at the National Institute of Environmental Health Sciences (NIEHS), National Institutes of Health and performed for NIEHS under contracts 75N94025C00006, 75N96025C00003, 75N96024C00005, 75N96024C00002, GS-00F-173CA/75N96022F00055, 75N96023A00001, 75N96023D00001, GS00Q14OADU417 (Order No. HHSN273201600015U), HHSN273201500006C, HHSN273201400015C, and HHSN273201400027C.

Abstract

Background: 1,4-Dichlorobenzene (1,4-DCB) is a chlorinated aromatic hydrocarbon that is used in various industrial and household applications, including as a fumigant for moth control, a deodorizer in urinal cakes, and an air freshener in domestic and public settings. Short-term in vivo transcriptomic studies were used to assess the biological potency of 1,4-DCB. The data from these studies are intended to support risk assessment and establishment of acceptable exposure levels of 1,4-DCB in environmental and occupational settings.

Methods: Short-term in vivo biological potency studies on 1,4-DCB in adult female Sprague Dawley (Hsd:Sprague Dawley® SD®) rats and B6D2F1/Crl mice were conducted. Animals were exposed to 1,4-DCB via whole-body inhalation for 6 hours plus the time to achieve 90% of the target concentration after the beginning of vapor generation (T_{90}) per day for 5 consecutive days (study days 0–4) at exposure concentrations of 0, 1, 10, 50, 150, 400, or 800 ppm for rats and 0, 1, 10, 50, 150, or 400 ppm for mice. Blood was collected from animals dedicated to internal concentration assessment in all groups. On study day 5, the day after the final day of exposure, animals were euthanized, standard toxicological measures were assessed, and the heart, kidney, liver, lung, and ovary were assayed in gene expression studies using the TempO-Seq assay. Modeling was conducted to identify the benchmark doses (BMDs) associated with apical toxicological endpoints and transcriptional changes in the heart, kidney, liver, lung, and ovary. A benchmark response of 1 standard deviation from the mean was used to model all apical endpoints, whereas a benchmark response set to a 25% change in the median response was used to model the gene expression data.

Results: Several clinical pathology and organ weight measurements showed exposure-related changes from which BMD values were calculated. In rats, the effects, and their BMDs and benchmark dose lower confidence limits [BMD_{LS}] in ppm, included significantly increased relative liver weight (191.4 [127.6]), increased relative left kidney weight (219.2 [89.4]), increased absolute liver weight (245.5 [163.4]), increased cholesterol concentration (259.4 [126.2]), increased absolute left kidney weight (259.8 [93.3]), increased reticulocyte count (437.0 [307.0]), and increased triglyceride concentration (489.4 [332.3]). In mice, the effects, and their BMDs (BMD_{LS}) in ppm, included significantly decreased albumin/globulin ratio (15.1 [2.2]), increased relative liver weight (70.2 [47.4]), increased cholesterol concentration (71.0 [43.1]), and increased absolute liver weight (83.7 [59.2]).

Following the last exposure (study day 4), 1,4-DCB concentrations in rats increased proportionally to the exposure concentration up to 150 ppm in blood, 50 ppm in liver, and 400 ppm in lung. At higher exposure concentrations, blood, liver, and lung concentrations increased more than proportionally to the exposure concentration, demonstrating saturation of metabolism and/or clearance processes. In mice, 1,4-DCB concentrations increased proportionally to the exposure concentration in blood and tissues up to 10 ppm. At exposure concentrations ≥50 ppm, blood and tissue concentration increased more than proportionally to the exposure concentration. In general, 1,4-DCB tissue concentrations were similar to blood concentrations in rats and mice, demonstrating low tissue distribution and/or retention. Blood and tissue concentrations on the day after the last exposure (study day 5) were much lower than those on the last day of exposure (study day 4) in both rats and mice, demonstrating rapid elimination of 1,4-DCB. In general, when normalized to the theoretical inhaled dose, rats had

higher blood and tissue concentrations of 1,4-DCB than mice at the lower exposure concentrations, although the difference was smaller at 400 ppm.

In both rats and mice, no Gene Ontology (GO) biological process in the heart, kidney, liver, lung, or ovary had BMD values below the lower limit of extrapolation (<0.333 ppm). The most sensitive gene sets for which a reliable estimate of the BMD could be made are given below for each tissue and species, with their BMDs (BMD_Ls) in ppm.

In the heart, the most sensitive gene sets in rats were cell cycle phase transition (141.4 [55.9]) and mitotic cell cycle phase transition (141.4 [55.9]), whereas in mice, the most sensitive gene set was organic hydroxy compound biosynthetic process (91.0 [25.1]). In the kidney, the most sensitive gene sets in rats were cell cycle phase transition (121.0 [42.2]) and mitotic cell cycle phase transition (121.0 [42.2]), and in mice, the most sensitive gene set was circadian rhythm (16.9 [2.0]). In the liver, the most sensitive gene set in rats was xenobiotic metabolic process (87.6 [59.6]), whereas the most sensitive gene sets in mice were regulation of chromosome segregation (6.3 [0.9]), positive regulation of cell cycle phase transition (6.3 [0.9]), and positive regulation of mitotic cell cycle phase transition (6.3 [0.9]). In the lung, the most sensitive gene sets in rats and mice were chromosome segregation (208.6 [55.4]) and DNA replication (1.4 [0.5]), respectively. In the ovary, the most sensitive gene set in rats was ameboidal-type cell migration (223.1 [90.9]). There were no active GO terms (i.e., no gene expression response at the gene set level) in the ovaries of mice exposed to 1,4-DCB.

Summary: Taken together, in rats, the most sensitive gene set and apical endpoint BMD (BMD_L) values that could be reliably determined occurred at 87.6 (59.6) and 191.4 (127.6) ppm, respectively. In mice, the most sensitive gene set and apical endpoint BMD (BMD_L) values that could be reliably determined occurred at 1.4 (0.5) and 15.1 (2.2) ppm, respectively.

Background

1,4-Dichlorobenzene (1,4-DCB) (CASRN: 106-46-7, U.S. Environmental Protection Agency [U.S. EPA] Chemical Dashboard: DTXSID1020431, PubChem CID: 4685, European Committee Number: 203-400-5), also known as para-DCB, is an organochlorine compound classified under chlorinated aromatic hydrocarbons.[2] 1,4-DCB is frequently used in various industrial and household applications.[2] Industrially, it is used in the synthesis of resins.[2; 3] With its distinctive, penetrating, and mothball-like odor, it is widely used as a fumigant for moth control and as a deodorizer in urinal cakes; it is has also been used an air freshener in domestic and public settings.[2] Additionally, 1,4-DCB is registered as a pesticide by the U.S. EPA.[4]

The Occupational Safety and Health Administration has set a maximum workplace air concentration of 75 ppm of 1,4-DCB for an 8-hour workday,[5] whereas the American Conference of Governmental Industrial Hygienists advises that the average airborne exposure should not exceed 10 ppm for an 8-hour work shift.[6] Under the Safe Drinking Water Act, both the federal maximum contaminant level goal and the maximum contaminant level for 1,4-DCB are set to 75 µg/L.[7] California's Office of Environmental Health Hazard Assessment has developed acute, chronic, and 8-hour reference exposure levels of 1,500, 0.8, and 1.7 ppb, respectively.[8] The U.S. Department of Health and Human Services has concluded that 1,4-DCB is reasonably anticipated to be a human carcinogen,[9] and the International Agency for Research on Cancer (IARC) has classified it as possibly carcinogenic to humans (Group 2B).[10] This conclusion is based on evidence from animal studies.[9; 10] Owing to its carcinogenic properties, the use of 1,4-DCB has been prohibited in the European Union for air fresheners since 2014 and in mothballs since 2007.[11]

Exposure to 1,4-DCB can occur through various routes, including inhalation, ingestion, and dermal contact.[2] Inhalation exposure is particularly significant because of the volatility of 1,4-DCB, making occupational exposure a concern in industrial settings.[2] Inhalation exposure is also of concern in environments where it is used as a deodorizer or fumigant.[2] Data from animal experiments suggest that 1,4-DCB is rapidly and extensively absorbed through inhalation and oral routes, whereas no data on dermal absorption are available.[2] Data from both humans and experimental animals suggest that the compound widely distributes throughout the body, particularly in lipid-rich tissues, because of its lipophilicity.[2] 1,4-DCB is primarily metabolized in the liver by cytochrome P450 enzymes, mainly CYP2E1, resulting in an epoxide that is subsequently hydrolyzed to more water-soluble metabolites such as 2,5-dichlorophenol.[2; 12] These metabolites are then conjugated and primarily excreted through urine, with minor excretion via feces and exhaled air as demonstrated in animal studies.[2]

Short-term exposure to high concentrations of 1,4-DCB in humans can lead to acute central nervous system effects such as dizziness, headache, and nausea, as well as skin and eye irritation upon direct contact.[2] Subacute or subchronic exposure to 1,4-DCB in animal models has also been linked to liver and kidney damage; hepatotoxicity is indicated by elevated liver enzymes and histopathological changes such as liver cell hypertrophy and necrosis, and nephrotoxicity manifests as proximal tubular damage and altered renal function markers.[2] Chronic exposure has been associated with liver and kidney cancer, and there is sufficient evidence of carcinogenicity in animal studies,[2; 10] leading to the classification of 1,4-DCB as a possible human carcinogen by IARC.[10]

The primary mechanism of 1,4-DCB toxicity involves its bioactivation to reactive intermediates, such as epoxides, which are conjugated to glutathione during hepatic metabolism.[2; 12] These intermediates can induce oxidative stress and covalently bind to cellular macromolecules, leading to lipid peroxidation, protein damage, and DNA adduct formation.[2] This oxidative damage is a significant factor contributing to the hepatotoxicity and nephrotoxicity observed in various studies.[2]

The primary purpose of these short-term toxicity studies is to characterize the biological potency of 1,4-DCB via inhalation exposure. The data from these studies are intended to support risk assessment and establishment of acceptable exposure levels of 1,4-DCB in environmental and occupational settings.

Materials and Methods

Chemistry

Procurement and Characterization of 1,4-Dichlorobenzene

1,4-Dichlorobenzene (1,4-DCB) was obtained from Finetech Industry Limited (Wuhan, China) in a single lot (20240416001). Identity, purity, and stability analyses were conducted by the analytical chemistry laboratory at Battelle (Columbus, OH). Reports on analyses performed in support of the 1,4-DCB studies are on file at the National Institute of Environmental Health Sciences (NIEHS).

The identity and purity of lot 20240416001, a white crystal at room temperature, was evaluated using gas chromatography (GC) with mass spectrometry (MS) detection. The MS spectrum was consistent with the National Institute of Standards and Technology library spectrum for 1,4-DCB and a certified reference material of 1,4-DCB. The overall purity of the test article was estimated at approximately 100%.

Bulk 1,4-DCB was stored in the original shipping container at room temperature. Reanalysis of the bulk chemical was performed by the analytical chemistry laboratory within 30 days of study termination and no degradation was detected.

Vapor Generation and Exposure System

A diagram of the generation and distribution system is shown in Figure A-3. Solid 1,4-DCB was melted in a heated reservoir and pumped through heated lines by a fluid metering pump into a heated glass vaporizer column filled with glass beads and wrapped with heat tape. A waste collection flask was connected to the bottom of the column to collect residual 1,4-DCB not completely vaporized within the vaporizer column. Preheated nitrogen entered the column from below, vaporized 1,4-DCB, and carried the vapor from the generator cabinet located in the control room to the distribution manifold located in the exposure room through a heated Teflon® transport line. The nitrogen-test article mixture was diluted with heated air before it entered the distribution manifold. Concentration in the manifold was determined by the chemical pump rate, dilution air flow rate, nitrogen flow rate, and special modifications to the distribution manifold (Appendix A).

Individual heated Teflon delivery lines carried the vapor from the exposure valves in the distribution cabinet to the chamber inlets. The exposure valves diverted vapor delivery to the manifold exhaust until the generation system was stable, and exposures were ready to proceed. The rate of 1,4-DCB vapor delivery to each chamber was controlled by precision metering valves at the manifold. When the exposure started, the exposure valves actuated, directing the vapor into the chamber inlet, where it was diluted with conditioned air to achieve the desired exposure concentration. Conditioned air was a temperature-controlled and filtered mix of air derived from each exposure chamber's wet and dry air duct supplies.

The exposure system consisted of seven exposure chambers with target test article concentrations of 0 (control group), 1, 10, 50, 150, 400, and 800 ppm. The inhalation exposure chamber (Lab Products, Inc., Seaford, DE) was designed so that uniform vapor concentrations could be

maintained throughout the chamber with catch pans in place. The total active mixing volume of each chamber was 1.7 m^3. A small particle detector (Model 3022A; TSI, Inc., Shoreview, MN) was used in the exposure chambers, both with and without animals, to ensure vapor (not aerosol) was produced. No particle counts above the minimum resolvable level were detected.

Vapor Concentration Monitoring

Exposure chamber and room concentrations of 1,4-DCB were monitored using an online GC equipped with a flame ionization detector (FID) (Table A-1). All chambers were sampled at approximately twice per hour during exposure through Teflon tubing connected to each exposure chamber's relative-humidity sampling lines at a location close to the GC/FID. The samples flowed into a 16-port Hastelloy®-C stream-select valve that directed a continuous stream of sampled atmosphere to a 6-port Hastelloy-C gas-sampling valve with a 1 mL sample loop. Valves were mounted in a dedicated valve oven to maintain temperature. A vacuum regulator maintained a constant vacuum in the sample loop to compensate for variations in sample line pressure. An in-line flow meter between the vacuum regulator and GC allowed for digital measurement of sample flow.

The average concentrations were all within the acceptance criteria of 10% for all exposure groups. Concentration relative standard deviation was within acceptance criteria of 10% except for the 1 ppm chamber (rat and mouse). The number of acceptable samples was ≥94% for all exposure groups of every study except for the 1 ppm rat and mouse chambers, which were 65% and 74%, respectively. The individual concentration data collected from the exposure room frequently exceeded the limit of detection (LOD; 0.02 ppm) with concentrations ≤0.053 ppm during the rat study and ≤0.034 ppm during the mouse study. The control chambers remained below the LOD for the entirety of both studies. These deviations from the acceptance criteria were considered to have no effect on the study results. Additional details are provided in Appendix A.

Chamber Atmosphere Characterization

Buildup and decay rates for chamber vapor concentrations were determined prior to (without animals) and during (with animals) the studies. The time to achieve 90% of the target concentration after the beginning of vapor generation (T_{90}) and the time for the chamber concentration to decay to 10% of the target concentration after vapor generation was terminated (T_{10}) were estimated from the concentration versus time curves. At a chamber airflow rate of 15 ft^3/min, the theoretical T_{90} value was 9.2 minutes. The estimated values in both rat and mouse studies ranged from 8 to 19 minutes, and a value of 12 minutes was used for the studies. Estimated T_{10} for both studies ranged from 9 to 13 minutes.

Prior to the studies, the persistence of 1,4-DCB was monitored in the 400 and 800 ppm chambers after exposure without animals present. The concentration of 1,4-DCB reached 1% of starting concentration (T_1) in ≤37 minutes. During the studies and with animals present, T_1 was ≤75 minutes. The reason for the prolonged T_1 values is unknown, but the prolonged T_1 values were considered to have no effect on study findings given the low levels compared to the target chamber concentrations.

The uniformity of 1,4-DCB vapor concentration was evaluated in all exposure chambers without animals present and repeated during the studies with animals present in the lowest (1 ppm) and

highest (800 or 400 ppm for rats and mice, respectively) exposure concentration chambers. Concentrations were measured at 12 chamber positions, one in the front and one in the back, for each of the six possible animal cage positions per chamber. Chamber concentration uniformity was maintained throughout the studies.

To measure the stability and purity of 1,4-DCB in the generation and delivery system, samples of the test atmosphere were collected from the distribution line, generator reservoir, and the highest, lowest, and control exposure concentration chambers for both species at the beginning and end of the exposure day. Exposure atmosphere samples were collected with sorbent gas-sampling tubes in series with a silica gel sorbent tube. Samples were extracted with methanol for analysis. In addition, analysis was performed on a second set of samples collected from the same locations and exposure times and extracted in acetone to determine whether any impurities in 1,4-DCB were obscured by methanol. No impurity peaks were present in any samples. 1,4-DCB was not detected in the silica gel samples, demonstrating 100% capture of the inhalation exposure atmosphere onto sorbent media. The stability and purity of 1,4-DCB were maintained throughout the exposure system.

Study Design for Rats

Female Sprague Dawley (Hsd:Sprague Dawley® SD®) rats were obtained from Inotiv (Envigo, at time of procurement, Indianapolis, IN). Sprague Dawley rats were employed to represent the Division of Translational Toxicology (DTT)'s typical rat strain of choice. Females were chosen instead of males to reduce the overall study size and limit the complexity of comparisons between the mouse data set (see further justification below) and the rat data set. On receipt, the rats were 7 weeks of age. Animals were quarantined for 8 days and then randomly assigned to one of seven exposure groups. The rats in each exposure group were exposed to 1,4-DCB via whole-body inhalation for 6 hours plus T_{90} per day for 5 consecutive days (study days 0–4) at exposure concentrations of 0, 1, 10, 50, 150, 400, or 800 ppm. There were 5 core female rats in each exposed group and 10 in the 0 ppm group to establish a more confident estimate of variance in the control group; an additional 3 rats were added to each group for internal concentration assessment. Immediately following the final exposure on study day 4, blood, lung, and liver samples were collected from the internal concentration assessment animals once chamber concentrations were at or below the regulatory limit of 5 ppm without additional health and safety considerations. Euthanasia, blood/serum collection, and tissue sample collection for all core animals were completed on study day 5, the day following the final exposure. In addition, blood, lung, and liver samples were collected from three core animals in each group on study day 5 for internal concentration assessment. Animal identification numbers and FASTQ data file names for each animal are presented in Appendix C.

Study Design for Mice

Female B6D2F1/Crl mice were obtained from Charles River Laboratory (Raleigh, NC). Given previously observed carcinogenic effects in the lung in female mice and in the liver in male and female mice,[13] these studies employed the same strain/sex in which these effects were observed to allow for phenotypic anchoring of the biological interpretation of the data generated in the proposed studies. Females accounted for both carcinogenic responses (liver and lung) with exposure to 1,4-DCB, hence they were chosen instead of males. This decision reduced the overall study size and limited the complexity of comparisons between the mouse and rat data

sets. On receipt, the mice were 6 weeks of age. Animals were quarantined for 5 days and then randomly assigned to one of six exposure groups. The mice in each exposure group were exposed to 1,4-DCB via whole-body inhalation for 6 hours plus T_{90} per day for 5 consecutive days (study days 0–4) at exposure concentrations of 0, 1, 10, 50, 150, or 400 ppm. There were 5 core female mice in each exposed group and 10 in the 0 ppm group to establish a more confident estimate of variance in the control group; an additional 3 mice were added to each group for internal concentration assessment. Immediately following the final exposure on study day 4, blood, lung, and liver samples were collected from the internal concentration assessment animals once chamber concentrations fell below the regulatory limit of 5 ppm without additional health and safety considerations. Euthanasia, blood/serum collection, and tissue sample collection for all surviving core animals were completed on study day 5, the day following the final exposure. In addition, blood, lung, and liver samples were collected from up to three core females in each group on study day 5 for internal concentration assessment. Animal identification numbers and FASTQ data file names for each animal are presented in Appendix C.

Exposure Concentration Selection Rationale

The exposure concentrations evaluated in these studies were based on data in the published literature as described in the background of this report. In addition, a pilot study was conducted during the prestudy exposure engineering phase to confirm concentrations would be well tolerated for the duration of the planned study. Informed by the pilot exposure in a small number of animals, the highest concentrations were selected to be 800 ppm and 400 ppm for rats and mice, respectively. The lowest concentration of 1 ppm was selected to be tenfold less than the second lowest nonzero exposure concentration to produce a no-effect level at the transcriptome level.

Clinical Examinations and Sample Collection

Clinical Observations

All animals were observed twice daily for signs of mortality or moribundity, except for the day of receipt and at removal when animals were observed once. Clinical observations were performed once prior to exposure on study day 0 and at study termination.

Body and Organ Weights

Animals were weighed during quarantine for randomization, on the first day of exposure (study day 0), daily thereafter (prior to exposure), and on the day of necropsy (study day 4 or 5). During necropsy for all core animals, the heart, liver, kidneys, and lungs were removed, and organ weights were recorded; bilateral organs were weighed separately.

Clinical Pathology

Animals were anesthetized with a 70% carbon dioxide (CO_2)/30% oxygen (O_2) mixture and bled in random order 1 day after the final day of exposure. After blood collection, animals were euthanized by exsanguination (rats) or CO_2/O_2 (70%/30%) followed by exsanguination (mice). Blood samples were collected within approximately a 2-hour and 30-minute window because extended times were needed for chambers to fall below regulatory limits. Blood was taken via retro orbital plexus (rats) or retro orbital sinus (mice) and collected into tubes containing

tripotassium ethylenediaminetetraacetic acid (K_3 EDTA) for hematology analysis (rats only) and into serum collection tubes without anticoagulant for clinical chemistry (rats and mice). The following hematology parameters were measured on a Sysmex XN-2000V (Sysmex America, Lincolnshire, IL) for rats: erythrocyte count, hemoglobin, hematocrit, mean cell volume, mean cell hemoglobin, mean cell hemoglobin concentration, white blood cell count and differential, reticulocyte count, and platelet count. Manual hematocrit was determined using a microcentrifuge and capillary reader. Blood smears were prepared, and qualitative evaluation of cellular morphology was performed per study protocol. The following clinical chemistry parameters were measured on a Roche cobas® c501 Chemistry Analyzer (Roche Diagnostics, Indianapolis, IN) for rats and mice: alanine aminotransferase, albumin, alkaline phosphatase, aspartate aminotransferase, total bile acids, total bilirubin, direct bilirubin, cholesterol, creatine kinase, creatinine, glucose, sorbitol dehydrogenase, total protein, triglycerides, and blood urea nitrogen. Globulin, albumin/globulin ratio, and indirect bilirubin were calculated based on direct measurements (e.g., indirect bilirubin = total bilirubin − direct bilirubin). Individual animal and summary clinical chemistry and hematology data are available in Appendix G.

Internal Concentration Assessment

An assessment was conducted to determine systemic exposure and tissue distribution and evaluate whether the test chemical had bioaccumulative properties (i.e., whether the half-life was >24 hours). Blood, lung, and liver samples were collected from the internal concentration assessment animals immediately following the last exposure on study day 4 (once chamber concentrations were at or below the regulatory limit of 5 ppm without additional health and safety considerations) and on study day 5 (approximately 18 hours following the last exposure) from core animals designated for internal concentration assessment. On study day 4, blood was collected via cardiac puncture for all surviving rats and mice (up to 3/exposure group) while animals were anesthetized with CO_2/O_2 (70%/30%). On study day 5, blood samples from designated core animals (3/exposure group) were taken via retro orbital plexus (rats) or retro orbital sinus (mice) while animals were anesthetized with CO_2/O_2 (70%/30%). Blood samples were collected within a 2-hour window. Blood was collected into tubes containing K_3 EDTA and three aliquots of 100 µL were transferred into headspace vials and kept on wet ice. Internal standard $^{13}C_6$ 1,4-DCB (added as a mixture of $^{13}C_6$ 1,2-DCB and $^{13}C_6$ 1,4-DCB) was added to aliquoted samples and then stored frozen (−85°C to −60°C). All samples were frozen within 2 hours of collection. After blood collection, animals were euthanized by exsanguination and lung and liver tissues were collected (following organ weight measurements for core animals designated for internal concentration assessment) from each animal within approximately 2 hours and 30 minutes of each other. Up to three aliquots of approximately 100 mg (rats) or 50 mg (mice) lung and liver tissue were collected from each animal and flash frozen. Samples were stored frozen (−85°C to −60°C) until analysis as described in Appendix B.

Transcriptomics

Sample Collection for Transcriptomics

The majority of all tissues from all animals were collected within approximately 10 minutes of euthanasia. Tissue samples were collected following organ weight measurements in the following order: lung, heart, liver (left lobe), kidney, and ovary (no ovary weights were taken) from all remaining animals on study day 5 for transcriptomic analysis. Two samples of lung,

heart, liver, and kidney tissue (approximately 5 mm^3) were collected and placed into cryotubes containing RNA*later*™ (Thermo Fisher Scientific, Waltham, MA). The ovaries were collected whole bilaterally (one sample) and placed into cryotubes containing RNA*later*. The tissue samples were stored at 2°C to 8°C for approximately 55 hours for rats or up to 48 hours for mice. The RNA*later* was then removed and the samples were stored in a −85°C to −60°C freezer until processed for RNA isolation.

RNA Isolation, Library Creation, and Sequencing

RNA isolation was performed on tissue samples preserved in RNA*later*. Tissues were homogenized in QIAzol lysis buffer (Qiagen Inc., Valencia, CA) using the TissueLyser II bead-beating system followed by RNA extraction using the RNeasy 96 QIAcube HT kits (Qiagen Inc., Valencia, CA) with a DNA digestion step. The concentration and purity of all isolated samples were determined from absorbency readings taken at 260 and 280 nm using a NanoDrop ND-2000 Spectrophotometer (NanoDrop Technologies, Wilmington, DE). The readings accurately determined the concentration of each sample while ensuring that an acceptable purity (A_{260}/A_{280} ratio) between 1.80 and 2.20 was achieved. Further quality control (QC) evaluation of each RNA sample was performed using the RNA 6000 Nano kit and analyzed with a 2100 Bioanalyzer (Agilent Technology, Foster City, CA), which evaluates the RNA Integrity Number (RIN). RIN must be >3.0 to meet acceptable quality for TempO-Seq analysis. All samples were divided into at least two aliquots. One aliquot was used for BioSpyder TempO-Seq S1500+ analysis. Any tissue samples remaining after RNA isolation were stored at −85ºC to −60ºC until submitted frozen to the Frozen Tissue Bank.

Isolated RNA was utilized for analysis using either the Rat S1500+ v1.2 TempO-Seq or Mouse S1500+ v1.2 TempO-Seq (BioSpyder, Carlsbad, CA) platform with a minimum of 500 mapped read counts/transcript and approximately 1.5 million counts/sample. Work instructions developed by Battelle using the BioSpyder User Guide[14] were followed, including the optimized overnight annealing procedure, outlined as follows. Two microliters of each diluted RNA sample (50 ng/µL) was hybridized with the S1500+ surrogate detector oligo pool mix (2 µL per sample) in a 384-well plate using the following thermocycler settings: 70°C for 10 minutes, followed by a gradual decrease to 45°C over 50 minutes, held at 45°C for 16 hours, and ending with a decrease to 25°C. The plates were held at 25°C for no longer than 8 hours. After annealing, the annealed RNA was transferred to 96-well plates for nuclease digestion (24 µL nuclease mix addition followed by 90 minutes at 37°C), followed by ligation (24 µL ligation mix addition followed by 60 minutes at 37°C) and heat denaturation (at 80°C for 15 minutes). For amplification, polymerase chain reaction (PCR) Pre-Mix and Primers were transferred from the BioSpyder S1500+ surrogate kit 96-well plates into a 384-well plate. Ten microliters of each ligated product were then added to the 384-well plate, sealed, and centrifuged briefly before 30 cycles of amplification.

All steps during the TempO-Seq S1500+ surrogate assay were performed using a QuantStudio 6 Flex System. The amplification step produced well-specific barcoded primer pairs that allowed identification of each well after being combined into a single sequencing library. Five microliters of amplified libraries were pooled together and purified using NucleoSpin gel and a PCR clean-up kit (Macherey-Nagel Inc., Allentown, PA). Once cleaned, the library concentration was determined by quantitative PCR using a KAPA Library Quantification Kit (Roche Sequencing, Indianapolis, IN), and the library was diluted to a final concentration of 400 pM. A PhiX control

library (Illumina, San Diego, CA) was spiked into the final library as a system control. The final library was loaded onto an Illumina next generation sequencing cartridge, NovaSeq 6000 S1 Reagent Kit v1.5 (100 cycles) (Illumina, San Diego, CA), along with the BioSpyder-provided custom sequencing primer. Processing of sequencing data was conducted using Illumina's BCL2FASTQ software employing default parameter settings.

Sequence Data Processing

FASTQ files of TempO-Seq reads were aligned to the probe sequences from the target platform using Bowtie version 1.3.1[15] with the following parameters: -v 3 -k 1 -m 1 --best --strata. This configuration allows up to three mismatches and reports the single best alignment. After alignment, the total sequenced reads, the percentage of reads aligning to the platform manifest, the alignment rate, and the percentage of expressed probes (≥5 reads per probe) were calculated for each sample.

Sequencing Quality Checks and Outlier Removal

Each sample was evaluated for quality using the following metrics: sequencing depth, alignment to the platform manifest, number of aligned reads, % of probes with at least five reads, average per base quality, and per base N content. Samples were flagged for values below the following thresholds for the QC metrics: sequencing depth <300 K, total alignment rate <40%, unique alignment rate <30%, number of aligned reads <300 K, or percentage of probes with at least five reads <50%. FastQC was run on all samples to ensure adequate per base quality and per base N content, where N represents bases that could not be identified. Ten samples were flagged after applying the per-sample QC metrics. In addition, principal component, hierarchical cluster, and inter-replicate correlation analyses were used collectively to identify outlier samples. These analyses confirmed the 10 flagged samples as outliers, identified additional outliers, and discovered a set of mouse kidney samples with potential tissue contamination. A total of 7 rat and 13 mouse samples were removed before downstream analysis, with 192 rat and 162 mouse samples available for downstream analysis.

The processing of samples from the study of 1,4-DCB was conducted in parallel with one other chemical (1,2-dichlorobenzene) that was studied under a similar protocol, therefore allowing for a more powerful collective assessment of the data. Specifically, during RNA isolation and extraction, the samples from both studies were distributed over twelve 96-well plates (i.e., three plates per species per chemical). Prior to amplification and library generation, the samples were randomized over five 384-well plates (i.e., one plate per tissue). The sample layout on the plate avoided the edge wells to preclude edge-well effects, which can affect downstream sequencing results. The final sample counts used for benchmark dose (BMD) analysis of the transcriptomics data are shown in Table 1.

Table 1. Final Sample Counts for Benchmark Dose Analysis of the Transcriptomics Data

	0 ppm	1 ppm	10 ppm	50 ppm	150 ppm	400 ppm	800 ppm
Rats							
Heart	10	5	5	5	5	5	5
Kidney	10	4	5	5	5	5	5
Liver	10	5	5	5	5	5	5

	0 ppm	1 ppm	10 ppm	50 ppm	150 ppm	400 ppm	800 ppm
Lung	8	4	4	5	4	3	5
Ovary	10	5	5	5	5	5	5
Mice							
Heart	10	5	5	5	5	5	NA
Kidney	6	4	4	4	4	5	NA
Liver	7	5	4	5	4	5	NA
Lung	10	5	5	5	5	5	NA
Ovary	10	5	5	5	5	5	NA

NA = not applicable.

Data Normalization

The aligned read counts for attenuated probes were properly readjusted to calculate unattenuated equivalent counts using the attenuation factors provided in the platform manifest. To account for between-sample sequencing depth variation, unattenuated read counts were normalized at the probe level by applying reads per million normalization. A pseudo-read-count of 1.0 was added to each normalized expression value, and then the values were log2-transformed to complete the normalization. Principal component-based visualizations of the final expression data set used from modeling are available in Appendix D.

Data Analysis

Statistical Analysis of Body Weights, Organ Weights, and Clinical Pathology

Two approaches were employed to assess the significance of pairwise comparisons between exposed and 0 ppm groups in the analysis of continuous variables. Organ and body weight data, which have approximately normal distributions, were analyzed using the parametric multiple comparison procedures of Williams[16; 17] and Dunnett.[18] Clinical pathology data, which typically have skewed distributions, were analyzed using the nonparametric multiple comparison methods of Shirley[19] and Dunn.[20] The Jonckheere test[21] was used to assess the significance of dose-response trends and to determine whether a trend-sensitive test (Williams or Shirley test) was more appropriate for pairwise comparisons than a test that assumes no monotonic dose response (Dunnett or Dunn test). Trend-sensitive tests were used when the Jonckheere test was significant at $p \leq 0.01$.

Prior to analysis, values identified by the outlier test of Dixon and Massey[22] were examined by NIEHS staff. Values from animals suspected of illness from causes other than experimental exposure and values that the laboratory indicated as inadequate because of measurement problems were eliminated from the analysis.

A no-observed-effect level (NOEL) was identified as the highest exposure concentration not showing a significant ($p \leq 0.05$) pairwise difference relative to the 0 ppm group. A lowest-observed-effect level (LOEL) was identified as the lowest exposure concentration demonstrating a significant ($p \leq 0.05$) pairwise difference relative to the 0 ppm group. Throughout the results

section for apical endpoints, interpretation of BMDs is made in relationship to NOEL and LOEL values for specific endpoints, as defined here, and are not meant to reflect an overall study NOEL or LOEL.

Benchmark Dose Analysis of Body Weights, Organ Weights, and Clinical Pathology

Data files for apical endpoints, including clinical pathology, organ weights, and body weights, were created using nontransformed individual animal data. With the exception of body weights and body weight gain, to be included in the data file, an endpoint had to show a significant trend and at least one significant pairwise response. The expression data files were then loaded into BMDExpress 3.2.0119 using a "generic" platform annotation. BMD modeling was conducted with ToxicR Laplace model averaging, applying a benchmark response (BMR) of 1 standard deviation. Constant variance was assumed in the BMD modeling. Results from the BMD analysis were subsequently subjected to a defined category analysis in which modeled responses were excluded if they did not meet the following criteria: $R^2 > 0.6$, BMD/benchmark dose lower confidence limits (BMD_L) < 10, and BMD < highest dose. Some endpoints that met the initial statistical criteria for inclusion (i.e., significant trend and at least one significant pairwise response) did not yield a BMD result because no viable model was obtained.

Benchmark Dose Analysis of Transcriptomics Data

The BMD analysis of the transcriptomic data was performed in a manner consistent with the guidance provided in the National Toxicology Program best practices for genomic dose-response modeling as reviewed by an independent panel of experts in October 2017. These recommendations are described in the 2018 publication *National Toxicology Program Approach to Genomic Dose-Response Modeling*.[23]

Dose-response modeling of transcriptional effects was carried out using BMDExpress 3.20.0095, a robust, interactive, and user-friendly update of BMDExpress software[24] that can be downloaded at no cost (https://github.com/auerbachs/BMDExpress-3/releases). The initial mapped read counts from the TempO-Seq data from each well were counts per million normalized. The values were log2 transformed and imported into BMDExpress. The platform selection in BMDExpress was S1500_Plus_Rat for rats (date: October 31, 2024) and S1500_Plus_Mouse for mice (date: October 31, 2024). Before importing the data into BMDExpress, all detection oligos (DO) with "0" count values in any sample were excluded.

In BMDExpress, the data underwent a twofold prefiltering process. First, a Williams trend test[16; 17] was performed with nominal p value < 0.05 with 10,000 permutations. The DOs that passed the Williams trend test were then subject to the Curve Fit Prefilter for which the Hill, Power, Linear, Exponential 3, and Exponential 5 models were selected. A BMR factor of 2 standard deviations was used and the variance setting was constant.

The BMD analysis on the transcripts that passed the Curve Fit Prefilter was conducted using the ToxicR MAP/Laplace Bayesian MA fitting approach, implemented in BMDExpress. All continuous models (Hill, Power, Exponential 3, Exponential 5) were utilized. The parameters were set as follows: BMR type as relative deviation; BMR factor at 25%; variance as constant; and a Step Function Threshold at 0.5.

Gene set analysis (a.k.a. Functional Classification) was carried out using Gene Ontology biological process (GO BP) gene sets. For the GO analysis, the following settings were selected: (1) remove BMD > highest dose from category descriptive statistics; (2) remove BMD with R^2 < the cutoff of 0.6; (3) remove DOs with step function lower than first dose; (4) minimum number of genes in gene set of 40; (5) maximum number of genes in gene set of 500; (5) under DO to gene conversion, identify conflicting probe sets with correlation cutoff for conflicting probe sets of 0.5. Individual gene functional classification was conducted similarly to the GO gene set analysis, except that the maximum and minimum gene set size requirements were omitted.

Active GO BP terms were identified using criteria requiring at least three genes and being at least 5% populated. BMD, BMD_L, and benchmark dose upper confidence limit (BMD_U) values at the 5% level (i.e., 5th percentile) were reported as potency metrics for the active GO BP gene sets. BMD, BMD_L, and BMD_U values for the individual gene analyses reflected the average of DOs met the fit criteria and corresponded to that gene. The exact BMD modeling pipeline parameters used to analyze the data presented in this report were evaluated using the data from Gwinn et. al.[25] and compared to the EPA Transcriptomic Assessment Product analysis pipeline.[26] The results of this analysis can be found in Appendix G under G.5.1 Analysis Pipeline Evaluation.

Empirical False Discovery Rate Determination for Genomic Dose-response Modeling

Synthetic null data were generated using the probe-filtered (i.e., "no 0") 0 ppm data from each tissue from the 1,2-dichlorobenzene rat and mouse studies that were performed in combination and that used a similar protocol as the 1,4-DCB studies reported here. The synthetic null data were generated using the Synthetic and Null Data Generator (SaNDGen; https://rstudio.niehs.nih.gov/sandgen/), which employed the normal distribution method previously described for generating synthetic data.[27] In short, for each set of tissue/species, 0 ppm data were used to generate a distribution for each probe. This distribution was resampled to generate 1,000 values for each probe. These values were distributed into synthetic samples, which were then organized into 20 different experiments paralleling the distribution of samples in the experimental study (i.e., 10 samples in the 0 ppm group and 5 for each exposed group). Each of the 20 synthetic null experiments was processed through BMDExpress using the identical parameters used to analyze the experimental data. The resultant data were then used to determine the empirical false discovery rates, which are reported as percentages of possible genes and GO BPs. The results of the empirical false discovery rate analysis are available in Appendix D. The associated bm2 analysis files that are the basis of the empirical false discovery rate can be found in Appendix G.

Data Accessibility

Primary and analyzed data used in this study are available to the public at https://doi.org/10.22427/NIEHS-DATA-NIEHS-13.[28]

Results

Apical Endpoint Analysis

Animal Condition, Body Weights, and Organ Weights

Rats

One internal concentration assessment animal in the 800 ppm group was found dead on study day 4. All core rats exposed to 1,4-dichlorobenzene (1,4-DCB) survived to the end of the study. In the 800 ppm group, all core rats began exhibiting piloerection, bilateral dilated pupil, and moderate tremors on study day 0, with two of the rats also noted with lacrimation post exposure, one each on study days 1 and 3 (Appendix G). No significant change in terminal body weight was observed with exposure to 1,4-DCB (Table 2).

At study termination, absolute and relative left kidney weights were significantly increased in the ≥400 ppm groups with benchmark doses (benchmark dose lower confidence limits)—BMDs (BMD_{LS})—of 259.8 (93.3) and 219.2 (89.4) ppm, respectively (Table 3). There was also a significant increase in relative right kidney weight at 400 ppm; a BMD (BMD_L) was not determined for increased relative right kidney weight because no viable model was available. A significant increase in absolute and relative liver weights occurred in the ≥400 ppm groups with BMDs (BMD_{LS}) of 245.5 (163.4) and 191.4 (127.6) ppm, respectively. The organ weights mentioned above all exhibited positive trends. The BMDs for all organ weights were reviewed by a subject matter expert for anomalous modeling results (i.e., when the traditional statistics are notably different from the calculated BMD values). Significant trend and pairwise comparisons were not observed in absolute right kidney weight or absolute or relative heart or lung weights (Appendix G).

Mice

One internal concentration assessment animal in the 50 ppm group was found dead on study day 2. All core mice exposed to 1,4-DCB survived to the end of the study with no adverse clinical observations noted (Appendix G). There were no significant changes in terminal body weight in core mice exposed to 1,4-DCB (Table 2).

At study termination, absolute and relative liver weights were significantly increased in the ≥150 ppm groups with both endpoints exhibiting a positive trend. The BMDs (BMD_{LS}) for increased absolute and relative liver weights were 83.7 (59.2) and 70.2 (47.4) ppm, respectively (Table 3). Significant trend and pairwise comparisons were not observed in absolute or relative left or right kidney weights or absolute or relative heart or lung weights (Appendix G).

Table 2. Summary of Body Weights and Body Weight Gain of Female Rats and Mice Exposed to 1,4-Dichlorobenzene for Five Days

Endpoint[a,b]	0 ppm	1 ppm	10 ppm	50 ppm	150 ppm	400 ppm	800 ppm	BMD_{1Std} (ppm)	BMD_{L1Std} (ppm)
Rats									
n	10	5	5	5	5	5	5	NA	NA
Body Weight									
Study Day									
0	190.0 ± 3.8	186.5 ± 4.0	188.0 ± 4.9	193.5 ± 4.7	193.5 ± 4.6	190.1 ± 2.8	186.9 ± 1.9	ND	ND
5	197.3 ± 4.0	188.6 ± 5.2	193.5 ± 5.4	196.6 ± 3.0	192.5 ± 5.8	189.5 ± 2.7	193.0 ± 2.6	ND	ND
Body Weight Gain									
Study Day Interval									
0–5	7.3 ± 0.9	2.1 ± 1.9	5.5 ± 0.7	3.1 ± 2.0	−1.0 ± 4.1**	−0.6 ± 1.5*	6.1 ± 1.5	ND	ND
Mice									
n	10	5	5	5	5	5	NA	NA	NA
Body Weight									
Study Day									
0	18.3 ± 0.4	18.0 ± 0.3	18.5 ± 0.5	17.9 ± 0.4	18.4 ± 0.3	18.5 ± 0.4	NA	ND	ND
5	18.4 ± 0.4	18.4 ± 0.3	18.7 ± 0.5	18.5 ± 0.3	19.0 ± 0.3	19.3 ± 0.6	NA	ND	ND
Body Weight Gain									
Study Day Interval									
0–5	0.1 ± 0.1**	0.4 ± 0.1	0.2 ± 0.4	0.6 ± 0.3	0.7 ± 0.1*	0.8 ± 0.2*	NA	NVM	NVM

Statistical significance for an exposed group indicates a significant pairwise test compared to the 0 ppm group. Statistical significance for the 0 ppm group indicates a significant trend test.
*Statistically significant at $p \leq 0.05$; **$p \leq 0.01$.
BMD_{1Std} = benchmark dose corresponding to a benchmark response set to 1 standard deviation from the mean; BMD_{L1Std} = benchmark dose lower confidence limit corresponding to a benchmark response set to 1 standard deviation from the mean; NA = not applicable; ND = not determined; NVM = nonviable model.
[a]Data are displayed as mean ± standard error of the mean; body weight data are presented in grams.
[b]Statistical analysis performed by the Jonckheere (trend) and Williams or Dunnett (pairwise) tests

Table 3. Summary of Select Organ Weights of Female Rats and Mice Exposed to 1,4-Dichlorobenzene for Five Days

Endpoint[a,b,c]	0 ppm	1 ppm	10 ppm	50 ppm	150 ppm	400 ppm	800 ppm	BMD_{1Std} (ppm)	BMD_{L1Std} (ppm)
Rats									
n	10	5	5	5	5	5	5	NA	NA
Terminal Body Wt. (g)	197.3 ± 4.0	188.6 ± 5.2	193.5 ± 5.4	196.6 ± 3.0	192.5 ± 5.8	189.5 ± 2.7	193.0 ± 2.6	ND	ND
Left Kidney									
Absolute (g)	0.62 ± 0.01**	0.62 ± 0.02	0.62 ± 0.02	0.62 ± 0.01	0.63 ± 0.02	0.67 ± 0.00*	0.68 ± 0.03*	259.8	93.3
Relative (mg/g)[d]	3.14 ± 0.06**	3.29 ± 0.08	3.20 ± 0.09	3.15 ± 0.05	3.27 ± 0.11	3.53 ± 0.05**	3.52 ± 0.15**	219.2	89.4
Right Kidney									
Relative (mg/g)	3.22 ± 0.06*	3.39 ± 0.08	3.35 ± 0.07	3.23 ± 0.06	3.38 ± 0.13	3.62 ± 0.09**	3.47 ± 0.13	NVM	NVM
Liver									
Absolute (g)	7.40 ± 0.18**	7.29 ± 0.33	7.25 ± 0.25	7.73 ± 0.13	7.43 ± 0.29	8.68 ± 0.27**	11.50 ± 0.40**	245.5	163.4
Relative (mg/g)	37.51 ± 0.75**	38.60 ± 0.90	37.46 ± 0.77	39.38 ± 0.97	38.54 ± 0.60	45.81 ± 1.42**	59.64 ± 2.21**	191.4	127.6
Mice									
n	10	5	5	5	5	5	NA	NA	NA
Terminal Body Wt. (g)	18.4 ± 0.4	18.4 ± 0.3	18.7 ± 0.5	18.5 ± 0.3	19.0 ± 0.3	19.3 ± 0.6	NA	ND	ND
Liver									
Absolute (g)	0.87 ± 0.02**	0.92 ± 0.03	0.88 ± 0.04	0.92 ± 0.04	1.08 ± 0.03**	1.65 ± 0.04**	NA	83.7	59.2
Relative (mg/g)	47.44 ± 0.80**	49.78 ± 1.57	47.02 ± 1.17	49.55 ± 2.32	56.92 ± 0.88**	85.72 ± 1.11**	NA	70.2	47.4

Statistical significance for an exposed group indicates a significant pairwise test compared to the 0 ppm group. Statistical significance for the 0 ppm group indicates a significant trend test.

*Statistically significant at $p \leq 0.05$; **$p \leq 0.01$.

BMD_{1Std} = benchmark dose corresponding to a benchmark response set to 1 standard deviation from the mean; BMD_{L1Std} = benchmark dose lower confidence limit corresponding to a benchmark response set to 1 standard deviation from the mean; NA = not applicable; ND = not determined; NVM = nonviable model.

[a]Descriptions of organ weight endpoints and changes are provided in Appendix F.

[b]Data are displayed as mean ± standard error of the mean.

[c]Statistical analysis performed by the Jonckheere (trend) and Williams or Dunnett (pairwise) tests.

[d]Relative organ weights (organ weight-to-body weight ratios) are given as mg organ weight/g body weight.

Clinical Pathology

Rats

At study termination, the reticulocyte count had a positive trend with a significant increase at 800 ppm; the BMD (BMD_L) was 437.0 (307.0) ppm (Table 4). Sorbitol dehydrogenase (SDH) activity and triglyceride concentration had positive trends with significant increases in the 800 ppm group (Table 5). The BMD (BMD_L) for increased triglycerides was 489.4 (332.3) ppm, whereas a BMD (BMD_L) for SDH was not determined because no viable model was available. Cholesterol concentration had a positive trend with significant increases in the 400 and 800 ppm groups; the BMD (BMD_L) was 259.4 (126.2) ppm.

Mice

Because of serum volume limitations (i.e., quantity not sufficient), some pairwise statistical comparisons across different exposure groups and involving different parameters (Appendix G) were underpowered and may not accurately reflect the existence of "no effect."

The albumin/globulin (A/G) ratio had a negative trend with a significant decrease in the 400 ppm group (Table 5); the decrease was driven by a (nonsignificant) increase in globulin concentration (Appendix G). The BMD (BMD_L) for decreased A/G ratio was 15.1 (2.2) ppm. Cholesterol concentration had a positive trend with significant increases in the 150 and 400 ppm groups; the BMD (BMD_L) was 71.0 (43.1) ppm.

Table 4. Summary of Select Hematology Data for Female Rats Exposed to 1,4-Dichlorobenzene for Five Days

Endpoint[a,b]	0 ppm	1 ppm	10 ppm	50 ppm	150 ppm	400 ppm	800 ppm	BMD_{1Std} (ppm)	BMD_{L1Std} (ppm)
n	10	5	5	5	5	5	5	NA	NA
Reticulocytes (10^6/μL)	0.2350 ± 0.0071**	0.2148 ± 0.0098	0.2385 ± 0.0093	0.2546 ± 0.0081	0.2214 ± 0.0166	0.2436 ± 0.0112	0.3177 ± 0.0137**	437.0	307.0

Statistical significance for an exposed group indicates a significant pairwise test compared to the 0 ppm group. Statistical significance for the 0 ppm group indicates a significant trend test.

**Statistically significant at $p \leq 0.01$.

BMD_{1Std} = benchmark dose corresponding to a benchmark response set to 1 standard deviation from the mean; BMD_{L1Std} = benchmark dose lower confidence limit corresponding to a benchmark response set to 1 standard deviation from the mean; NA = not applicable.

[a]Data are displayed as mean ± standard error of the mean.

[b]Statistical analysis performed by the Jonckheere (trend) and Shirley or Dunn (pairwise) tests.

Table 5. Summary of Select Clinical Chemistry Data for Female Rats and Mice Exposed to 1,4-Dichlorobenzene for Five Days

Endpoint[a,b,c]	0 ppm	1 ppm	10 ppm	50 ppm	150 ppm	400 ppm	800 ppm	BMD_{1Std} (ppm)	BMD_{L1Std} (ppm)
Rats									
Sorbitol Dehydrogenase (IU/L)	10.2 ± 0.6* (10)	13.1 ± 3.1 (5)	9.7 ± 0.6 (5)	9.4 ± 1.3 (5)	10.6 ± 2.6 (5)	40.4 ± 23.7 (5)	23.6 ± 1.5* (5)	NVM	NVM
Triglycerides (mg/dL)	54.9 ± 3.6** (10)	75.6 ± 5.2 (5)	69.0 ± 7.1 (5)	73.6 ± 9.4 (5)	62.2 ± 8.1 (5)	70.0 ± 6.4 (5)	112.8 ± 10.4** (5)	489.4	332.3
Cholesterol (mg/dL)	91.7 ± 4.2** (10)	92.4 ± 2.2 (5)	96.0 ± 6.5 (5)	99.0 ± 8.1 (5)	105.2 ± 4.3 (5)	111.0 ± 4.6* (5)	143.2 ± 5.3** (5)	259.4	126.2
Mice									
A/G Ratio	2.94 ± 0.11** (3)	2.86 (1)	2.78 ± 0.03 (2)	–[d]	2.59 (1)	2.26 ± 0.02* (2)	NA	15.1	2.2
Cholesterol (mg/dL)	124.3 ± 3.6** (8)	113.7 ± 5.2 (3)	117.7 ± 2.7 (3)	126.5 ± 9.0 (4)	159.3 ± 4.4* (4)	269.3 ± 15.1* (3)	NA	71.0	43.1

Statistical significance for an exposed group indicates a significant pairwise test compared to the 0 ppm group. Statistical significance for the 0 ppm group indicates a significant trend test.
*Statistically significant at $p \leq 0.05$; **$p \leq 0.01$.
BMD_{1Std} = benchmark dose corresponding to a benchmark response set to 1 standard deviation from the mean; BMD_{L1Std} = benchmark dose lower confidence limit corresponding to a benchmark response set to 1 standard deviation from the mean; NA = not applicable; NVM = nonviable model; A/G ratio = albumin/globulin ratio.
[a]Data are displayed as mean ± standard error of the mean (number of animals).
[b]Statistical analysis performed by the Jonckheere (trend) and Shirley or Dunn (pairwise) tests. Data with sample size of one were included in the trend test but excluded from the pairwise test.
[c]Clinical chemistry data not reported were removed as outliers or were due to preanalytical or analytical conditions or errors, including but not limited to below linearity, short sample, quantity not sufficient, or extreme hemolysis.
[d]No data were available due to insufficient volume available for analysis.

Apical Endpoint Benchmark Dose Summary

A summary of the calculated BMDs for each toxicological endpoint, by species, is provided in Table 6. The endpoint-specific lowest-observed-effect level (LOEL) and no-observed-effect level (NOEL) are included and could be informative for endpoints that lack a calculated BMD either because no viable model was available or because the estimated BMD was below the lower limit of extrapolation (<0.333 ppm).

Table 6. BMD, BMD_L, LOEL, and NOEL Summary for Apical Endpoints, Sorted by BMD or LOEL from Low to High for Female Rats and Mice Exposed to 1,4-Dichlorobenzene for Five Days

Endpoint	BMD_{1Std} (ppm)	BMD_{L1Std} (ppm)	LOEL (ppm)[a]	NOEL (ppm)	Direction of Change
Rats					
Relative Liver Weight	191.4	127.6	400	150	UP
Relative Left Kidney Weight	219.2	89.4	400	150	UP
Absolute Liver Weight	245.5	163.4	400	150	UP
Cholesterol	259.4	126.2	400	150	UP
Absolute Left Kidney Weight	259.8	93.3	400	150	UP
Reticulocytes	437.0	307.0	800	400	UP
Triglycerides	489.4	332.3	800	400	UP
Relative Right Kidney Weight	NVM	NVM	**400**	150	UP
Sorbitol Dehydrogenase	NVM	NVM	**800**	400	UP
Mice					
A/G Ratio	15.1	2.2	400	150	DOWN
Relative Liver Weight	70.2	47.4	150	50	UP
Cholesterol	71.0	43.1	150	50	UP
Absolute Liver Weight	83.7	59.2	150	50	UP
Body Weight Gain	NVM	NVM	**150**	50	UP

BMD = benchmark dose; BMD_L = benchmark dose lower confidence limit; LOEL = lowest-observed-effect level; NOEL = no-observed-effect level; BMD_{1Std} = benchmark dose corresponding to a benchmark response set to 1 standard deviation from the mean; BMD_{L1Std} = benchmark dose lower confidence limit corresponding to a benchmark response set to 1 standard deviation from the mean; NVM = no viable model; A/G ratio = albumin/globulin ratio.
[a]Values in bold text indicate the LOEL of endpoints for which a BMD could not be calculated.

Gene Set Benchmark Dose Analysis

Chemical-induced alterations in heart, kidney, liver, lung, and ovary gene transcript expression were examined to determine those gene sets most sensitive to 1,4-DCB exposure. To that end, BMD analysis of transcripts and gene sets (Gene Ontology [GO] biological process) was conducted to determine the potency of the chemical to elicit gene expression changes in the heart, kidney, liver, lung, and ovary. This analysis used transcript-level BMD data to assess an aggregate score of gene set potency (5th percentile of transcript BMDs) and enrichment.

The "active" gene sets with the lowest 5th percentile BMD values are shown in the heart (Table 7), kidney (Table 8), liver (Table 9), lung (Table 10), and ovary (Table 11), with a summary of the top gene set per tissue based on lowest BMD 5th percentile provided in

Table 12. No gene sets had estimated 5th percentile BMD values <0.333 ppm. The gene sets shown in Table 7 to Table 11 should be interpreted with caution from the standpoint of the underlying biological mechanism and any relationship to toxicity or toxic agents referenced in the GO term definitions. The data primarily should be considered as a metric of potency for chemical-induced transcriptional changes (i.e., a concerted biological change) that could serve as a surrogate of estimated biological potency and, by extension, toxicological potency when more definitive toxicological data are unavailable.

Heart

Rats

The most sensitive GO biological processes for which a BMD value could be reliably calculated were cell cycle phase transition (GO:0044770) and mitotic cell cycle phase transition (GO:0044772), both with a 5th percentile BMD (BMD_L) of 141.4 (55.9) ppm (Table 7).

Mice

The most sensitive GO biological processes for which a BMD value could be reliably calculated were organic hydroxy compound biosynthetic process (GO:1901617) and circadian rhythm (GO:0007623) with 5th percentile BMDs (BMD_{LS}) of 91.0 (25.1) and 139.5 (37.4) ppm, respectively (Table 7). The full list of affected gene sets in the heart of female rats and mice can be found in Appendix G.

Kidney

Rats

The most sensitive GO biological processes for which a BMD value could be reliably calculated were cell cycle phase transition (GO:0044770) and mitotic cell cycle phase transition (GO:0044772), both with a 5th percentile BMD (BMD_L) of 121.0 (42.2) ppm (Table 8).

Mice

The most sensitive GO biological processes for which a BMD value could be reliably calculated were circadian rhythm (GO:0007623) and organic hydroxy compound transport (GO:0015850) with 5th percentile BMDs (BMD_{LS}) of 16.9 (2.0) and 17.6 (3.9) ppm, respectively (Table 8). The full list of affected gene sets in the kidney of female rats and mice can be found in Appendix G.

Liver

Rats

The most sensitive GO biological processes for which a BMD value could be reliably calculated were xenobiotic metabolic process (GO:0006805), long-chain fatty acid metabolic process (GO:0001676), icosanoid metabolic process (GO:0006690), and unsaturated fatty acid metabolic process (GO:0033559) with 5th percentile BMDs (BMD_{LS}) of 87.6 (59.6), 92.8 (52.7), 92.8 (52.7), and 92.8 (52.7) ppm, respectively (Table 9).

Mice

The most sensitive GO biological processes for which a BMD value could be reliably calculated were regulation of chromosome segregation (GO:0051983), positive regulation of cell cycle

phase transition (GO:1901989), and positive regulation of mitotic cell cycle phase transition (GO:1901992), all three with a 5th percentile BMD (BMD_L) of 6.3 (0.9) ppm (Table 9). The full list of affected gene sets in the liver of female rats and mice can be found in Appendix G.

Lung

Rats

The most sensitive GO biological processes for which a BMD value could be reliably calculated were chromosome segregation (GO:0007059) and nonmembrane-bounded organelle assembly (GO:0140694) with 5th percentile BMDs (BMD_{LS}) of 208.6 (55.4) and 236.8 (65.6) ppm, respectively (Table 10).

Mice

The most sensitive GO biological processes for which a BMD value could be reliably calculated were DNA replication (GO:0006260) and xenobiotic metabolic process (GO:0006805) with 5th percentile BMDs (BMD_{LS}) of 1.4 (0.5) and 2.9 (0.4) ppm, respectively (Table 10). The full list of affected gene sets in the lung of female rats and mice can be found in Appendix G.

Ovary

Rats

The most sensitive GO biological processes for which a BMD value could be reliably calculated were ameboidal-type cell migration (GO:0001667) and positive regulation of apoptotic signaling pathway (GO:2001235) with 5th percentile BMDs (BMD_{LS}) of 223.1 (90.9) and 282.7 (140.2) ppm, respectively (Table 11). The full list of affected gene sets in the ovary of female rats can be found in Appendix G.

Mice

In mice exposed to 1,4-DCB, there were no active GO terms (i.e., no gene expression response at the gene set level).

Table 7. Top 10 Heart Gene Ontology Biological Process Gene Sets Ranked by Potency of Perturbation, Sorted by 5th Percentile Benchmark Dose, for Female Rats and Mice Exposed to 1,4-Dichlorobenzene for Five Days

Category Name[a,b]	Input Genes/Platform Genes in Gene Set (% Coverage)	BMD_{rd25} 5th Percentile of Gene Set Transcripts (BMD_{Lrd25}–BMD_{Urd25}) (ppm)[c]	Genes with Changed Direction Up/Down
Rats			
GO:0044770 cell cycle phase transition	5/58 (8.6%)	141.4 (55.9–292.9)	0/5
GO:0044772 mitotic cell cycle phase transition	5/52 (9.6%)	141.4 (55.9–292.9)	0/5
GO:0051301 cell division	6/84 (7.1%)	181.5 (65.8–517.4)	0/6
GO:0007049 cell cycle	4/45 (8.9%)	192.5 (68.7–382.0)	0/4
GO:0000226 microtubule cytoskeleton organization	4/80 (5.0%)	197.5 (80.5–710.7)	0/4
GO:0007059 chromosome segregation	4/41 (9.8%)	202.9 (85.1–551.4)	0/4
GO:1903047 mitotic cell cycle process	11/149 (7.4%)	242.4 (96.3–435.9)	0/11
GO:0022402 cell cycle process	12/194 (6.2%)	282.0 (108.6–1,328.0)	0/12
GO:0019730 antimicrobial humoral response	5/43 (11.6%)	333.8 (156.8–476.7)	2/3
GO:0006959 humoral immune response	5/80 (6.3%)	347.4 (174.4–695.6)	2/3
Mice			
GO:1901617 organic hydroxy compound biosynthetic process	3/52 (5.8%)	91.0 (25.1–495.5)	3/0
GO:0007623 circadian rhythm	3/49 (6.1%)	139.5 (37.4–273.5)	2/1
GO:0030595 leukocyte chemotaxis	3/49 (6.1%)	178.4 (91.9–411.5)	3/0
GO:0097529 myeloid leukocyte migration	3/51 (5.9%)	178.4 (91.9–411.5)	3/0

BMD_{rd25} = benchmark dose corresponding to a benchmark response set to a 25% change in the median response; BMD_{Lrd25} = benchmark dose lower confidence limit corresponding to a benchmark response set to a 25% change in the median response; BMD_{Urd25} = benchmark dose upper confidence limit corresponding to a benchmark response set to a 25% change in the median response; GO = Gene Ontology.

[a]Active genes and GO biological process definitions are available in Appendix E and in the Chemical Effects in Biological Systems (CEBS) data repository: https://doi.org/10.22427/NTP-DATA-002-00600-0002-000-0.

[b]Only four heart GO biological process gene sets were active in mice.

[c]5th percentile = the value below which 5% of transcript benchmark dose values fall.

Table 8. Top 10 Kidney Gene Ontology Biological Process Gene Sets Ranked by Potency of Perturbation, Sorted by 5th Percentile Benchmark Dose, for Female Rats and Mice Exposed to 1,4-Dichlorobenzene for Five Days

Category Name[a]	Input Genes/Platform Genes in Gene Set (% Coverage)	BMD_{rd25} 5th Percentile of Gene Set Transcripts (BMD_{Lrd25}–BMD_{Urd25}) (ppm)[b]	Genes with Changed Direction Up/Down
Rats			
GO:0044770 cell cycle phase transition	4/58 (6.9%)	121.0 (42.2–652.8)	1/3
GO:0044772 mitotic cell cycle phase transition	4/52 (7.7%)	121.0 (42.2–652.8)	1/3
GO:0001822 kidney development	6/57 (10.5%)	197.7 (91.7–305.6)	5/1
GO:0019218 regulation of steroid metabolic process	5/49 (10.2%)	224.1 (73.8–NC)	4/1
GO:0030324 lung development	4/45 (8.9%)	224.1 (73.8–NC)	3/1
GO:0006694 steroid biosynthetic process	6/54 (11.1%)	225.9 (89.2–NC)	4/2
GO:0008203 cholesterol metabolic process	5/54 (9.3%)	225.9 (89.2–NC)	3/2
GO:0016125 sterol metabolic process	5/56 (8.9%)	225.9 (89.2–NC)	3/2
GO:0046165 alcohol biosynthetic process	6/42 (14.3%)	225.9 (89.2–NC)	5/1
GO:0001676 long-chain fatty acid metabolic process	5/55 (9.1%)	226.7 (96.8–365.3)	5/0
Mice			
GO:0007623 circadian rhythm	5/49 (10.2%)	16.9 (2.0–793.4)	3/2
GO:0015850 organic hydroxy compound transport	4/58 (6.9%)	17.6 (3.9–778.1)	3/1
GO:0006869 lipid transport	5/77 (6.5%)	22.5 (5.6–84.1)	4/1
GO:0010565 regulation of cellular ketone metabolic process	3/56 (5.4%)	107.2 (74.6–880.6)	3/0
GO:0006805 xenobiotic metabolic process	6/56 (10.7%)	108.3 (48.2–389.5)	6/0
GO:0015718 monocarboxylic acid transport	3/52 (5.8%)	112.1 (76.4–186.6)	2/1
GO:0048511 rhythmic process	6/89 (6.7%)	129.9 (83.8–241.2)	4/2
GO:0033559 unsaturated fatty acid metabolic process	5/40 (12.5%)	136.9 (55.1–282.5)	5/0
GO:0006631 fatty acid metabolic process	8/117 (6.8%)	139.4 (60.5–491.7)	8/0
GO:0006690 icosanoid metabolic process	5/43 (11.6%)	139.4 (60.5–491.7)	5/0

BMD_{rd25} = benchmark dose corresponding to a benchmark response set to a 25% change in the median response; BMD_{Lrd25} = benchmark dose lower confidence limit corresponding to a benchmark response set to a 25% change in the median response; BMD_{Urd25} = benchmark dose upper confidence limit corresponding to a benchmark response set to a 25% change in the median response; GO = Gene Ontology; NC = nonconvergent.

[a]Active genes and GO biological process definitions are available in Appendix E and in the Chemical Effects in Biological Systems (CEBS) data repository: https://doi.org/10.22427/NTP-DATA-002-00600-0002-000-0.

[b]5th percentile = the value below which 5% of transcript benchmark dose values fall.

Table 9. Top 10 Liver Gene Ontology Biological Process Gene Sets Ranked by Potency of Perturbation, Sorted by 5th Percentile Benchmark Dose, for Female Rats and Mice Exposed to 1,4-Dichlorobenzene for Five Days

Category Name[a]	Input Genes/Platform Genes in Gene Set (% Coverage)	BMD_{rd25} 5th Percentile of Gene Set Transcripts (BMD_{Lrd25}–BMD_{Urd25}) (ppm)[b]	Genes with Changed Direction Up/Down
Rats			
GO:0006805 xenobiotic metabolic process	20/59 (33.9%)	87.6 (59.6–136.7)	18/2
GO:0001676 long-chain fatty acid metabolic process	16/55 (29.1%)	92.8 (52.7–142.7)	15/1
GO:0006690 icosanoid metabolic process	14/50 (28.0%)	92.8 (52.7–142.7)	13/1
GO:0033559 unsaturated fatty acid metabolic process	16/54 (29.6%)	92.8 (52.7–142.7)	15/1
GO:0120254 olefinic compound metabolic process	15/64 (23.4%)	116.4 (63.4–152.0)	13/2
GO:0006720 isoprenoid metabolic process	17/41 (41.5%)	143.6 (107.8–165.0)	15/2
GO:0071384 cellular response to corticosteroid stimulus	9/55 (16.4%)	153.0 (59.6–271.9)	6/3
GO:0071385 cellular response to glucocorticoid stimulus	8/52 (15.4%)	153.0 (59.6–271.9)	5/3
GO:0098754 detoxification	16/58 (27.6%)	153.4 (98.2–219.2)	16/0
GO:0071383 cellular response to steroid hormone stimulus	10/62 (16.1%)	158.6 (44.1–339.0)	6/4
Mice			
GO:0051983 regulation of chromosome segregation	22/45 (48.9%)	6.3 (0.9–28.2)	19/3
GO:1901989 positive regulation of cell cycle phase transition	19/53 (35.9%)	6.3 (0.9–28.2)	15/4
GO:1901992 positive regulation of mitotic cell cycle phase transition	17/43 (39.5%)	6.3 (0.9–28.2)	13/4
GO:0007051 spindle organization	15/40 (37.5%)	6.9 (1.1–32.3)	15/0
GO:0045931 positive regulation of mitotic cell cycle	19/60 (31.7%)	6.9 (1.1–32.3)	13/6
GO:0007088 regulation of mitotic nuclear division	18/47 (38.3%)	7.7 (1.1–39.5)	15/3
GO:0033044 regulation of chromosome organization	27/69 (39.1%)	7.7 (1.1–39.5)	20/7
GO:0044770 cell cycle phase transition	28/63 (44.4%)	7.7 (1.1–39.5)	21/7
GO:0044772 mitotic cell cycle phase transition	22/55 (40.0%)	7.7 (1.1–39.5)	17/5
GO:0051783 regulation of nuclear division	19/52 (36.5%)	7.7 (1.1–39.5)	16/3

BMD_{rd25} = benchmark dose corresponding to a benchmark response set to a 25% change in the median response; BMD_{Lrd25} = benchmark dose lower confidence limit corresponding to a benchmark response set to a 25% change in the median response; BMD_{Urd25} = benchmark dose upper confidence limit corresponding to a benchmark response set to a 25% change in the median response; GO = Gene Ontology.

[a]Active genes and GO biological process definitions are available in Appendix E and in the Chemical Effects in Biological Systems (CEBS) data repository: https://doi.org/10.22427/NTP-DATA-002-00600-0002-000-0.

[b]5th percentile = the value below which 5% of transcript benchmark dose values fall.

Table 10. Top 10 Lung Gene Ontology Biological Process Gene Sets Ranked by Potency of Perturbation, Sorted by 5th Percentile Benchmark Dose for Female Rats and Mice Exposed to 1,4-Dichlorobenzene for Five Days

Category Name[a]	Input Genes/Platform Genes in Gene Set (% Coverage)	BMD_{rd25} 5th Percentile of Gene Set Transcripts (BMD_{Lrd25}–BMD_{Urd25}) (ppm)[b]	Genes with Changed Direction Up/Down
Rats			
GO:0007059 chromosome segregation	9/41 (22.0%)	208.6 (55.4–1,082.9)	0/9
GO:0140694 nonmembrane-bounded organelle assembly	6/59 (10.2%)	236.8 (65.6–NC)	0/6
GO:0007049 cell cycle	6/45 (13.3%)	247.7 (69.6–NC)	0/6
GO:0048568 embryonic organ development	5/47 (10.6%)	264.4 (73.4–2,060.4)	3/2
GO:0045931 positive regulation of mitotic cell cycle	3/51 (5.9%)	288.7 (135.6–NC)	0/3
GO:1901989 positive regulation of cell cycle phase transition	3/43 (7.0%)	288.7 (135.6–NC)	0/3
GO:1901990 regulation of mitotic cell cycle phase transition	7/94 (7.5%)	288.7 (135.6–NC)	1/6
GO:0051301 cell division	8/84 (9.5%)	289.6 (102.8–NC)	0/8
GO:1901987 regulation of cell cycle phase transition	11/116 (9.5%)	293.1 (122.5–NC)	1/10
GO:0050728 negative regulation of inflammatory response	5/51 (9.8%)	293.3 (143.2–448.6)	2/3
Mice			
GO:0006260 DNA replication	3/43 (7.0%)	1.4 (0.5–1,130.8)	3/0
GO:0006805 xenobiotic metabolic process	5/56 (8.9%)	2.9 (0.4–54.2)	4/1
GO:0000209 protein polyubiquitination	3/42 (7.1%)	3.8 (0.8–14.9)	3/0
GO:0016567 protein ubiquitination	4/68 (5.9%)	3.8 (0.8–14.9)	4/0
GO:0032446 protein modification by small protein conjugation	4/79 (5.1%)	3.8 (0.8–14.9)	4/0
GO:0006575 cellular modified amino acid metabolic process	5/59 (8.5%)	14.1 (2.1–56.6)	5/0
GO:0048545 response to steroid hormone	3/52 (5.8%)	68.8 (9.1–117.4)	2/1
GO:0008203 cholesterol metabolic process	3/48 (6.3%)	75.4 (33.3–148.1)	2/1
GO:0016125 sterol metabolic process	3/49 (6.1%)	75.4 (33.3–148.1)	2/1
GO:1902652 secondary alcohol metabolic process	3/53 (5.7%)	75.4 (33.3–148.1)	2/1

BMD_{rd25} = benchmark dose corresponding to a benchmark response set to a 25% change in the median response; BMD_{Lrd25} = benchmark dose lower confidence limit corresponding to a benchmark response set to a 25% change in the median response; BMD_{Urd25} = benchmark dose upper confidence limit corresponding to a benchmark response set to a 25% change in the median response; GO = Gene Ontology; NC = nonconvergent.

[a]Active genes and GO biological process definitions are available in Appendix E and in the Chemical Effects in Biological Systems (CEBS) data repository: https://doi.org/10.22427/NTP-DATA-002-00600-0002-000-0.

[b]5th percentile = the value below which 5% of transcript benchmark dose values fall.

Table 11. Top 10 Ovary Gene Ontology Biological Process Gene Sets Ranked by Potency of Perturbation, Sorted by 5th Percentile Benchmark Dose, for Female Rats Exposed to 1,4-Dichlorobenzene for Five Days

Category Name[a]	Input Genes/Platform Genes in Gene Set (% Coverage)	BMD_{rd25} 5th Percentile of Gene Set Transcripts (BMD_{Lrd25}–BMD_{Urd25}) (ppm)[b]	Genes with Changed Direction Up/Down
GO:0001667 ameboidal-type cell migration	5/55 (9.1%)	223.1 (90.9–432.8)	4/1
GO:2001235 positive regulation of apoptotic signaling pathway	6/58 (10.3%)	282.7 (140.2–432.6)	3/3
GO:0061041 regulation of wound healing	5/59 (8.5%)	309.9 (178.5–463.5)	3/2
GO:0048639 positive regulation of developmental growth	5/50 (10.0%)	332.8 (176.6–485.1)	3/2
GO:0030307 positive regulation of cell growth	3/47 (6.4%)	335.6 (203.0–460.4)	2/1
GO:0015850 organic hydroxy compound transport	5/60 (8.3%)	347.9 (198.4–485.0)	0/5
GO:0002526 acute inflammatory response	3/43 (7.0%)	354.0 (206.0–481.4)	3/0
GO:2001242 regulation of intrinsic apoptotic signaling pathway	6/75 (8.0%)	366.2 (144.6–NC)	4/2
GO:0051385 response to mineralocorticoid	3/45 (6.7%)	382.1 (233.3–525.2)	1/2
GO:1903034 regulation of response to wounding	5/69 (7.3%)	383.0 (243.8–527.7)	3/2

BMD_{rd25} = benchmark dose corresponding to a benchmark response set to a 25% change in the median response; BMD_{Lrd25} = benchmark dose lower confidence limit corresponding to a benchmark response set to a 25% change in the median response; BMD_{Urd25} = benchmark dose upper confidence limit corresponding to a benchmark response set to a 25% change in the median response; GO = Gene Ontology; NC = nonconvergent.

[a]Active genes and GO biological process definitions are available in Appendix E and in the Chemical Effects in Biological Systems (CEBS) data repository: https://doi.org/10.22427/NTP-DATA-002-00600-0002-000-0.

[b]5th percentile = the value below which 5% of transcript benchmark dose values fall.

Gene Set Benchmark Dose Summary

A summary of the most potent gene set per tissue is provided in Table 12. In rats exposed to 1,4-DCB, the liver had the gene set with the lowest BMD 5th percentile value, corresponding to xenobiotic metabolic process (GO:0006805) with a BMD (BMD_L) of 87.6 (59.6) ppm. In mice, the lung had the gene set with the lowest BMD 5th percentile value, corresponding to DNA replication (GO:0006260) with a BMD (BMD_L) of 1.4 (0.5) ppm.

Table 12. Most Potent Gene Ontology Biological Process Gene Set per Tissue, Sorted by 5th Percentile Benchmark Dose, for Female Rats and Mice Exposed to 1,4-Dichlorobenzene for Five Days

Tissue	Category Name[a]	Input Genes/Platform Genes in Gene Set (% Coverage)	BMD_{rd25} 5th Percentile of Gene Set Transcripts (BMD_{Lrd25}–BMD_{Urd25}) (ppm)[b]	Genes with Changed Direction Up/Down
Rats				
Liver	**GO:0006805** xenobiotic metabolic process	20/59 (33.9%)	87.6[c] (59.6–136.7)	18/2
Kidney	**GO:0044770** cell cycle phase transition	4/58 (6.9%)	121.0 (42.2–652.8)	1/3
Heart	**GO:0044770** cell cycle phase transition	5/58 (8.6%)	141.4 (55.9–292.9)	0/5
Lung	**GO:0007059** chromosome segregation	9/41 (22.0%)	208.6 (55.4–1,082.9)	0/9
Ovary	**GO:0001667** ameboidal-type cell migration	5/55 (9.1%)	223.1 (90.9–432.8)	4/1
Mice				
Lung	**GO:0006260** DNA replication	3/43 (7.0%)	1.4[c] (0.5–1,130.8)	3/0
Liver	**GO:0051983** regulation of chromosome segregation	22/45 (48.9%)	6.3 (0.9–28.2)	19/3
Kidney	**GO:0007623** circadian rhythm	5/49 (10.2%)	16.9 (2.0–793.4)	3/2
Heart	**GO:1901617** organic hydroxy compound biosynthetic process	3/52 (5.8%)	91.0 (25.1–495.5)	3/0

BMD_{rd25} = benchmark dose corresponding to a benchmark response set to a 25% change in the median response; BMD_{Lrd25} = benchmark dose lower confidence limit corresponding to a benchmark response set to a 25% change in the median response; BMD_{Urd25} = benchmark dose upper confidence limit corresponding to a benchmark response set to a 25% change in the median response; GO = Gene Ontology.

[a]Active genes and GO biological process definitions are available in Appendix E and in the Chemical Effects in Biological Systems (CEBS) data repository: https://doi.org/10.22427/NTP-DATA-002-00600-0002-000-0.

[b]5th percentile = the value below which 5% of transcript benchmark dose values fall.

[c]Transcriptional point of departure determined based on the lowest Gene Ontology biological process BMD_{rd25} 5th percentile value.

Gene Benchmark Dose Analysis

The top 10 genes ranked by BMD potency are shown in the heart (Table 13), kidney (Table 14), liver (Table 15), lung (Table 16), and ovary (Table 17). No genes had estimated median BMD values <0.333 ppm with the exception of one lung gene in mice. As with the GO analysis, the biological or toxicological significance of the changes in gene expression shown in Table 13 to Table 17 should be interpreted with caution. The data primarily should be considered as a metric of potency for chemical-induced transcriptional changes that could serve as a conservative surrogate of estimated biological potency, and by extension toxicological potency, when more definitive toxicological data are unavailable.

Heart

Rats

The most sensitive upregulated genes with a calculated BMD were *Spp1* (secreted phosphoprotein 1) and *Dbp* (D-box binding PAR bZIP transcription factor) with BMDs (BMD_{LS}) of 108.2 (30.6) and 189.0 (183.6) ppm, respectively. The most sensitive genes exhibiting a decrease in expression were *Lck* (LCK proto-oncogene, Src family tyrosine kinase), *Ccnb2* (cyclin B2), *Ccnb2-ps2* (cyclin B2, pseudogene 2), *Ccna2* (cyclin A2), *Kif18b* (kinesin family member 18B), *Prc1* (protein regulator of cytokinesis 1), *Mki67* (marker of proliferation Ki-67), and *Rt1-da* (RT1 class II, locus Da) with BMDs (BMD_{LS}) of 31.7 (6.0), 124.3 (51.4), 124.3 (51.4), 158.4 (60.3), 165.4 (51.1), 173.4 (45.9), 176.8 (47.7), and 187.5 (72.3) ppm, respectively.

Mice

The most sensitive upregulated genes with a calculated BMD were *Krt18* (keratin 18), *S100a4* (S100 calcium-binding protein A4), *Star* (steroidogenic acute regulatory protein), *Ephx1* (epoxide hydrolase 1, microsomal), *Dbp* (D site albumin promoter binding protein), *Abcg1* (ATP-binding cassette subfamily G member 1), and *Bhlhe40* (basic helix-loop-helix family, member e40) with BMDs (BMD_{LS}) of 0.6 (0.1), 1.3 (0.1), 3.4 (0.5), 52.9 (13.9), 60.3 (18.1), 91.1 (34.2), and 93.4 (38.8) ppm, respectively. The most sensitive genes exhibiting a decrease in expression were *Lcn2* (lipocalin 2), *Ddit4* (DNA-damage-inducible transcript 4), and *Ifi44* (interferon-induced protein 44) with BMDs (BMD_{LS}) of 4.5 (0.6), 21.8 (4.0), and 95.0 (21.3) ppm, respectively.

Table 13. Top 10 Heart Genes Ranked by Potency of Perturbation, Sorted by Benchmark Dose Median, for Female Rats and Mice Exposed to 1,4-Dichlorobenzene for Five Days

Gene Symbol[a]	BMD_{rd25} (BMD_{Lrd25}–BMD_{Urd25}) in ppm	Maximum Fold Change	Direction of Expression Change
Rats			
Lck	31.7 (6.0–NC)	1.4	DOWN
Spp1	108.2 (30.6–345.5)	1.7	UP
Ccnb2	124.3 (51.4–277.6)	2.1	DOWN
Ccnb2-ps2	124.3 (51.4–277.6)	2.1	DOWN
Ccna2	158.4 (60.3–308.2)	2.1	DOWN
Kif18b	165.4 (51.1–324.1)	2.3	DOWN

Gene Symbol[a]	BMD_{rd25} (BMD_{Lrd25}–BMD_{Urd25}) in ppm	Maximum Fold Change	Direction of Expression Change
Prc1	173.4 (45.9–395.4)	2.0	DOWN
Mki67	176.8 (47.7–372.0)	1.9	DOWN
Rt1-da	187.5 (72.3–411.3)	1.6	DOWN
Dbp	189.0 (183.6–228.8)	6.9	UP
Mice			
Krt18	0.6 (0.1–128.8)	2.7	UP
S100a4	1.3 (0.1–150.1)	2.0	UP
Star	3.4 (0.5–66.1)	1.8	UP
Lcn2	4.5 (0.6–33.0)	1.7	DOWN
Ddit4	21.8 (4.0–82.2)	2.3	DOWN
Ephx1	52.9 (13.9–109.4)	1.9	UP
Dbp	60.3 (18.1–122.4)	4.7	UP
Abcg1	91.1 (34.2–176.0)	2.0	UP
Bhlhe40	93.4 (38.8–174.3)	1.8	UP
Ifi44	95.0 (21.3–431.5)	1.6	DOWN

BMD_{rd25} = benchmark dose corresponding to a benchmark response set to a 25% change in the median response; BMD_{Lrd25} = benchmark dose lower confidence limit corresponding to a benchmark response set to a 25% change in the median response; BMD_{Urd25} = benchmark dose upper confidence limit corresponding to a benchmark response set to a 25% change in the median response; NC = nonconvergent.
[a]Gene definitions are available in Appendix E and in the Chemical Effects in Biological Systems (CEBS) data repository: https://doi.org/10.22427/NTP-DATA-002-00600-0002-000-0.

Kidney

Rats

The most sensitive genes exhibiting an increase in expression were *Srebf1* (sterol regulatory element binding transcription factor 1), *Cyp4a2* (cytochrome P450, family 4, subfamily a, polypeptide 2), and *Cyp4a3* (cytochrome P450, family 4, subfamily a, polypeptide 3) with calculated BMD (BMD_{LS}) of 31.8 (7.8), 125.1 (49.5), and 137.6 (56.5) ppm, respectively. The most sensitive downregulated genes with a calculated BMD were *Ccnb2* (cyclin B2), *Ccnb2-ps2* (cyclin B2, pseudogene 2), *Kif22* (kinesin family member 22), *Mki67* (marker of proliferation Ki-67), *Cks2* (CDC28 protein kinase regulatory subunit 2), *Dhcr7* (7-dehydrocholesterol reductase), and *Mfap4* (microfibril associated protein 4) with BMDs (BMD_{LS}) of 77.8 (29.5), 77.8 (29.5), 139.6 (48.2), 150.4 (59.2), 164.3 (55.0), 190.4 (20.9), and 210.5 (55.7) ppm, respectively.

Mice

The most sensitive genes exhibiting an increase in expression were *Ces1g* (carboxylesterase 1G), *Acaa1b* (acetyl-Coenzyme A acyltransferase 1B), *Dbp* (D site albumin promoter binding protein), *Ces1d* (carboxylesterase 1D), *Hlf* (hepatic leukemia factor), and *Slc51a* (solute carrier family 51, alpha subunit) with calculated BMDs (BMD_{LS}) of 7.6 (2.2), 15.3 (3.2), 16.6 (1.9), 17.1 (2.1), 21.7 (5.7), and 26.9 (5.6) ppm, respectively. The most sensitive genes exhibiting a decrease in expression were *Chn1* (chimerin 1), *Nfil3* (nuclear factor, interleukin 3, regulated), *Abcc3* (ATP-binding cassette, sub-family C member 3), and *Rnf125* (ring finger protein 125)

with calculated BMDs (BMD_{LS}) of 5.4 (0.9), 15.4 (3.2), 18.0 (5.6), and 20.5 (3.2) ppm, respectively.

Table 14. Top 10 Kidney Genes Ranked by Potency of Perturbation, Sorted by Benchmark Dose Median, for Female Rats and Mice Exposed to 1,4-Dichlorobenzene for Five Days

Gene Symbol[a]	BMD_{rd25} (BMD_{Lrd25}–BMD_{Urd25}) in ppm	Maximum Fold Change	Direction of Expression Change
Rats			
Srebf1	31.8 (7.8–123.9)	1.6	UP
Ccnb2	77.8 (29.5–183.5)	1.8	DOWN
Ccnb2-ps2	77.8 (29.5–183.5)	1.8	DOWN
Cyp4a2	125.1 (49.5–193.2)	3.1	UP
Cyp4a3	137.6 (56.5–190.5)	2.9	UP
Kif22	139.6 (48.2–291.1)	1.8	DOWN
Mki67	150.4 (59.2–331.7)	1.7	DOWN
Cks2	164.3 (55.0–1,122.1)	1.6	DOWN
Dhcr7	190.4 (20.9–NC)	1.5	DOWN
Mfap4	210.5 (55.7–447.5)	1.9	DOWN
Mice			
Chn1	5.4 (0.9–213.8)	1.5	DOWN
Ces1g	7.6 (2.2–19.4)	1.7	UP
Acaa1b	15.3 (3.2–268.4)	1.5	UP
Nfil3	15.4 (3.2–75.5)	2.1	DOWN
Dbp	16.6 (1.9–100.5)	4.1	UP
Ces1d	17.1 (2.1–1,486.2)	1.5	UP
Abcc3	18.0 (5.6–70.0)	1.6	DOWN
Rnf125	20.5 (3.2–175.4)	1.6	DOWN
Hlf	21.7 (5.7–79.0)	1.7	UP
Slc51a	26.9 (5.6–98.2)	1.7	UP

BMD_{rd25} = benchmark dose corresponding to a benchmark response set to a 25% change in the median response; BMD_{Lrd25} = benchmark dose lower confidence limit corresponding to a benchmark response set to a 25% change in the median response; BMD_{Urd25} = benchmark dose upper confidence limit corresponding to a benchmark response set to a 25% change in the median response; NC = nonconvergent.
[a]Gene definitions are available in Appendix E and in the Chemical Effects in Biological Systems (CEBS) data repository: https://doi.org/10.22427/NTP-DATA-002-00600-0002-000-0.

Liver

Rats

The most sensitive genes exhibiting an increase in expression were *Cyp2b2* (cytochrome P450, family 2, subfamily b, polypeptide 2), *Cyp2b1* (cytochrome P450, family 2, subfamily b, polypeptide 1), *Abcc3* (ATP-binding cassette subfamily C member 3), *Ugt2b1* (UDP glucuronosyltransferase 2 family, polypeptide B1), *Ephx1* (epoxide hydrolase 1), *Cyp2c6* (cytochrome P450, family 2, subfamily C, polypeptide 6), *Loc100911718* (cytochrome P450 2C6-like), and *Aldh1a1* (aldehyde dehydrogenase 1 family, member A1) with calculated BMD (BMD_{LS}) of 48.4 (25.0), 69.9 (43.9), 103.8 (60.2), 105.4 (75.3), 115.8 (61.5), 117.1 (65.4), 117.1

(65.4), and 127.6 (110.1) ppm, respectively. The most sensitive downregulated genes with a calculated BMD were *Car3*/*Ca3* (carbonic anhydrase 3) and *Egr1* (early growth response 1) with BMDs (BMD_{L}s) of 117.8 (41.2) and 127.0 (30.5) ppm, respectively.

Mice

The most sensitive upregulated genes with a calculated BMD were *Cdc20* (cell division cycle 20), *Cdk1* (cyclin dependent kinase 1), *Mest* (mesoderm specific transcript), *Gstp2* (glutathione S-transferase, pi 2), *Ccnb1* (cyclin B1), *Cyp2a5* (cytochrome P450, family 2, subfamily a, polypeptide 5), *Cyp2c29* (cytochrome P450, family 2, subfamily c, polypeptide 29), *Ube2c* (ubiquitin-conjugating enzyme E2C), and *Gsta13* (glutathione S-transferase alpha 13) with BMDs (BMD_{L}s) of 5.6 (0.7), 5.6 (0.8), 5.9 (1.4), 6.6 (4.2), 6.9 (1.1), 8.3 (6.0), 8.4 (5.2), 8.5 (1.1), and 9.2 (4.0) ppm, respectively. One gene, *Cpsf4l* (cleavage and polyadenylation specific factor 4-like), was downregulated with a BMD (BMD_{L}) of 8.9 (1.9) ppm.

Table 15. Top 10 Liver Genes Ranked by Potency of Perturbation, Sorted by Benchmark Dose Median, for Female Rats and Mice Exposed to 1,4-Dichlorobenzene for Five Days

Gene Symbol[a]	BMD_{rd25} (BMD_{Lrd25}–BMD_{Urd25}) in ppm	Maximum Fold Change	Direction of Expression Change
Rats			
Cyp2b2	48.4 (25.0–78.3)	87.1	UP
Cyp2b1	69.9 (43.9–101.5)	195.0	UP
Abcc3	103.8 (60.2–157.7)	4.8	UP
Ugt2b1	105.4 (75.3–172.0)	5.5	UP
Ephx1	115.8 (61.5–183.9)	5.6	UP
Cyp2c6	117.1 (65.4–120.1)	3.7	UP
Loc100911718	117.1 (65.4–120.1)	3.7	UP
Car3/Ca3	117.8 (41.2–266.8)	2.3	DOWN
Egr1	127.0 (30.5–318.2)	2.5	DOWN
Aldh1a1	127.6 (110.1–130.6)	8.0	UP
Mice			
Cdc20	5.6 (0.7–28.7)	7.8	UP
Cdk1	5.6 (0.8–24.0)	5.3	UP
Mest	5.9 (1.4–49.6)	1.5	UP
Gstp2	6.6 (4.2–17.5)	3.6	UP
Ccnb1	6.9 (1.1–32.3)	4.4	UP
Cyp2a5	8.3 (6.0–29.6)	11.6	UP
Cyp2c29	8.4 (5.2–8.7)	6.2	UP
Ube2c	8.5 (1.1–46.7)	2.3	UP
Cpsf4l	8.9 (1.9–26.0)	2.2	DOWN
Gsta13	9.2 (4.0–16.5)	209.7	UP

BMD_{rd25} = benchmark dose corresponding to a benchmark response set to a 25% change in the median response; BMD_{Lrd25} = benchmark dose lower confidence limit corresponding to a benchmark response set to a 25% change in the median response; BMD_{Urd25} = benchmark dose upper confidence limit corresponding to a benchmark response set to a 25% change in the median response.

[a]Gene definitions are available in Appendix E and in the Chemical Effects in Biological Systems (CEBS) data repository: https://doi.org/10.22427/NTP-DATA-002-00600-0002-000-0.

Lung

Rats

The most sensitive genes exhibiting an increase in expression were *Junb* (JunB proto-oncogene, AP-1 transcription factor subunit), *Meg3* (maternally expressed 3), *Ier3* (immediate early response 3), and *Ccl12* (C-C motif chemokine ligand 12) with calculated BMD (BMD_{LS}) of 121.9 (39.9), 146.1 (40.1), 182.4 (51.2), and 217.6 (62.0) ppm, respectively. The most sensitive downregulated genes with a calculated BMD were *Ddit4* (DNA-damage-inducible transcript 4), *Cebpd* (CCAAT/enhancer binding protein delta), *Slc6a8* (solute carrier family 6 member 8), *Cenpf* (centromere protein F), *Cenpw* (centromere protein W), and *Papss2* (3'-phosphoadenosine 5'-phosphosulfate synthase 2) with BMDs (BMD_{LS}) of 92.8 (13.6), 132.6 (41.7), 141.9 (48.1), 169.3 (51.1), 177.3 (58.2), and 198.6 (83.7) ppm, respectively.

Mice

The most sensitive lung gene in mice, exhibiting an increase in expression, was *Ces1g* (carboxylesterase 1G) with an estimated median BMD <0.333 ppm. The most sensitive upregulated genes with a calculated BMD were *Dtl* (denticleless E3 ubiquitin protein ligase), *Ccna1* (cyclin A1), *Atp2b2* (ATPase, Ca++ transporting, plasma membrane 2), *Ugt1a6a* (UDP glucuronosyltransferase 1 family, polypeptide A6A), *Gins2* (GINS complex subunit 2), *Pole* (polymerase (DNA directed), epsilon), *Ugt1a6b* (UDP glucuronosyltransferase 1 family, polypeptide A6B), *Uhrf1* (ubiquitin-like, containing PHD and RING finger domains, 1), and *Ube2t* (ubiquitin-conjugating enzyme E2T) with BMDs (BMD_{LS}) of 0.6 (0.2), 0.6 (0.3), 0.8 (0.3), 1.0 (0.3), 1.3 (0.5), 1.5 (0.5), 1.6 (0.5), 1.9 (0.6), and 2.8 (0.8) ppm, respectively.

Table 16. Top 10 Lung Genes Ranked by Potency of Perturbation, Sorted by Benchmark Dose Median, for Female Rats and Mice Exposed to 1,4-Dichlorobenzene for Five Days

Gene Symbol[a]	BMD_{rd25} (BMD_{Lrd25}–BMD_{Urd25}) in ppm	Maximum Fold Change	Direction of Expression Change
Rats			
Ddit4	92.8 (13.6–256.6)	2.2	DOWN
Junb	121.9 (39.9–278.5)	1.8	UP
Cebpd	132.6 (41.7–216.4)	2.0	DOWN
Slc6a8	141.9 (48.1–1,438.7)	1.5	DOWN
Meg3	146.1 (40.1–395.1)	1.9	UP
Cenpf	169.3 (51.1–1,294.8)	1.6	DOWN
Cenpw	177.3 (58.2–542.9)	1.7	DOWN
Ier3	182.4 (51.2–426.7)	1.6	UP
Papss2	198.6 (83.7–NC)	1.4	DOWN
Ccl12	217.6 (62.0–475.4)	1.9	UP
Mice			
Ces1g	<0.333[b] (NR)	3.5	UP
Dtl	0.6 (0.2–2.0)	2.1	UP

Gene Symbol[a]	BMD_{rd25} (BMD_{Lrd25}–BMD_{Urd25}) in ppm	Maximum Fold Change	Direction of Expression Change
Ccna1	0.6 (0.3–1.7)	2.4	UP
Atp2b2	0.8 (0.3–3.7)	1.6	UP
Ugt1a6a	1.0 (0.3–9.4)	1.6	UP
Gins2	1.3 (0.5–37.8)	1.6	UP
Pole	1.5 (0.5–2,223.9)	1.5	UP
Ugt1a6b	1.6 (0.5–11.1)	1.6	UP
Uhrf1	1.9 (0.6–1,766.4)	1.5	UP
Ube2t	2.8 (0.8–11.3)	1.6	UP

BMD_{rd25} = benchmark dose corresponding to a benchmark response set to a 25% change in the median response; BMD_{Lrd25} = benchmark dose lower confidence limit corresponding to a benchmark response set to a 25% change in the median response; BMD_{Urd25} = benchmark dose upper confidence limit corresponding to a benchmark response set to a 25% change in the median response; NC = nonconvergent; NR = the BMD_{Lrd25}–BMD_{Urd25} range is not reportable because the BMD_{rd25} median is below the lower limit of extrapolation (<1/3 of the lowest nonzero exposure concentration tested).
[a]Gene definitions are available in Appendix E and in the Chemical Effects in Biological Systems (CEBS) data repository: https://doi.org/10.22427/NTP-DATA-002-00600-0002-000-0.
[b]<0.333 = a best-fit model was identified and a BMD_{rd25} was estimated that was <1/3 of the lowest nonzero exposure concentration tested.

Ovary

Rats

The most sensitive genes exhibiting an increase in expression were *S100a9* (S100 calcium-binding protein A9), *Acss1* (acyl-CoA synthetase short-chain family member 1), *Cxcl12* (C-X-C motif chemokine ligand 12), *Slc26a2* (solute carrier family 26 member 2), and *Vnn1* (vanin 1) with calculated BMD (BMD_{LS}) of 199.6 (78.7), 213.3 (63.5), 246.7 (103.1), 258.7 (84.0), and 310.0 (166.8) ppm, respectively. The most sensitive downregulated genes with a calculated BMD were *Fosl1* (FOS like 1, AP-1 transcription factor subunit), *Apoa1* (apolipoprotein A1), *Tnfrsf12a* (TNF receptor superfamily member 12A), *Aen* (apoptosis enhancing nuclease), and *Slc51a* (solute carrier family 51 member A) with BMDs (BMD_{LS}) of 127.2 (22.7), 187.9 (47.2), 255.3 (113.7), 291.1 (93.4), and 314.8 (131.0) ppm, respectively.

Mice

Only eight genes met the criteria. Of these eight genes, the most sensitive upregulated genes with a calculated BMD were *Cyp2a4* (cytochrome P450, family 2, subfamily a, polypeptide 4), *Gdf7* (growth differentiation factor 7), *Dbp* (D site albumin promoter binding protein), *Hoxa10* (homeobox A10), and *Tuba4a* (tubulin, alpha 4A) with BMDs (BMD_{LS}) of 48.8 (14.5), 82.1 (23.7), 83.6 (25.6), 103.4 (21.3), and 230.8 (112.7) ppm, respectively. The most sensitive genes exhibiting a decrease in expression were *H2-q6* (histocompatibility 2, Q region locus 6), *Hmgcs2* (3-hydroxy-3-methylglutaryl-Coenzyme A synthase 2), and *Clu* (clusterin) with BMDs (BMD_{LS}) of 172.4 (73.4), 266.2 (197.3), and 384.1 (260.5) ppm, respectively.

Table 17. Top 10 Ovary Genes Ranked by Potency of Perturbation, Sorted by Benchmark Dose Median, for Female Rats and Mice Exposed to 1,4-Dichlorobenzene for Five Days

Gene Symbol[a,b]	BMD_{rd25} (BMD_{Lrd25}–BMD_{Urd25}) in ppm	Maximum Fold Change	Direction of Expression Change
Rats			
Fosl1	127.2 (22.7–291.4)	11.4	DOWN
Apoa1	187.9 (47.2–378.4)	3.2	DOWN
S100a9	199.6 (78.7–432.2)	1.8	UP
Acss1	213.3 (63.5–449.8)	1.8	UP
Cxcl12	246.7 (103.1–433.5)	1.7	UP
Tnfrsf12a	255.3 (113.7–412.3)	3.9	DOWN
Slc26a2	258.7 (84.0–430.3)	1.7	UP
Aen	291.1 (93.4–2,345.0)	1.5	DOWN
Vnn1	310.0 (166.8–452.8)	6.9	UP
Slc51a	314.8 (131.0–483.1)	3.1	DOWN
Mice			
Cyp2a4	48.8 (14.5–123.1)	2.2	UP
Gdf7	82.1 (23.7–170.5)	5.4	UP
Dbp	83.6 (25.6–102.8)	2.3	UP
Hoxa10	103.4 (21.3–212.0)	2.8	UP
H2-q6	172.4 (73.4–1,326.3)	1.5	DOWN
Tuba4a	230.8 (112.7–529.2)	1.5	UP
Hmgcs2	266.2 (197.3–401.9)	1.4	DOWN
Clu	384.1 (260.5–737.6)	1.3	DOWN

BMD_{rd25} = benchmark dose corresponding to a benchmark response set to a 25% change in the median response; BMD_{Lrd25} = benchmark dose lower confidence limit corresponding to a benchmark response set to a 25% change in the median response; BMD_{Urd25} = benchmark dose upper confidence limit corresponding to a benchmark response set to a 25% change in the median response.
[a]Gene definitions are available in Appendix E and in the Chemical Effects in Biological Systems (CEBS) data repository: https://doi.org/10.22427/NTP-DATA-002-00600-0002-000-0.
[b]Only eight ovary genes met the criteria in mice.

Theoretical Inhaled Dose

To provide information relevant for route-to-route extrapolation, to allow for comparison between two dichlorobenzene isomers, and to normalize data for comparison of internal dose between species, a theoretical inhaled mg/kg/day dose was calculated for each species and exposure group. Information relevant to the calculations is provided below, with the calculated theoretical inhaled doses shown in Table 18.

- Estimates of minute volume (Mv) were based on EPA's *Methods for Derivation of Inhalation Reference Concentrations and Application of Inhalation Dosimetry*[29] as well as *Recommendations for and Documentation of Biological Values for Use in Risk Assessment*.[30]

- Study day 0 body weights (BW) were used in the calculations due to the short duration of the study and minimal effects on body weight.
- Target exposure concentrations, rather than actual exposure concentrations, were used for the calculations due to the high degree of congruency.

The inhaled dose over a 6-hour exposure period was calculated as:

Dose (mg/kg/day) = C [(mg/m^3)/1,000)] × Mv (L/min) × 360 min/day exposure ÷ BW (kg)

where

C (mg/m^3) = 0.0409 × C (ppm) × molecular weight of test article

Mv (L/min) is estimated as LnMv = b0 + b1 × Ln(BW) where b0 and b1 are −0.578 and 0.821 for rats and 0.326 and 1.050 for mice, respectively.[29; 30]

Table 18. Theoretical Inhaled Daily Dose (mg/kg/day) of 1,4-Dichlorobenzene Following Six-hour Whole-Body Inhalation Exposure

	0 ppm	1 ppm	10 ppm	50 ppm	150 ppm	400 ppm	800 ppm
Rat	0	1.64	16.36	81.58	245.18	653.76	1,305.97
Mouse	0	2.46	24.58	122.86	368.16	982.02	NA

Within each exposure group and species, calculations were performed for the core and internal concentration assessment animals separately, using group mean body weight data. The data presented here and used for internal dose assessment normalization (mg/kg/day) are a mean of the values calculated by the core and internal concentration assessment animals.
NA = not applicable.

Internal Concentration Assessment

1,4-DCB concentrations were quantified in blood, lung, and liver on study day 4 (following the last exposure) and study day 5 (approximately 18 hours following the last exposure) using a validated analytical method (Appendix B). Data are reported before and after normalizing to the exposure concentration (ppm) and the estimated theoretical inhaled dose (mg/kg/day).

Rats

On study day 4, blood 1,4-DCB concentration increased with increasing exposure concentration (Table 19). The increase was proportional to the exposure concentration up to 150 ppm as evidenced by the dose-normalized values (72.1–99.8 [ng/mL]/[mg/kg/day]). At 400 and 800 ppm, blood concentrations increased more than proportionally to the exposure concentration with normalized values of 152 and 136 (ng/mL)/(mg/kg/day), respectively, demonstrating saturation of metabolism and/or clearance processes.

On study day 4, 1,4-DCB liver concentrations, in general, were similar to blood although lung concentrations were lower than those for blood (except the 800 ppm group), suggesting low tissue distribution and/or retention. As evidenced by the normalized values, liver concentration increased proportionally to the exposure concertation up to 50 ppm (101–127 [ng/g]/[mg/kg/day]) but increased more than proportionally to the exposure concentration ≥150 ppm with normalized values ranging from 155 to 231 (ng/g)/(mg/kg/day). In general, lung

concentrations increased proportionally to the exposure concentration with normalized values ranging from 30.2 to 73.4 (ng/g)/(mg/kg/day), except at the highest exposure concentration at which the increase was more than proportional to the exposure concentration with a normalized value of 185 (ng/g)/(mg/kg/day).

On study day 5, blood, liver, and lung concentrations were much lower than on study day 4, demonstrating rapid elimination of 1,4-DCB. As observed for study day 4, concentrations in general were similar between blood and liver but lower in lung.

Mice

On study day 4, blood 1,4-DCB concentration increased with increasing exposure concentration (Table 20). The increase was proportional to the exposure concentration up to 10 ppm as evidenced by the dose-normalized values (6.89–10.7 [ng/mL]/[mg/kg/day]). At concentrations ≥50 ppm, blood concentration increased more than proportionally to exposure concentration with normalized values ranging from 32 to 95.6 (ng/mL)/(mg/kg/day).

On study day 4, 1,4-DCB liver and lung concentrations, in general, were similar to blood (with the exception of lung concentrations in the 50 and 400 ppm groups) suggesting low tissue distribution and/or retention. As evidenced by the dose-normalized values, liver (3.84–10.1 [ng/g]/[mg/kg/day]) and lung (2.36–4.37 [ng/g]/[mg/kg/day]) concentrations increased proportionally to the exposure concentration up to 10 ppm, but the increase was more than proportional at concentrations ≥50 ppm (liver, 48.1–143 [ng/g]/[mg/kg/day]; lung, 38.3–209 [ng/g]/[mg/kg/day]).

On study day 5, blood, liver, and lung concentrations were much lower than on study day 4 with values falling below the limit of detection at 1 ppm for the tissues, demonstrating rapid elimination of 1,4-DCB. As observed for study day 4, concentrations in general were similar among blood, liver, and lung.

In general, when normalized to the theoretical inhaled dose, rats had higher blood and tissue concentrations of 1,4-DCB than mice at the lower exposure concentrations, although the difference was smaller at 400 ppm.

Table 19. Summary of Blood, Lung, and Liver Concentration Data for Female Rats Exposed to 1,4-Dichlorobenzene for Five Days

Endpoint[a,b]	0 ppm	1 ppm	10 ppm	50 ppm	150 ppm	400 ppm	800 ppm
Study Day 4							
n	3	3	3	3	3	3	2
Blood							
Blood concentration (ng/mL)[c]	0.398 ± 0.0127**	152 ± 11.0*	1,400 ± 70.2**	8,140 ± 690**	17,700 ± 2,370**	99,100 ± 5,000**	178,000 ± 52,500**
Normalized blood concentration [(ng/mL)/(mg/kg/day)][d,e]	–[f]	92.8 ± 6.70	85.6 ± 4.29	99.8 ± 8.45	72.1 ± 9.66	152 ± 7.65	136 ± 40.2
Normalized blood concentration [(ng/mL)/ppm][e]	–	152 ± 11.0	140 ± 7.02	163 ± 13.8	118 ± 15.8	248 ± 12.5	222 ± 65.6
Liver							
Liver concentration (ng/g)	0.873 ± 0.0422**	208 ± 11.1*	1,680 ± 185**	8,270 ± 771**	37,900 ± 5,060**	151,000 ± 12,700**	207,000 ± 89,000**
Normalized liver concentration [(ng/g)/(mg/kg/day)][d,e]	–	127 ± 6.80	103 ± 11.3	101 ± 9.45	155 ± 20.7	231 ± 19.5	159 ± 68.1
Normalized liver concentration [(ng/g)/ppm][e]	–	208 ± 11.1	168 ± 18.5	165 ± 15.4	253 ± 33.8	378 ± 31.9	259 ± 111
Lung							
Lung concentration (ng/g)	0.408 ± 0.0132**	120 ± 36.5*	595 ± 158**	3,830 ± 1,390**	7,410 ± 305**	37,800 ± 2,580**	242,000 ± 134,000**
Normalized lung concentration [(ng/g)/(mg/kg/day)][d,e]	–	73.4 ± 22.3	36.4 ± 9.65	47.0 ± 17.1	30.2 ± 1.24	57.8 ± 3.95	185 ± 103
Normalized lung concentration [(ng/g)/ppm][e]	–	120 ± 36.5	59.5 ± 15.8	76.7 ± 27.9	49.4 ± 2.03	94.4 ± 6.46	303 ± 168
Study Day 5							
n	3	3	3	3	3	3	3
Blood							
Blood concentration (ng/mL)	0.477 ± 0.0264**	4.69 ± 0.736*	36.3 ± 4.94**	250 ± 27.6**	1,180 ± 165**	2,610 ± 636**	4,430 ± 537**
Normalized blood concentration [(ng/mL)/(mg/kg/day)]	–	2.87 ± 0.450	2.22 ± 0.302	3.07 ± 0.338	4.82 ± 0.673	4.00 ± 0.973	3.39 ± 0.411
Normalized blood concentration [(ng/mL)/ppm]	–	4.69 ± 0.736	3.63 ± 0.494	5.01 ± 0.551	7.88 ± 1.10	6.53 ± 1.59	5.54 ± 0.671

Endpoint[a,b]	0 ppm	1 ppm	10 ppm	50 ppm	150 ppm	400 ppm	800 ppm
Liver							
Liver concentration (ng/g)	0.760 ± 0.0563**	7.13 ± 1.29*	69.2 ± 24.2**	158 ± 13.5**	1,300 ± 225**	2,480 ± 413**	3,810 ± 665**
Normalized liver concentration [(ng/g)/(mg/kg/day)]	–	4.35 ± 0.787	4.23 ± 1.48	1.94 ± 0.166	5.31 ± 0.919	3.80 ± 0.632	2.92 ± 0.509
Normalized liver concentration [(ng/g)/ppm]	–	7.13 ± 1.29	6.92 ± 2.42	3.17 ± 0.271	8.68 ± 1.50	6.21 ± 1.03	4.77 ± 0.831
Lung							
Lung concentration (ng/g)	0.482 ± 0.0559**	4.31 ± 1.03*	22.3 ± 3.66**	352 ± 51.9**	446 ± 42.1**	1,660 ± 810**	1,970 ± 381**
Normalized lung concentration [(ng/g)/(mg/kg/day)]	–	2.63 ± 0.631	1.37 ± 0.224	4.32 ± 0.636	1.82 ± 0.172	2.53 ± 1.24	1.51 ± 0.292
Normalized lung concentration [(ng/g)/ppm]	–	4.31 ± 1.03	2.23 ± 0.366	7.05 ± 1.04	2.97 ± 0.281	4.14 ± 2.03	2.46 ± 0.477

Statistical significance for an exposed group indicates a significant pairwise test compared to the 0 ppm group. Statistical significance for the 0 ppm group indicates a significant trend test.
*Statistically significant at $p \leq 0.05$; **$p \leq 0.01$.
[a]Data are presented as mean ± standard error.
[b]If over 20% of the animals in a group were above the limit of detection (LOD), one-half of the LOD was substituted for values below the LOD. LOD for blood = 0.0960 ng/mL; LOD for liver = 0.288 ng/g; LOD for lung = 0.288 ng/g.
[c]Statistical analysis performed by the Jonckheere (trend) and the Shirley or Dunn (pairwise) tests.
[d]Theoretical inhaled doses estimated for the 1, 10, 50, 150, 400 and 800 ppm groups are 1.64, 16.36, 81.58, 245.18, 653.76 and 1,305.97 mg/kg/day, respectively.
[e]Normalized concentrations were calculated by dividing the measured concentration in either ng/mL for blood or ng/g for tissues by either the theoretical inhaled dose (mg/kg/day) or nominal exposure concentration (ppm). No statistical analysis was performed on normalized endpoints.
[f]Not applicable.

Table 20. Summary of Blood, Lung, and Liver Concentration Data for Female Mice Exposed to 1,4-Dichlorobenzene for Five Days

Endpoint[a,b]	0 ppm	1 ppm	10 ppm	50 ppm	150 ppm	400 ppm
Study Day 4						
n	3	3	3[c]	2	3	3
Blood						
Blood concentration (ng/mL)	BD[d]	16.9 ± 2.75	263 ± 28.7	4,940 ± 260	11,800 ± 1,380	93,900 ± 12,700
Normalized blood concentration [(ng/mL)/(mg/kg/day)][e,f]	–[g]	6.89 ± 1.12	10.7 ± 1.17	40.2 ± 2.12	32.0 ± 3.74	95.6 ± 12.9
Normalized blood concentration [(ng/mL)/ppm][f]	–	16.9 ± 2.75	26.3 ± 2.87	98.8 ± 5.20	78.4 ± 9.18	235 ± 31.7
Liver						
Liver concentration (ng/g)	BD	9.43 ± 0.558	248 ± 19.5	5,910 ± 335	18,900 ± 1,940	141,000 ± 23,100
Normalized liver concentration [(ng/g)/(mg/kg/day)][e,f]	–	3.84 ± 0.227	10.1 ± 0.792	48.1 ± 2.73	51.3 ± 5.28	143 ± 23.6
Normalized liver concentration [(ng/g)/ppm][f]	–	9.43 ± 0.558	24.8 ± 1.95	118 ± 6.70	126 ± 13.0	352 ± 57.8
Lung						
Lung concentration (ng/g)	BD	10.7 ± 1.85	58.1 ± 3.30	14,600 ± 5,200	14,100 ± 4,000	205,000 ± 72,700
Normalized lung concentration [(ng/g)/(mg/kg/day)][e,f]	–	4.37 ± 0.755	2.36 ± 0.134	119 ± 42.3	38.3 ± 10.9	209 ± 74.1
Normalized lung concentration [(ng/g)/ppm][f]	–	10.7 ± 1.85	5.81 ± 0.330	292 ± 104	94.0 ± 26.7	513 ± 182
Study Day 5						
n	3[h]	3	3	3	3	3
Blood						
Blood concentration (ng/mL)	BD	0.0983 ± 0.0252	0.492 ± 0.264	2.24 ± 1.02	20.1 ± 8.44	23.8 ± 17.3
Normalized blood concentration [(ng/mL)/(mg/kg/day)]	–	0.0400 ± 0.0102	0.0200 ± 0.0107	0.0182 ± 0.00826	0.0545 ± 0.0229	0.0242 ± 0.0176
Normalized blood concentration [(ng/mL)/ppm]	–	0.0983 ± 0.0252	0.0492 ± 0.0264	0.0447 ± 0.0203	0.134 ± 0.0563	0.0595 ± 0.0433

Endpoint[a,b]	0 ppm	1 ppm	10 ppm	50 ppm	150 ppm	400 ppm
Liver						
Liver concentration (ng/g)	BD	BD	0.656 ± 0.193	3.97 ± 0.833	27.3 ± 9.22	25.8 ± 12.1
Normalized liver concentration [(ng/g)/(mg/kg/day)]	–	BD	0.0267 ± 0.00786	0.0323 ± 0.00678	0.0742 ± 0.0250	0.0263 ± 0.0123
Normalized liver concentration [(ng/g)/ppm]	–	BD	0.0656 ± 0.0193	0.0793 ± 0.0167	0.182 ± 0.0614	0.0646 ± 0.0303
Lung						
Lung concentration (ng/g)	BD	BD	0.713 ± 0.414	1.27 ± 0.330	15.6 ± 3.46	27.0 ± 22.6
Normalized lung concentration [(ng/g)/(mg/kg/day)]	–	BD	0.0290 ± 0.0168	0.0103 ± 0.00269	0.0423 ± 0.00941	0.0275 ± 0.0230
Normalized lung concentration [(ng/g)/ppm]	–	BD	0.0713 ± 0.0414	0.0254 ± 0.00661	0.104 ± 0.0231	0.0676 ± 0.0565

BD = below detection; group did not have more than 20% of its values above the limit of detection (LOD).
[a]Data are presented as mean ± standard error.
[b]If over 20% of the animals in a group were above the LOD, one-half of the LOD was substituted for values below the LOD. LOD for blood = 0.0960 ng/mL; LOD for liver = 0.288 ng/g; LOD for lung = 0.288 ng/g.
[c]n = 2 for lung. One animal was identified as an outlier and thus excluded from analysis.
[d]When the 0 ppm group did not have over 20% of its values above the LOD, no mean or standard error was calculated, and no statistical analysis was performed.
[e]Theoretical inhaled doses estimated for the 1, 10, 50, 150, and 400 ppm groups are 2.46, 24.58, 122.86, 368.16, and 982.02 mg/kg/day, respectively.
[f]Normalized concentrations were calculated by dividing the measured concentration in either ng/mL for blood or ng/g for tissues by either the theoretical inhaled dose (mg/kg/day) or nominal exposure concentration (ppm). No statistical analysis was performed on normalized endpoints.
[g]Not applicable.
[h]n = 2 for blood and lung. One animal for blood and one animal for lung were identified as outliers and thus excluded from analysis.

Summary

1,4-Dichlorobenzene (1,4-DCB) is a chlorinated aromatic hydrocarbon that is used in various industrial and household applications, including as a fumigant for moth control, a deodorizer in urinal cakes, and an air freshener in domestic and public settings. These studies used a transcriptomic approach and standard toxicological endpoints to estimate the in vivo biological potency of 1,4-DCB. The data from these studies are intended to support risk assessment and establishment of acceptable exposure levels of 1,4-DCB in environmental and occupational settings.

In rats exposed to 1,4-DCB, the most sensitive apical endpoint was an increase in relative liver weight with a calculated benchmark dose (benchmark dose lower confidence limit)—BMD (BMD_L)—of 191.4 (127.6) ppm. Increases in relative left kidney weight and absolute liver weight were the next most sensitive apical endpoint changes observed with BMDs (BMD_Ls) of 219.2 (89.4) and 245.5 (163.4) ppm, respectively. In mice exposed to 1,4-DCB, the most sensitive apical endpoint was a decrease in albumin/globulin ratio with a BMD (BMD_L) of 15.1 (2.2) ppm. The next most sensitive apical endpoints observed were increases in relative liver weight and cholesterol concentration with BMDs (BMD_Ls) of 70.2 (47.4) and 71.0 (43.1) ppm, respectively.

In the heart, transcriptional changes at the gene set level were calculated to occur at a BMD (BMD_L) as low as 141.4 (55.9) ppm, corresponding to cell cycle phase transition (GO:0044770) and mitotic cell cycle phase transition (GO:0044772), and as low as 91.0 (25.1) ppm in mice, corresponding to organic hydroxy compound biosynthetic process (GO:1901617). The most sensitive heart genes for which a reliable BMD could be determined were *Lck,* with a BMD (BMD_L) of 31.7 (6.0) ppm, in rats and *Krt18*, with a BMD (BMD_L) of 0.6 (0.1) ppm, in mice.

In the kidney, transcriptional changes at the gene set level were calculated to occur at a BMD (BMD_L) as low as 121.0 (42.2) ppm in rats, corresponding to cell cycle phase transition (GO:0044770) and mitotic cell cycle phase transition (GO:0044772), and as low as 16.9 (2.0) ppm in mice, corresponding to circadian rhythm (GO:0007623). The most sensitive kidney gene in rats for which a reliable BMD could be determined was *Srebf1* with a BMD (BMD_L) of 31.8 (7.8) ppm. The most sensitive kidney gene in mice for which a reliable BMD could be determined was *Chn1* with a BMD (BMD_L) of 5.4 (0.9) ppm.

In the liver, transcriptional changes at the gene set level were calculated to occur at a BMD (BMD_L) as low as 87.6 (59.6) ppm in rats, corresponding to xenobiotic metabolic process (GO:0006805), and as low as 6.3 (0.9) ppm in mice, corresponding to regulation of chromosome segregation (GO:0051983), positive regulation of cell cycle phase transition (GO:1901989), and positive regulation of mitotic cell cycle phase transition (GO:1901992). The most sensitive liver genes for which a reliable BMD could be determined were *Cyp2b2* in rats and *Cdc20* in mice with BMDs (BMD_Ls) of 48.4 (25.0) and 5.6 (0.7) ppm, respectively.

In the lung, transcriptional changes at the gene set level were calculated to occur at a BMD (BMD_L) as low as 208.6 (55.4) ppm in rats, corresponding to chromosome segregation (GO:0007059), and as low as 1.4 (0.5) ppm in mice, corresponding to DNA replication (GO:0006260). One lung gene in mice had a BMD estimate below the lower limit of extrapolation (<0.333 ppm). The most sensitive lung genes for which a reliable BMD could be

determined were *Ddit4*, with a BMD (BMD_L) of 92.8 (13.6) ppm, in rats and *Dtl* and *Ccna1* in mice, with BMDs (BMD_{LS}) of 0.6 (0.2) and 0.6 (0.3) ppm, respectively.

In the ovary, transcriptional changes at the gene set level were calculated to occur at a BMD (BMD_L) as low as 223.1 (90.9) ppm in rats, corresponding to ameboidal-type cell migration (GO:0001667). There were no active GO terms (i.e., no gene expression response at the gene set level) in mice exposed to 1,4-DCB. The most sensitive ovary genes for which a reliable BMD could be determined were *Fosl1* in rats and *Cyp2a4* in mice with BMDs (BMD_{LS}) of 127.2 (22.7) and 48.8 (14.5) ppm, respectively.

Under the conditions of this short-term transcriptomic study in female Sprague Dawley (Hsd:Sprague Dawley® SD®) rats and B6D2F1/Crl mice, the most sensitive point of departure with a reliable estimate in rats was a transcriptional change in a heart gene, *Lck*, with a BMD (BMD_L) of 31.7 (6.0) ppm. Apical endpoints and transcriptional changes at the gene set level provided potency estimates slightly higher than *Lck*. In mice, the most sensitive point of departure with a reliable estimate was a transcriptional change in a heart gene, *Krt18*, and two lung genes, *Dtl* and *Ccna1*, with BMDs (BMD_{LS}) of 0.6 (0.1), 0.6 (0.2), and 0.6 (0.3) ppm, respectively. Transcriptional changes at the gene set level provided potency estimates slightly higher than *Krt18*, *Dtl*, and *Ccna1* and apical endpoints provided potency estimates higher than *Krt18*, *Dtl*, and *Ccna1*.

References

1. National Information Standards Organization (NISO). CRediT (Contributor Roles Taxonomy). Baltimore, MD: National Information Standards Organization; 2024. [Accessed: July 26, 2024]. https://credit.niso.org/

2. Agency for Toxic Substances and Disease Registry (ATSDR). Toxicological profile for dichlorobenzenes. Atlanta, GA: U.S. Department of Health and Human Services, Public Health Service, Agency for Toxic Substances and Disease Registry; 2006. [Accessed: April 29, 2025]. https://www.atsdr.cdc.gov/ToxProfiles/tp10.pdf

3. National Center for Biotechnology Information (NCBI). PubChem compound summary for CID 4685, 1,4-dichlorobenzene. Bethesda, MD: U.S. Department of Health and Human Services, National Institutes of Health, National Library of Medicine, National Center for Biotechnology Information; 2025. [Accessed: April 29, 2025]. https://pubchem.ncbi.nlm.nih.gov/compound/1_4-Dichlorobenzene

4. U.S. Environmental Protection Agency (USEPA). Notice of pesticide reregistration: Paradichlorobenzene. Washington, DC: U.S. Environmental Protection Agency, Office of Pesticide Programs; 2014. EPA Reg. No. 81433-1. [Accessed: September 16, 2025]. https://www3.epa.gov/pesticides/chem_search/ppls/081433-00001-20140828.pdf

5. Occupational Safety and Health Administration (OSHA). 29 CFR § 1910.1000: Table Z-1 limits for air contaminants. Washington, DC: U.S. Department of Labor, Occupational Safety and Health Administration; 2025. [Accessed: April 29, 2025]. https://www.osha.gov/laws-regs/regulations/standardnumber/1910/1910.1000TABLEZ1

6. American Conference of Governmental Industrial Hygienists (ACGIH). ACGIH Data Hub: p-Dichlorobenzene. Cincinnati, OH: American Conference of Governmental Industrial Hygienists; 2025. [Accessed: September 16, 2025]. https://www.acgih.org/p-dichlorobenzene/

7. U.S. Environmental Protection Agency (USEPA). National Primary Drinking Water Regulations. Washington, DC: U.S. Environmental Protection Agency; 2024. [Accessed: September 16, 2025]. https://www.epa.gov/ground-water-and-drinking-water/national-primary-drinking-water-regulations

8. Office of Environmental Health Hazard Assessment (OEHHA). Air Toxics Hot Spots Program: 1,4-Dichlorobenzene Reference Exposure Levels: Technical support document for the derivation of noncancer Reference Exposure Levels: Appendix D1. Sacramento, CA: California Environmental Protection Agency, Office of Environmental Health Hazard Assessment, Air and Site Assessment and Climate Indicators Branch; 2025. [Accessed: September 16, 2025]. https://oehha.ca.gov/sites/default/files/media/2025-07/1%2C4-DCB%20REL071825_2.pdf

9. National Toxicology Program (NTP). 1,4-Dichlorobenzene. In: 15th Report on Carcinogens. Research Triangle Park, NC: U.S. Department of Health and Human Services, Public Health Service, National Toxicology Program; 2021. [Accessed: April 29, 2025]. https://ntp.niehs.nih.gov/sites/default/files/ntp/roc/content/profiles/dichlorobenzene.pdf

10. International Agency for Research on Cancer (IARC). Some chemicals that cause tumours of the kidney or urinary bladder in rodents and some other substances. (IARC monographs on the evaluation of carcinogenic risks to humans; vol. 73). Lyon, France: International Agency for Research on Cancer; 1999. [Accessed: April 29, 2025]. https://publications.iarc.who.int/91

11. European Commission (EC). Commission Regulation (EU) No 474/2014 of 8 May 2014 amending Annex XVII to Regulation (EC) No 1907/2006 of the European Parliament and of the Council on the Registration, Evaluation, Authorisation and Restriction of Chemicals ('REACH') as regards 1,4-dichlorobenzene (text with EEA relevance). OJ L 136, p. 19–22. 2014. [Accessed: October 6, 2025]. http://data.europa.eu/eli/reg/2014/474/oj

12. Hissink E, van Ommen B, Bogaards JJ, van Bladeren PJ. Hepatic epoxide concentrations during biotransformation of 1,2- and 1,4-dichlorobenzene: The use of in vitro and in vivo metabolism, kinetics and PB-PK modeling. In: Snyder R, Kocsis JJ, Sipes IG, Kalf GF, Jollow DJ, Greim H, Monks TJ, Witmer CM, editors. Biological Reactive Intermediates V: Basic Mechanistic Research in Toxicology and Human Risk Assessment. New York, NY: Springer; 1996. p. 129-133. https://doi.org/10.1007/978-1-4757-9480-9_18

13. Aiso S, Takeuchi T, Arito H, Nagano K, Yamamoto S, Matsushima T. Carcinogenicity and chronic toxicity in mice and rats exposed by inhalation to para-dichlorobenzene for two years. J Vet Med Sci. 2005; 67(10):1019-1029. https://doi.org/10.1292/jvms.67.1019

14. BioSpyder. TempO-Seq® assay user guide. Carlsbad, CA: BioSpyder Technologies, Inc.; 2022. Document 100802 rev C. [Accessed: August 25, 2025]. https://www.biospyder.com/s/100802-TempO-Seq-User-Guide-rev-C-r8r7.pdf

15. Langmead B, Trapnell C, Pop M, Salzberg SL. Ultrafast and memory-efficient alignment of short DNA sequences to the human genome. Genome Biol. 2009; 10(3):R25. https://doi.org/10.1186/gb-2009-10-3-r25

16. Williams DA. A test for differences between treatment means when several dose levels are compared with a zero dose control. Biometrics. 1971; 27(1):103-117. https://doi.org/10.2307/2528930

17. Williams DA. The comparison of several dose levels with a zero dose control. Biometrics. 1972; 28(2):519-531. https://doi.org/10.2307/2556164

18. Dunnett CW. A multiple comparison procedure for comparing several treatments with a control. J Am Stat Assoc. 1955; 50(272):1096-1121. https://doi.org/10.1080/01621459.1955.10501294

19. Shirley E. A non-parametric equivalent of Williams' test for contrasting increasing dose levels of a treatment. Biometrics. 1977; 33(2):386-389. https://doi.org/10.2307/2529789

20. Dunn OJ. Multiple comparisons using rank sums. Technometrics. 1964; 6(3):241-252. https://doi.org/10.1080/00401706.1964.10490181

21. Jonckheere AR. A distribution-free k-sample test against ordered alternatives. Biometrika. 1954; 41(1-2):133-145. https://doi.org/10.1093/biomet/41.1-2.133

22. Dixon WJ, Massey FJ. Introduction to statistical analysis. 2nd ed. New York, NY: McGraw-Hill; 1957.

23. National Toxicology Program (NTP). NTP research report on National Toxicology Program approach to genomic dose-response modeling. Research Triangle Park, NC: U.S. Department of Health and Human Services, Public Health Service, National Toxicology Program; 2018. NTP Research Report No. 5. https://doi.org/10.22427/NTP-RR-5

24. Yang L, Allen BC, Thomas RS. BMDExpress: A software tool for the benchmark dose analyses of genomic data. BMC Genomics. 2007; 8:387. https://doi.org/10.1186/1471-2164-8-387

25. Gwinn WM, Auerbach SS, Parham F, Stout MD, Waidyanatha S, Mutlu E, Collins B, Paules RS, Merrick BA, Ferguson S, et al. Evaluation of 5-day in vivo rat liver and kidney with high-throughput transcriptomics for estimating benchmark doses of apical outcomes. Toxicol Sci. 2020; 176(2):343-354. https://doi.org/10.1093/toxsci/kfaa081

26. Brennan A, Chang D, Cowden J, Davidson-Fritz S, Dean J, Devito M, Ford J, Everett L, Harrill A, Hester S, et al. Standard methods for development of EPA Transcriptomic Assessment Products (ETAPs). Research Triangle Park, NC: U.S. Environmental Protection Agency, Office of Research and Development, Center for Public Health and Environmental Assessment, Center for Computational Toxicology and Exposure; 2024. EPA Report No. EPA/600/X-23/083. [Accessed: February 10, 2026]. https://doi.org/10.23645/epacomptox.25365496

27. Auerbach SS, Ballin JD, Blake JC, Browning DB, Collins BJ, Cora MC, Fernando RA, Fostel JM, Liu YF, Luh J, et al. NIEHS report on the in vivo repeat dose biological potency study of perfluorohexanesulfonamide (CASRN 41997-13-1) in Sprague Dawley (Hsd:Sprague Dawley® SD®) rats (gavage studies). Research Triangle Park, NC: U.S. Department of Health and Human Services, Public Health Service, National Institute of Environmental Health Sciences; 2023. NIEHS Report 10. https://doi.org/10.22427/niehs-10

28. National Toxicology Program (NTP). NIEHS 13: Chemical Effects in Biological Systems (CEBS) data repository. Research Triangle Park, NC: U.S. Department of Health and Human Services, Public Health Service, National Toxicology Program; 2025. https://doi.org/10.22427/NIEHS-DATA-NIEHS-13

29. U.S. Environmental Protection Agency (USEPA). Methods for derivation of inhalation reference concentrations and application of inhalation dosimetry. Research Triangle Park, NC: U.S. Environmental Protection Agency, Office of Research and Development, Office of Health and Environmental Assessment, Environmental Criteria and Assessment Office; 1994. EPA Report No. EPA/600/8-90/066F. [Accessed: October 21, 2025]. https://www.epa.gov/risk/methods-derivation-inhalation-reference-concentrations-and-application-inhalation-dosimetry

30. U.S. Environmental Protection Agency (USEPA). Recommendations for and documentation of biological values for use in risk assessment. Cincinnati, OH: U.S. Environmental Protection Agency, Office of Research and Development, Office of Health and Environmental Assessment, Environmental Criteria and Assessment Office; 1988. EPA Report No. EPA/600/6-87/008. [Accessed: October 6, 2025]. https://assessments.epa.gov/risk/document/&deid%3D34855

31. Liu J, Hara K, Kashimura S, Hamanaka T, Tomojiri S, Tanaka K. Gas chromatographic-mass spectrometric analysis of dichlorobenzene isomers in human blood with headspace solid-phase microextraction. J Chromatogr B Biomed Sci Appl. 1999; 731(2):217-221. https://doi.org/10.1016/s0378-4347(99)00226-1

32. Watanabe K, Hasegawa K, Yamagishi I, Nozawa H, Takaba M, Suzuki O. Simple isotope dilution headspace-GC-MS analysis of naphthalene and p-dichlorobenzene in whole blood and urine. Anal Sci. 2009; 25(11):1301-1305. https://doi.org/10.2116/analsci.25.1301

33. Gene Ontology Consortium (GOC). Geneontology: The gene ontology resource. 2025. [Accessed: October 17, 2025]. https://geneontology.org/

34. Medical College of Wisconsin. Rat Genome Database. Milwaukee, WI: Medical College of Wisconsin; 2025. [Accessed: October 17, 2025]. https://rgd.mcw.edu/

35. UniProt Consortium. UniProtKB. 2025. [Accessed: October 17, 2025]. https://www.uniprot.org/uniprotkb/

36. National Center for Biotechnology Information (NCBI). Entrez Gene. Bethesda, MD: U.S. Department of Health and Human Services, National Institutes of Health, National Library of Medicine, National Center for Biotechnology Information; 2025. [Accessed: October 17, 2025]. https://www.ncbi.nlm.nih.gov/gene/

Appendix A. Chemical Characterization and Generation of Chamber Concentrations

Table of Contents

Tables

Figures

A.1. Procurement and Characterization of 1,4-Dichlorobenzene

1,4-Dichlorobenzene (1,4-DCB) was obtained from Finetech Industry Limited (Wuhan, China) in a single lot (20240416001). Identity, purity, and stability analyses were conducted by the analytical chemistry laboratory at Battelle (Columbus, OH). Reports on analyses performed in support of the 1,4-DCB studies are on file at the National Institute of Environmental Health Sciences (NIEHS).

The identity and purity of lot 20240416001, a white crystal at room temperature, was evaluated using gas chromatography (GC) with mass spectrometry (MS) detection (Table A-1, System A). The MS spectrum (Figure A-1) was consistent with the National Institute of Standards and Technology library spectrum for 1,4-DCB (Figure A-2) and a certified reference material of 1,4-DCB (lot LRAD1967, Sigma Aldrich). There were no impurity peaks present at ≥0.1%. The overall purity of the test article was estimated at approximately 100%.

Bulk 1,4-DCB was stored in the original shipping container at room temperature. Reanalysis of the bulk chemical was performed by the analytical chemistry laboratory within 30 days of study termination and no degradation was detected (Table A-1, System B).

A.2. Vapor Concentration Monitoring

Exposure chamber and room concentrations of 1,4-DCB were monitored using an online GC equipped with a flame ionization detector (FID) (Table A-1, System C). All chambers were sampled at approximately twice per hour during exposure through Teflon tubing connected to each exposure chamber's relative-humidity sampling lines at a location close to the GC/FID. The samples flowed into a 16-port Hastelloy®-C stream-select valve that directed a continuous stream of sampled atmosphere to a 6-port Hastelloy-C gas-sampling valve with a 1 mL sample loop. Valves were mounted in a dedicated valve oven located on top of the GC oven. The valve oven temperature was maintained at approximately 175°C. A vacuum regulator maintained a constant vacuum in the sample loop to compensate for variations in sample line pressure. An in-line flow meter between the vacuum regulator and GC allowed for digital measurement of sample flow (approximately 1 L/min).

The online GCs were checked for suitability before the start of each exposure day and after every ninth sample throughout the exposure period using a standard 1,4-DCB vapor supplied by a standard generator (KIN-TEK Analytical, Inc., La Marque, TX). The online GC/FID at the testing facility was calibrated by quantitative determination of 1,4-DCB in exposure chamber samples on sorbent tubes (ORBO-101 and ORBO-100; graphitized carbon black; Supelco; Bellefonte, PA) and analyzed using an offline GC/FID at the analytical chemistry laboratory (Table A-1, System D). Prior to the study, stability of 1,4-DCB on sorbent tubes was confirmed for up to 7 days when stored at ambient (extracted) or refrigerated (either extracted or unextracted) temperatures. Known volumes of atmosphere from each inhalation exposure chamber were collected using a calibrated critical-orifice controlled sampler at a constant flow rate. The sorbent samples were extracted with acetone containing propylbenzene internal standard (IS) and transferred to autosampler vials for analysis on the offline GC/FID. Online GC/FID calibration was established by correlating the chamber concentrations determined from

analysis of the sorbent gas-sampling tubes against the online monitor peak area determined at the time of sampling.

Summaries of the chamber vapor concentrations are given in Table A-2. The mean concentrations were all within the acceptance criteria of 10% for all exposure groups. Concentration relative standard deviation (RSD) was within acceptance criteria of 10% except for the 1 ppm chamber (rat and mouse). For the 1 ppm chamber, mainly because of the sensitivity of and fluctuation in the siphon/dilution system, the concentration RSD was 18% in the rat study and 22% in the mouse study. The high RSD of the 1 ppm chamber was considered to have no effect on the study results. The number of acceptable samples was ≥94% for all exposure groups of every study except for the 1 ppm rat and mouse chambers, which were 65% and 74%, respectively. The individual concentration data collected from the exposure room frequently exceeded the limit of detection (LOD; 0.02 ppm) with concentrations ≤0.053 ppm during the rat study and ≤0.034 ppm during the mouse study. The control chambers remained below the LOD for the entirety of both studies. These deviations were considered to have no effect on the study results, given that the mean concentrations were 100% of targets for both 1 ppm and 10 ppm chambers.

A.3. Vapor Generation and Exposure System

A diagram of the generation and distribution system is shown in Figure A-3. Solid 1,4-DCB was melted in a heated reservoir (target >150°F) and pumped through heated lines (approximately 140°F) by a fluid metering pump into a heated (approximately 280°F) glass vaporizer column containing 6 mm glass beads and wrapped around the full length by heat tape. A waste collection flask was connected to the bottom of the column for collection of residual 1,4-DCB not completely vaporized within the vaporizer column.

Preheated (approximately 260°F) nitrogen entered the column from below, vaporized 1,4-DCB, and carried the vapor from the generator cabinet located in the control room to the distribution manifold located in the exposure room through a heated (approximately 300°F) Teflon® transport line. The mixture of nitrogen and 1,4-DCB was diluted with heated (approximately 160°F) air before it entered the distribution manifold. The pressure in the distribution manifold was kept fixed, which ensured constant flow through the manifold and into all chambers as the flow of vapor to each chamber was adjusted. Concentration in the manifold was determined by the chemical pump rate, dilution air flow rate, nitrogen flow rate, and special modifications to the distribution manifold. Specifically, to achieve the 1 ppm exposure concentration, siphon/heated dilution lines were used to reduce the main manifold concentration approximately 30-fold before delivering the vapor to the 1 ppm chamber. Additionally, to ensure appropriate build up and decay times, heated entrainment air was added to the 10, 50, and 150 ppm delivery lines. Heated dilution air was also added to the 1 ppm siphon exhaust line to prevent potential blockage caused by solidified 1,4-DCB, which was at high concentration in the line.

Individual heated (approximately 200°F) Teflon delivery lines carried the vapor from the exposure valves in the distribution cabinet to the chamber inlets. The exposure valves diverted vapor delivery to the manifold exhaust until the generation system was stable, and exposures were ready to proceed. 1,4-DCB vapor delivery rates to each chamber were controlled by precision metering valves at the manifold. When the exposure started, the exposure valves

actuated and directed the vapor into the chamber inlet where it was diluted with conditioned air to achieve the desired exposure concentration.

Conditioned air was defined as the mix of air derived from each exposure chamber's wet and dry air duct supplies. The temperature of the resultant mixture of air was adjusted by passage over a temperature-controlled radiator after sequential treatment with Purafil®, charcoal, and high-efficiency particulate air (HEPA) filters. Air for the ducts was either passed over desiccant lowering the dew point (dry duct) or injected with clean steam raising the dew point (wet duct). Approximately 10% excess capacity of vapor was available for adjustments to chamber concentrations, as necessary. The excess capacity was emptied into the exhaust line from the manifold through a manually controlled adjustable flowmeter valve set to maintain constant pressure within the manifold. An alarm system automatically alerted the operator when any temperature controller detected a temperature outside of operating range. In addition, a variable power transformer limited power to each heater, thereby guarding against a temperature controller failure that could lead to excessive heating.

The exposure system consisted of seven exposure chambers with target test article concentrations of 0 (control group), 1, 10, 50, 150, 400, and 800 ppm. The inhalation exposure chamber (Lab Products, Inc., Seaford, DE) was designed so that uniform vapor concentrations could be maintained throughout the chamber with catch pans in place. The total active mixing volume of each chamber was 1.7 m^3. A small particle detector (Model 3022A; TSI, Inc., Shoreview, MN) was used in the exposure chambers, both with and without animals, to ensure vapor (not aerosol) was produced. Particle counts of fewer than 200 particles/cm^3 are typical of an exposure atmosphere when no generation is occurring. Particle counts above this level, especially if the counts increase with exposure concentration and are above the level during the off-exposure period, suggest a contribution to the aerosol concentration from the generation system. No particle counts above the minimum resolvable level were detected.

A.4. Chamber Atmosphere Characterization

Buildup and decay rates for chamber vapor concentrations were determined prior to (without animals) and during (with animals) the studies. The time to achieve 90% of the target concentration after the beginning of vapor generation (T_{90}) and the time for the chamber concentration to decay to 10% of the target concentration after vapor generation was terminated (T_{10}) were estimated from the concentration versus time curves.

The theoretical prediction of T_{90} as suggested by a 1.7 m^3 chamber mixing volume and a 15 ft^3/min flow rate was approximately 9.2 minutes. Estimated T_{90} ranged from 8 to 13 minutes for all chambers without animals except the 1 ppm chamber, which had a T_{90} of 19 minutes. Estimated T_{10} ranged from 9 to 13 minutes without animals. Buildup and decay of vapor concentrations were measured for the lowest (1 ppm) and highest (800 ppm for rat; 400 ppm for mouse) exposure concentration chambers during the studies. For the rat study, T_{90} ranged from 9 to 10 minutes and T_{10} ranged from 10 to 12 minutes. For the mouse study, T_{90} ranged from 11 to 13 minutes and T_{10} ranged from 10 to 11 minutes for both chambers. A T_{90} value of 12 minutes was used for the studies.

Prior to the studies, the persistence of 1,4-DCB was monitored in the 400 and 800 ppm chambers after exposure without animals present. The concentration of 1,4-DCB reached 1% of starting

concentration (T_1) in ≤37 minutes. During the studies and with animals present, T_1 was ≤75 minutes. The reason for the prolonged T_1 values is unknown, but the prolonged T_1 values were considered to have no effect on study findings given the low levels compared to the target chamber concentrations.

Concentration uniformity was evaluated in all exposure chambers without animals present. Vapor was sampled from 12 chamber positions, one in the front and one in the back, for each of the six possible animal cage positions per chamber and measured using the online monitor (Table A-1, System C). Uniformity measurements were all within the acceptable criterion of <5% of the RSD. Uniformity measurements were made during the studies from the lowest (1 ppm) and highest (800 ppm for rat; 400 ppm for mouse) exposure concentration chambers. All measurements met acceptable criteria and were comparable to the results prior to study start.

To measure stability and purity of 1,4-DCB in the generation and delivery system, samples of the test atmosphere were collected from the distribution line, generator reservoir, and the highest, lowest, and control exposure concentration chambers for both studies at the beginning and end of the exposure day and extracted with methanol. In addition, analysis was performed on a second set of samples collected from the same locations and exposure times and extracted in a second solvent (acetone) to demonstrate that any impurities in 1,4-DCB (if present) were not obscured by the primary solvent (methanol). Exposure atmosphere samples were collected on ORBO 101 (800 and 400 ppm for rats and mice, respectively) and ORBO 100 (1 ppm and control) CarboTrap B sorbent tubes. All sample collections included an SKC, Inc. (Eighty Four, PA) silica gel sorbent tube arranged in series with the ORBO primary tube. Samples were shipped on ice to the analytical chemistry laboratory for analysis (Table A-1, System D). No impurity peaks were present in any samples. Peaks were not observed in the silica gel samples, demonstrating 100% capture of the inhalation exposure atmosphere onto the ORBO 101 and ORBO 100 sorbent media. Stability and purity of 1,4-DCB was maintained throughout the exposure system.

To demonstrate acceptable stability and composition of the test article in the inhalation exposure system while animals were present in the exposure chambers, samples for stability analysis were collected by the testing facility from the distribution line, the two highest and the lowest exposure concentration chambers, and the vapor generator reservoir during the rat study. Additionally, the exposure system reservoir was sampled during the mouse study. The purity of 1,4-DCB in the exposure system with animals present in the exposure chambers was approximately 100%. Impurities with peak areas >0.1% of the total peak area were not present.

Table A-1. Gas Chromatography Systems Used in the Five-day Inhalation Studies of 1,4-Dichlorobenzene

Detection System	Column	Carrier Gas	Oven Temperature Program
System A			
Mass spectrometry with electron impact ionization	Restek Rtx-1 (30 m × 0.25 mm ID, 1.0 µm film thickness)	Helium at 1 mL/min	80°C for 2 minutes, then 5°C/min to 250°C, held for 5 minutes
System B			
Mass spectrometry with electron impact ionization	Restek Rtx-1 (30 m × 0.25 mm ID, 1.0 µm film thickness)	Helium at 1 mL/min	80°C for 2 minutes, then 10°C/min to 250°C, held for 5 minutes
System C			
Flame ionization (250°C)	Restek Rtx-5 (15 m × 0.53 mm ID, 1.5 µm film thickness)	Nitrogen at 7.9 psi	Isothermal at 110°C
System D			
Flame ionization (250°C)	Agilent DB-5a (30 m × 0.32 mm ID, 1.5 µm film thickness)	Helium at 1 mL/min	80°C for 2 minutes, then 5°C/min to 150°C, then 20°C/min to 250°C, held for 4 minutes

ID = internal diameter.

Table A-2. Summary of Chamber Concentrations in the Five-day Inhalation Study of 1,4-Dichlorobenzene

Exposure Date	Target Concentration (ppm)	Total Number of Readings	Determined Concentration (ppm)[a]	Percent of Target ± RSD	Acceptable Samples (%)[b]
Rat Chambers					
January 23–27, 2025	0 (Room)	84	ND[c]	NA	35
	0	80	ND[c]	NA	96
	1	130	1.00 ± 0.18	100 ± 18	65
	10	80	10.0 ± 0.4	100 ± 4	99
	50	80	49.8 ± 0.5	100 ± 1	100
	150	80	152 ± 2	102 ± 2	100
	400	80	403 ± 9	101 ± 2	100
	800	111	795 ± 11	99 ± 1	100
Mouse Chambers					
February 13–17, 2025	0 (Room)	83	ND[c]	NA	54
	0	83	ND	NA	100
	1	114	0.974 ± 0.215	97 ± 22	74
	10	80	9.99 ± 0.39	100 ± 4	94
	50	82	49.8 ± 0.5	100 ± 1	100
	150	82	150 ± 2	100 ± 1	100
	400	120	396 ± 9	99 ± 2	98

RSD = relative standard deviation; ND = not detectable; NA = not applicable.
[a]Data shown as mean of readings ± standard deviation.
[b]Acceptable range: Target concentration ± 10%; except for room and 0 ppm chamber: <limit of detection (LOD; 0.02 ppm).
[c]Daily mean concentrations were below the LOD; however, some individual readings were above the LOD with maximum readings of 0.053 and 0.034 ppm in the rat and mouse exposure rooms, respectively.

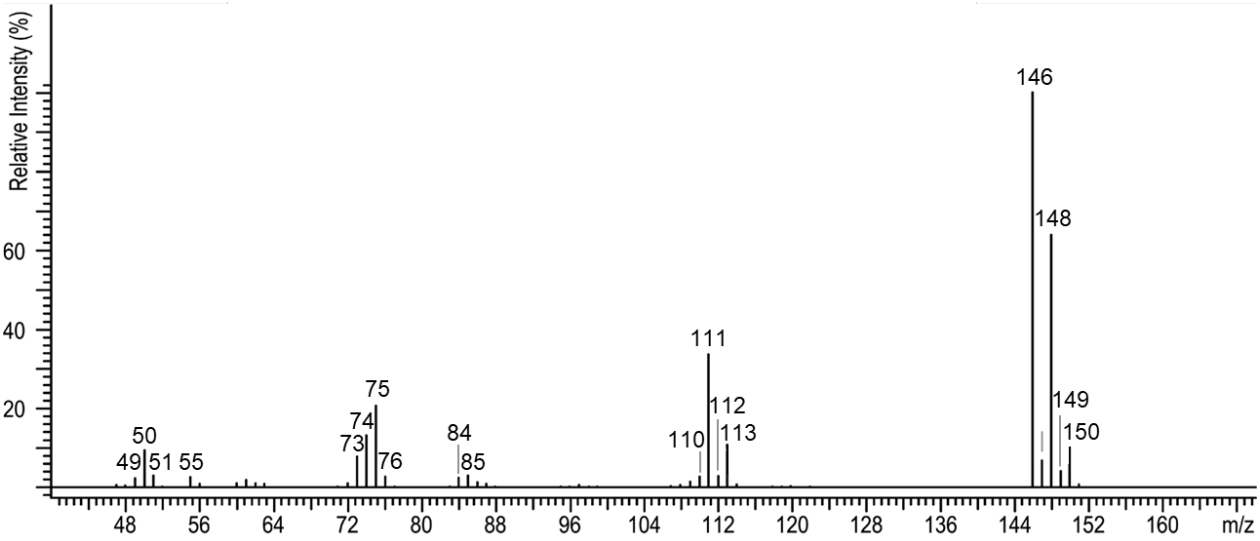

Figure A-1. Mass Spectrum of 1,4-Dichlorobenzene

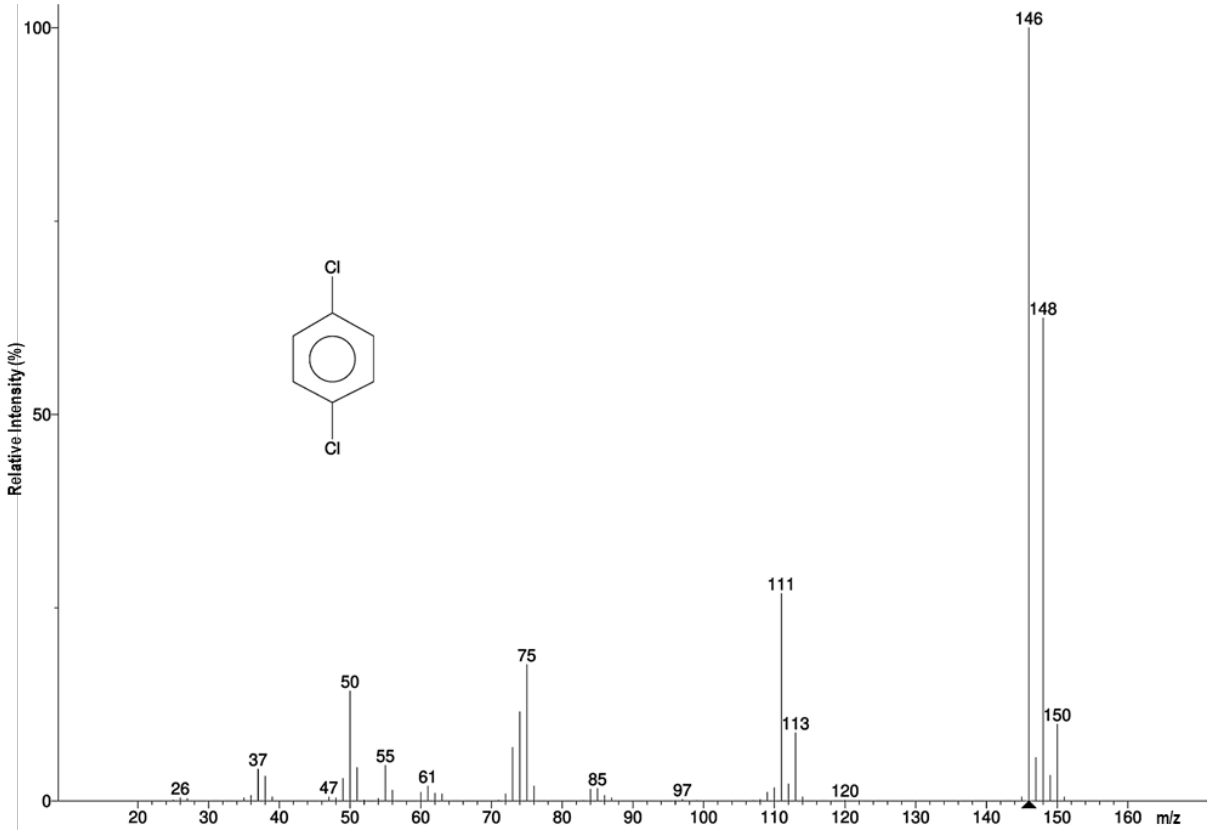

Figure A-2. Library Reference Spectrum of 1,4-Dichlorobenzene

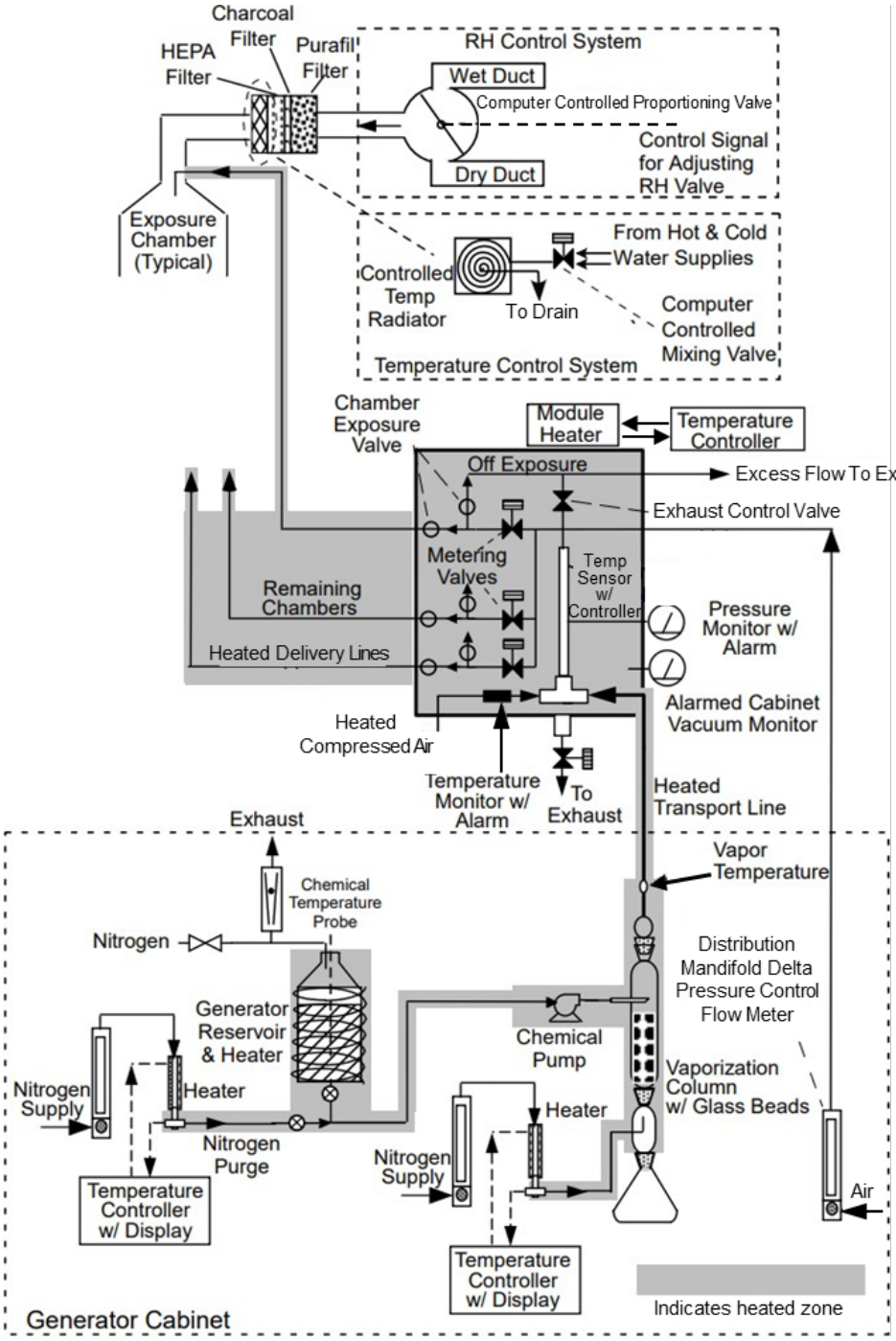

Figure A-3. Schematic of the Vapor Generation and Delivery System in the Inhalation Studies of 1,4-Dichlorobenzene

Appendix B. Internal Concentration Assessment

Table of Contents

Tables

B.1. Validation of Analytical Method

A method utilizing headspace solid-phase microextraction-gas chromatography mass spectrometry (HS-SPME-GC/MS; Table B-1) was adapted from the literature[31; 32] and validated for simultaneous quantitation of 1,2-dichlorobenzene (1,2-DCB) and 1,4-dichlorobenzene (1,4-DCB) in blood, liver, and lung.

Experiments were designed to demonstrate the linearity, sensitivity, selectivity, intra- and interday accuracy and precision, and reproducibility. Accuracy and precision were evaluated as percent relative error (% RE) and percent relative standard deviation (% RSD), respectively. The lower limit of quantitation (LLOQ) was the lowest calibration standard that could be accurately quantitated for six replicates within 20% RE and reproducible within 20% RSD. The limit of detection (LOD) was defined as 3 times the standard deviation of the LLOQ response, expressed as concentration. The ability to quantitate analyte concentrations above the validated range was also evaluated by preparing samples in respective matrices with concentrations above the upper limit of the validated range and diluting into the validated range using various approaches. The validated method was used to demonstrate the performance of the method to quantify analytes in study matrices (Hsd:Sprague Dawley® SD® [HSD] rat, B6D2F1/Crl mouse and B6C3F1 mouse blood, liver, and lung). HSD rat, B6D2F1/Crl mouse, and B6C3F1 mouse blood, liver, and lung were obtained from various sources, including BioIVT (Westbury, NY), Southern Research (Birmingham, AL), Battelle (Columbus, OH), and/or AmplifyBio (West Jefferson, OH). The stability of analytes in blood and tissues during sample storage to cover the study sample storage duration and under the conditions of the sample analysis was also assessed.

The method was validated in male HSD rat blood over an analyte concentration range of 0.5 to 250 ng/mL using seven concentrations. Quality control (QC) standards were prepared at 1, 25, and 200 ng/mL. 1,2- and 1,4-DCB solvent standards containing both analytes were prepared in acetone. $^{13}C_6$ 1,4-DCB (added as a mixture of $^{13}C_6$ 1,2-DCB and $^{13}C_6$ 1,4-DCB; Cambridge Isotope Laboratories, Inc., Tewksbury, MA) was used as the internal standard (IS). The working IS solution was prepared as 250 ng/mL of $^{13}C_6$ 1,4-DCB and $^{13}C_6$ 1,2-DCB in acetone.

Blood calibration standards and QC samples were prepared by aliquoting 20 µL analyte spiking solution in acetone into 180 µL HSD rat blood. Then, 100 µL of analyte-spiked blood was transferred into a 2 mL headspace vial, and 25 µL IS solution (250 ng/mL) in acetone was added prior to immediately capping the vials. Method (with IS) and matrix blanks (without IS) were prepared similarly except analyte spiking solution was not added to method and matrix blanks. Liver and lung QC samples were prepared by homogenizing 100 mg tissue in 170 µL phosphate buffered saline (PBS) with one 5 mm stainless-steel bead in the presence of 75 µL IS (or acetone for blanks without IS) and appropriate 30 µL analyte standard spiking solution (or acetone for blanks) using the TissueLyser at 25 Hz for 60 seconds 2 to 3 times until complete homogenization was observed. The final tissue dilution was 1:3. One hundred twenty-five microliters of the processed homogenate was transferred into individual 2 mL headspace vials and immediately capped. Stability of analytes during sample analysis at ambient temperature and during sample storage in ultracold temperature was assessed by preparing QC samples as described above with IS present and comparing to freshly prepared QC samples on day 0. The final IS concentration in all calibration standards, blanks, and QC samples was 50 ng/mL. All

samples were analyzed using the HS-SPME-GC/MS method (Table B-1) and quantified as described in section B.3.

Validation data for 1,4-DCB are shown in Table B-2. Calibration curves were linear ($r^2 \geq 0.99$) over the range (0.5 to 250 ng/mL) with an intra- and interday accuracy and precision of ≤ ±10.9% RE and ≤10.2% RSD, respectively. The intra- and interday accuracy and precision for QC standards were ≤ ±14.8% RE and ≤13.6% RSD, respectively. Carryover was assessed by comparing responses from three air blanks that were run immediately following the highest calibration standard of 250 ng/mL and met the acceptance criteria of <30% of the average response of the lowest standard (0.5 ng/mL). Selectivity was assessed by analyzing six replicates of blanks from two different lots of blood, with and without IS. Interference was minimal; the responses were 0.8%–20.0% of the lowest calibration concentration response (0.5 ng/mL). With each analytical batch, two air blanks were also analyzed to assess carryover. The air blanks were empty, 2 mL screw-top vials that did not go through sample processing. There was no appreciable carryover.

Dilution verification was conducted using different dilution schemes (i.e., using blood or blood diluted with acetone with or without IS) to determine if concentrations above the validated range could be quantified after diluting into the validated range. Because the blood sample collection during the study included the addition of IS, the data for blood prepared with IS and then diluted with blood containing IS are reported (Table B-3). In blood, 1,4-DCB concentrations up to 100,000 ng/mL can be quantified with good precision (≤ 0.9% RSD). The RE was ≤ ±24.2% for up to 20,000 ng/mL, demonstrating that 1,4-DCB can be quantified up to 20,000 ng/mL after diluting into range. Estimated RE ranged between ≤ ±30% and ≤ ±43.1% for concentrations >20,000 ng/mL.

The validated method was used to assess the performance in secondary (study) matrices with QC samples prepared as described above. The estimated RSD in all secondary matrices was ≤5.5% (Table B-4). Estimated RE in B6D2F1/Crl mouse blood (≤ ±9.0%), whereas the RE in all other tissues was 29.0%–44.7%. Overall data showed that the method is acceptable for quantitation of 1,4-DCB in secondary matrices, with the caveat that there is higher variability in some matrices. Dilution verification was also conducted for rat liver QC samples prepared at 150,000 ng/g and diluted using blood after homogenization (Table B-4). The accuracy of the dilutions was 25.3% and precision was 11.7%, demonstrating that liver samples could be diluted into the validated range for analysis. Because lung and liver homogenates behaved similarly, this assessment was not conducted for lung.

Analyte stability in blood and tissues was evaluated after storing QC samples under analysis conditions for 21 days or at –70°C for 100 or 149 days and then analyzing with freshly prepared samples on day 0 (Table B-5). When samples were prepared with IS present, 1,4-DCB showed acceptable stability in blood for up to 21 days at ambient temperature and for up to 149 days when frozen. 1,4-DCB was stable in liver at –70°C for up to 100 days. Stability of 1,4-DCB in lung was not evaluated and was expected to be similar to the liver.

B.2. Study Sample Collection

Blood, lung, and liver samples were collected from the internal concentration assessment animals immediately following the last exposure on study day 4 (once chamber concentrations were at or

below the regulatory limit of 5 ppm without additional health and safety considerations). Blood, lung, and liver samples were also collected from core animals designated for internal concentration assessment on study day 5 (approximately 18 hours following the last exposure).

B.2.1. Blood

On study day 4, blood was collected from the internal concentration assessment animals via cardiac puncture for all surviving rats and mice (up to 3/exposure group) while animals were anesthetized with CO_2/O_2 (70%/30%). On study day 5, blood samples from designated core animals (3/exposure group) were taken via retro orbital plexus (rats) or retro orbital sinus (mice) while animals were anesthetized with CO_2/O_2 (70%/30%). All blood samples were collected within a 2-hour window. Blood was collected into tubes containing tripotassium ethylenediaminetetraacetic acid (K_3 EDTA) and three aliquots of 100 µL were transferred into headspace vials and kept on wet ice. To aliquoted blood, IS (25 µL of 250 ng/mL of combined $^{13}C_6$ 1,4-DCB and $^{13}C_6$ 1,2-DCB in acetone) was added and kept on wet ice until transferred to frozen storage (−85°C to −60°C). The final IS concentration in samples was 50 ng/mL.

All samples were frozen within 2 hours of collection. QC samples were also prepared at the analytical chemistry laboratory to track the impacts of storage and shipping, if any, by spiking 0.1 mL blank blood aliquots with 25 ng/mL 1,2- and 1,4-DCB. At the testing facility, these blood aliquots were spiked with IS and processed similarly to study samples.

B.2.2. Lung and Liver

After blood collection, animals were euthanized by exsanguination and lung and liver tissues were collected (following organ weight measurements for core animals designated for internal concentration assessment) from each animal within approximately 2 hours and 30 minutes of each other. Up to three aliquots of approximately 100 mg (rats) or 50 mg (mice) (exact weights were recorded) lung and liver tissue were collected from each animal and flash frozen. Samples were stored frozen (−85°C to −60°C) until analyzed.

B.2.3. Study Sample Preparation

One blood aliquot from each animal was directly analyzed for 1,4-DCB using the validated method using conditions given in Table B-1. Calibration standards, QC samples (1 and 100 ng/mL), matrix blanks, method blanks, and tracking QC samples prepared in HSD rat blood were run with each analytical batch. Blood samples with 1,4-DCB concentrations above the validated method were reanalyzed after diluting into the validated range using blood diluent with IS present at the same concentration as study samples such that the final IS concentration in the sample was 50 ng/mL.

Rat lung and liver study samples were homogenized as described above under section B.1. Mouse liver and lung study samples were prepared by homogenizing 50 mg of tissue with 100 µL of PBS and 37.5 µL IS as described for rat but with one 3 mm stainless-steel bead. The final IS concentration in tissues was 50 ng/mL. After homogenization, samples were centrifuged at approximately 20,800 rcf for approximately 10 minutes. One hundred twenty-five microliters of the supernatant was transferred to individual 2 mL headspace vials, immediately sealed, and analyzed by HS-SPME-GC/MS (Table B-1). Lung and liver samples with concentrations above

the validated method were reanalyzed after diluting with HSD rat blood without IS into the validated range and IS at a final concentration of 50 ng/mL was added following dilution.

B.3. Instrumentation and Quantitation

All samples were analyzed using the HS-SPME-GC/MS method (Table B-1) and quantified using blood calibration curves. The peak area response ratio (analyte/IS) was calculated in each injection for 1,4-DCB. A linear regression equation with 1/x weighting was calculated relating the peak area response ratio (y) to the nominal concentration (x) in blood calibration standards for 1,4-DCB.

The concentration of each calibration standard, QC standard, and blank was calculated in nanograms per milliliter using its individual response ratio and the regression equation. Tissue concentration was converted to ng/g using the tissue weight and homogenization parameters (1 part tissue to 2 parts PBS/acetone).

Data from the study samples were considered valid if they were bracketed by valid QC sets. In general, each sample set, method blank, and control was bracketed by two QC sets, which consisted of a calibration blank and two concentrations of calibration standards. A QC set passed when the measured concentration for QC standards was ≤15% of its nominal value for at least 67% of all QC standards and at least 50% of the QC standards at each concentration level (high or low) having determined concentrations ≤15% of the nominal value. All QC standard sets met these acceptance criteria.

Seventeen tracking blood QC standards were analyzed with the study samples. Estimated REs for 14 out of the 17 the tracking QC standards ranged from –3.6% to 25.6%, demonstrating that there was no appreciable analyte loss during sample collection and storage.

Table B-1. Analytical System and Parameters Used in the Internal Concentration Assessment of 1,4-Dichlorobenzene

Instrument and Parameter	System A
System	Agilent GC 7890B plus Agilent MS 5977B
Sampling	
Headspace Autosampler	PAL RSI 85 Autosampler (CTC Analytics AG, Zwingen, Switzerland)
Solid Phase Microextraction	Topaz inlet liner (0.75 mm × 6.35 mm × 78.5 mm) and 100% polydimethylsiloxane fiber
Sample Incubation Temperature	40°C
Sample Incubation Time	10 minutes
Fiber Conditioning Temperature	300°C
Pre-desorption Conditioning Time	5 minutes
Sampling Time	15 minutes
Sample Vial Penetration Speed	20 mm/sec
Inlet Penetration Speed	100 mm/sec

Instrument and Parameter	System A
Sample Desorption Time	2 minutes
Post-desorption Conditioning Time	15 minutes
Column and Program	
Column	Restek Rtx-5 (30 m × 0.25 mm ID, 0.25 µm film thickness)
Carrier Gas	Helium at 1 mL/min
Oven Temperature Program	80°C for 2 minutes, then 5°C/min to 100°C, then 25°C/min to 250°C, 5-minute hold
Inlet Temperature	250°C
Inlet Purge Flow, Time	50.0 mL/min at 0.2 minutes
GC Cycle Time	22 minutes
Solvent Delay	3.5 to 4 minutes
Retention Time	~5.7 minutes
Auxiliary Temperature	250°C
MS Detector	
Source Temperature	230°C
Quadrupole Temperature	150°C
Ionization Mode	Electron Ionization Positive (EI+)
Acquisition Mode	SIM for 30 minutes m/z 146 (1,4-DCB quantitation ion) m/z, 75 (1,4-DCB confirmation ion) m/z 152 ($^{13}C_6$ 1,4-DCB quantitation ion) m/z 81 ($^{13}C_6$ 1,4-DCB confirmation ion)

GC = gas chromatography; MS = mass spectrometry; ID = internal diameter; EI = electron ionization; SIM = single ion monitoring.

Table B-2. Method Validation Data for 1,4-Dichlorobenzene in Rat Blood

Parameter	Male Sprague Dawley Rat
Matrix Concentration Range (ng/mL)	0.5–250[a]
Sensitivity	
LLOQ (ng/mL)	0.5
LOD (ng/mL)	0.0960
Coefficient of determination (r^2)	>0.99
Accuracy (% RE)	
Calibration standards intraday	≤ ±10.9
Calibration standards interday	≤ ±3.0
QC standards intraday[b]	≤ ±14.8
QC standards interday[b]	≤ ±3.5
Precision (% RSD)	
Calibration standards intraday	≤10.2

Parameter	Male Sprague Dawley Rat
Calibration standards interday	≤9.3
QC standards intraday[b]	≤7.3
QC standards interday[b]	≤13.6

LLOQ = lower limit of quantitation; LOD = limit of detection; RE = relative error; QC = quality control; RSD = relative standard deviation.
[a]Range validated with seven matrix calibration standards.
[b]Quality control standards prepared at 1, 25, and 200 ng/mL. n = 4 for intraday and n = 12 for interday.

Table B-3. Method Dilution Verification Data for 1,4-Dichlorobenzene in Male Sprague Dawley Rat Blood

Parameter[a]	9,900 ng/mL[b]	19,600 ng/mL[c]	47,600 ng/mL[d]	90,900 ng/mL[e]
Accuracy (% RE)	24.2	16.3	43.1	–30.0
Precision (% RSD)	0.9	0.0	0.2	0.3

RE = relative error; RSD = relative standard deviation.
[a]All values are a result of three replicate quality control standards.
[b]50-fold dilution with blood containing internal standard (IS).
[c]100-fold dilution with blood containing IS.
[d]250-fold dilution with blood containing IS.
[e]500-fold dilution with blood containing IS.

Table B-4. Secondary Matrix Evaluation Data for 1,4-Dichlorobenzene

Matrix	Accuracy (%RE)	Precision (%RSD)
Harlan Sprague Dawley Rat Blood[a]	≤ ±29.0	≤5.5
Harlan Sprague Dawley Rat Liver[b]	37.3	3.3
Harlan Sprague Dawley Rat Liver, Dilution Verification[c]	25.3	11.7
Harlan Sprague Dawley Rat Lung[b]	34.0	3.9
B6C3F1 Mouse Blood[d]	≤ ±29.0	≤3.4
B6C3F1 Mouse Liver[b]	38.3	2.5
B6C3F1 Mouse Lung[b]	44.7	4.7
B6D2F1 Mouse Blood[e]	≤ ±9.0	≤0.9

RE = relative error; RSD = relative standard deviation.
[a]Results from one analysis of six 1 ng/mL quality control (QC) standards and one analysis of three 1 ng/mL and three 25 ng/mL QC standards.
[b]Results from one analysis of six 3.0 ng/g QC standards (1 part tissue:2 parts water).
[e]Results from one analysis of four 150,000 ng/g samples diluted with blood at a 250-fold dilution.
[d]Results from two analyses of six 1 ng/mL QC standards.
[e]Results from one analysis of three 1 ng/mL and one analysis of three 25 ng/mL QC standards.

Table B-5. Storage Stability of 1,4-Dichlorobenzene in Sample Matrices

Matrix	Environment	Percent of Day 0
Sprague Dawley Rat Blood[a]	Ambient, light	81.1 to 110.6
Sprague Dawley Rat Blood[b]	–70°C, dark	74.7 to 88.7
Harlan Sprague Dawley Rat Liver[c]	–70°C, dark	99.0 to 110.9

[a]Four replicate quality control (QC) standards at three concentrations (1, 25, and 200 ng/mL); processed with internal standard (IS), stored at ambient temperature in the light for 21 days, and injected with freshly processed matrix calibration standards.
[b]Four replicate QC standards at three concentrations (1, 25, and 200 ng/mL); processed with IS, stored at –70°C for 149 days, and injected with freshly processed matrix calibration standards.
[c]Four replicate QC standards at three concentrations (3, 75, and 600 ng/g); stored at –70°C for 100 days and injected with freshly processed matrix calibration standards.

Appendix C. Animal Identifiers

Tables

Table C-1. Animal Numbers and FASTQ Data File Names for Female Rats Exposed to 1,4-Dichlorobenzene for Five Days

Animal Number	Selection	Group	Exposure Concentration (ppm)	Survived to Study Termination	Tissue	FASTQ File ID
1	Core Animals	Vehicle Control	0	Yes	Heart	4DR1F1HE_S118_R1_001.fastq.gz
1	Core Animals	Vehicle Control	0	Yes	Kidney	4DR1F1KI_S117_R1_001.fastq.gz
1	Core Animals	Vehicle Control	0	Yes	Liver	4DR1F1LI_S127_R1_001.fastq.gz
1	Core Animals	Vehicle Control	0	Yes	Lung	4DR1F1LU_S127_R1_001.fastq.gz
1	Core Animals	Vehicle Control	0	Yes	Ovary	4DR1F1OV_S53_R1_001.fastq.gz
2	Core Animals	Vehicle Control	0	Yes	Heart	4DR1F2HE_S149_R1_001.fastq.gz
2	Core Animals	Vehicle Control	0	Yes	Kidney	4DR1F2KI_S148_R1_001.fastq.gz
2	Core Animals	Vehicle Control	0	Yes	Liver	4DR1F2LI_S118_R1_001.fastq.gz
2	Core Animals	Vehicle Control	0	Yes	Lung	4DR1F2LU_S118_R1_001.fastq.gz[a]
2	Core Animals	Vehicle Control	0	Yes	Ovary	4DR1F2OV_S44_R1_001.fastq.gz
3	Core Animals	Vehicle Control	0	Yes	Heart	4DR1F3HE_S131_R1_001.fastq.gz
3	Core Animals	Vehicle Control	0	Yes	Kidney	4DR1F3KI_S130_R1_001.fastq.gz
3	Core Animals	Vehicle Control	0	Yes	Liver	4DR1F3LI_S140_R1_001.fastq.gz
3	Core Animals	Vehicle Control	0	Yes	Lung	4DR1F3LU_S140_R1_001.fastq.gz
3	Core Animals	Vehicle Control	0	Yes	Ovary	4DR1F3OV_S66_R1_001.fastq.gz
4	Core Animals	Vehicle Control	0	Yes	Heart	4DR1F4HE_S128_R1_001.fastq.gz
4	Core Animals	Vehicle Control	0	Yes	Kidney	4DR1F4KI_S127_R1_001.fastq.gz
4	Core Animals	Vehicle Control	0	Yes	Liver	4DR1F4LI_S137_R1_001.fastq.gz
4	Core Animals	Vehicle Control	0	Yes	Lung	4DR1F4LU_S137_R1_001.fastq.gz
4	Core Animals	Vehicle Control	0	Yes	Ovary	4DR1F4OV_S63_R1_001.fastq.gz
5	Core Animals	Vehicle Control	0	Yes	Heart	4DR1F5HE_S138_R1_001.fastq.gz
5	Core Animals	Vehicle Control	0	Yes	Kidney	4DR1F5KI_S137_R1_001.fastq.gz
5	Core Animals	Vehicle Control	0	Yes	Liver	4DR1F5LI_S147_R1_001.fastq.gz
5	Core Animals	Vehicle Control	0	Yes	Lung	4DR1F5LU_S147_R1_001.fastq.gz
5	Core Animals	Vehicle Control	0	Yes	Ovary	4DR1F5OV_S73_R1_001.fastq.gz
6	Core Animals	Vehicle Control	0	Yes	Heart	4DR1F6HE_S139_R1_001.fastq.gz
6	Core Animals	Vehicle Control	0	Yes	Kidney	4DR1F6KI_S138_R1_001.fastq.gz
6	Core Animals	Vehicle Control	0	Yes	Liver	4DR1F6LI_S148_R1_001.fastq.gz
6	Core Animals	Vehicle Control	0	Yes	Lung	4DR1F6LU_S148_R1_001.fastq.gz
6	Core Animals	Vehicle Control	0	Yes	Ovary	4DR1F6OV_S74_R1_001.fastq.gz
7	Core Animals	Vehicle Control	0	Yes	Heart	4DR1F7HE_S126_R1_001.fastq.gz
7	Core Animals	Vehicle Control	0	Yes	Kidney	4DR1F7KI_S125_R1_001.fastq.gz
7	Core Animals	Vehicle Control	0	Yes	Liver	4DR1F7LI_S135_R1_001.fastq.gz
7	Core Animals	Vehicle Control	0	Yes	Lung	4DR1F7LU_S135_R1_001.fastq.gz
7	Core Animals	Vehicle Control	0	Yes	Ovary	4DR1F7OV_S61_R1_001.fastq.gz
8	Core Animals	Vehicle Control	0	Yes	Heart	4DR1F8HE_S150_R1_001.fastq.gz
8	Core Animals	Vehicle Control	0	Yes	Kidney	4DR1F8KI_S149_R1_001.fastq.gz

Animal Number	Selection	Group	Exposure Concentration (ppm)	Survived to Study Termination	Tissue	FASTQ File ID
8	Core Animals	Vehicle Control	0	Yes	Liver	4DR1F8LI_S119_R1_001.fastq.gz
8	Core Animals	Vehicle Control	0	Yes	Lung	4DR1F8LU_S119_R1_001.fastq.gz[a]
8	Core Animals	Vehicle Control	0	Yes	Ovary	4DR1F8OV_S45_R1_001.fastq.gz
9	Core Animals	Vehicle Control	0	Yes	Heart	4DR1F9HE_S133_R1_001.fastq.gz
9	Core Animals	Vehicle Control	0	Yes	Kidney	4DR1F9KI_S132_R1_001.fastq.gz
9	Core Animals	Vehicle Control	0	Yes	Liver	4DR1F9LI_S142_R1_001.fastq.gz
9	Core Animals	Vehicle Control	0	Yes	Lung	4DR1F9LU_S142_R1_001.fastq.gz
9	Core Animals	Vehicle Control	0	Yes	Ovary	4DR1F9OV_S68_R1_001.fastq.gz
10	Core Animals	Vehicle Control	0	Yes	Heart	4DR1F10HE_S132_R1_001.fastq.gz
10	Core Animals	Vehicle Control	0	Yes	Kidney	4DR1F10KI_S131_R1_001.fastq.gz
10	Core Animals	Vehicle Control	0	Yes	Liver	4DR1F10LI_S141_R1_001.fastq.gz
10	Core Animals	Vehicle Control	0	Yes	Lung	4DR1F10LU_S141_R1_001.fastq.gz
10	Core Animals	Vehicle Control	0	Yes	Ovary	4DR1F10OV_S67_R1_001.fastq.gz
11	ICA Animals	Vehicle Control	0	Yes	None	NA
12	ICA Animals	Vehicle Control	0	Yes	None	NA
13	ICA Animals	Vehicle Control	0	Yes	None	NA
101	Core Animals	1,4-Dichlorobenzene	1	Yes	Heart	4DR2F101HE_S140_R1_001.fastq.gz
101	Core Animals	1,4-Dichlorobenzene	1	Yes	Kidney	4DR2F101KI_S139_R1_001.fastq.gz
101	Core Animals	1,4-Dichlorobenzene	1	Yes	Liver	4DR2F101LI_S149_R1_001.fastq.gz
101	Core Animals	1,4-Dichlorobenzene	1	Yes	Lung	4DR2F101LU_S149_R1_001.fastq.gz
101	Core Animals	1,4-Dichlorobenzene	1	Yes	Ovary	4DR2F101OV_S75_R1_001.fastq.gz
102	Core Animals	1,4-Dichlorobenzene	1	Yes	Heart	4DR2F102HE_S152_R1_001.fastq.gz
102	Core Animals	1,4-Dichlorobenzene	1	Yes	Kidney	4DR2F102KI_S151_R1_001.fastq.gz
102	Core Animals	1,4-Dichlorobenzene	1	Yes	Liver	4DR2F102LI_S121_R1_001.fastq.gz
102	Core Animals	1,4-Dichlorobenzene	1	Yes	Lung	4DR2F102LU_S121_R1_001.fastq.gz[a]
102	Core Animals	1,4-Dichlorobenzene	1	Yes	Ovary	4DR2F102OV_S47_R1_001.fastq.gz
103	Core Animals	1,4-Dichlorobenzene	1	Yes	Heart	4DR2F103HE_S144_R1_001.fastq.gz
103	Core Animals	1,4-Dichlorobenzene	1	Yes	Kidney	4DR2F103KI_S143_R1_001.fastq.gz
103	Core Animals	1,4-Dichlorobenzene	1	Yes	Liver	4DR2F103LI_S153_R1_001.fastq.gz
103	Core Animals	1,4-Dichlorobenzene	1	Yes	Lung	4DR2F103LU_S153_R1_001.fastq.gz
103	Core Animals	1,4-Dichlorobenzene	1	Yes	Ovary	4DR2F103OV_S79_R1_001.fastq.gz
104	Core Animals	1,4-Dichlorobenzene	1	Yes	Heart	4DR2F104HE_S119_R1_001.fastq.gz
104	Core Animals	1,4-Dichlorobenzene	1	Yes	Kidney	4DR2F104KI_S118_R1_001.fastq.gz
104	Core Animals	1,4-Dichlorobenzene	1	Yes	Liver	4DR2F104LI_S128_R1_001.fastq.gz
104	Core Animals	1,4-Dichlorobenzene	1	Yes	Lung	4DR2F104LU_S128_R1_001.fastq.gz
104	Core Animals	1,4-Dichlorobenzene	1	Yes	Ovary	4DR2F104OV_S54_R1_001.fastq.gz
105	Core Animals	1,4-Dichlorobenzene	1	Yes	Heart	4DR2F105HE_S113_R1_001.fastq.gz
105	Core Animals	1,4-Dichlorobenzene	1	Yes	Kidney	NA
105	Core Animals	1,4-Dichlorobenzene	1	Yes	Liver	4DR2F105LI_S122_R1_001.fastq.gz

Animal Number	Selection	Group	Exposure Concentration (ppm)	Survived to Study Termination	Tissue	FASTQ File ID
105	Core Animals	1,4-Dichlorobenzene	1	Yes	Lung	4DR2F105LU_S122_R1_001.fastq.gz
105	Core Animals	1,4-Dichlorobenzene	1	Yes	Ovary	4DR2F105OV_S48_R1_001.fastq.gz
106	ICA Animals	1,4-Dichlorobenzene	1	Yes	None	NA
107	ICA Animals	1,4-Dichlorobenzene	1	Yes	None	NA
108	ICA Animals	1,4-Dichlorobenzene	1	Yes	None	NA
201	Core Animals	1,4-Dichlorobenzene	10	Yes	Heart	4DR3F201HE_S129_R1_001.fastq.gz
201	Core Animals	1,4-Dichlorobenzene	10	Yes	Kidney	4DR3F201KI_S128_R1_001.fastq.gz
201	Core Animals	1,4-Dichlorobenzene	10	Yes	Liver	4DR3F201LI_S138_R1_001.fastq.gz
201	Core Animals	1,4-Dichlorobenzene	10	Yes	Lung	4DR3F201LU_S138_R1_001.fastq.gz
201	Core Animals	1,4-Dichlorobenzene	10	Yes	Ovary	4DR3F201OV_S64_R1_001.fastq.gz
202	Core Animals	1,4-Dichlorobenzene	10	Yes	Heart	4DR3F202HE_S123_R1_001.fastq.gz
202	Core Animals	1,4-Dichlorobenzene	10	Yes	Kidney	4DR3F202KI_S122_R1_001.fastq.gz
202	Core Animals	1,4-Dichlorobenzene	10	Yes	Liver	4DR3F202LI_S132_R1_001.fastq.gz
202	Core Animals	1,4-Dichlorobenzene	10	Yes	Lung	4DR3F202LU_S132_R1_001.fastq.gz
202	Core Animals	1,4-Dichlorobenzene	10	Yes	Ovary	4DR3F202OV_S58_R1_001.fastq.gz
203	Core Animals	1,4-Dichlorobenzene	10	Yes	Heart	4DR3F203HE_S134_R1_001.fastq.gz
203	Core Animals	1,4-Dichlorobenzene	10	Yes	Kidney	4DR3F203KI_S133_R1_001.fastq.gz
203	Core Animals	1,4-Dichlorobenzene	10	Yes	Liver	4DR3F203LI_S143_R1_001.fastq.gz
203	Core Animals	1,4-Dichlorobenzene	10	Yes	Lung	4DR3F203LU_S143_R1_001.fastq.gz
203	Core Animals	1,4-Dichlorobenzene	10	Yes	Ovary	4DR3F203OV_S69_R1_001.fastq.gz
204	Core Animals	1,4-Dichlorobenzene	10	Yes	Heart	4DR3F204HE_S151_R1_001.fastq.gz
204	Core Animals	1,4-Dichlorobenzene	10	Yes	Kidney	4DR3F204KI_S150_R1_001.fastq.gz
204	Core Animals	1,4-Dichlorobenzene	10	Yes	Liver	4DR3F204LI_S120_R1_001.fastq.gz
204	Core Animals	1,4-Dichlorobenzene	10	Yes	Lung	4DR3F204LU_S120_R1_001.fastq.gz[a]
204	Core Animals	1,4-Dichlorobenzene	10	Yes	Ovary	4DR3F204OV_S46_R1_001.fastq.gz
205	Core Animals	1,4-Dichlorobenzene	10	Yes	Heart	4DR3F205HE_S130_R1_001.fastq.gz
205	Core Animals	1,4-Dichlorobenzene	10	Yes	Kidney	4DR3F205KI_S129_R1_001.fastq.gz
205	Core Animals	1,4-Dichlorobenzene	10	Yes	Liver	4DR3F205LI_S139_R1_001.fastq.gz
205	Core Animals	1,4-Dichlorobenzene	10	Yes	Lung	4DR3F205LU_S139_R1_001.fastq.gz
205	Core Animals	1,4-Dichlorobenzene	10	Yes	Ovary	4DR3F205OV_S65_R1_001.fastq.gz
206	ICA Animals	1,4-Dichlorobenzene	10	Yes	None	NA
207	ICA Animals	1,4-Dichlorobenzene	10	Yes	None	NA
208	ICA Animals	1,4-Dichlorobenzene	10	Yes	None	NA
301	Core Animals	1,4-Dichlorobenzene	50	Yes	Heart	4DR4F301HE_S135_R1_001.fastq.gz
301	Core Animals	1,4-Dichlorobenzene	50	Yes	Kidney	4DR4F301KI_S134_R1_001.fastq.gz
301	Core Animals	1,4-Dichlorobenzene	50	Yes	Liver	4DR4F301LI_S144_R1_001.fastq.gz
301	Core Animals	1,4-Dichlorobenzene	50	Yes	Lung	4DR4F301LU_S144_R1_001.fastq.gz
301	Core Animals	1,4-Dichlorobenzene	50	Yes	Ovary	4DR4F301OV_S70_R1_001.fastq.gz
302	Core Animals	1,4-Dichlorobenzene	50	Yes	Heart	4DR4F302HE_S114_R1_001.fastq.gz

Animal Number	Selection	Group	Exposure Concentration (ppm)	Survived to Study Termination	Tissue	FASTQ File ID
302	Core Animals	1,4-Dichlorobenzene	50	Yes	Kidney	4DR4F302KI_S113_R1_001.fastq.gz
302	Core Animals	1,4-Dichlorobenzene	50	Yes	Liver	4DR4F302LI_S123_R1_001.fastq.gz
302	Core Animals	1,4-Dichlorobenzene	50	Yes	Lung	4DR4F302LU_S123_R1_001.fastq.gz
302	Core Animals	1,4-Dichlorobenzene	50	Yes	Ovary	4DR4F302OV_S49_R1_001.fastq.gz
303	Core Animals	1,4-Dichlorobenzene	50	Yes	Heart	4DR4F303HE_S143_R1_001.fastq.gz
303	Core Animals	1,4-Dichlorobenzene	50	Yes	Kidney	4DR4F303KI_S142_R1_001.fastq.gz
303	Core Animals	1,4-Dichlorobenzene	50	Yes	Liver	4DR4F303LI_S152_R1_001.fastq.gz
303	Core Animals	1,4-Dichlorobenzene	50	Yes	Lung	4DR4F303LU_S152_R1_001.fastq.gz
303	Core Animals	1,4-Dichlorobenzene	50	Yes	Ovary	4DR4F303OV_S78_R1_001.fastq.gz
304	Core Animals	1,4-Dichlorobenzene	50	Yes	Heart	4DR4F304HE_S116_R1_001.fastq.gz
304	Core Animals	1,4-Dichlorobenzene	50	Yes	Kidney	4DR4F304KI_S115_R1_001.fastq.gz
304	Core Animals	1,4-Dichlorobenzene	50	Yes	Liver	4DR4F304LI_S125_R1_001.fastq.gz
304	Core Animals	1,4-Dichlorobenzene	50	Yes	Lung	4DR4F304LU_S125_R1_001.fastq.gz
304	Core Animals	1,4-Dichlorobenzene	50	Yes	Ovary	4DR4F304OV_S51_R1_001.fastq.gz
305	Core Animals	1,4-Dichlorobenzene	50	Yes	Heart	4DR4F305HE_S121_R1_001.fastq.gz
305	Core Animals	1,4-Dichlorobenzene	50	Yes	Kidney	4DR4F305KI_S120_R1_001.fastq.gz
305	Core Animals	1,4-Dichlorobenzene	50	Yes	Liver	4DR4F305LI_S130_R1_001.fastq.gz
305	Core Animals	1,4-Dichlorobenzene	50	Yes	Lung	4DR4F305LU_S130_R1_001.fastq.gz
305	Core Animals	1,4-Dichlorobenzene	50	Yes	Ovary	4DR4F305OV_S56_R1_001.fastq.gz
306	ICA Animals	1,4-Dichlorobenzene	50	Yes	None	NA
307	ICA Animals	1,4-Dichlorobenzene	50	Yes	None	NA
308	ICA Animals	1,4-Dichlorobenzene	50	Yes	None	NA
401	Core Animals	1,4-Dichlorobenzene	150	Yes	Heart	4DR5F401HE_S146_R1_001.fastq.gz
401	Core Animals	1,4-Dichlorobenzene	150	Yes	Kidney	4DR5F401KI_S145_R1_001.fastq.gz
401	Core Animals	1,4-Dichlorobenzene	150	Yes	Liver	4DR5F401LI_S155_R1_001.fastq.gz
401	Core Animals	1,4-Dichlorobenzene	150	Yes	Lung	4DR5F401LU_S155_R1_001.fastq.gz
401	Core Animals	1,4-Dichlorobenzene	150	Yes	Ovary	4DR5F401OV_S81_R1_001.fastq.gz
402	Core Animals	1,4-Dichlorobenzene	150	Yes	Heart	4DR5F402HE_S148_R1_001.fastq.gz
402	Core Animals	1,4-Dichlorobenzene	150	Yes	Kidney	4DR5F402KI_S147_R1_001.fastq.gz
402	Core Animals	1,4-Dichlorobenzene	150	Yes	Liver	4DR5F402LI_S117_R1_001.fastq.gz
402	Core Animals	1,4-Dichlorobenzene	150	Yes	Lung	4DR5F402LU_S117_R1_001.fastq.gz[a]
402	Core Animals	1,4-Dichlorobenzene	150	Yes	Ovary	4DR5F402OV_S43_R1_001.fastq.gz
403	Core Animals	1,4-Dichlorobenzene	150	Yes	Heart	4DR5F403HE_S137_R1_001.fastq.gz
403	Core Animals	1,4-Dichlorobenzene	150	Yes	Kidney	4DR5F403KI_S136_R1_001.fastq.gz
403	Core Animals	1,4-Dichlorobenzene	150	Yes	Liver	4DR5F403LI_S146_R1_001.fastq.gz
403	Core Animals	1,4-Dichlorobenzene	150	Yes	Lung	4DR5F403LU_S146_R1_001.fastq.gz
403	Core Animals	1,4-Dichlorobenzene	150	Yes	Ovary	4DR5F403OV_S72_R1_001.fastq.gz
404	Core Animals	1,4-Dichlorobenzene	150	Yes	Heart	4DR5F404HE_S117_R1_001.fastq.gz
404	Core Animals	1,4-Dichlorobenzene	150	Yes	Kidney	4DR5F404KI_S116_R1_001.fastq.gz

Animal Number	Selection	Group	Exposure Concentration (ppm)	Survived to Study Termination	Tissue	FASTQ File ID
404	Core Animals	1,4-Dichlorobenzene	150	Yes	Liver	4DR5F404LI_S126_R1_001.fastq.gz
404	Core Animals	1,4-Dichlorobenzene	150	Yes	Lung	4DR5F404LU_S126_R1_001.fastq.gz
404	Core Animals	1,4-Dichlorobenzene	150	Yes	Ovary	4DR5F404OV_S52_R1_001.fastq.gz
405	Core Animals	1,4-Dichlorobenzene	150	Yes	Heart	4DR5F405HE_S127_R1_001.fastq.gz
405	Core Animals	1,4-Dichlorobenzene	150	Yes	Kidney	4DR5F405KI_S126_R1_001.fastq.gz
405	Core Animals	1,4-Dichlorobenzene	150	Yes	Liver	4DR5F405LI_S136_R1_001.fastq.gz
405	Core Animals	1,4-Dichlorobenzene	150	Yes	Lung	4DR5F405LU_S136_R1_001.fastq.gz
405	Core Animals	1,4-Dichlorobenzene	150	Yes	Ovary	4DR5F405OV_S62_R1_001.fastq.gz
406	ICA Animals	1,4-Dichlorobenzene	150	Yes	None	NA
407	ICA Animals	1,4-Dichlorobenzene	150	Yes	None	NA
408	ICA Animals	1,4-Dichlorobenzene	150	Yes	None	NA
501	Core Animals	1,4-Dichlorobenzene	400	Yes	Heart	4DR6F501HE_S145_R1_001.fastq.gz
501	Core Animals	1,4-Dichlorobenzene	400	Yes	Kidney	4DR6F501KI_S144_R1_001.fastq.gz
501	Core Animals	1,4-Dichlorobenzene	400	Yes	Liver	4DR6F501LI_S154_R1_001.fastq.gz
501	Core Animals	1,4-Dichlorobenzene	400	Yes	Lung	4DR6F501LU_S154_R1_001.fastq.gz
501	Core Animals	1,4-Dichlorobenzene	400	Yes	Ovary	4DR6F501OV_S80_R1_001.fastq.gz
502	Core Animals	1,4-Dichlorobenzene	400	Yes	Heart	4DR6F502HE_S147_R1_001.fastq.gz
502	Core Animals	1,4-Dichlorobenzene	400	Yes	Kidney	4DR6F502KI_S146_R1_001.fastq.gz
502	Core Animals	1,4-Dichlorobenzene	400	Yes	Liver	4DR6F502LI_S156_R1_001.fastq.gz
502	Core Animals	1,4-Dichlorobenzene	400	Yes	Lung	4DR6F502LU_S156_R1_001.fastq.gz[b]
502	Core Animals	1,4-Dichlorobenzene	400	Yes	Ovary	4DR6F502OV_S82_R1_001.fastq.gz
503	Core Animals	1,4-Dichlorobenzene	400	Yes	Heart	4DR6F503HE_S115_R1_001.fastq.gz
503	Core Animals	1,4-Dichlorobenzene	400	Yes	Kidney	4DR6F503KI_S114_R1_001.fastq.gz
503	Core Animals	1,4-Dichlorobenzene	400	Yes	Liver	4DR6F503LI_S124_R1_001.fastq.gz
503	Core Animals	1,4-Dichlorobenzene	400	Yes	Lung	4DR6F503LU_S124_R1_001.fastq.gz
503	Core Animals	1,4-Dichlorobenzene	400	Yes	Ovary	4DR6F503OV_S50_R1_001.fastq.gz
504	Core Animals	1,4-Dichlorobenzene	400	Yes	Heart	4DR6F504HE_S141_R1_001.fastq.gz
504	Core Animals	1,4-Dichlorobenzene	400	Yes	Kidney	4DR6F504KI_S140_R1_001.fastq.gz
504	Core Animals	1,4-Dichlorobenzene	400	Yes	Liver	4DR6F504LI_S150_R1_001.fastq.gz
504	Core Animals	1,4-Dichlorobenzene	400	Yes	Lung	4DR6F504LU_S150_R1_001.fastq.gz[b]
504	Core Animals	1,4-Dichlorobenzene	400	Yes	Ovary	4DR6F504OV_S76_R1_001.fastq.gz
505	Core Animals	1,4-Dichlorobenzene	400	Yes	Heart	4DR6F505HE_S136_R1_001.fastq.gz
505	Core Animals	1,4-Dichlorobenzene	400	Yes	Kidney	4DR6F505KI_S135_R1_001.fastq.gz
505	Core Animals	1,4-Dichlorobenzene	400	Yes	Liver	4DR6F505LI_S145_R1_001.fastq.gz
505	Core Animals	1,4-Dichlorobenzene	400	Yes	Lung	4DR6F505LU_S145_R1_001.fastq.gz
505	Core Animals	1,4-Dichlorobenzene	400	Yes	Ovary	4DR6F505OV_S71_R1_001.fastq.gz
506	ICA Animals	1,4-Dichlorobenzene	400	Yes	None	NA
507	ICA Animals	1,4-Dichlorobenzene	400	Yes	None	NA
508	ICA Animals	1,4-Dichlorobenzene	400	Yes	None	NA

Animal Number	Selection	Group	Exposure Concentration (ppm)	Survived to Study Termination	Tissue	FASTQ File ID
601	Core Animals	1,4-Dichlorobenzene	800	Yes	Heart	4DR7F601HE_S124_R1_001.fastq.gz
601	Core Animals	1,4-Dichlorobenzene	800	Yes	Kidney	4DR7F601KI_S123_R1_001.fastq.gz
601	Core Animals	1,4-Dichlorobenzene	800	Yes	Liver	4DR7F601LI_S133_R1_001.fastq.gz
601	Core Animals	1,4-Dichlorobenzene	800	Yes	Lung	4DR7F601LU_S133_R1_001.fastq.gz
601	Core Animals	1,4-Dichlorobenzene	800	Yes	Ovary	4DR7F601OV_S59_R1_001.fastq.gz
602	Core Animals	1,4-Dichlorobenzene	800	Yes	Heart	4DR7F602HE_S120_R1_001.fastq.gz
602	Core Animals	1,4-Dichlorobenzene	800	Yes	Kidney	4DR7F602KI_S119_R1_001.fastq.gz
602	Core Animals	1,4-Dichlorobenzene	800	Yes	Liver	4DR7F602LI_S129_R1_001.fastq.gz
602	Core Animals	1,4-Dichlorobenzene	800	Yes	Lung	4DR7F602LU_S129_R1_001.fastq.gz
602	Core Animals	1,4-Dichlorobenzene	800	Yes	Ovary	4DR7F602OV_S55_R1_001.fastq.gz
603	Core Animals	1,4-Dichlorobenzene	800	Yes	Heart	4DR7F603HE_S122_R1_001.fastq.gz
603	Core Animals	1,4-Dichlorobenzene	800	Yes	Kidney	4DR7F603KI_S121_R1_001.fastq.gz
603	Core Animals	1,4-Dichlorobenzene	800	Yes	Liver	4DR7F603LI_S131_R1_001.fastq.gz
603	Core Animals	1,4-Dichlorobenzene	800	Yes	Lung	4DR7F603LU_S131_R1_001.fastq.gz
603	Core Animals	1,4-Dichlorobenzene	800	Yes	Ovary	4DR7F603OV_S57_R1_001.fastq.gz
604	Core Animals	1,4-Dichlorobenzene	800	Yes	Heart	4DR7F604HE_S142_R1_001.fastq.gz
604	Core Animals	1,4-Dichlorobenzene	800	Yes	Kidney	4DR7F604KI_S141_R1_001.fastq.gz
604	Core Animals	1,4-Dichlorobenzene	800	Yes	Liver	4DR7F604LI_S151_R1_001.fastq.gz
604	Core Animals	1,4-Dichlorobenzene	800	Yes	Lung	4DR7F604LU_S151_R1_001.fastq.gz
604	Core Animals	1,4-Dichlorobenzene	800	Yes	Ovary	4DR7F604OV_S77_R1_001.fastq.gz
605	Core Animals	1,4-Dichlorobenzene	800	Yes	Heart	4DR7F605HE_S125_R1_001.fastq.gz
605	Core Animals	1,4-Dichlorobenzene	800	Yes	Kidney	4DR7F605KI_S124_R1_001.fastq.gz
605	Core Animals	1,4-Dichlorobenzene	800	Yes	Liver	4DR7F605LI_S134_R1_001.fastq.gz
605	Core Animals	1,4-Dichlorobenzene	800	Yes	Lung	4DR7F605LU_S134_R1_001.fastq.gz
605	Core Animals	1,4-Dichlorobenzene	800	Yes	Ovary	4DR7F605OV_S60_R1_001.fastq.gz
606	ICA Animals	1,4-Dichlorobenzene	800	Yes	None	NA
607	ICA Animals	1,4-Dichlorobenzene	800	Yes	None	NA
608	ICA Animals	1,4-Dichlorobenzene	800	No	None	NA

ICA = internal concentration assessment; NA = no transcriptomics data collected for selected animal.
[a]Removed due to quality control fail.
[b]Removed due to principal component analysis/inter-replicate correlation analysis outlier.

Table C-2. Animal Numbers and FASTQ Data File Names for Female Mice Exposed to 1,4-Dichlorobenzene for Five Days

Animal Number	Selection	Group	Exposure Concentration (ppm)	Survived to Study Termination	Tissue	FASTQ File ID
1	Core Animals	Vehicle Control	0	Yes	Heart	4DM1F1HE_S43_R1_001.fastq.gz
1	Core Animals	Vehicle Control	0	Yes	Kidney	4DM1F1KI_S43_R1_001.fastq.gz[a]
1	Core Animals	Vehicle Control	0	Yes	Liver	4DM1F1LI_S49_R1_001.fastq.gz
1	Core Animals	Vehicle Control	0	Yes	Lung	4DM1F1LU_S49_R1_001.fastq.gz

Animal Number	Selection	Group	Exposure Concentration (ppm)	Survived to Study Termination	Tissue	FASTQ File ID
1	Core Animals	Vehicle Control	0	Yes	Ovary	4DM1F1OV_S131_R1_001.fastq.gz
2	Core Animals	Vehicle Control	0	Yes	Heart	4DM1F2HE_S66_R1_001.fastq.gz
2	Core Animals	Vehicle Control	0	Yes	Kidney	4DM1F2KI_S66_R1_001.fastq.gz
2	Core Animals	Vehicle Control	0	Yes	Liver	4DM1F2LI_S72_R1_001.fastq.gz
2	Core Animals	Vehicle Control	0	Yes	Lung	4DM1F2LU_S72_R1_001.fastq.gz
2	Core Animals	Vehicle Control	0	Yes	Ovary	4DM1F2OV_S154_R1_001.fastq.gz
3	Core Animals	Vehicle Control	0	Yes	Heart	4DM1F3HE_S41_R1_001.fastq.gz
3	Core Animals	Vehicle Control	0	Yes	Kidney	4DM1F3KI_S41_R1_001.fastq.gz
3	Core Animals	Vehicle Control	0	Yes	Liver	4DM1F3LI_S47_R1_001.fastq.gz
3	Core Animals	Vehicle Control	0	Yes	Lung	4DM1F3LU_S47_R1_001.fastq.gz
3	Core Animals	Vehicle Control	0	Yes	Ovary	4DM1F3OV_S129_R1_001.fastq.gz
4	Core Animals	Vehicle Control	0	Yes	Heart	4DM1F4HE_S53_R1_001.fastq.gz
4	Core Animals	Vehicle Control	0	Yes	Kidney	4DM1F4KI_S53_R1_001.fastq.gz[a]
4	Core Animals	Vehicle Control	0	Yes	Liver	4DM1F4LI_S59_R1_001.fastq.gz
4	Core Animals	Vehicle Control	0	Yes	Lung	4DM1F4LU_S59_R1_001.fastq.gz
4	Core Animals	Vehicle Control	0	Yes	Ovary	4DM1F4OV_S141_R1_001.fastq.gz
5	Core Animals	Vehicle Control	0	Yes	Heart	4DM1F5HE_S61_R1_001.fastq.gz
5	Core Animals	Vehicle Control	0	Yes	Kidney	4DM1F5KI_S61_R1_001.fastq.gz[a]
5	Core Animals	Vehicle Control	0	Yes	Liver	4DM1F5LI_S67_R1_001.fastq.gz
5	Core Animals	Vehicle Control	0	Yes	Lung	4DM1F5LU_S67_R1_001.fastq.gz
5	Core Animals	Vehicle Control	0	Yes	Ovary	4DM1F5OV_S149_R1_001.fastq.gz
6	Core Animals	Vehicle Control	0	Yes	Heart	4DM1F6HE_S58_R1_001.fastq.gz
6	Core Animals	Vehicle Control	0	Yes	Kidney	4DM1F6KI_S58_R1_001.fastq.gz
6	Core Animals	Vehicle Control	0	Yes	Liver	4DM1F6LI_S64_R1_001.fastq.gz[b]
6	Core Animals	Vehicle Control	0	Yes	Lung	4DM1F6LU_S64_R1_001.fastq.gz
6	Core Animals	Vehicle Control	0	Yes	Ovary	4DM1F6OV_S146_R1_001.fastq.gz
7	Core Animals	Vehicle Control	0	Yes	Heart	4DM1F7HE_S71_R1_001.fastq.gz
7	Core Animals	Vehicle Control	0	Yes	Kidney	4DM1F7KI_S71_R1_001.fastq.gz
7	Core Animals	Vehicle Control	0	Yes	Liver	4DM1F7LI_S42_R1_001.fastq.gz
7	Core Animals	Vehicle Control	0	Yes	Lung	4DM1F7LU_S42_R1_001.fastq.gz
7	Core Animals	Vehicle Control	0	Yes	Ovary	4DM1F7OV_S124_R1_001.fastq.gz
8	Core Animals	Vehicle Control	0	Yes	Heart	4DM1F8HE_S59_R1_001.fastq.gz
8	Core Animals	Vehicle Control	0	Yes	Kidney	4DM1F8KI_S59_R1_001.fastq.gz
8	Core Animals	Vehicle Control	0	Yes	Liver	4DM1F8LI_S65_R1_001.fastq.gz[b]
8	Core Animals	Vehicle Control	0	Yes	Lung	4DM1F8LU_S65_R1_001.fastq.gz
8	Core Animals	Vehicle Control	0	Yes	Ovary	4DM1F8OV_S147_R1_001.fastq.gz
9	Core Animals	Vehicle Control	0	Yes	Heart	4DM1F9HE_S57_R1_001.fastq.gz

Animal Number	Selection	Group	Exposure Concentration (ppm)	Survived to Study Termination	Tissue	FASTQ File ID
9	Core Animals	Vehicle Control	0	Yes	Kidney	4DM1F9KI_S57_R1_001.fastq.gz[b]
9	Core Animals	Vehicle Control	0	Yes	Liver	4DM1F9LI_S63_R1_001.fastq.gz[b]
9	Core Animals	Vehicle Control	0	Yes	Lung	4DM1F9LU_S63_R1_001.fastq.gz
9	Core Animals	Vehicle Control	0	Yes	Ovary	4DM1F9OV_S145_R1_001.fastq.gz
10	Core Animals	Vehicle Control	0	Yes	Heart	4DM1F10HE_S72_R1_001.fastq.gz
10	Core Animals	Vehicle Control	0	Yes	Kidney	4DM1F10KI_S72_R1_001.fastq.gz
10	Core Animals	Vehicle Control	0	Yes	Liver	4DM1F10LI_S43_R1_001.fastq.gz
10	Core Animals	Vehicle Control	0	Yes	Lung	4DM1F10LU_S43_R1_001.fastq.gz
10	Core Animals	Vehicle Control	0	Yes	Ovary	4DM1F10OV_S125_R1_001.fastq.gz
11	ICA Animals	Vehicle Control	0	Yes	None	NA
12	ICA Animals	Vehicle Control	0	Yes	None	NA
13	ICA Animals	Vehicle Control	0	Yes	None	NA
101	Core Animals	1,4-Dichlorobenzene	1	Yes	Heart	4DM2F101HE_S50_R1_001.fastq.gz
101	Core Animals	1,4-Dichlorobenzene	1	Yes	Kidney	4DM2F101KI_S50_R1_001.fastq.gz
101	Core Animals	1,4-Dichlorobenzene	1	Yes	Liver	4DM2F101LI_S56_R1_001.fastq.gz
101	Core Animals	1,4-Dichlorobenzene	1	Yes	Lung	4DM2F101LU_S56_R1_001.fastq.gz
101	Core Animals	1,4-Dichlorobenzene	1	Yes	Ovary	4DM2F101OV_S138_R1_001.fastq.gz
102	Core Animals	1,4-Dichlorobenzene	1	Yes	Heart	4DM2F102HE_S52_R1_001.fastq.gz
102	Core Animals	1,4-Dichlorobenzene	1	Yes	Kidney	4DM2F102KI_S52_R1_001.fastq.gz
102	Core Animals	1,4-Dichlorobenzene	1	Yes	Liver	4DM2F102LI_S58_R1_001.fastq.gz
102	Core Animals	1,4-Dichlorobenzene	1	Yes	Lung	4DM2F102LU_S58_R1_001.fastq.gz
102	Core Animals	1,4-Dichlorobenzene	1	Yes	Ovary	4DM2F102OV_S140_R1_001.fastq.gz
103	Core Animals	1,4-Dichlorobenzene	1	Yes	Heart	4DM2F103HE_S62_R1_001.fastq.gz
103	Core Animals	1,4-Dichlorobenzene	1	Yes	Kidney	4DM2F103KI_S62_R1_001.fastq.gz
103	Core Animals	1,4-Dichlorobenzene	1	Yes	Liver	4DM2F103LI_S68_R1_001.fastq.gz
103	Core Animals	1,4-Dichlorobenzene	1	Yes	Lung	4DM2F103LU_S68_R1_001.fastq.gz
103	Core Animals	1,4-Dichlorobenzene	1	Yes	Ovary	4DM2F103OV_S150_R1_001.fastq.gz
104	Core Animals	1,4-Dichlorobenzene	1	Yes	Heart	4DM2F104HE_S44_R1_001.fastq.gz
104	Core Animals	1,4-Dichlorobenzene	1	Yes	Kidney	4DM2F104KI_S44_R1_001.fastq.gz
104	Core Animals	1,4-Dichlorobenzene	1	Yes	Liver	4DM2F104LI_S50_R1_001.fastq.gz
104	Core Animals	1,4-Dichlorobenzene	1	Yes	Lung	4DM2F104LU_S50_R1_001.fastq.gz
104	Core Animals	1,4-Dichlorobenzene	1	Yes	Ovary	4DM2F104OV_S132_R1_001.fastq.gz
105	Core Animals	1,4-Dichlorobenzene	1	Yes	Heart	4DM2F105HE_S38_R1_001.fastq.gz
105	Core Animals	1,4-Dichlorobenzene	1	Yes	Kidney	4DM2F105KI_S38_R1_001.fastq.gz[a]
105	Core Animals	1,4-Dichlorobenzene	1	Yes	Liver	4DM2F105LI_S44_R1_001.fastq.gz
105	Core Animals	1,4-Dichlorobenzene	1	Yes	Lung	4DM2F105LU_S44_R1_001.fastq.gz
105	Core Animals	1,4-Dichlorobenzene	1	Yes	Ovary	4DM2F105OV_S126_R1_001.fastq.gz

Animal Number	Selection	Group	Exposure Concentration (ppm)	Survived to Study Termination	Tissue	FASTQ File ID
106	ICA Animals	1,4-Dichlorobenzene	1	Yes	None	NA
107	ICA Animals	1,4-Dichlorobenzene	1	Yes	None	NA
108	ICA Animals	1,4-Dichlorobenzene	1	Yes	None	NA
201	Core Animals	1,4-Dichlorobenzene	10	Yes	Heart	4DM3F201HE_S49_R1_001.fastq.gz
201	Core Animals	1,4-Dichlorobenzene	10	Yes	Kidney	4DM3F201KI_S49_R1_001.fastq.gz
201	Core Animals	1,4-Dichlorobenzene	10	Yes	Liver	4DM3F201LI_S55_R1_001.fastq.gz
201	Core Animals	1,4-Dichlorobenzene	10	Yes	Lung	4DM3F201LU_S55_R1_001.fastq.gz
201	Core Animals	1,4-Dichlorobenzene	10	Yes	Ovary	4DM3F201OV_S137_R1_001.fastq.gz
202	Core Animals	1,4-Dichlorobenzene	10	Yes	Heart	4DM3F202HE_S48_R1_001.fastq.gz
202	Core Animals	1,4-Dichlorobenzene	10	Yes	Kidney	4DM3F202KI_S48_R1_001.fastq.gz[a]
202	Core Animals	1,4-Dichlorobenzene	10	Yes	Liver	4DM3F202LI_S54_R1_001.fastq.gz
202	Core Animals	1,4-Dichlorobenzene	10	Yes	Lung	4DM3F202LU_S54_R1_001.fastq.gz
202	Core Animals	1,4-Dichlorobenzene	10	Yes	Ovary	4DM3F202OV_S136_R1_001.fastq.gz
203	Core Animals	1,4-Dichlorobenzene	10	Yes	Heart	4DM3F203HE_S54_R1_001.fastq.gz
203	Core Animals	1,4-Dichlorobenzene	10	Yes	Kidney	4DM3F203KI_S54_R1_001.fastq.gz
203	Core Animals	1,4-Dichlorobenzene	10	Yes	Liver	4DM3F203LI_S60_R1_001.fastq.gz
203	Core Animals	1,4-Dichlorobenzene	10	Yes	Lung	4DM3F203LU_S60_R1_001.fastq.gz
203	Core Animals	1,4-Dichlorobenzene	10	Yes	Ovary	4DM3F203OV_S142_R1_001.fastq.gz
204	Core Animals	1,4-Dichlorobenzene	10	Yes	Heart	4DM3F204HE_S60_R1_001.fastq.gz
204	Core Animals	1,4-Dichlorobenzene	10	Yes	Kidney	4DM3F204KI_S60_R1_001.fastq.gz
204	Core Animals	1,4-Dichlorobenzene	10	Yes	Liver	4DM3F204LI_S66_R1_001.fastq.gz[b]
204	Core Animals	1,4-Dichlorobenzene	10	Yes	Lung	4DM3F204LU_S66_R1_001.fastq.gz
204	Core Animals	1,4-Dichlorobenzene	10	Yes	Ovary	4DM3F204OV_S148_R1_001.fastq.gz
205	Core Animals	1,4-Dichlorobenzene	10	Yes	Heart	4DM3F205HE_S40_R1_001.fastq.gz
205	Core Animals	1,4-Dichlorobenzene	10	Yes	Kidney	4DM3F205KI_S40_R1_001.fastq.gz
205	Core Animals	1,4-Dichlorobenzene	10	Yes	Liver	4DM3F205LI_S46_R1_001.fastq.gz
205	Core Animals	1,4-Dichlorobenzene	10	Yes	Lung	4DM3F205LU_S46_R1_001.fastq.gz
205	Core Animals	1,4-Dichlorobenzene	10	Yes	Ovary	4DM3F205OV_S128_R1_001.fastq.gz
206	ICA Animals	1,4-Dichlorobenzene	10	Yes	None	NA
207	ICA Animals	1,4-Dichlorobenzene	10	Yes	None	NA
208	ICA Animals	1,4-Dichlorobenzene	10	Yes	None	NA
301	Core Animals	1,4-Dichlorobenzene	50	Yes	Heart	4DM4F301HE_S45_R1_001.fastq.gz
301	Core Animals	1,4-Dichlorobenzene	50	Yes	Kidney	4DM4F301KI_S45_R1_001.fastq.gz
301	Core Animals	1,4-Dichlorobenzene	50	Yes	Liver	4DM4F301LI_S51_R1_001.fastq.gz
301	Core Animals	1,4-Dichlorobenzene	50	Yes	Lung	4DM4F301LU_S51_R1_001.fastq.gz
301	Core Animals	1,4-Dichlorobenzene	50	Yes	Ovary	4DM4F301OV_S133_R1_001.fastq.gz
302	Core Animals	1,4-Dichlorobenzene	50	Yes	Heart	4DM4F302HE_S39_R1_001.fastq.gz

Animal Number	Selection	Group	Exposure Concentration (ppm)	Survived to Study Termination	Tissue	FASTQ File ID
302	Core Animals	1,4-Dichlorobenzene	50	Yes	Kidney	4DM4F302KI_S39_R1_001.fastq.gz
302	Core Animals	1,4-Dichlorobenzene	50	Yes	Liver	4DM4F302LI_S45_R1_001.fastq.gz
302	Core Animals	1,4-Dichlorobenzene	50	Yes	Lung	4DM4F302LU_S45_R1_001.fastq.gz
302	Core Animals	1,4-Dichlorobenzene	50	Yes	Ovary	4DM4F302OV_S127_R1_001.fastq.gz
303	Core Animals	1,4-Dichlorobenzene	50	Yes	Heart	4DM4F303HE_S65_R1_001.fastq.gz
303	Core Animals	1,4-Dichlorobenzene	50	Yes	Kidney	4DM4F303KI_S65_R1_001.fastq.gz[a]
303	Core Animals	1,4-Dichlorobenzene	50	Yes	Liver	4DM4F303LI_S71_R1_001.fastq.gz
303	Core Animals	1,4-Dichlorobenzene	50	Yes	Lung	4DM4F303LU_S71_R1_001.fastq.gz
303	Core Animals	1,4-Dichlorobenzene	50	Yes	Ovary	4DM4F303OV_S153_R1_001.fastq.gz
304	Core Animals	1,4-Dichlorobenzene	50	Yes	Heart	4DM4F304HE_S63_R1_001.fastq.gz
304	Core Animals	1,4-Dichlorobenzene	50	Yes	Kidney	4DM4F304KI_S63_R1_001.fastq.gz
304	Core Animals	1,4-Dichlorobenzene	50	Yes	Liver	4DM4F304LI_S69_R1_001.fastq.gz
304	Core Animals	1,4-Dichlorobenzene	50	Yes	Lung	4DM4F304LU_S69_R1_001.fastq.gz
304	Core Animals	1,4-Dichlorobenzene	50	Yes	Ovary	4DM4F304OV_S151_R1_001.fastq.gz
305	Core Animals	1,4-Dichlorobenzene	50	Yes	Heart	4DM4F305HE_S67_R1_001.fastq.gz
305	Core Animals	1,4-Dichlorobenzene	50	Yes	Kidney	4DM4F305KI_S67_R1_001.fastq.gz
305	Core Animals	1,4-Dichlorobenzene	50	Yes	Liver	4DM4F305LI_S73_R1_001.fastq.gz
305	Core Animals	1,4-Dichlorobenzene	50	Yes	Lung	4DM4F305LU_S73_R1_001.fastq.gz
305	Core Animals	1,4-Dichlorobenzene	50	Yes	Ovary	4DM4F305OV_S155_R1_001.fastq.gz
306	ICA Animals	1,4-Dichlorobenzene	50	Yes	None	NA
307	ICA Animals	1,4-Dichlorobenzene	50	No	None	NA
308	ICA Animals	1,4-Dichlorobenzene	50	Yes	None	NA
401	Core Animals	1,4-Dichlorobenzene	150	Yes	Heart	4DM5F401HE_S56_R1_001.fastq.gz
401	Core Animals	1,4-Dichlorobenzene	150	Yes	Kidney	4DM5F401KI_S56_R1_001.fastq.gz
401	Core Animals	1,4-Dichlorobenzene	150	Yes	Liver	4DM5F401LI_S62_R1_001.fastq.gz
401	Core Animals	1,4-Dichlorobenzene	150	Yes	Lung	4DM5F401LU_S62_R1_001.fastq.gz
401	Core Animals	1,4-Dichlorobenzene	150	Yes	Ovary	4DM5F401OV_S144_R1_001.fastq.gz
402	Core Animals	1,4-Dichlorobenzene	150	Yes	Heart	4DM5F402HE_S69_R1_001.fastq.gz
402	Core Animals	1,4-Dichlorobenzene	150	Yes	Kidney	4DM5F402KI_S69_R1_001.fastq.gz[a]
402	Core Animals	1,4-Dichlorobenzene	150	Yes	Liver	4DM5F402LI_S40_R1_001.fastq.gz
402	Core Animals	1,4-Dichlorobenzene	150	Yes	Lung	4DM5F402LU_S40_R1_001.fastq.gz
402	Core Animals	1,4-Dichlorobenzene	150	Yes	Ovary	4DM5F402OV_S122_R1_001.fastq.gz
403	Core Animals	1,4-Dichlorobenzene	150	Yes	Heart	4DM5F403HE_S42_R1_001.fastq.gz
403	Core Animals	1,4-Dichlorobenzene	150	Yes	Kidney	4DM5F403KI_S42_R1_001.fastq.gz
403	Core Animals	1,4-Dichlorobenzene	150	Yes	Liver	4DM5F403LI_S48_R1_001.fastq.gz[c]
403	Core Animals	1,4-Dichlorobenzene	150	Yes	Lung	4DM5F403LU_S48_R1_001.fastq.gz
403	Core Animals	1,4-Dichlorobenzene	150	Yes	Ovary	4DM5F403OV_S130_R1_001.fastq.gz

Animal Number	Selection	Group	Exposure Concentration (ppm)	Survived to Study Termination	Tissue	FASTQ File ID
404	Core Animals	1,4-Dichlorobenzene	150	Yes	Heart	4DM5F404HE_S64_R1_001.fastq.gz
404	Core Animals	1,4-Dichlorobenzene	150	Yes	Kidney	4DM5F404KI_S64_R1_001.fastq.gz
404	Core Animals	1,4-Dichlorobenzene	150	Yes	Liver	4DM5F404LI_S70_R1_001.fastq.gz
404	Core Animals	1,4-Dichlorobenzene	150	Yes	Lung	4DM5F404LU_S70_R1_001.fastq.gz
404	Core Animals	1,4-Dichlorobenzene	150	Yes	Ovary	4DM5F404OV_S152_R1_001.fastq.gz
405	Core Animals	1,4-Dichlorobenzene	150	Yes	Heart	4DM5F405HE_S68_R1_001.fastq.gz
405	Core Animals	1,4-Dichlorobenzene	150	Yes	Kidney	4DM5F405KI_S68_R1_001.fastq.gz
405	Core Animals	1,4-Dichlorobenzene	150	Yes	Liver	4DM5F405LI_S74_R1_001.fastq.gz
405	Core Animals	1,4-Dichlorobenzene	150	Yes	Lung	4DM5F405LU_S74_R1_001.fastq.gz
405	Core Animals	1,4-Dichlorobenzene	150	Yes	Ovary	4DM5F405OV_S156_R1_001.fastq.gz
406	ICA Animals	1,4-Dichlorobenzene	150	Yes	None	NA
407	ICA Animals	1,4-Dichlorobenzene	150	Yes	None	NA
408	ICA Animals	1,4-Dichlorobenzene	150	Yes	None	NA
501	Core Animals	1,4-Dichlorobenzene	400	Yes	Heart	4DM6F501HE_S55_R1_001.fastq.gz
501	Core Animals	1,4-Dichlorobenzene	400	Yes	Kidney	4DM6F501KI_S55_R1_001.fastq.gz
501	Core Animals	1,4-Dichlorobenzene	400	Yes	Liver	4DM6F501LI_S61_R1_001.fastq.gz
501	Core Animals	1,4-Dichlorobenzene	400	Yes	Lung	4DM6F501LU_S61_R1_001.fastq.gz
501	Core Animals	1,4-Dichlorobenzene	400	Yes	Ovary	4DM6F501OV_S143_R1_001.fastq.gz
502	Core Animals	1,4-Dichlorobenzene	400	Yes	Heart	4DM6F502HE_S47_R1_001.fastq.gz
502	Core Animals	1,4-Dichlorobenzene	400	Yes	Kidney	4DM6F502KI_S47_R1_001.fastq.gz
502	Core Animals	1,4-Dichlorobenzene	400	Yes	Liver	4DM6F502LI_S53_R1_001.fastq.gz
502	Core Animals	1,4-Dichlorobenzene	400	Yes	Lung	4DM6F502LU_S53_R1_001.fastq.gz
502	Core Animals	1,4-Dichlorobenzene	400	Yes	Ovary	4DM6F502OV_S135_R1_001.fastq.gz
503	Core Animals	1,4-Dichlorobenzene	400	Yes	Heart	4DM6F503HE_S70_R1_001.fastq.gz
503	Core Animals	1,4-Dichlorobenzene	400	Yes	Kidney	4DM6F503KI_S70_R1_001.fastq.gz
503	Core Animals	1,4-Dichlorobenzene	400	Yes	Liver	4DM6F503LI_S41_R1_001.fastq.gz
503	Core Animals	1,4-Dichlorobenzene	400	Yes	Lung	4DM6F503LU_S41_R1_001.fastq.gz
503	Core Animals	1,4-Dichlorobenzene	400	Yes	Ovary	4DM6F503OV_S123_R1_001.fastq.gz
504	Core Animals	1,4-Dichlorobenzene	400	Yes	Heart	4DM6F504HE_S51_R1_001.fastq.gz
504	Core Animals	1,4-Dichlorobenzene	400	Yes	Kidney	4DM6F504KI_S51_R1_001.fastq.gz
504	Core Animals	1,4-Dichlorobenzene	400	Yes	Liver	4DM6F504LI_S57_R1_001.fastq.gz
504	Core Animals	1,4-Dichlorobenzene	400	Yes	Lung	4DM6F504LU_S57_R1_001.fastq.gz
504	Core Animals	1,4-Dichlorobenzene	400	Yes	Ovary	4DM6F504OV_S139_R1_001.fastq.gz
505	Core Animals	1,4-Dichlorobenzene	400	Yes	Heart	4DM6F505HE_S46_R1_001.fastq.gz
505	Core Animals	1,4-Dichlorobenzene	400	Yes	Kidney	4DM6F505KI_S46_R1_001.fastq.gz
505	Core Animals	1,4-Dichlorobenzene	400	Yes	Liver	4DM6F505LI_S52_R1_001.fastq.gz
505	Core Animals	1,4-Dichlorobenzene	400	Yes	Lung	4DM6F505LU_S52_R1_001.fastq.gz

Animal Number	Selection	Group	Exposure Concentration (ppm)	Survived to Study Termination	Tissue	FASTQ File ID
505	Core Animals	1,4-Dichlorobenzene	400	Yes	Ovary	4DM6F505OV_S134_R1_001.fastq.gz
506	ICA Animals	1,4-Dichlorobenzene	400	Yes	None	NA
507	ICA Animals	1,4-Dichlorobenzene	400	Yes	None	NA
508	ICA Animals	1,4-Dichlorobenzene	400	Yes	None	NA

ICA = internal concentration assessment; NA = no transcriptomics data collected for selected animal.
[a]Removed due to potential tissue contamination.
[b]Removed due to quality control fail.
[c]Removed due to principal component analysis/inter-replicate correlation analysis outlier.

Appendix D. Transcriptomic Quality Control and Empirical False Discovery Rate

Table of Contents

Tables

Figures

D.1. Gene Expression Quality Control

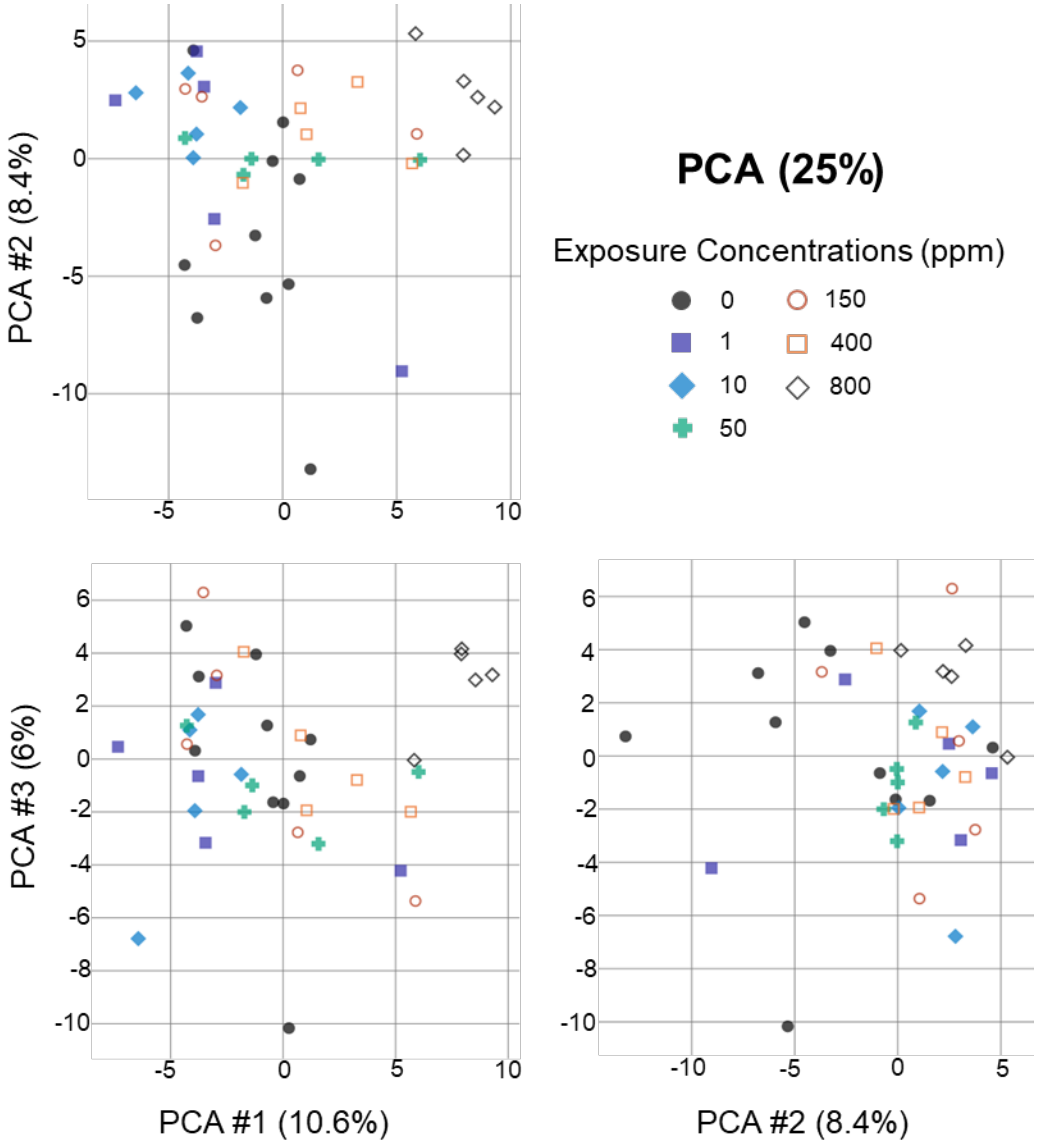

Figure D-1. A Principal Component Analysis of the Normalized Data from the Heart of Female Rats

A principal component analysis (PCA) plot enables visualization of global transcriptional changes in two dimensions, with each plot showing a different angle on the basis of the principal components plotted. Global transcript data are shown for individual animals (dots) within each exposure group (designated by color). Dots that are spatially closer to each other indicate more similarity in global expression profiles; dots that are farther apart indicate dissimilarity in global expression profiles for those animals. The data represented in the plot are those employed in dose response modeling (i.e., if outliers were identified in the quality control process, they were removed from the data set and are not present in the plot). Visual inspection does not suggest subgrouping of the data other than exposure concentration-related changes, which indicates any technical batch-related effects are minimal.

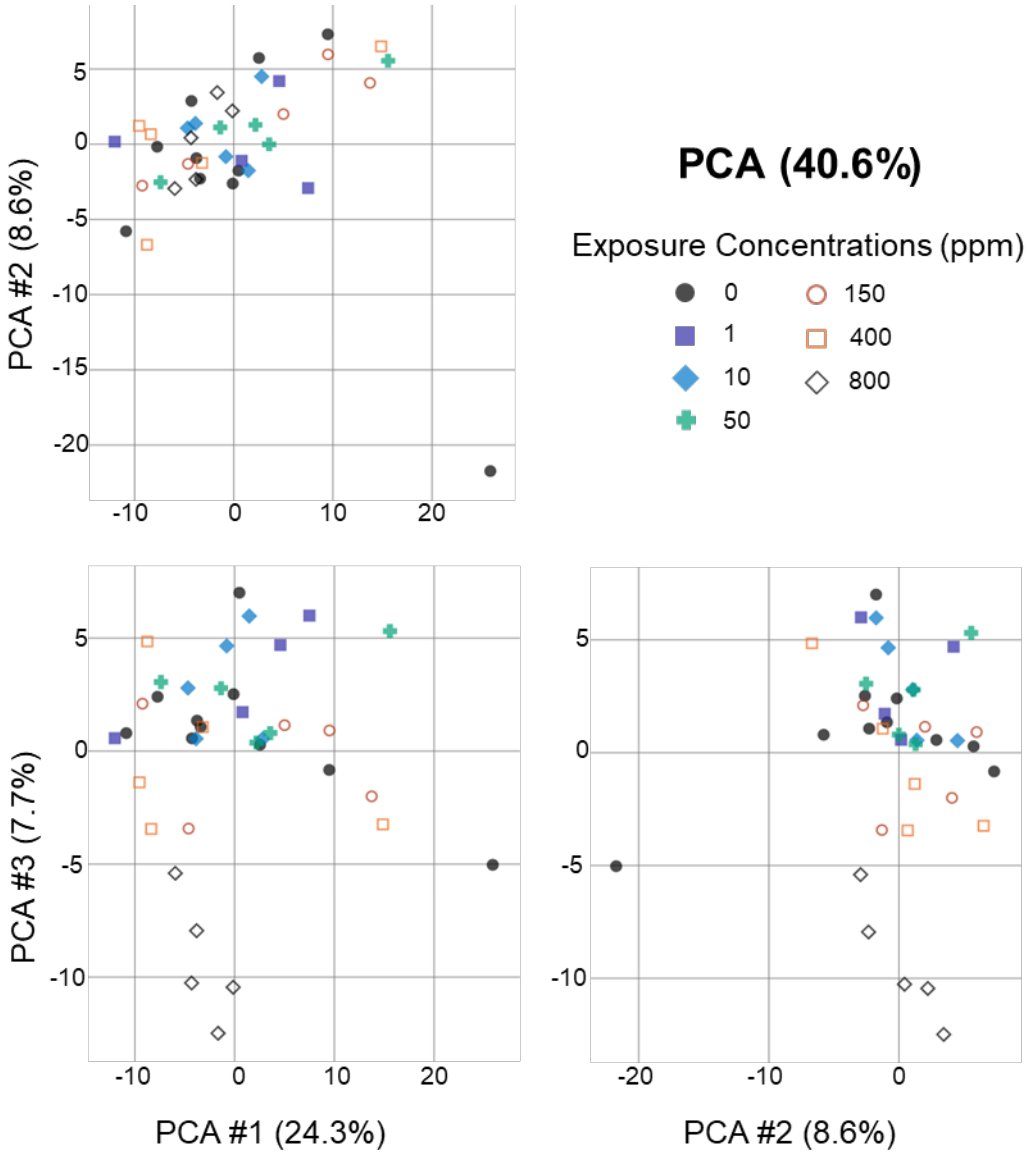

Figure D-2. A Principal Component Analysis of the Normalized Data from the Kidney of Female Rats

A principal component analysis (PCA) plot enables visualization of global transcriptional changes in two dimensions, with each plot showing a different angle on the basis of the principal components plotted. Global transcript data are shown for individual animals (dots) within each exposure group (designated by color). Dots that are spatially closer to each other indicate more similarity in global expression profiles; dots that are farther apart indicate dissimilarity in global expression profiles for those animals. The data represented in the plot are those employed in dose response modeling (i.e., if outliers were identified in the quality control process, they were removed from the data set and are not present in the plot). Visual inspection does not suggest subgrouping of the data other than exposure concentration-related changes, which indicates any technical batch-related effects are minimal.

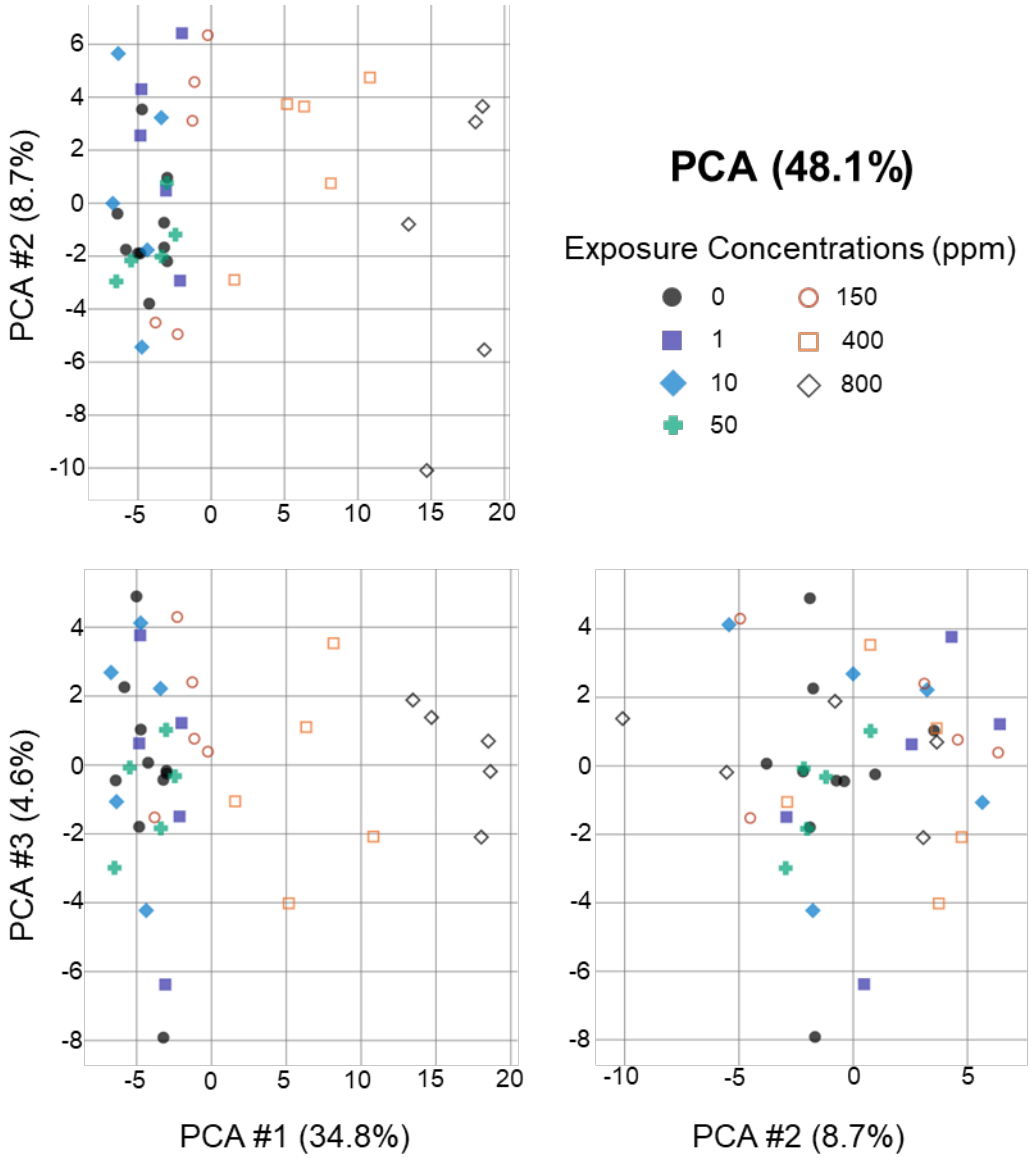

Figure D-3. A Principal Component Analysis of the Normalized Data from the Liver of Female Rats

A principal component analysis (PCA) plot enables visualization of global transcriptional changes in two dimensions, with each plot showing a different angle on the basis of the principal components plotted. Global transcript data are shown for individual animals (dots) within each exposure group (designated by color). Dots that are spatially closer to each other indicate more similarity in global expression profiles; dots that are farther apart indicate dissimilarity in global expression profiles for those animals. The data represented in the plot are those employed in dose response modeling (i.e., if outliers were identified in the quality control process, they were removed from the data set and are not present in the plot). Visual inspection does not suggest subgrouping of the data other than exposure concentration-related changes, which indicates any technical batch-related effects are minimal.

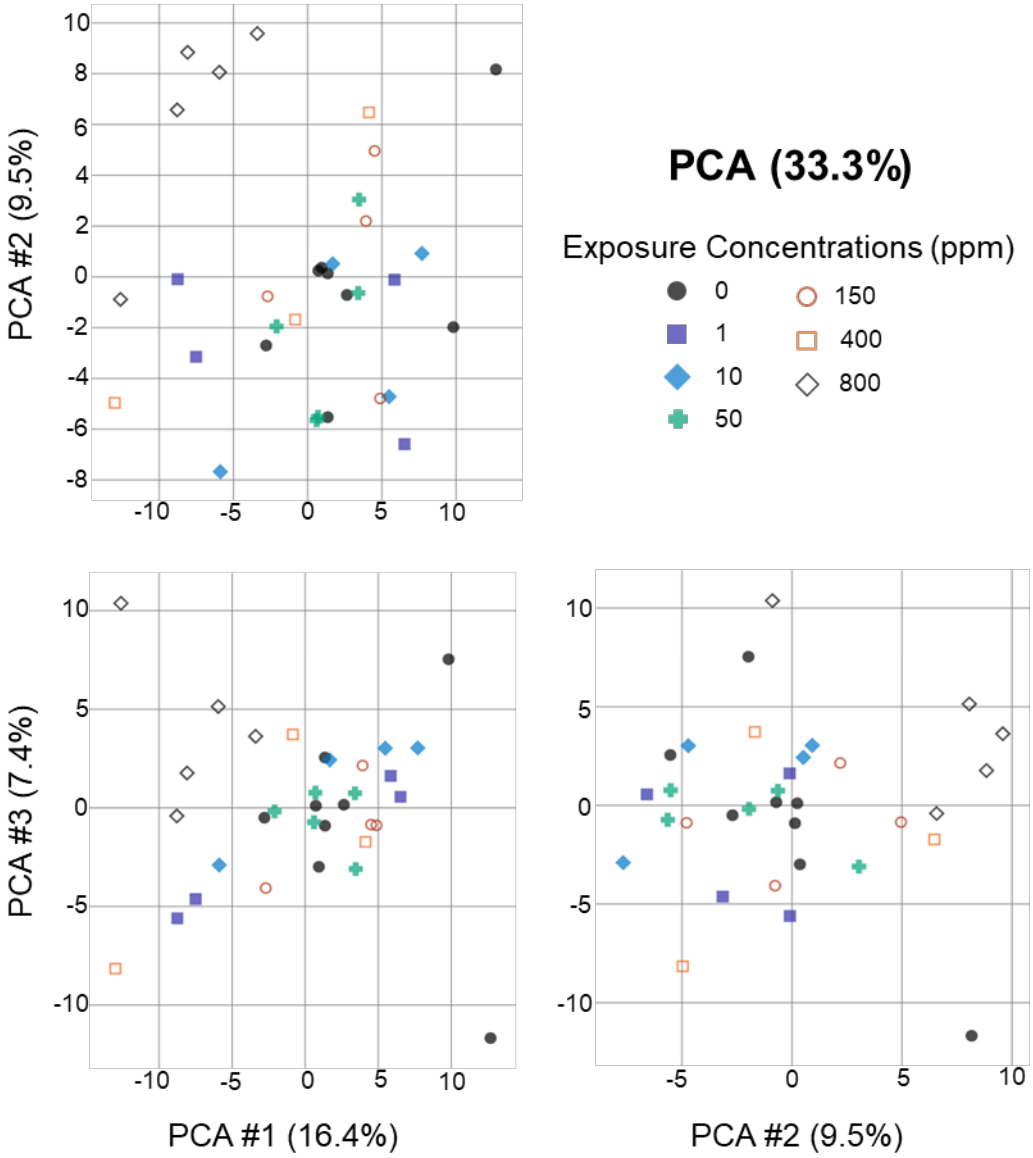

Figure D-4. A Principal Component Analysis of the Normalized Data from the Lung of Female Rats

A principal component analysis (PCA) plot enables visualization of global transcriptional changes in two dimensions, with each plot showing a different angle on the basis of the principal components plotted. Global transcript data are shown for individual animals (dots) within each exposure group (designated by color). Dots that are spatially closer to each other indicate more similarity in global expression profiles; dots that are farther apart indicate dissimilarity in global expression profiles for those animals. The data represented in the plot are those employed in dose response modeling (i.e., if outliers were identified in the quality control process, they were removed from the data set and are not present in the plot). Visual inspection does not suggest subgrouping of the data other than exposure concentration-related changes, which indicates any technical batch-related effects are minimal.

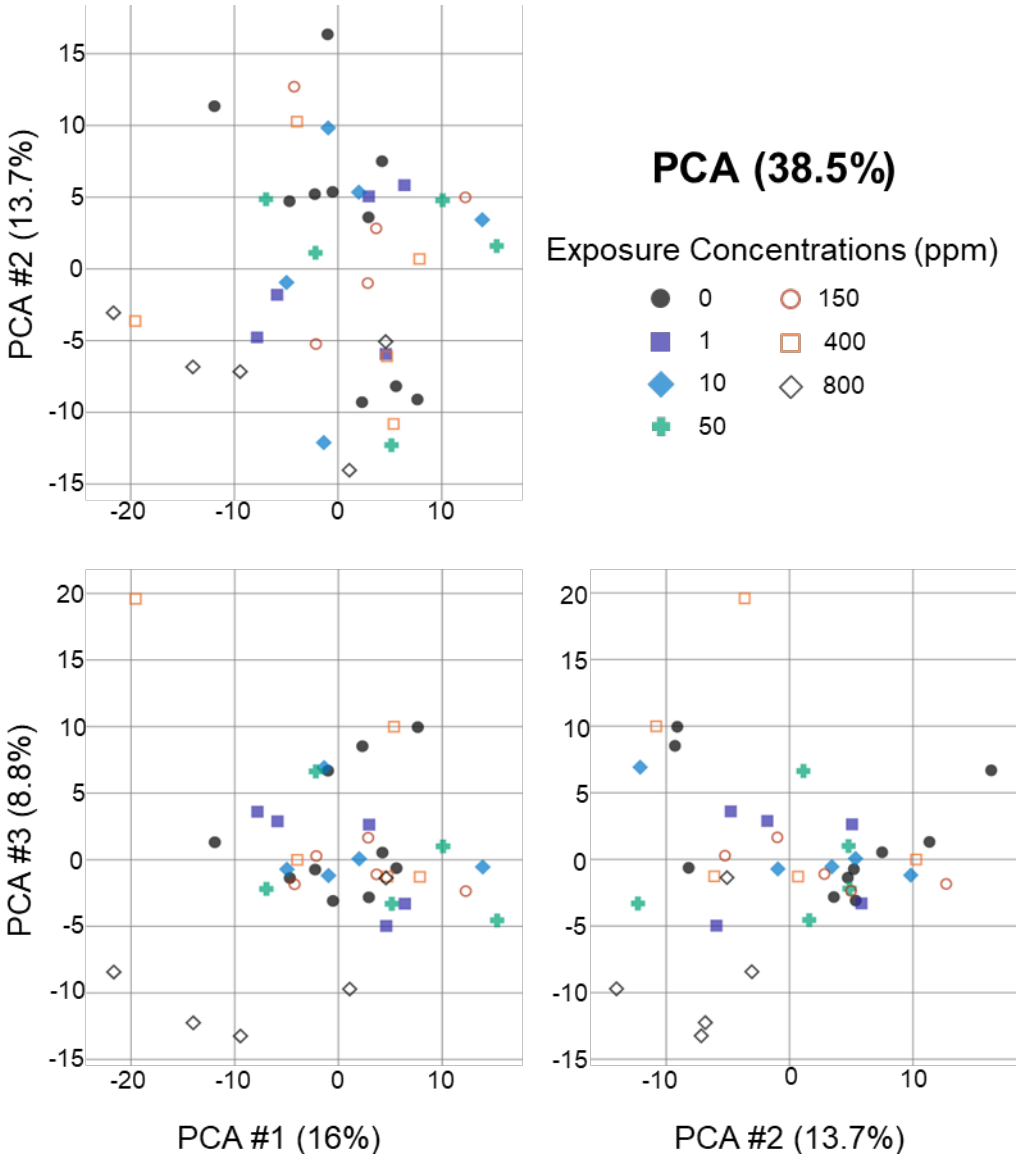

Figure D-5. A Principal Component Analysis of the Normalized Data from the Ovary of Female Rats

A principal component analysis (PCA) plot enables visualization of global transcriptional changes in two dimensions, with each plot showing a different angle on the basis of the principal components plotted. Global transcript data are shown for individual animals (dots) within each exposure group (designated by color). Dots that are spatially closer to each other indicate more similarity in global expression profiles; dots that are farther apart indicate dissimilarity in global expression profiles for those animals. The data represented in the plot are those employed in dose response modeling (i.e., if outliers were identified in the quality control process, they were removed from the data set and are not present in the plot). Visual inspection does not suggest subgrouping of the data other than exposure concentration-related changes, which indicates any technical batch-related effects are minimal.

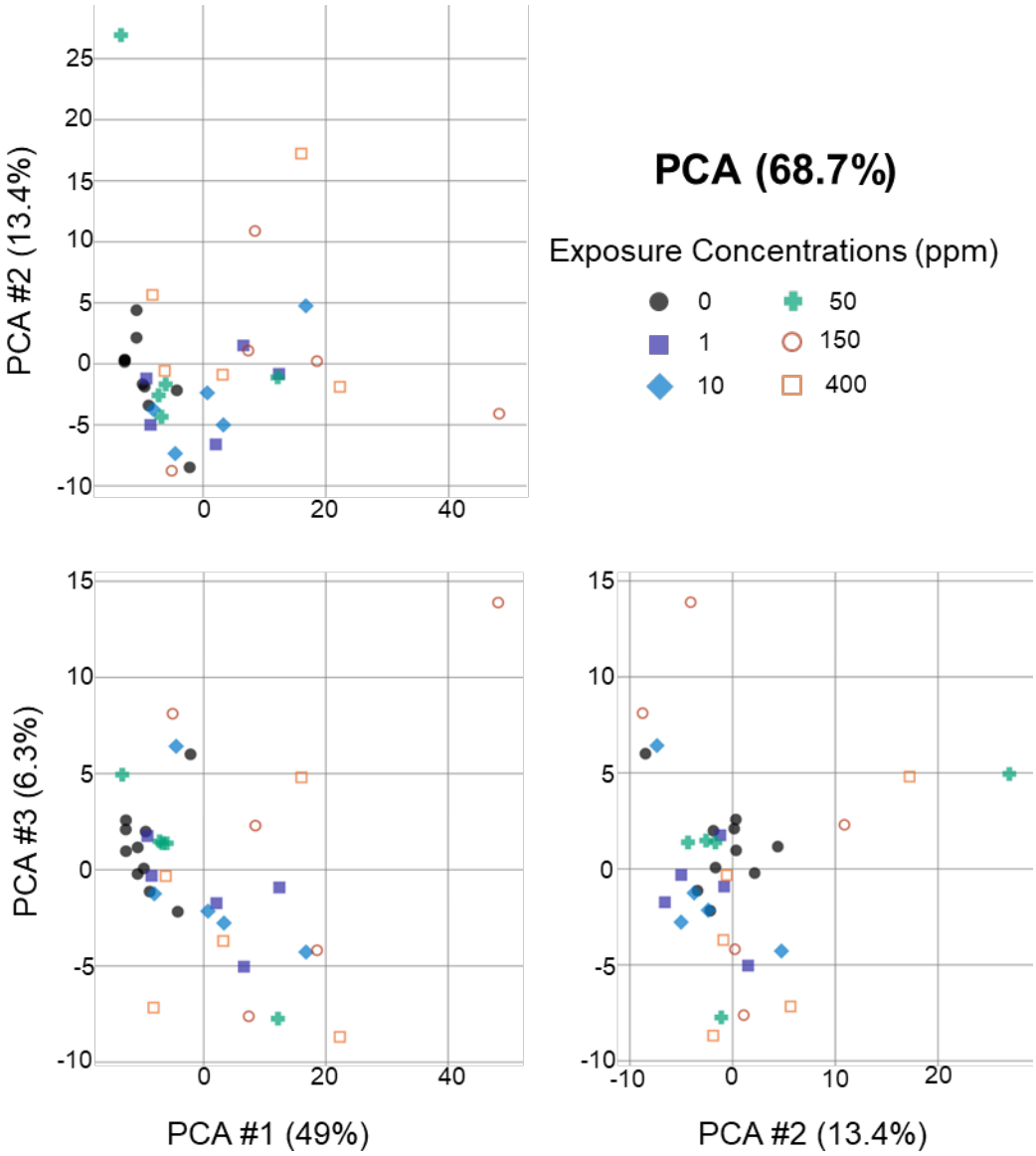

Figure D-6. A Principal Component Analysis of the Normalized Data from the Heart of Female Mice

A principal component analysis (PCA) plot enables visualization of global transcriptional changes in two dimensions, with each plot showing a different angle on the basis of the principal components plotted. Global transcript data are shown for individual animals (dots) within each exposure group (designated by color). Dots that are spatially closer to each other indicate more similarity in global expression profiles; dots that are farther apart indicate dissimilarity in global expression profiles for those animals. The data represented in the plot are those employed in dose response modeling (i.e., if outliers were identified in the quality control process, they were removed from the data set and are not present in the plot). Visual inspection does not suggest subgrouping of the data other than exposure concentration-related changes, which indicates any technical batch-related effects are minimal.

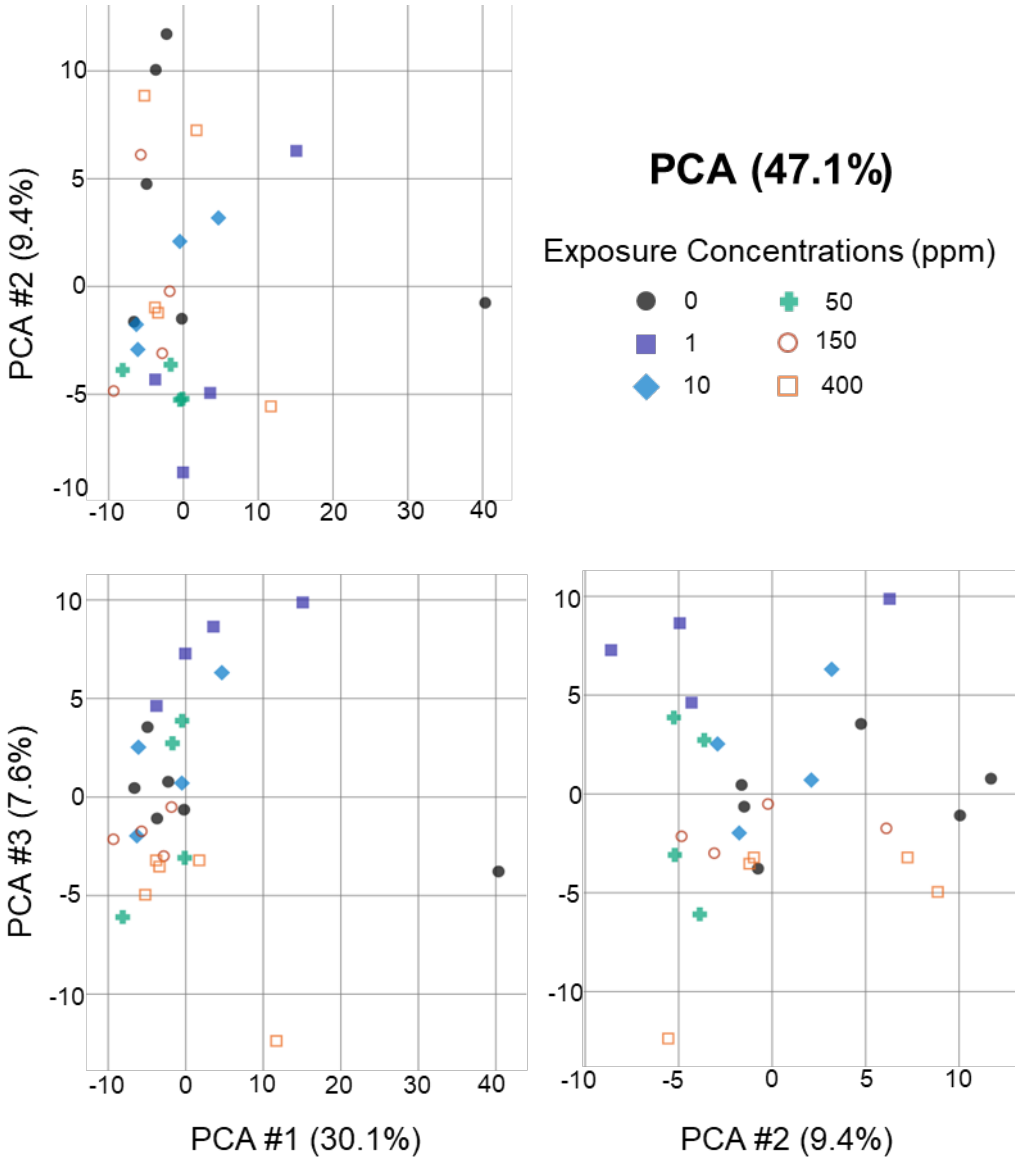

Figure D-7. A Principal Component Analysis of the Normalized Data from the Kidney of Female Mice

A principal component analysis (PCA) plot enables visualization of global transcriptional changes in two dimensions, with each plot showing a different angle on the basis of the principal components plotted. Global transcript data are shown for individual animals (dots) within each exposure group (designated by color). Dots that are spatially closer to each other indicate more similarity in global expression profiles; dots that are farther apart indicate dissimilarity in global expression profiles for those animals. The data represented in the plot are those employed in dose response modeling (i.e., if outliers were identified in the quality control process, they were removed from the data set and are not present in the plot). Visual inspection does not suggest subgrouping of the data other than exposure concentration-related changes, which indicates any technical batch-related effects are minimal.

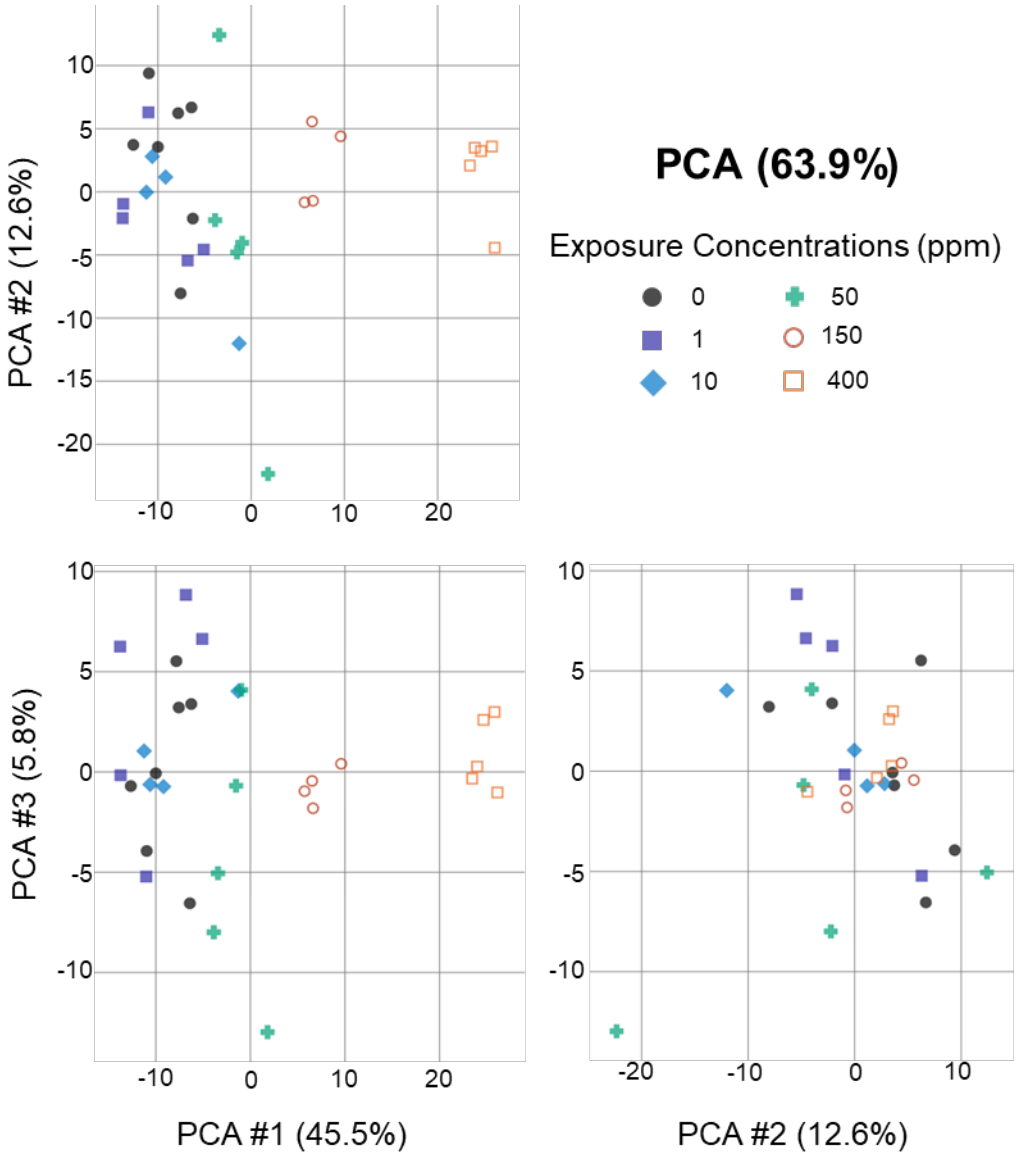

Figure D-8. A Principal Component Analysis of the Normalized Data from the Liver of Female Mice

A principal component analysis (PCA) plot enables visualization of global transcriptional changes in two dimensions, with each plot showing a different angle on the basis of the principal components plotted. Global transcript data are shown for individual animals (dots) within each exposure group (designated by color). Dots that are spatially closer to each other indicate more similarity in global expression profiles; dots that are farther apart indicate dissimilarity in global expression profiles for those animals. The data represented in the plot are those employed in dose response modeling (i.e., if outliers were identified in the quality control process, they were removed from the data set and are not present in the plot). Visual inspection does not suggest subgrouping of the data other than exposure concentration-related changes, which indicates any technical batch-related effects are minimal.

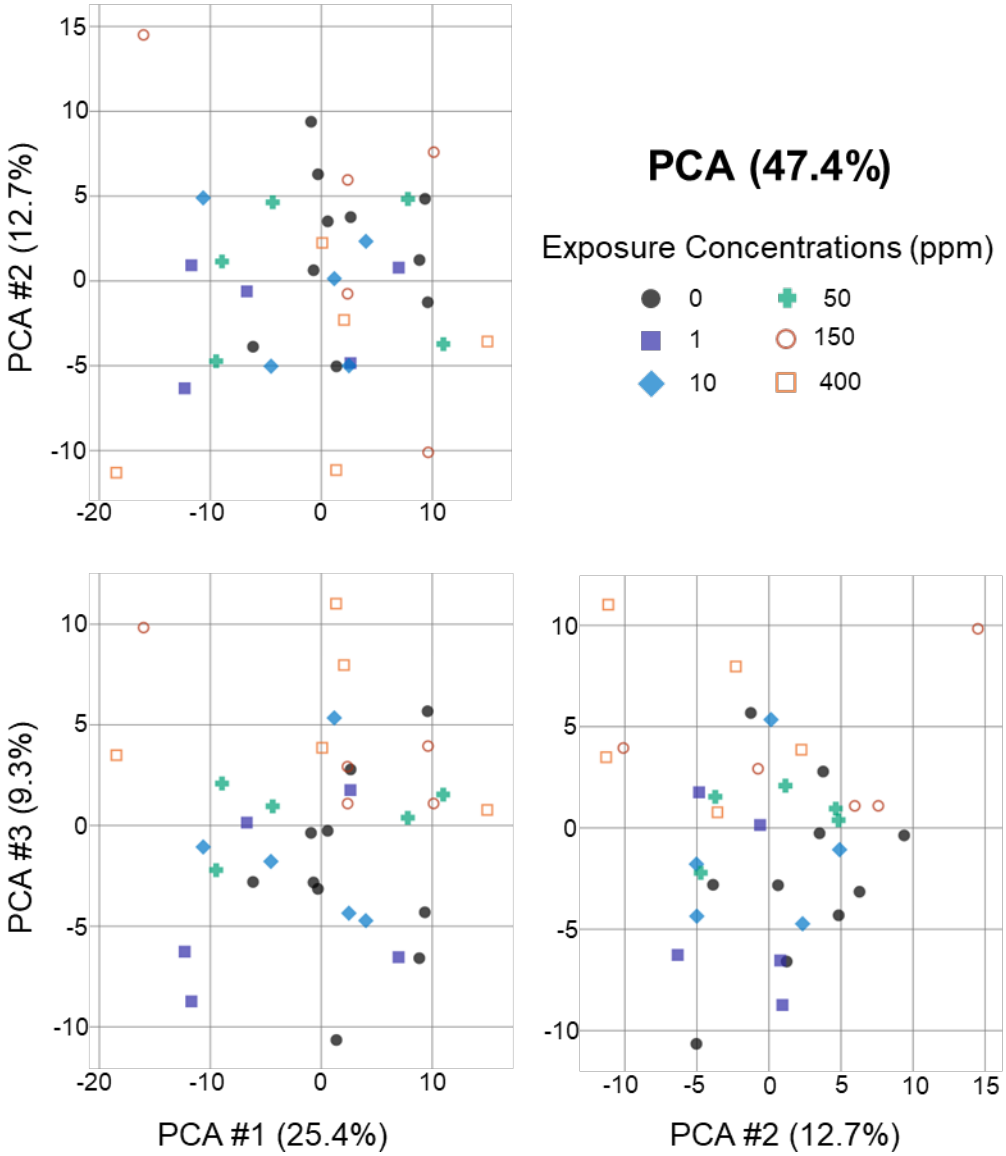

Figure D-9. A Principal Component Analysis of the Normalized Data from the Lung of Female Mice

A principal component analysis (PCA) plot enables visualization of global transcriptional changes in two dimensions, with each plot showing a different angle on the basis of the principal components plotted. Global transcript data are shown for individual animals (dots) within each exposure group (designated by color). Dots that are spatially closer to each other indicate more similarity in global expression profiles; dots that are farther apart indicate dissimilarity in global expression profiles for those animals. The data represented in the plot are those employed in dose response modeling (i.e., if outliers were identified in the quality control process, they were removed from the data set and are not present in the plot). Visual inspection does not suggest subgrouping of the data other than exposure concentration-related changes, which indicates any technical batch-related effects are minimal.

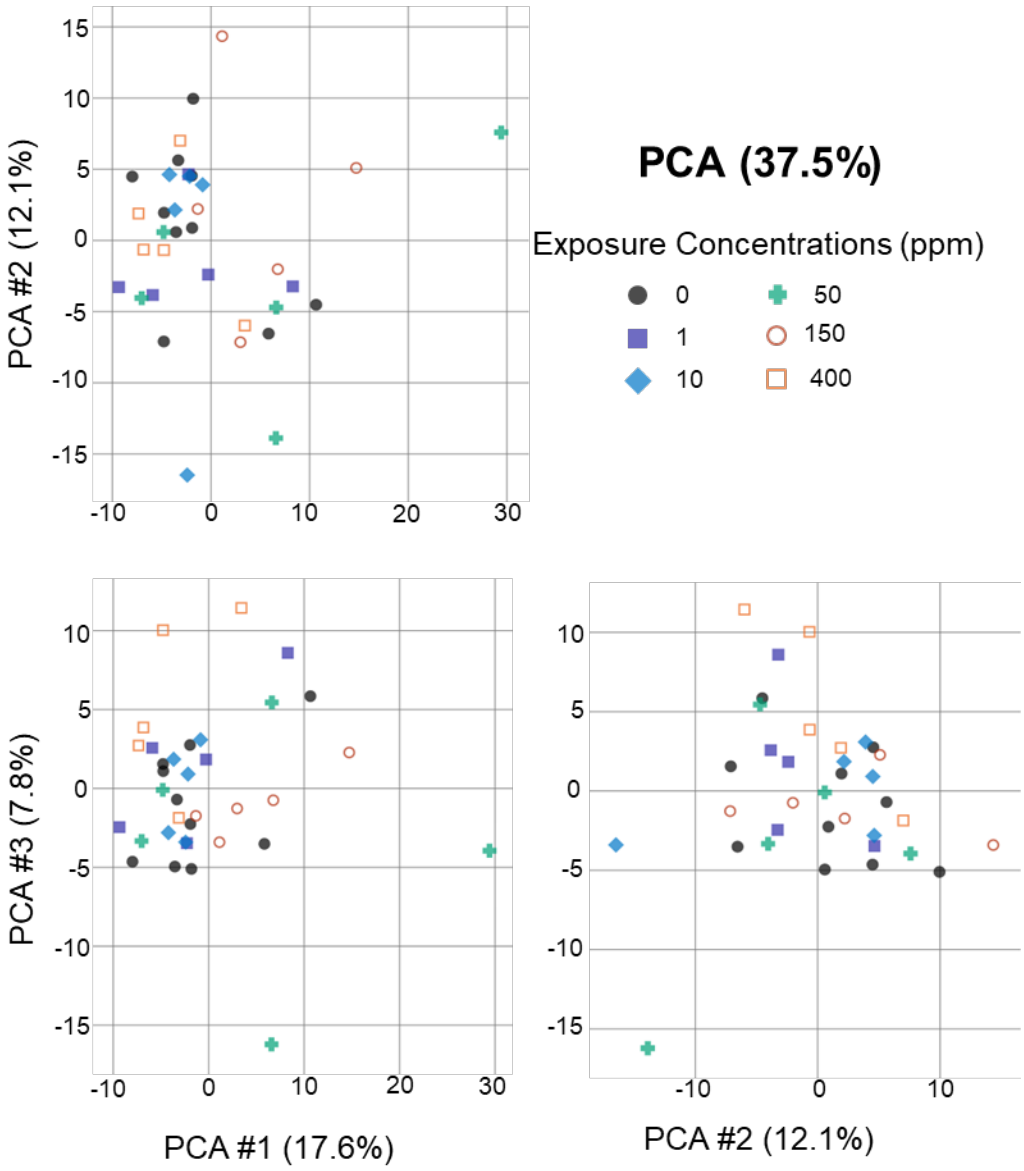

Figure D-10. A Principal Component Analysis of the Normalized Data from the Ovary of Female Mice

A principal component analysis (PCA) plot enables visualization of global transcriptional changes in two dimensions, with each plot showing a different angle on the basis of the principal components plotted. Global transcript data are shown for individual animals (dots) within each exposure group (designated by color). Dots that are spatially closer to each other indicate more similarity in global expression profiles; dots that are farther apart indicate dissimilarity in global expression profiles for those animals. The data represented in the plot are those employed in dose response modeling (i.e., if outliers were identified in the quality control process, they were removed from the data set and are not present in the plot). Visual inspection does not suggest subgrouping of the data other than exposure concentration-related changes, which indicates any technical batch-related effects are minimal.

D.2. Empirical False Discovery Rate

D.2.1. Methods

Synthetic null data were generated using the probe-filtered (i.e., "no 0") 0 ppm data from each tissue in the 1,2-dichlorobenzene rat and mouse studies. The synthetic null data were generated using the Synthetic and Null Data Generator (SaNDGen; https://rstudio.niehs.nih.gov/sandgen/), which employed the normal distribution method previously described for generating synthetic data.[27] In short, for each set of tissue/species, 0 ppm data were used to generate a distribution for each probe. This distribution was resampled to generate 1,000 values for each probe. These values were distributed into synthetic samples, which were then organized into 20 different experiments paralleling the distribution of samples in the experimental study, i.e., 10 samples in the 0 ppm group and 5 for each nonzero exposure concentration. Each of the 20 synthetic null experiments was processed through BMDExpress using the identical parameters used to analyze the experimental data. The resultant data were then used to determine the empirical false discovery rates (eFDR), which are reported as percentages of possible genes and Gene Ontology (GO) biological processes. The associated bm2 analysis files that are the basis of the empirical false discovery rate can be found in Appendix G.

D.2.2. Results

In all species-tissue combinations, the gene-level eFDR was <1%, with a range of 0% to 0.21% (Table D-1). Most gene-level eFDR values were below 0.5%. In all cases, the eFDR for GO biological processes was 0% across all species-tissue combinations.

Table D-1. Empirical False Discovery Results

Species	Tissue	Gene eFDR (%)		GO Biological Process eFDR (%)	
		Mean	Range	Mean	Range
Mouse	Heart	0.07	0–0.2	0	0
Mouse	Kidney	0.03	0–0.09	0	0
Mouse	Liver	0.05	0–0.21	0	0
Mouse	Lung	0.06	0–0.14	0	0
Mouse	Ovary	0.03	0–0.09	0	0
Rat	Heart	0.04	0–0.2	0	0
Rat	Kidney	0.02	0–0.005	0	0
Rat	Liver	0.03	0–0.01	0	0
Rat	Lung	0.03	0–0.007	0	0
Rat	Ovary	0.02	0–0.005	0	0

eFDR = empirical false discovery rate; GO = Gene Ontology.

Appendix E. Gene Set and Gene Definitions

Tables

Table E-1. Active Genes and Definitions within Top 10 Heart Gene Ontology Biological Process Gene Sets Ranked by Potency of Perturbation, Sorted by 5th Percentile Benchmark Dose, for Female Rats and Mice Exposed to 1,4-Dichlorobenzene for Five Days

Category Name[a,b]	Input Genes/Platform Genes in Gene Set (% Coverage)	Active Genes	BMD_{rd25} 5th Percentile of Gene Set Transcripts (BMD_{Lrd25}–BMD_{Urd25}) (ppm)[c]	Definition
Rats				
GO:0044770 cell cycle phase transition	5/58 (8.6%)	*Usp22; Cks2; Ccnb2; Ccnb2-ps2; Ccna2*	141.4 (55.9–292.9)	The cell cycle process by which a cell commits to entering the next cell cycle phase.
GO:0044772 mitotic cell cycle phase transition	5/52 (9.6%)	*Usp22; Cks2; Ccnb2; Ccnb2-ps2; Ccna2*	141.4 (55.9–292.9)	The cell cycle process by which a cell commits to entering the next mitotic cell cycle phase.
GO:0051301 cell division	6/84 (7.1%)	*Nuf2; Cdca5; Kif18b; Ccnb2; Ccnb2-ps2; Ccna2*	181.5 (65.8–517.4)	The process resulting in division and partitioning of components of a cell to form more cells; may or may not be accompanied by the physical separation of a cell into distinct, individually membrane-bounded daughter cells.
GO:0007049 cell cycle	4/45 (8.9%)	*Mki67; Cdca5; Kif18b; Cenpf*	192.5 (68.7–382.0)	The progression of biochemical and morphological phases and events that occur in a cell during successive cell replication or nuclear replication events. Canonically, the cell cycle comprises the replication and segregation of genetic material followed by the division of the cell, but in endocycles or syncytial cells nuclear replication or nuclear division may not be followed by cell division.
GO:0000226 microtubule cytoskeleton organization	4/80 (5.0%)	*Prc1; Nuf2; Kif18b; Ccnb2*	197.5 (80.5–710.7)	A process that is carried out at the cellular level, which results in the assembly, arrangement of constituent parts, or disassembly of cytoskeletal structures comprising microtubules and their associated proteins.

Category Name[a,b]	Input Genes/Platform Genes in Gene Set (% Coverage)	Active Genes	BMD_{rd25} 5th Percentile of Gene Set Transcripts (BMD_{Lrd25}–BMD_{Urd25}) (ppm)[c]	Definition
GO:0007059 chromosome segregation	4/41 (9.8%)	*Smc2; Nuf2; Kif18b; Cenpf*	202.9 (85.1–551.4)	The process in which genetic material, in the form of chromosomes, is organized into specific structures and then physically separated and apportioned to two or more sets. In eukaryotes, chromosome segregation begins with the condensation of chromosomes, includes chromosome separation, and ends when chromosomes have completed movement to the spindle poles.
GO:1903047 mitotic cell cycle process	11/149 (7.4%)	*Usp22; Smc2; Prc1; Nuf2; Cdca5; Kif18b; Cks2; Ckap2; Ccnb2; Ccnb2-ps2; Ccna2*	242.4 (96.3–435.9)	A process that is part of the mitotic cell cycle.
GO:0022402 cell cycle process	12/194 (6.2%)	*Usp22; Smc2; Prc1; Nuf2; Cdca5; Kif18b; Cks2; Ckap2; Cenpf; Ccnb2; Ccnb2-ps2; Ccna2*	282.0 (108.6–1,328.0)	The cellular process that ensures successive accurate and complete genome replication and chromosome segregation.
GO:0019730 antimicrobial humoral response	5/43 (11.6%)	*Loc102549061; Hist1h2bq; H2bc8; Ccl7; Ccl2*	333.8 (156.8–476.7)	An immune response against microbes mediated through a body fluid. Examples of this process are seen in the antimicrobial humoral response of Drosophila melanogaster and Mus musculus.
GO:0006959 humoral immune response	5/80 (6.3%)	*Loc102549061; Hist1h2bq; H2bc8; Ccl7; Ccl2*	347.4 (174.4–695.6)	An immune response mediated through a body fluid.
Mice				
GO:1901617 organic hydroxy compound biosynthetic process	3/52 (5.8%)	*Star; Hmgcs2; Ephx1*	91.0 (25.1–495.5)	The chemical reactions and pathways resulting in the formation of organic hydroxy compound.
GO:0007623 circadian rhythm	3/49 (6.1%)	*Bhlhe40; Dbp; Nfil3*	139.5 (37.4–273.5)	Any biological process in an organism that recurs with a regularity of approximately 24 hours.
GO:0030595 leukocyte chemotaxis	3/49 (6.1%)	*Ccl2; Ccl7; Cxcl1*	178.4 (91.9–411.5)	The movement of a leukocyte in response to an external stimulus.

Category Name[a,b]	Input Genes/Platform Genes in Gene Set (% Coverage)	Active Genes	BMD_{rd25} 5th Percentile of Gene Set Transcripts (BMD_{Lrd25}–BMD_{Urd25}) (ppm)[c]	Definition
GO:0097529 myeloid leukocyte migration	3/51 (5.9%)	*Ccl2; Ccl7; Cxcl1*	178.4 (91.9–411.5)	The movement of a myeloid leukocyte within or between different tissues and organs of the body.

BMD_{rd25} = benchmark dose corresponding to a benchmark response set to a 25% change in the median response; BMD_{Lrd25} = benchmark dose lower confidence limit corresponding to a benchmark response set to a 25% change in the median response; BMD_{Urd25} = benchmark dose upper confidence limit corresponding to a benchmark response set to a 25% change in the median response; GO = Gene Ontology.

[a]Definitions of GO terms were adapted from the Gene Ontology Resource.[33] Official gene symbols from the Rat Genome Database[34] are shown in the "Active Genes" column.

[b]Only four heart GO biological process gene sets were active in mice.

[c]5th percentile = the value below which 5% of transcript benchmark dose values fall.

GO process descriptions and retrieval dates: https://doi.org/10.22427/NTP-DATA-002-00600-0002-000-0.

Table E-2. Active Genes and Definitions within Top 10 Kidney Gene Ontology Biological Process Gene Sets Ranked by Potency of Perturbation, Sorted by 5th Percentile Benchmark Dose, for Female Rats and Mice Exposed to 1,4-Dichlorobenzene for Five Days

Category Name[a]	Input Genes/Platform Genes in Gene Set (% Coverage)	Active Genes	BMD_{rd25} 5th Percentile of Gene Set Transcripts (BMD_{Lrd25}–BMD_{Urd25}) (ppm)[b]	Definition
Rats				
GO:0044770 cell cycle phase transition	4/58 (6.9%)	*Hspa8; Cks2; Ccnb2; Ccnb2-ps2*	121.0 (42.2–652.8)	The cell cycle process by which a cell commits to entering the next cell cycle phase.
GO:0044772 mitotic cell cycle phase transition	4/52 (7.7%)	*Hspa8; Cks2; Ccnb2; Ccnb2-ps2*	121.0 (42.2–652.8)	The cell cycle process by which a cell commits to entering the next mitotic cell cycle phase.
GO:0001822 kidney development	6/57 (10.5%)	*Thra; Hspa8; Hmgcs2; Cyp4a3; Cyp4a2; Agtr1a*	197.7 (91.7–305.6)	The process whose specific outcome is the progression of the kidney over time, from its formation to the mature structure. The kidney is an organ that filters the blood and/or excretes the end products of body metabolism in the form of urine.
GO:0019218 regulation of steroid metabolic process	5/49 (10.2%)	*Srebf1; Por; Nr1d1; Insig1; Dhcr7*	224.1 (73.8–NC)	Any process that modulates the frequency, rate or extent of the chemical reactions and pathways involving steroids.
GO:0030324 lung development	4/45 (8.9%)	*Srebf1; Thra; Hmgcs2; Dhcr7*	224.1 (73.8–NC)	The process whose specific outcome is the progression of the lung over time, from its formation to the mature structure. In all air-breathing vertebrates the lungs are developed from the ventral wall of the oesophagus as a pouch which divides into two sacs. In amphibians and many reptiles the lungs retain very nearly this primitive sac-like character, but in the higher forms the connection with the esophagus becomes elongated into the windpipe and the inner walls of the sacs become more and more divided, until, in the mammals, the air spaces become minutely divided into tubes ending in small air cells, in the walls of which the blood circulates in a fine network of capillaries. In mammals the lungs are more or less divided into lobes, and each lung occupies a separate cavity in the thorax.

Category Name[a]	Input Genes/Platform Genes in Gene Set (% Coverage)	Active Genes	BMD_{rd25} 5th Percentile of Gene Set Transcripts (BMD_{Lrd25}–BMD_{Urd25}) (ppm)[b]	Definition
GO:0006694 steroid biosynthetic process	6/54 (11.1%)	*Srebf1; Insig1; Hsd17b10; Hmgcs2; Dhcr7; Cyp1a1*	225.9 (89.2–NC)	The chemical reactions and pathways resulting in the formation of steroids, compounds with a 1,2,cyclopentanoperhydrophenanthrene nucleus; includes de novo formation and steroid interconversion by modification.
GO:0008203 cholesterol metabolic process	5/54 (9.3%)	*Tsku; Srebf1; Insig1; Hmgcs2; Dhcr7*	225.9 (89.2–NC)	The chemical reactions and pathways involving cholesterol, cholest-5-en-3 beta-ol, the principal sterol of vertebrates and the precursor of many steroids, including bile acids and steroid hormones. It is a component of the plasma membrane lipid bilayer and of plasma lipoproteins and can be found in all animal tissues.
GO:0016125 sterol metabolic process	5/56 (8.9%)	*Tsku; Srebf1; Insig1; Hmgcs2; Dhcr7*	225.9 (89.2–NC)	The chemical reactions and pathways involving sterols, steroids with one or more hydroxyl groups and a hydrocarbon side-chain in the molecule.
GO:0046165 alcohol biosynthetic process	6/42 (14.3%)	*Srebf1; Pck1; Insig1; Hmgcs2; Ephx1; Dhcr7*	225.9 (89.2–NC)	The chemical reactions and pathways resulting in the formation of alcohols, any of a class of compounds containing one or more hydroxyl groups attached to a saturated carbon atom.
GO:0001676 long-chain fatty acid metabolic process	5/55 (9.1%)	*Fads1; Ephx1; Cyp4a3; Cyp4a2; Cyp1a1*	226.7 (96.8–365.3)	The chemical reactions and pathways involving long-chain fatty acids, A long-chain fatty acid is a fatty acid with a chain length between C13 and C22.
Mice				
GO:0007623 circadian rhythm	5/49 (10.2%)	*Bhlhe40; Dbp; Nfil3; Ces1d; Bdnf*	16.9 (2.0–793.4)	Any biological process in an organism that recurs with a regularity of approximately 24 hours.

Category Name[a]	Input Genes/Platform Genes in Gene Set (% Coverage)	Active Genes	BMD_{rd25} 5th Percentile of Gene Set Transcripts (BMD_{Lrd25}–BMD_{Urd25}) (ppm)[b]	Definition
GO:0015850 organic hydroxy compound transport	4/58 (6.9%)	*Ces1d; Ces1g; Abcc3; Slc51a*	17.6 (3.9–778.1)	The directed movement of an organic hydroxy compound (organic alcohol) into, out of or within a cell, or between cells, by means of some agent such as a transporter or pore. An organic hydroxy compound is an organic compound having at least one hydroxy group attached to a carbon atom.
GO:0006869 lipid transport	5/77 (6.5%)	*Ces1d; Ces1g; Abcc3; Fabp1; Slc51a*	22.5 (5.6–84.1)	The directed movement of lipids into, out of or within a cell, or between cells, by means of some agent such as a transporter or pore. Lipids are compounds soluble in an organic solvent but not, or sparingly, in an aqueous solvent.
GO:0010565 regulation of cellular ketone metabolic process	3/56 (5.4%)	*Ces1d; Ces1g; Fabp1*	107.2 (74.6–880.6)	Any process that modulates the chemical reactions and pathways involving any of a class of organic compounds that contain the carbonyl group, CO, and in which the carbonyl group is bonded only to carbon atoms. The general formula for a ketone is RCOR, where R and R are alkyl or aryl groups.
GO:0006805 xenobiotic metabolic process	6/56 (10.7%)	*Cyp2a5; Ugt2b5; Gsta2; Gsta1; Acaa1b; Cyp2e1*	108.3 (48.2–389.5)	The chemical reactions and pathways involving a xenobiotic compound, a compound foreign to living organisms. Used of chemical compounds, e.g., a xenobiotic chemical, such as a pesticide.
GO:0015718 monocarboxylic acid transport	3/52 (5.8%)	*Abcc3; Fabp1; Slc51a*	112.1 (76.4–186.6)	The directed movement of monocarboxylic acids into, out of or within a cell, or between cells, by means of some agent such as a transporter or pore.
GO:0048511 rhythmic process	6/89 (6.7%)	*Bhlhe40; Dbp; Nfil3; Ces1d; Hlf; Bdnf*	129.9 (83.8–241.2)	Any process pertinent to the generation and maintenance of rhythms in the physiology of an organism.
GO:0033559 unsaturated fatty acid metabolic process	5/40 (12.5%)	*Cyp2a5; Cyp4a10; Ces2e; Cyp4a14; Cyp2e1*	136.9 (55.1–282.5)	The chemical reactions and pathways involving an unsaturated fatty acid, any fatty acid containing one or more double bonds between carbon atoms.

Category Name[a]	Input Genes/Platform Genes in Gene Set (% Coverage)	Active Genes	BMD_{rd25} 5th Percentile of Gene Set Transcripts (BMD_{Lrd25}–BMD_{Urd25}) (ppm)[b]	Definition
GO:0006631 fatty acid metabolic process	8/117 (6.8%)	*Cyp2a5; Cyp4a10; Ces1d; Ces2e; Ces1g; Acaa1b; Cyp4a14; Cyp2e1*	139.4 (60.5–491.7)	The chemical reactions and pathways involving fatty acids, aliphatic monocarboxylic acids liberated from naturally occurring fats and oils by hydrolysis.
GO:0006690 icosanoid metabolic process	5/43 (11.6%)	*Cyp2a5; Cyp4a10; Ces2e; Cyp4a14; Cyp2e1*	139.4 (60.5–491.7)	The chemical reactions and pathways involving icosanoids, any of a group of C20 polyunsaturated fatty acids.

BMD_{rd25} = benchmark dose corresponding to a benchmark response set to a 25% change in the median response; BMD_{Lrd25} = benchmark dose lower confidence limit corresponding to a benchmark response set to a 25% change in the median response; BMD_{Urd25} = benchmark dose upper confidence limit corresponding to a benchmark response set to a 25% change in the median response; GO = Gene Ontology; NC = nonconvergent.
[a]Definitions of GO terms were adapted from the Gene Ontology Resource.[33] Official gene symbols from the Rat Genome Database[34] are shown in the "Active Genes" column.
[b]5th percentile = the value below which 5% of transcript benchmark dose values fall.
GO process descriptions and retrieval dates: https://doi.org/10.22427/NTP-DATA-002-00600-0002-000-0.

Table E-3. Active Genes and Definitions within Top 10 Liver Gene Ontology Biological Process Gene Sets Ranked by Potency of Perturbation, Sorted by 5th Percentile Benchmark Dose, for Female Rats and Mice Exposed to 1,4-Dichlorobenzene for Five Days

Category Name[a]	Input Genes/Platform Genes in Gene Set (% Coverage)	Active Genes	BMD_{rd25} 5th Percentile of Gene Set Transcripts (BMD_{Lrd25}–BMD_{Urd25}) (ppm)[b]	Definition
Rats				
GO:0006805 xenobiotic metabolic process	20/59 (33.9%)	*Ugt2b1; Gstp1; Gstm2; Gsta4; Gsta1; Gsta3; Gsta2; Gsta5; Fmo1; Cyp3a2; Cyp3a23-3a1; Cyp2j4; Cyp2e1; Cyp2c6; Cyp2c11; Cyp2b2; Cyp2b1; Cbr1; Acaa1b; Acaa1a*	87.6 (59.6–136.7)	The chemical reactions and pathways involving a xenobiotic compound, a compound foreign to living organisms. Used of chemical compounds, e.g., a xenobiotic chemical, such as a pesticide.
GO:0001676 long-chain fatty acid metabolic process	16/55 (29.1%)	*Mgll; Gstp1; Gstm2; Gsta1; Fads1; Ephx1; Elovl6; Cyp2j4; Cyp2e1; Cyp2c6; Cyp2c11; Cyp2b2; Cyp2b1; Cpt2; Acot4; Acadl*	92.8 (52.7–142.7)	The chemical reactions and pathways involving long-chain fatty acids, A long-chain fatty acid is a fatty acid with a chain length between C13 and C22.
GO:0006690 icosanoid metabolic process	14/50 (28.0%)	*Mif; Mgll; Gstp1; Gsta1; Gsta2; Fads1; Ephx1; Cyp2j4; Cyp2e1; Cyp2c6; Cyp2c11; Cyp2b2; Cyp2b1; Comt*	92.8 (52.7–142.7)	The chemical reactions and pathways involving icosanoids, any of a group of C20 polyunsaturated fatty acids.
GO:0033559 unsaturated fatty acid metabolic process	16/54 (29.6%)	*Mif; Mgll; Gstp1; Gstm2; Gsta1; Gsta2; Fads1; Ephx1; Elovl6; Cyp2j4; Cyp2e1; Cyp2c6; Cyp2c11; Cyp2b2; Cyp2b1; Comt*	92.8 (52.7–142.7)	The chemical reactions and pathways involving an unsaturated fatty acid, any fatty acid containing one or more double bonds between carbon atoms.

Category Name[a]	Input Genes/Platform Genes in Gene Set (% Coverage)	Active Genes	BMD_{rd25} 5th Percentile of Gene Set Transcripts (BMD_{Lrd25}–BMD_{Urd25}) (ppm)[b]	Definition
GO:0120254 olefinic compound metabolic process	15/64 (23.4%)	*Srd5a1; Mgll; Gstp1; Gstm2; Gsta1; Fads1; Ephx1; Cyp3a2; Cyp2j4; Cyp2e1; Cyp2c6; Cyp2c11; Cyp2b2; Cyp2b1; Aldh1a1*	116.4 (63.4–152.0)	The chemical reactions and pathways involving an olefinic compound, any compound which contains a carbon-carbon double bond (aka C=C).
GO:0006720 isoprenoid metabolic process	17/41 (41.5%)	*Srd5a1; Pecr; Mvd; Lss; Idi1; Hmgcs1; Hmgcr; Fdps; Fdft1; Dhdds; Cyp3a2; Cyp2j4; Cyp2e1; Cyp2c6; Cyp2c11; Aldh1a1; Acat2*	143.6 (107.8–165.0)	The chemical reactions and pathways involving isoprenoid compounds, isoprene (2-methylbuta-1,3-diene) or compounds containing or derived from linked isoprene (3-methyl-2-butenylene) residues.
GO:0071384 cellular response to corticosteroid stimulus	9/55 (16.4%)	*Ugt2b1; Srd5a1; Ran; Pck1; Orm1; Gstp1; Ephx1; Eif4ebp1; Agtr1a*	153.0 (59.6–271.9)	Any process that results in a change in state or activity of a cell (in terms of movement, secretion, enzyme production, gene expression, etc.) as a result of a corticosteroid hormone stimulus. A corticosteroid is a steroid hormone that is produced in the adrenal cortex. Corticosteroids are involved in a wide range of physiologic systems such as stress response, immune response and regulation of inflammation, carbohydrate metabolism, protein catabolism, blood electrolyte levels, and behavior. They include glucocorticoids and mineralocorticoids.
GO:0071385 cellular response to glucocorticoid stimulus	8/52 (15.4%)	*Ugt2b1; Srd5a1; Pck1; Orm1; Gstp1; Ephx1; Eif4ebp1; Agtr1a*	153.0 (59.6–271.9)	Any process that results in a change in state or activity of a cell (in terms of movement, secretion, enzyme production, gene expression, etc.) as a result of a glucocorticoid stimulus. Glucocorticoids are hormonal C21 corticosteroids synthesized from cholesterol with the ability to bind with the cortisol receptor and trigger similar effects. Glucocorticoids act primarily on carbohydrate and protein metabolism and have anti-inflammatory effects.

Category Name[a]	Input Genes/Platform Genes in Gene Set (% Coverage)	Active Genes	BMD_{rd25} 5th Percentile of Gene Set Transcripts (BMD_{Lrd25}–BMD_{Urd25}) (ppm)[b]	Definition
GO:0098754 detoxification	16/58 (27.6%)	*Txnrd2; Txnrd1; Srxn1; Sod2; Slc22a1; Prdx3; Prdx2; Prdx1; Nqo1; Gstp1; Gstm2; Gsta3; Gsta2; Gsr; Aldh1a1; Akr7a3*	153.4 (98.2–219.2)	Any process that reduces or removes the toxicity of a toxic substance. These may include transport of the toxic substance away from sensitive areas and to compartments or complexes whose purpose is sequestration of the toxic substance.
GO:0071383 cellular response to steroid hormone stimulus	10/62 (16.1%)	*Ugt2b1; Srd5a1; Ran; Pck1; Orm1; Gstp1; Ephx1; Eif4ebp1; Egr1; Agtr1a*	158.6 (44.1–339.0)	Any process that results in a change in state or activity of a cell (in terms of movement, secretion, enzyme production, gene expression, etc.) as a result of a steroid hormone stimulus.
Mice				
GO:0051983 regulation of chromosome segregation	22/45 (48.9%)	*Nuf2; Ube2c; Aurkb; Smarcd2; Ccnb1; Cdk1; Cdc23; Spc24; Zwilch; Smc4; Cdc20; Knl1; Becn1; Tacc3; Cdca2; Ncapg2; Bub1; Hnrnpu; Birc5; Fbxo5; Ndc80; Chtf18*	6.3 (0.9–28.2)	Any process that modulates the frequency, rate or extent of chromosome segregation, the process in which genetic material, in the form of chromosomes, is organized and then physically separated and apportioned to two or more sets.
GO:1901989 positive regulation of cell cycle phase transition	19/53 (35.9%)	*Ezh2; Ube2c; Ccnb1; Ccnd1; Cdk1; Cdc23; Rrm1; Cdc20; Ccnd2; Lmnb1; Aurka; Egfr; App; Birc5; Rrm2; Rad51c; Fbxo5; Ccne2; Dtl*	6.3 (0.9–28.2)	Any process that activates or increases the frequency, rate or extent of cell cycle phase transition.
GO:1901992 positive regulation of mitotic cell cycle phase transition	17/43 (39.5%)	*Ube2c; Ccnb1; Ccnd1; Cdk1; Cdc23; Rrm1; Cdc20; Ccnd2; Lmnb1; Egfr; App; Birc5; Rrm2; Rad51c; Fbxo5; Ccne2; Dtl*	6.3 (0.9–28.2)	Any process that activates or increases the frequency, rate, or extent of mitotic cell cycle phase transition.

Category Name[a]	Input Genes/Platform Genes in Gene Set (% Coverage)	Active Genes	BMD_{rd25} 5th Percentile of Gene Set Transcripts (BMD_{Lrd25}–BMD_{Urd25}) (ppm)[b]	Definition
GO:0007051 spindle organization	15/40 (37.5%)	*Nuf2; Aurkb; Aspm; Ccnb1; Cdc20; Uhrf1; Tacc3; Aurka; Haus3; Birc5; Ccnb2; Fbxo5; Ndc80; Stmn1; Kif11*	6.9 (1.1–32.3)	A process that is carried out at the cellular level which results in the assembly, arrangement of constituent parts, or disassembly of the spindle, the array of microtubules and associated molecules that forms between opposite poles of a eukaryotic cell during DNA segregation and serves to move the duplicated chromosomes apart.
GO:0045931 positive regulation of mitotic cell cycle	19/60 (31.7%)	*Ube2c; Meis2; Ccnb1; Ccnd1; Cdk1; Cdc23; Rrm1; Cdc20; Stat5b; Ccnd2; Lmnb1; Egfr; App; Birc5; Rrm2; Rad51c; Fbxo5; Ccne2; Dtl*	6.9 (1.1–32.3)	Any process that activates or increases the rate or extent of progression through the mitotic cell cycle.
GO:0007088 regulation of mitotic nuclear division	18/47 (38.3%)	*Nuf2; Ube2c; Aurkb; Chek1; Ccnb1; Cdc23; Spc24; Igf1; Zwilch; Cdc20; Il1b; Knl1; Cdca2; Bub1; Birc5; Fgfr2; Fbxo5; Ndc80*	7.7 (1.1–39.5)	Any process that modulates the frequency, rate or extent of mitosis.
GO:0033044 regulation of chromosome organization	27/69 (39.1%)	*Nuf2; Ube2c; Aurkb; Smarcd2; Ccnb1; Trp53; Cdk1; Dkc1; Cdc23; Spc24; Zwilch; Smc4; Cdc20; Top2a; Knl1; Becn1; Tacc3; Bub1; Hnrnpu; Birc5; Fen1; Pnkp; Fbxo5; Wdhd1; Mcm2; Ndc80; Senp6*	7.7 (1.1–39.5)	Any process that modulates the frequency, rate or extent of a process involved in the formation, arrangement of constituent parts, or disassembly of a chromosome.

Category Name[a]	Input Genes/Platform Genes in Gene Set (% Coverage)	Active Genes	BMD_{rd25} 5th Percentile of Gene Set Transcripts (BMD_{Lrd25}–BMD_{Urd25}) (ppm)[b]	Definition
GO:0044770 cell cycle phase transition	28/63 (44.4%)	*Ezh2; Ptprc; Ube2c; Akap8l; Aurkb; Chek1; Ccnb1; Ccnd1; Cdk1; Timeless; Id4; Cdc20; Ccng1; Ccnd2; Nfib; Tacc3; Pole; Ccna2; Cks1b; App; Birc5; Tcf19; Ccnb2; Abcb1a; Ccne2; Arpp19; Ndc80; Skp2*	7.7 (1.1–39.5)	The cell cycle process by which a cell commits to entering the next cell cycle phase.
GO:0044772 mitotic cell cycle phase transition	22/55 (40.0%)	*Ezh2; Ube2c; Chek1; Ccnb1; Ccnd1; Cdk1; Id4; Ccng1; Ccnd2; Nfib; Tacc3; Pole; Ccna2; Cks1b; App; Birc5; Tcf19; Ccnb2; Abcb1a; Ccne2; Arpp19; Skp2*	7.7 (1.1–39.5)	The cell cycle process by which a cell commits to entering the next mitotic cell cycle phase.
GO:0051783 regulation of nuclear division	19/52 (36.5%)	*Nuf2; Ube2c; Aurkb; Chek1; Ccnb1; Cdc23; Spc24; Igf1; Zwilch; Cdc20; Il1b; Knl1; Cdca2; Bub1; Birc5; Rad51ap1; Fgfr2; Fbxo5; Ndc80*	7.7 (1.1–39.5)	Any process that modulates the frequency, rate or extent of nuclear division, the partitioning of the nucleus and its genetic information.

BMD_{rd25} = benchmark dose corresponding to a benchmark response set to a 25% change in the median response; BMD_{Lrd25} = benchmark dose lower confidence limit corresponding to a benchmark response set to a 25% change in the median response; BMD_{Urd25} = benchmark dose upper confidence limit corresponding to a benchmark response set to a 25% change in the median response; GO = Gene Ontology.

[a]Definitions of GO terms were adapted from the Gene Ontology Resource.[33] Official gene symbols from the Rat Genome Database[34] are shown in the "Active Genes" column.

[b]5th percentile = the value below which 5% of transcript benchmark dose values fall.

GO process descriptions and retrieval dates: https://doi.org/10.22427/NTP-DATA-002-00600-0002-000-0.

Table E-4. Active Genes and Definitions within Top 10 Lung Gene Ontology Biological Process Gene Sets Ranked by Potency of Perturbation, Sorted by 5th Percentile Benchmark Dose, for Female Rats and Mice Exposed to 1,4-Dichlorobenzene for Five Days

Category Name[a]	Input Genes/Platform Genes in Gene Set (% Coverage)	Active Genes	BMD_{rd25} 5th Percentile of Gene Set Transcripts (BMD_{Lrd25}–BMD_{Urd25}) (ppm)[b]	Definition
Rats				
GO:0007059 chromosome segregation	9/41 (22.0%)	*Ttk; Smc2; Nuf2; Mad2l1; Kif18b; Dlgap5; Ctcf; Cenpw; Cenpf*	208.6 (55.4–1,082.9)	The process in which genetic material, in the form of chromosomes, is organized into specific structures and then physically separated and apportioned to two or more sets. In eukaryotes, chromosome segregation begins with the condensation of chromosomes, includes chromosome separation, and ends when chromosomes have completed movement to the spindle poles.
GO:0140694 nonmembrane-bounded organelle assembly	6/59 (10.2%)	*Plk4; Dlgap5; Cirbp; Cenpw; Cdc20; Ccnb2*	236.8 (65.6–NC)	This biological process involves the aggregation, arrangement, and bonding together of a set of components to form a non-membrane-bounded organelle. Unlike traditional organelles enclosed by lipid membranes (e.g., nucleus, mitochondria), membraneless organelles are dynamic structures formed through processes like liquid-liquid phase separation. Examples include the nucleolus, stress granules, and P bodies. These organelles play crucial roles in various cellular functions, such as RNA processing, signal transduction, and stress responses. Their assembly is essential for maintaining cellular organization and function.
GO:0007049 cell cycle	6/45 (13.3%)	*Mybl1; Mki67; Cdca5; Kif18b; Cenpw; Cenpf*	247.7 (69.6–NC)	The progression of biochemical and morphological phases and events that occur in a cell during successive cell replication or nuclear replication events. Canonically, the cell cycle comprises the replication and segregation of genetic material followed by the division of the cell, but in endocycles or syncytial cells nuclear replication or nuclear division may not be followed by cell division.

Category Name[a]	Input Genes/Platform Genes in Gene Set (% Coverage)	Active Genes	BMD_{rd25} 5th Percentile of Gene Set Transcripts (BMD_{Lrd25}–BMD_{Urd25}) (ppm)[b]	Definition
GO:0048568 embryonic organ development	5/47 (10.6%)	*Slc6a8; Junb; Hsd17b7; Gdnf; Cebpb*	264.4 (73.4–2,060.4)	Development, taking place during the embryonic phase, of a tissue or tissues that work together to perform a specific function or functions. Development pertains to the process whose specific outcome is the progression of a structure over time, from its formation to the mature structure. Organs are commonly observed as visibly distinct structures but may also exist as loosely associated clusters of cells that work together to perform a specific function or functions.
GO:0045931 positive regulation of mitotic cell cycle	3/51 (5.9%)	*Cdca5; Crebbp; Cdc20*	288.7 (135.6–NC)	Any process that activates or increases the rate or extent of progression through the mitotic cell cycle.
GO:1901989 positive regulation of cell cycle phase transition	3/43 (7.0%)	*Cdca5; Crebbp; Cdc20*	288.7 (135.6–NC)	Any process that activates or increases the frequency, rate or extent of cell cycle phase transition.
GO:1901990 regulation of mitotic cell cycle phase transition	7/94 (7.5%)	*Ttk; Mad2l1; Cdca5; Ier3; Crebbp; Cenpf; Cdc20*	288.7 (135.6–NC)	Any process that modulates the frequency, rate or extent of mitotic cell cycle phase transition.
GO:0051301 cell division	8/84 (9.5%)	*Nuf2; Cdca5; Kif18b; Cenpw; Cdc20; Ccnb2; Ccnb2-ps2; Ccna2*	289.6 (102.8–NC)	The process resulting in division and partitioning of components of a cell to form more cells; may or may not be accompanied by the physical separation of a cell into distinct, individually membrane-bounded daughter cells.
GO:1901987 regulation of cell cycle phase transition	11/116 (9.5%)	*Ttk; Mapk14; Mad2l1; Cdca5; Ier3; Cry1; Crebbp; Cirbp; Cenpf; Cdc20; Apbb2*	293.1 (122.5–NC)	Any process that modulates the frequency, rate or extent of cell cycle phase transition.
GO:0050728 negative regulation of inflammatory response	5/51 (9.8%)	*Nr1d2; Ier3; Hgf; Enpp3; Ahr*	293.3 (143.2–448.6)	Any process that stops, prevents, or reduces the frequency, rate or extent of the inflammatory response.

Category Name[a]	Input Genes/Platform Genes in Gene Set (% Coverage)	Active Genes	BMD_{rd25} 5th Percentile of Gene Set Transcripts (BMD_{Lrd25}–BMD_{Urd25}) (ppm)[b]	Definition
Mice				
GO:0006260 DNA replication	3/43 (7.0%)	*Pole; Dtl; Gins2*	1.4 (0.5–1,130.8)	The cellular metabolic process in which a cell duplicates one or more molecules of DNA. DNA replication begins when specific sequences, known as origins of replication, are recognized and bound by initiation proteins, and ends when the original DNA molecule has been completely duplicated and the copies topologically separated. The unit of replication usually corresponds to the genome of the cell, an organelle, or a virus. The template for replication can either be an existing DNA molecule or RNA.
GO:0006805 xenobiotic metabolic process	5/56 (8.9%)	*Gsta2; Gsta1; Cyp1a1; Ugt1a6a; Ugt1a6b*	2.9 (0.4–54.2)	The chemical reactions and pathways involving a xenobiotic compound, a compound foreign to living organisms. Used of chemical compounds, e.g., a xenobiotic chemical, such as a pesticide.
GO:0000209 protein polyubiquitination	3/42 (7.1%)	*Ube2t; Nqo1; Dtl*	3.8 (0.8–14.9)	Addition of multiple ubiquitin groups to a protein, forming a ubiquitin chain.
GO:0016567 protein ubiquitination	4/68 (5.9%)	*Uhrf1; Ube2t; Nqo1; Dtl*	3.8 (0.8–14.9)	The process in which one or more ubiquitin groups are added to a protein.
GO:0032446 protein modification by small protein conjugation	4/79 (5.1%)	*Uhrf1; Ube2t; Nqo1; Dtl*	3.8 (0.8–14.9)	A protein modification process in which one or more groups of a small protein, such as ubiquitin or a ubiquitin-like protein, are covalently attached to a target protein.
GO:0006575 cellular modified amino acid metabolic process	5/59 (8.5%)	*Gsta2; Mthfd1l; Gclc; Slc7a11; Gsta1*	14.1 (2.1–56.6)	The chemical reactions and pathways involving compounds derived from amino acids, organic acids containing one or more amino substituents.
GO:0048545 response to steroid hormone	3/52 (5.8%)	*Lox; Ugt1a6a; Ugt1a6b*	68.8 (9.1–117.4)	Any process that results in a change in state or activity of a cell or an organism (in terms of movement, secretion, enzyme production, gene expression, etc.) as a result of a steroid hormone stimulus.

Category Name[a]	Input Genes/Platform Genes in Gene Set (% Coverage)	Active Genes	BMD_{rd25} 5th Percentile of Gene Set Transcripts (BMD_{Lrd25}–BMD_{Urd25}) (ppm)[b]	Definition
GO:0008203 cholesterol metabolic process	3/48 (6.3%)	*Ces1g; Hmgcs2; Tsku*	75.4 (33.3–148.1)	The chemical reactions and pathways involving cholesterol, cholest-5-en-3 beta-ol, the principal sterol of vertebrates and the precursor of many steroids, including bile acids and steroid hormones. It is a component of the plasma membrane lipid bilayer and of plasma lipoproteins and can be found in all animal tissues.
GO:0016125 sterol metabolic process	3/49 (6.1%)	*Ces1g; Hmgcs2; Tsku*	75.4 (33.3–148.1)	The chemical reactions and pathways involving sterols, steroids with one or more hydroxyl groups and a hydrocarbon side-chain in the molecule.
GO:1902652 secondary alcohol metabolic process	3/53 (5.7%)	*Ces1g; Hmgcs2; Tsku*	75.4 (33.3–148.1)	The chemical reactions and pathways involving secondary alcohol.

BMD_{rd25} = benchmark dose corresponding to a benchmark response set to a 25% change in the median response; BMD_{Lrd25} = benchmark dose lower confidence limit corresponding to a benchmark response set to a 25% change in the median response; BMD_{Urd25} = benchmark dose upper confidence limit corresponding to a benchmark response set to a 25% change in the median response; GO = Gene Ontology; NC = nonconvergent.
[a]Definitions of GO terms were adapted from the Gene Ontology Resource.[33] Official gene symbols from the Rat Genome Database[34] are shown in the "Active Genes" column.
[b]5th percentile = the value below which 5% of transcript benchmark dose values fall.
GO process descriptions and retrieval dates: https://doi.org/10.22427/NTP-DATA-002-00600-0002-000-0.

Table E-5. Active Genes and Definitions within Top 10 Ovary Gene Ontology Biological Process Gene Sets Ranked by Potency of Perturbation, Sorted by 5th Percentile Benchmark Dose, for Female Rats Exposed to 1,4-Dichlorobenzene for Five Days

Category Name[a]	Input Genes/Platform Genes in Gene Set (% Coverage)	Active Genes	BMD_{rd25} 5th Percentile of Gene Set Transcripts (BMD_{Lrd25}–BMD_{Urd25}) (ppm)[b]	Definition
GO:0001667 ameboidal-type cell migration	5/55 (9.1%)	*S100a9; Nrp1; Kdr; Cxcl12; Apoa1*	223.1 (90.9–432.8)	Cell migration that is accomplished by extension and retraction of a pseudopodium.
GO:2001235 positive regulation of apoptotic signaling pathway	6/58 (10.3%)	*Vnn1; Tnfrsf12a; S100a9; Myc; Jak2; Ei24*	282.7 (140.2–432.6)	Any process that activates or increases the frequency, rate or extent of apoptotic signaling pathway.
GO:0061041 regulation of wound healing	5/59 (8.5%)	*Tnfrsf12a; S100a9; Plg; F2r; Anxa5*	309.9 (178.5–463.5)	Any process that modulates the rate, frequency, or extent of the series of events that restore integrity to a damaged tissue, following an injury.
GO:0048639 positive regulation of developmental growth	5/50 (10.0%)	*Tnfrsf12a; Nrp1; Mapk14; Cxcl12; Adrb2*	332.8 (176.6–485.1)	Any process that activates, maintains or increases the rate of developmental growth.
GO:0030307 positive regulation of cell growth	3/47 (6.4%)	*Tnfrsf12a; Nrp1; Cxcl12*	335.6 (203.0–460.4)	Any process that activates or increases the frequency, rate, extent or direction of cell growth.
GO:0015850 organic hydroxy compound transport	5/60 (8.3%)	*Slc51a; Slc10a2; Myc; Apoa1; Abcc4*	347.9 (198.4–485.0)	The directed movement of an organic hydroxy compound (organic alcohol) into, out of or within a cell, or between cells, by means of some agent such as a transporter or pore. An organic hydroxy compound is an organic compound having at least one hydroxy group attached to a carbon atom.
GO:0002526 acute inflammatory response	3/43 (7.0%)	*Vnn1; Hp; A2m*	354.0 (206.0–481.4)	Inflammation which comprises a rapid, short-lived, relatively uniform response to acute injury or antigenic challenge and is characterized by accumulations of fluid, plasma proteins, and granulocytic leukocytes. An acute inflammatory response occurs within a matter of minutes or hours, and either resolves within a few days or becomes a chronic inflammatory response.

Category Name[a]	Input Genes/Platform Genes in Gene Set (% Coverage)	Active Genes	BMD_{rd25} 5th Percentile of Gene Set Transcripts (BMD_{Lrd25}–BMD_{Urd25}) (ppm)[b]	Definition
GO:2001242 regulation of intrinsic apoptotic signaling pathway	6/75 (8.0%)	*Vnn1; S100a9; Myc; Herpud1; Ei24; Cxcl12*	366.2 (144.6–NC)	Any process that modulates the frequency, rate or extent of intrinsic apoptotic signaling pathway.
GO:0051385 response to mineralocorticoid	3/45 (6.7%)	*Maob; Grin2b; Fosl1*	382.1 (233.3–525.2)	Any process that results in a change in state or activity of a cell or an organism (in terms of movement, secretion, enzyme production, gene expression, etc.) as a result of a mineralocorticoid stimulus. Mineralocorticoids are hormonal C21 corticosteroids synthesized from cholesterol and characterized by their similarity to aldosterone. Mineralocorticoids act primarily on water and electrolyte balance.
GO:1903034 regulation of response to wounding	5/69 (7.3%)	*Tnfrsf12a; S100a9; Plg; F2r; Anxa5*	383.0 (243.8–527.7)	Any process that modulates the frequency, rate or extent of response to wounding.

BMD_{rd25} = benchmark dose corresponding to a benchmark response set to a 25% change in the median response; BMD_{Lrd25} = benchmark dose lower confidence limit corresponding to a benchmark response set to a 25% change in the median response; BMD_{Urd25} = benchmark dose upper confidence limit corresponding to a benchmark response set to a 25% change in the median response; GO = Gene Ontology; NC = nonconvergent.
[a]Definitions of GO terms were adapted from the Gene Ontology Resource.[33] Official gene symbols from the Rat Genome Database[34] are shown in the "Active Genes" column.
[b]5th percentile = the value below which 5% of transcript benchmark dose values fall.
GO process descriptions and retrieval dates: https://doi.org/10.22427/NTP-DATA-002-00600-0002-000-0.

Table E-6. Gene Identifiers and Definitions for Female Rats Exposed to 1,4-Dichlorobenzene for Five Days[a]

Gene Symbol	Entrez Gene IDs	Probe IDs[b]	Definition
Abcc3	140668	ABCC3_7941	Human Uniprot function (Human *ABCC3*): May act as an inducible transporter in the biliary and intestinal excretion of organic anions. Acts as an alternative route for the export of bile acids and glucuronides from cholestatic hepatocytes (By similarity). \{ECO:0000250\}.
Acss1	296259	ACSS1_32386	Human Uniprot function (Human *ACSS1*): Catalyzes the synthesis of acetyl-CoA from short-chain fatty acids (PubMed:16788062). Acetate is the preferred substrate (PubMed:16788062). Can also utilize propionate with a much lower affinity (By similarity). Provides acetyl-CoA that is utilized mainly for oxidation under ketogenic conditions (By similarity). Involved in thermogenesis under ketogenic conditions, using acetate as a vital fuel when carbohydrate availability is insufficient (By similarity). \{ECO:0000250|UniProtKB:Q99NB1, ECO:0000269|PubMed:16788062\}.
Aen	361594	AEN_7998	Human Uniprot function (Human *AEN*): Exonuclease with activity against single- and double-stranded DNA and RNA. Mediates p53-induced apoptosis. When induced by p53 following DNA damage, digests double-stranded DNA to form single-stranded DNA and amplifies DNA damage signals, leading to enhancement of apoptosis. \{ECO:0000269|PubMed:16171785, ECO:0000269|PubMed:18264133\}.
Aldh1a1	24188	ALDH1A1_8022	Human Uniprot function (Human *ALDH1A1*): Can convert/oxidize retinaldehyde to retinoic acid. Binds free retinal and cellular retinol-binding protein-bound retinal (By similarity). May have a broader specificity and oxidize other aldehydes in vivo (PubMed:19296407, PubMed:26373694, PubMed:25450233). \{ECO:0000250|UniProtKB:P51647, ECO:0000269|PubMed:19296407, ECO:0000269|PubMed:25450233, ECO:0000269|PubMed:26373694\}.
Apoa1	25081	APOA1_33150	Human Uniprot function (Human *APOA1*): Participates in the reverse transport of cholesterol from tissues to the liver for excretion by promoting cholesterol efflux from tissues and by acting as a cofactor for the lecithin cholesterol acyltransferase (LCAT). As part of the SPAP complex, activates spermatozoa motility. \{ECO:0000269|PubMed:1909888\}.
Car3/Ca3	54232	CAR3_8196	Rat Uniprot function (Rat *Car3*): Reversible hydration of carbon dioxide.
Ccl12	287562	CCL12_8217	Human Uniprot function (Human *CCL13*): Chemotactic factor that attracts monocytes, lymphocytes, basophils and eosinophils, but not neutrophils. Signals through CCR2B and CCR3 receptors. Plays a role in the accumulation of leukocytes at both sides of allergic and non-allergic inflammation. May be involved in the recruitment of monocytes into the arterial wall during the disease process of atherosclerosis. May play a role in the monocyte attraction in tissues chronically exposed to exogenous pathogens.
Ccna2	114494	CCNA2_8221	Human Uniprot function (Human *CCNA2*): Cyclin which controls both the G1/S and the G2/M transition phases of the cell cycle. Functions through the formation of specific serine/threonine protein kinase holoenzyme complexes with the cyclin-dependent protein kinases CDK1 or CDK2. The cyclin subunit confers the substrate specificity of these complexes and differentially interacts with and activates CDK1 and CDK2 throughout the cell cycle. \{ECO:0000269|PubMed:1312467\}.
Ccnb2	363088	CCNB2_8223	Human Uniprot function (Human *CCNB2*): Essential for the control of the cell cycle at the G2/M (mitosis) transition.
Ccnb2-ps2	100364016	CCNB2_8223	No description available.

Gene Symbol	Entrez Gene IDs	Probe IDs[b]	Definition
Cebpd	25695	CEBPD_8283	Human Uniprot function (Human *CEBPD*): Transcription activator that recognizes two different DNA motifs: the CCAAT homology common to many promoters and the enhanced core homology common to many enhancers (PubMed:16397300). Important transcription factor regulating the expression of genes involved in immune and inflammatory responses (PubMed:16397300, PubMed:1741402). Transcriptional activator that enhances IL6 transcription alone and as heterodimer with CEBPB (PubMed:1741402). \{ECO:0000269|PubMed:1741402\}.
Cenpf	257649	CENPF_8287	Human Uniprot function (Human *CENPF*): Required for kinetochore function and chromosome segregation in mitosis. Required for kinetochore localization of dynein, LIS1, NDE1, and NDEL1. Regulates recycling of the plasma membrane by acting as a link between recycling vesicles and the microtubule network though its association with STX4 and SNAP25. Acts as a potential inhibitor of pocket protein-mediated cellular processes during development by regulating the activity of RB proteins during cell division and proliferation. May play a regulatory or permissive role in the normal embryonic cardiomyocyte cell cycle and in promoting continued mitosis in transformed, abnormally dividing neonatal cardiomyocytes. Interaction with RB directs embryonic stem cells toward a cardiac lineage. Involved in the regulation of DNA synthesis and hence cell cycle progression, via its C-terminus. Has a potential role regulating skeletal myogenesis and in cell differentiation in embryogenesis. Involved in dendritic cell regulation of T-cell immunity against chlamydia. \{ECO:0000269|PubMed:12974617, ECO:0000269|PubMed:17600710, ECO:0000269|PubMed:7542657, ECO:0000269|PubMed:7651420\}.
Cenpw	689399	CENPW_32846	Human Uniprot function (Human *CENPW*): Component of the CENPA-NAC (nucleosome-associated) complex, a complex that plays a central role in assembly of kinetochore proteins, mitotic progression and chromosome segregation (By similarity). The CENPA-NAC complex recruits the CENPA-CAD (nucleosome distal) complex and may be involved in incorporation of newly synthesized CENPA into centromeres (By similarity). Part of a nucleosome-associated complex that binds specifically to histone H3-containing nucleosomes at the centromere, as opposed to nucleosomes containing CENPA. Component of the heterotetrameric CENP-T-W-S-X complex that binds and supercoils DNA, and plays an important role in kinetochore assembly. CENPW has a fundamental role in kinetochore assembly and function. It is one of the inner kinetochore proteins, with most further proteins binding downstream. Required for normal chromosome organization and normal progress through mitosis. \{ECO:0000250, ECO:0000269| PubMed:19070575, ECO:0000269|PubMed:19533040, ECO:0000269|PubMed:21695110, ECO:0000269|PubMed:22002061,ECO:0000269|PubMed:22304917\}.
Cks2	498709	CKS2_8325	Human Uniprot function (Human *CKS2*): Binds to the catalytic subunit of the cyclin dependent kinases and is essential for their biological function.
Cxcl12	24772	CXCL12_8410, CXCL12_32815	Human Uniprot function (Human *CXCL12*): Chemoattractant active on T-lymphocytes and monocytes but not neutrophils. Activates the C-X-C chemokine receptor CXCR4 to induce a rapid and transient rise in the level of intracellular calcium ions and chemotaxis. SDF-1-beta(3-72) and SDF-1-alpha(3-67) show a reduced chemotactic activity. Binding to cell surface proteoglycans seems to inhibit formation of SDF-1- alpha(3-67) and thus to preserve activity on local sites. Also binds to atypical chemokine receptor ACKR3, which activates the beta-arrestin pathway and acts as a scavenger receptor for SDF-1. Binds to the allosteric site (site 2) of integrins and activates integrins ITGAV:ITGB3, ITGA4:ITGB1 and ITGA5:ITGB1 in a CXCR4-independent manner (PubMed:29301984). Acts as a positive regulator of monocyte migration and a negative

Gene Symbol	Entrez Gene IDs	Probe IDs[b]	Definition
			regulator of monocyte adhesion via the LYN kinase. Stimulates migration of monocytes and T-lymphocytes through its receptors, CXCR4 and ACKR3, and decreases monocyte adherence to surfaces coated with ICAM-1, a ligand for beta-2 integrins. SDF1A/CXCR4 signaling axis inhibits beta-2 integrin LFA-1 mediated adhesion of monocytes to ICAM-1 through LYN kinase. Inhibits CXCR4-mediated infection by T-cell line-adapted HIV-1. Plays a protective role after myocardial infarction. Induces down-regulation and internalization of ACKR3 expressed in various cells. Has several critical functions during embryonic development; required for B-cell lymphopoiesis, myelopoiesis in bone marrow and heart ventricular septum formation. Stimulates the proliferation of bone marrow-derived B-cell progenitors in the presence of IL7 as well as growth of stromal cell-dependent pre-B-cells (By similarity). \{ECO:0000250|UniProtKB:P40224, ECO:0000269|PubMed:11069075, ECO:0000269|PubMed:11859124, ECO:0000269|PubMed:16107333, ECO:0000269|PubMed:18802065, ECO:0000269|PubMed:19255243, ECO:0000269|PubMed:29301984, ECO:0000269|PubMed:8752281\}.
Cyp2b1	24300	CYP2B1_32451, CYP2B2_32473	Human Uniprot function (Human *CYP2B6*): A cytochrome P450 monooxygenase involved in the metabolism of endocannabinoids and steroids (PubMed:21289075, PubMed:12865317). Mechanistically, uses molecular oxygen inserting one oxygen atom into a substrate, and reducing the second into a water molecule, with two electrons provided by NADPH via cytochrome P450 reductase (NADPH–hemoprotein reductase). Catalyzes the epoxidation of double bonds of arachidonoylethanolamide (anandamide) to 8,9-, 11,12-, and 14,15-epoxyeicosatrienoic acid ethanolamides (EpETrE-EAs), potentially modulating endocannabinoid system signaling (PubMed:21289075). Hydroxylates steroid hormones, including testosterone at C-16 and estrogens at C-2 (PubMed:12865317, PubMed:21289075). Plays a role in the oxidative metabolism of xenobiotics, including plant lipids and drugs (PubMed:11695850, PubMed:22909231). Acts as a 1,4-cineole 2-exo-monooxygenase (PubMed:11695850). \{ECO:0000269|PubMed:11695850, ECO:0000269|PubMed:12865317, ECO:0000269|PubMed:21289075, ECO:0000269|PubMed:22909231\}.; FUNCTION: Allele 2B6*9: Has low affinity for anandamide and can only produce 11,12 EpETrE-EAs. \{ECO:0000269|PubMed:21289075\}.
Cyp2b2	361523	CYP2B2_32473	Human Uniprot function (Human *CYP2B6*): A cytochrome P450 monooxygenase involved in the metabolism of endocannabinoids and steroids (PubMed:21289075, PubMed:12865317). Mechanistically, uses molecular oxygen inserting one oxygen atom into a substrate, and reducing the second into a water molecule, with two electrons provided by NADPH via cytochrome P450 reductase (NADPH–hemoprotein reductase). Catalyzes the epoxidation of double bonds of arachidonoylethanolamide (anandamide) to 8,9-, 11,12-, and 14,15-epoxyeicosatrienoic acid ethanolamides (EpETrE-EAs), potentially modulating endocannabinoid system signaling (PubMed:21289075). Hydroxylates steroid hormones, including testosterone at C-16 and estrogens at C-2 (PubMed:21289075, PubMed:12865317). Plays a role in the oxidative metabolism of xenobiotics, including plant lipids and drugs (PubMed:11695850, PubMed:22909231). Acts as a 1,4-cineole 2-exo-monooxygenase (PubMed:11695850). \{ECO:0000269|PubMed:11695850, ECO:0000269|PubMed:12865317, ECO:0000269|PubMed:21289075, ECO:0000269|PubMed:22909231\}.; FUNCTION: Allele 2B6*9: Has low affinity for anandamide and can only produce 11,12 EpETrE-EAs. \{ECO:0000269|PubMed:21289075\}.

Gene Symbol	Entrez Gene IDs	Probe IDs[b]	Definition
Cyp2c6	293989	CYP2C6V1_33169	Rat Uniprot function (Rat *Cyp2c6*): Cytochromes P450 are a group of heme-thiolate monooxygenases. In liver microsomes, this enzyme is involved in an NADPH-dependent electron transport pathway. It oxidizes a variety of structurally unrelated compounds, including steroids, fatty acids, and xenobiotics.
Cyp4a2	24306	CYP4A2_32530,CYP4A2_8426,CYP4A2_8425	Human Uniprot function (Human *CYP4A22*): Catalyzes the omega- and (omega-1)-hydroxylation of various fatty acids such as laurate and palmitate. Shows no activity toward arachidonic acid and prostaglandin A1. Lacks functional activity in the kidney and does not contribute to renal 20-hydroxyeicosatetraenoic acid (20-HETE) biosynthesis. \{ECO:0000269|PubMed:10860550, ECO:0000269|PubMed:15611369\}.
Cyp4a3	298423	CYP4A2_32530,CYP4A2_8426	Human Uniprot function (Human *CYP4Z1*): A cytochrome P450 monooxygenase that catalyzes omega and omega-1 hydroxylation of saturated fatty acids. Exhibits preferential omega versus omega-1 regioselectivity and (R) versus (S) stereoselectivity for hydroxylation of dodecanoic (lauric) acid. Mechanistically, uses molecular oxygen inserting one oxygen atom into a substrate, and reducing the second into a water molecule, with two electrons provided by NADPH via cytochrome P450 reductase (CPR; NADPH-ferrihemoprotein reductase). \{ECO:0000269|PubMed:10869363\}.
Dbp	24309	DBP_8439	Human Uniprot function (Human *DBP*): This transcriptional activator recognizes and binds to the sequence 5'-RTTAYGTAAY-3' found in the promoter of genes such as albumin, *CYP2A4* and *CYP2A5*. It is not essential for circadian rhythm generation, but modulates important clock output genes. May be a direct target for regulation by the circadian pacemaker component clock. May affect circadian period and sleep regulation.
Ddit4	140942	DDIT4_8450	Human Uniprot function (Human *DDIT4*): Regulates cell growth, proliferation and survival via inhibition of the activity of the mammalian target of rapamycin complex 1 (mTORC1). Inhibition of mTORC1 is mediated by a pathway that involves DDIT4/REDD1, AKT1, the TSC1-TSC2 complex and the GTPase RHEB. Plays an important role in responses to cellular energy levels and cellular stress, including responses to hypoxia and DNA damage. Regulates p53/TP53-mediated apoptosis in response to DNA damage via its effect on mTORC1 activity. Its role in the response to hypoxia depends on the cell type; it mediates mTORC1 inhibition in fibroblasts and thymocytes, but not in hepatocytes (By similarity). Required for mTORC1-mediated defense against viral protein synthesis and virus replication (By similarity). Inhibits neuronal differentiation and neurite outgrowth mediated by NGF via its effect on mTORC1 activity. Required for normal neuron migration during embryonic brain development. Plays a role in neuronal cell death. \{ECO:0000250, ECO:0000269|PubMed:15545625, ECO:0000269|PubMed:15632201, ECO:0000269|PubMed:15988001, ECO:0000269|PubMed:17005863, ECO:0000269|PubMed:17379067, ECO:0000269|PubMed:19557001, ECO:0000269|PubMed:20166753, ECO:0000269|PubMed:21460850\}.
Dhcr7	64191	DHCR7_8466	Human Uniprot function (Human *DHCR7*): 7-dehydrocholesterol reductase of the cholesterol biosynthetic pathway reducing the C7-C8 double bond of cholesta-5,7-dien-3beta-ol (7-dehydrocholesterol/7-DHC) and cholesta-5,7,24- trien-3beta-ol, two intermediates in that pathway. {ECO:0000269|PubMed:25637936, ECO:0000269|PubMed:9465114, ECO:0000269|PubMed:9634533}.

Gene Symbol	Entrez Gene IDs	Probe IDs[b]	Definition
Egr1	24330	EGR1_8533	Human Uniprot function (Human *EGR1*): Transcriptional regulator (PubMed:20121949). Recognizes and binds to the DNA sequence 5'-GCG(T/G)GGGCG-3'(EGR-site) in the promoter region of target genes (By similarity). Binds double-stranded target DNA, irrespective of the cytosine methylation status (PubMed:25258363, PubMed:25999311). Regulates the transcription of numerous target genes, and thereby plays an important role in regulating the response to growth factors, DNA damage, and ischemia. Plays a role in the regulation of cell survival, proliferation and cell death. Activates expression of p53/TP53 and TGFB1, and thereby helps prevent tumor formation. Required for normal progress through mitosis and normal proliferation of hepatocytes after partial hepatectomy. Mediates responses to ischemia and hypoxia; regulates the expression of proteins such as IL1B and CXCL2 that are involved in inflammatory processes and development of tissue damage after ischemia. Regulates biosynthesis of luteinizing hormone (LHB) in the pituitary (By similarity). Regulates the amplitude of the expression rhythms of clock genes: ARNTL/BMAL1, PER2 and NR1D1 in the liver via the activation of PER1 (clock repressor) transcription. Regulates the rhythmic expression of core-clock gene ARNTL/BMAL1 in the suprachiasmatic nucleus (SCN) (By similarity). \{ECO:0000250|UniProtKB:P08046, ECO:0000269|PubMed:20121949, ECO:0000269|PubMed:25258363, ECO:0000269|PubMed:25999311\}.
Ephx1	25315	EPHX1_8567	Human Uniprot function (Human *EPHX1*): Biotransformation enzyme that catalyzes the hydrolysis of arene and aliphatic epoxides to less reactive and more water soluble dihydrodiols by the trans addition of water (By similarity). Plays a role in the metabolism of endogenous lipids such as epoxide-containing fatty acids (PubMed:22798687). Metabolizes the abundant endocannabinoid 2-arachidonoylglycerol (2-AG) to free arachidonic acid (AA) and glycerol (PubMed:24958911). \{ECO:0000250|UniProtKB:P07687, ECO:0000269|PubMed:22798687, ECO:0000269|PubMed:24958911\}.
Fosl1	25445	FOSL1_8659	Human Entrez Gene Summary (Human *FOSL1*): The Fos gene family consists of 4 members: FOS, FOSB, FOSL1, and FOSL2. These genes encode leucine zipper proteins that can dimerize with proteins of the JUN family, thereby forming the transcription factor complex AP-1. As such, the FOS proteins have been implicated as regulators of cell proliferation, differentiation, and transformation. Several transcript variants encoding different isoforms have been found for this gene. [provided by RefSeq, Jul 2014]
Ier3	294235	IER3_8864	Human Uniprot function (Human *IER3*): May play a role in the ERK signaling pathway by inhibiting the dephosphorylation of ERK by phosphatase PP2A-PPP2R5C holoenzyme. Acts also as an ERK downstream effector mediating survival. As a member of the NUPR1/RELB/IER3 survival pathway, may provide pancreatic ductal adenocarcinoma with remarkable resistance to cell stress, such as starvation or gemcitabine treatment. \{ECO:0000269|PubMed:12356731, ECO:0000269|PubMed:16456541, ECO:0000269|PubMed:22565310\}.
Junb	24517	JUNB_8939	Human Uniprot function (Human *JUNB*): Transcription factor involved in regulating gene activity following the primary growth factor response. Binds to the DNA sequence 5'-TGA[CG]TCA-3'.
Kif18b	303575	KIF18B_32882	Human Uniprot function (Human *KIF18B*): In complex with KIF2C, constitutes the major microtubule plus-end depolymerizing activity in mitotic cells. Its major role may be to transport KIF2C and/or MAPRE1 along microtubules. \{ECO:0000269|PubMed:20600703, ECO:0000269|PubMed:21820309\}.

Gene Symbol	Entrez Gene IDs	Probe IDs[b]	Definition
Kif22	293502	KIF22_8963	Human Uniprot function (Human *KIF22*): Kinesin family member that is involved in spindle formation and the movements of chromosomes during mitosis and meiosis. Binds to microtubules and to DNA (By similarity). Plays a role in congression of laterally attached chromosomes in NDC80-depleted cells (PubMed:25743205). \{ECO:0000250|UniProtKB:Q9I869, ECO:0000269|PubMed:25743205\}.
Lck	313050	LCK_32705	Human Uniprot function (Human *Lck*): Non-receptor tyrosine-protein kinase that plays an essential role in the selection and maturation of developing T-cells in the thymus and in the function of mature T-cells. Plays a key role in T-cell antigen receptor (TCR)-linked signal transduction pathways. Constitutively associated with the cytoplasmic portions of the CD4 and CD8 surface receptors. Association of the TCR with a peptide antigen-bound MHC complex facilitates the interaction of CD4 and CD8 with MHC class II and class I molecules, respectively, thereby recruiting the associated LCK protein to the vicinity of the TCR/CD3 complex. LCK then phosphorylates tyrosine residues within the immunoreceptor tyrosine-based activation motifs (ITAM) of the cytoplasmic tails of the TCR-gamma chains and CD3 subunits, initiating the TCR/CD3 signaling pathway. Once stimulated, the TCR recruits the tyrosine kinase ZAP70, that becomes phosphorylated and activated by LCK. Following this, a large number of signaling molecules are recruited, ultimately leading to lymphokine production. LCK also contributes to signaling by other receptor molecules. Associates directly with the cytoplasmic tail of CD2, which leads to hyperphosphorylation and activation of LCK. Also plays a role in the IL2 receptor-linked signaling pathway that controls the T-cell proliferative response. Binding of IL2 to its receptor results in increased activity of LCK. Is expressed at all stages of thymocyte development and is required for the regulation of maturation events that are governed by both pre-TCR and mature alpha beta TCR. Phosphorylates other substrates, including RUNX3, PTK2B/PYK2, the microtubule-associated protein MAPT, RHOH or TYROBP. Interacts with FYB2 (PubMed:27335501). {ECO:0000269| PubMed:16339550, ECO:0000269|PubMed:16709819, ECO:0000269|PubMed:20028775, ECO:0000269|PubMed:20100835, ECO:0000269|PubMed:20851766, ECO:0000269|PubMed:21269457, ECO:0000269|PubMed:22080863, ECO:0000269|PubMed:27335501}.
Loc100911718	100911718	CYP2C6V1_33169	No description available.
Meg3	500717	RGD1566401_32721	No description available.
Mfap4	287382	MFAP4_32762	Human Uniprot function (Human *MFAP4*): Could be involved in calcium-dependent cell adhesion or intercellular interactions. May contribute to the elastic fiber assembly and/or maintenance(PubMed:26601954). \{ECO:0000269|PubMed:26601954\}.
Mki67	291234	MKI67_9232	Human Uniprot function (Human *MKI67*): Required to maintain individual mitotic chromosomes dispersed in the cytoplasm following nuclear envelope disassembly (PubMed:27362226). Associates with the surface of the mitotic chromosome, the perichromosomal layer, and covers a substantial fraction of the chromosome surface (PubMed:27362226). Prevents chromosomes from collapsing into a single chromatin mass by forming a steric and electrostatic charge barrier: the protein has a high net electrical charge and acts as a surfactant, dispersing chromosomes and enabling independent chromosome motility (PubMed:27362226). Binds DNA, with a preference for supercoiled DNA and AT-rich DNA (PubMed:10878551). Does not contribute to the internal structure of mitotic chromosomes (By similarity). May play a role in chromatin organization (PubMed:24867636). It is however unclear whether it plays a direct role in chromatin organization or whether it is an indirect consequence of its function in maintaining mitotic chromosomes

Gene Symbol	Entrez Gene IDs	Probe IDs[b]	Definition
			dispersed (Probable). \{ECO:0000250|UniProtKB:E9PVX6, ECO:0000269|PubMed:10878551, ECO:0000269|PubMed:24867636, ECO:0000269|PubMed:27362226\}.
Papss2	294103	PAPSS2_33237	Human Uniprot function (Human *PAPSS2*): Bifunctional enzyme with both ATP sulfurylase and APS kinase activity, which mediates two steps in the sulfate activation pathway. The first step is the transfer of a sulfate group to ATP to yield adenosine 5'-phosphosulfate (APS), and the second step is the transfer of a phosphate group from ATP to APS yielding 3'-phosphoadenylylsulfate (PAPS: activated sulfate donor used by sulfotransferase). In mammals, PAPS is the sole source of sulfate; APS appears to be only an intermediate in the sulfate-activation pathway. May have an important role in skeletogenesis during postnatal growth (By similarity). {ECO:0000250}.
Prc1	308761	PRC1_9556	Human Uniprot function (Human *PRC1*): Key regulator of cytokinesis that cross-links antiparallel microtubules at an average distance of 35 nM. Essential for controlling the spatiotemporal formation of the midzone and successful cytokinesis. Required for KIF14 localization to the central spindle and midbody. Required to recruit PLK1 to the spindle. Stimulates PLK1 phosphorylation of RACGAP1 to allow recruitment of ECT2 to the central spindle. Acts as an oncogene for promoting bladder cancer cells proliferation, apoptosis inhibition and carcinogenic progression (PubMed:17409436). \{ECO:0000269|PubMed:12082078, ECO:0000269|PubMed:15297875, ECO:0000269|PubMed:15625105, ECO:0000269|PubMed:16431929, ECO:0000269|PubMed:17409436, ECO:0000269|PubMed:19468300, ECO:0000269|PubMed:20691902, ECO:0000269|PubMed:9885575\}.
Rt1-da	294269	RT1-DA_9760	No description available.
S100a9	94195	S100A9_9775	Human Uniprot function (Human *S100A9*): S100A9 is a calcium- and zinc-binding protein which plays a prominent role in the regulation of inflammatory processes and immune response. It can induce neutrophil chemotaxis, adhesion, can increase the bactericidal activity of neutrophils by promoting phagocytosis via activation of SYK, PI3K/AKT, and ERK1/2 and can induce degranulation of neutrophils by a MAPK-dependent mechanism. Predominantly found as calprotectin (S100A8/A9) which has a wide plethora of intra and extracellular functions. The intracellular functions include: facilitating leukocyte arachidonic acid trafficking and metabolism, modulation of the tubulin-dependent cytoskeleton during migration of phagocytes and activation of the neutrophilic NADPH-oxidase. Activates NADPH-oxidase by facilitating the enzyme complex assembly at the cell membrane, transferring arachidonic acid, an essential cofactor, to the enzyme complex and S100A8 contributes to the enzyme assembly by directly binding to NCF2/ P67PHOX. The extracellular functions involve proinflammatory, antimicrobial, oxidant-scavenging and apoptosis-inducing activities. Its proinflammatory activity includes recruitment of leukocytes, promotion of cytokine and chemokine production, and regulation of leukocyte adhesion and migration. Acts as an alarmin or a danger associated molecular pattern (DAMP) molecule and stimulates innate immune cells via binding to pattern recognition receptors such as Toll-like receptor 4 (TLR4) and receptor for advanced glycation endproducts (AGER). Binding to TLR4 and AGER activates the MAP-kinase and NF-kappa-B signaling pathways resulting in the amplification of the proinflammatory cascade. Has antimicrobial activity toward bacteria and fungi and exerts its antimicrobial activity probably via chelation of $Zn^{(2+)}$ which is essential for microbial growth. Can induce cell death via autophagy and apoptosis and this occurs through the cross-talk of mitochondria and lysosomes via reactive oxygen species (ROS) and the process involves BNIP3. Can regulate neutrophil number and apoptosis by an anti-apoptotic effect; regulates cell survival via

Gene Symbol	Entrez Gene IDs	Probe IDs[b]	Definition
			ITGAM/ITGB and TLR4 and a signaling mechanism involving MEK-ERK. Its role as an oxidant scavenger has a protective role in preventing exaggerated tissue damage by scavenging oxidants. Can act as a potent amplifier of inflammation in autoimmunity as well as in cancer development and tumor spread. Has transnitrosylase activity; in oxidatively-modified low-density lipoprotein (LDL(ox))-induced S-nitrosylation of GAPDH on 'Cys-247' proposed to transfer the NO moiety from NOS2/iNOS to GAPDH via its own S-nitrosylated Cys-3. The iNOS-S100A8/A9 transnitrosylase complex is proposed to also direct selective inflammatory stimulus-dependent S-nitrosylation of multiple targets such as ANXA5, EZR, MSN and VIM by recognizing a [IL]-x-C-x-x-[DE] motif. \{ECO:0000269|PubMed:12626582, ECO:0000269|PubMed:15331440, ECO:0000269|PubMed:15598812, ECO:0000269|PubMed:15642721, ECO:0000269|PubMed:16258195, ECO:0000269|PubMed:19087201, ECO:0000269|PubMed:19122197, ECO:0000269|PubMed:19402754, ECO:0000269|PubMed:19534726, ECO:0000269|PubMed:19935772, ECO:0000269|PubMed:20103766, ECO:0000269|PubMed:21325622, ECO:0000269|PubMed:21487906, ECO:0000269|PubMed:22363402, ECO:0000269|PubMed:22804476, ECO:0000269|PubMed:22808130, ECO:0000269|PubMed:25417112, ECO:0000269|PubMed:8423249\}.
Slc26a2	117267	SLC26A2_33072	Human Uniprot function (Human *SLC26A2*): Sulfate transporter. May play a role in endochondral bone formation. \{ECO:0000269|PubMed:7923357\}.
Slc51a	303879	SLC51A_33157	Human Uniprot function (Human *SLC51A*): Essential component of the Ost-alpha/Ost-beta complex, a heterodimer that acts as the intestinal basolateral transporter responsible for bile acid export from enterocytes into portal blood. Efficiently transports the major species of bile acids. \{ECO:0000269|PubMed:16317684\}.
Slc6a8	50690	SLC6A8_32561	Human Uniprot function (Human *SLC6A8*): Required for the uptake of creatine in muscles and brain.
Spp1	25353	SPP1_9929	Human Uniprot function (Human *SPP1*): Binds tightly to hydroxyapatite. Appears to form an integral part of the mineralized matrix. Probably important to cell-matrix interaction.; FUNCTION: Acts as a cytokine involved in enhancing production of interferon-gamma and interleukin-12 and reducing production of interleukin-10 and is essential in the pathway that leads to type I immunity. \{ECO:0000250\}.
Srebf1	78968	SREBF1_32750	Human Uniprot function(Human *SREBF1*): [Sterol regulatory element-binding protein 1]: Precursor of the transcription factor form (Processed sterol regulatory element-binding protein 1), which is embedded in the endoplasmic reticulum membrane (PubMed:32322062). Low sterol concentrations promote processing of this form, releasing the transcription factor form that translocates into the nucleus and activates transcription of genes involved in cholesterol biosynthesis and lipid homeostasis (By similarity). \{ECO:0000250|UniProtKB:Q9WTN3, ECO:0000269|PubMed:32322062\}.; FUNCTION: [Processed sterol regulatory element-binding protein 1]: Key transcription factor that regulates expression of genes involved in cholesterol biosynthesis and lipid homeostasis (PubMed:8402897, PubMed:12177166, PubMed:32322062). Binds to the sterol regulatory element 1 (SRE-1) (5'-ATCACCCCAC-3'). Has dual sequence specificity binding to both an E-box motif (5'-ATCACGTGA-3') and to SRE-1 (5'-ATCACCCCAC-3') (PubMed:8402897, PubMed:12177166). Regulates the promoters of genes involved in cholesterol biosynthesis and the LDL receptor (LDLR) pathway of sterol regulation(PubMed:8402897, PubMed:12177166, PubMed:32322062). \{ECO:0000269|PubMed:12177166, ECO:0000269|PubMed:32322062, ECO:0000269|PubMed:8402897\}.; FUNCTION: [Isoform SREBP-1A]: Isoform expressed only in select tissues, which has higher transcriptional activity compared to SREBP-1C (By similarity). Able to stimulate both lipogenic and cholesterogenic gene expression(PubMed:12177166).

Gene Symbol	Entrez Gene IDs	Probe IDs[b]	Definition
			Has a role in the nutritional regulation of fatty acids and triglycerides in lipogenic organs such as the liver (By similarity). Required for innate immune response in macrophages by regulating lipid metabolism (By similarity). \{ECO:0000250|UniProtKB:Q9WTN3, ECO:0000269|PubMed:12177166\}.; FUNCTION: [Isoform SREBP-1C]: Predominant isoform expressed in most tissues, which has weaker transcriptional activity compared to isoform SREBP-1A (By similarity). Primarily controls expression of lipogenic gene (PubMed:12177166). Strongly activates global lipid synthesis in rapidly growing cells (By similarity). \{ECO:0000250|UniProtKB:Q9WTN3, ECO:0000269|PubMed:12177166\}.; FUNCTION: [Isoform SREBP-1aDelta]: The absence of Golgi proteolytic processing requirement makes this isoform constitutively active in transactivation of lipogenic gene promoters. \{ECO:0000305|PubMed:7759101\}.; FUNCTION: [Isoform SREBP-1cDelta]: The absence of Golgi proteolytic processing requirement makes this isoform constitutively active in transactivation of lipogenic gene promoters. \{ECO:0000305|PubMed:7759101\}.
Tnfrsf12a	302965	TNFRSF12A_10049	Human Uniprot function (Human *TNFRSF12A*): Receptor for TNFSF12/TWEAK. Weak inducer of apoptosis in some cell types. Promotes angiogenesis and the proliferation of endothelial cells. May modulate cellular adhesion to matrix proteins. \{ECO:0000269|PubMed:11728344\}.
Ugt2b1	286954	UGT2B10_33303, UGT2B1_33224	Human Uniprot function (Human *UGT2B17*): UDP-glucuronosyltransferase (UGT) that catalyzes phase II biotransformation reactions in which lipophilic substrates are conjugated with glucuronic acid to increase the metabolite's water solubility, thereby facilitating excretion into either the urine or bile (PubMed:8798464, PubMed:16595710, PubMed:18719240, PubMed:19022937, PubMed:23288867). Catalyzes the glucuronidation of endogenous steroid hormones such as androgens (epitestosterone, androsterone) and estrogens (estradiol, epiestradiol) (PubMed:8798464, PubMed:16595710, PubMed:18719240, PubMed:19022937, PubMed:23288867). \{ECO:0000269|PubMed:16595710, ECO:0000269|PubMed:18719240, ECO:0000269|PubMed:19022937, ECO:0000269|PubMed:23288867, ECO:0000269|PubMed:8798464\}.
Vnn1	29142	VNN1_10157	Human Uniprot function (Human *VNN1*): Amidohydrolase that hydrolyzes specifically one of the carboamide linkages in D-pantetheine thus recycling pantothenic acid (vitamin B5) and releasing cysteamine. \{ECO:0000269|PubMed:10567687, ECO:0000269|PubMed:11491533, ECO:0000269|PubMed:25478849\}

[a]Descriptions of orthologous human genes are shown due to the increased detail available in public resources such as UniprotKB[35] and Entrez Gene.[36] Gene definitions adapted from Human UniprotKB were used as the primary resource due to the greater breadth of annotation and depth of functional detail provided. Gene definitions adapted from Rat UniprotKB were used as the secondary resource if the primary source did not provide a detailed description of function. Human Entrez Gene was used as the third resource. Rat Entrez Gene was used as the fourth resource.
[b]In some cases, a probe may map to more than one gene, resulting in duplicate reporting of that probe mapped to different genes.
Gene definition version and retrieval dates: https://doi.org/10.22427/NTP-DATA-002-00600-0002-000-0.

Table E-7. Gene Identifiers and Definitions for Female Mice Exposed to 1,4-Dichlorobenzene for Five Days[a]

Gene Symbol	Entrez Gene IDs	Probe IDs[b]	Definition
Abcc3	76408	Abcc3_30114	Human Uniprot function (Human *ABCC3*): May act as an inducible transporter in the biliary and intestinal excretion of organic anions. Acts as an alternative route for the export of bile acids and glucuronides from cholestatic hepatocytes (By similarity). \{ECO:0000250\}.
Abcg1	11307	Abcg1_29054	Human Uniprot function (Human *ABCG1*): Catalyzes the efflux of phospholipids such as sphingomyelin, cholesterol and its oxygenated derivatives like 7beta-hydroxycholesterol and this transport is coupled to hydrolysis of ATP (PubMed:17408620, PubMed:24576892). The lipid efflux is ALB-dependent (PubMed:16702602). Is an active component of the macrophage lipid export complex. Could also be involved in intracellular lipid transport processes. The role in cellular lipid homeostasis may not be limited to macrophages. Prevents cell death by transporting cytotoxic 7beta-hydroxycholesterol (PubMed:17408620). \{ECO:0000269|PubMed:16702602, ECO:0000269|PubMed:17408620, ECO:0000269|PubMed:24576892\}.
Acaa1b	235674	Acaa1b_29729	Human Entrez Gene Summary (Human *ACAA1*):This gene encodes an enzyme operative in the beta-oxidation system of the peroxisomes. Deficiency of this enzyme leads to pseudo-Zellweger syndrome. Alternative splicing results in multiple transcript variants. [provided by RefSeq, Jul 2008]
Atp2b2	11941	Atp2b2_32103	Human Uniprot function (Human *ATP2B2*): This magnesium-dependent enzyme catalyzes the hydrolysis of ATP coupled with the transport of calcium out of the cell.
Bhlhe40	20893	Bhlhe40_32105,Bhlhe40_31406	Human Uniprot function (Human *BHLHE40*): Transcriptional repressor involved in the regulation of the circadian rhythm by negatively regulating the activity of the clock genes and clock-controlled genes (PubMed:12397359, PubMed:18411297). Acts as the negative limb of a novel autoregulatory feedback loop (DEC loop) which differs from the one formed by the PER and CRY transcriptional repressors (PER/CRY loop) (PubMed:14672706). Both these loops are interlocked as it represses the expression of PER1/2 and in turn is repressed by PER1/2 and CRY1/2 (PubMed:15193144). Represses the activity of the circadian transcriptional activator: CLOCK-ARNTL/BMAL1|ARNTL2/BMAL2 heterodimer by competing for the binding to E-box elements (5'-CACGTG-3') found within the promoters of its target genes (PubMed:15560782). Negatively regulates its own expression and the expression of DBP and BHLHE41/DEC2 (PubMed:14672706). Acts as a corepressor of RXR and the RXR-LXR heterodimers and represses the ligand-induced RXRA and NR1H3/LXRA transactivation activity (PubMed:19786558). May be involved in the regulation of chondrocyte differentiation via the cAMP pathway (PubMed:19786558). Represses the transcription of NR0B2 and attenuates the transactivation of NR0B2 by the CLOCK-ARNTL/BMAL1 complex (PubMed:28797635). Drives the circadian rhythm of blood pressure through transcriptional repression of ATP1B1 in the cardiovascular system (PubMed:30012868). \{ECO:0000269|PubMed:12397359, ECO:0000269|PubMed:14672706, ECO:0000269|PubMed:15193144, ECO:0000269|PubMed:15560782, ECO:0000269|PubMed:18411297, ECO:0000269|PubMed:19786558, ECO:0000269|PubMed:28797635, ECO:0000269|PubMed:30012868\}.
Ccna1	12427	Ccna1_31057	Human Uniprot function (Human *CCNA1*): May be involved in the control of the cell cycle at the G1/S (start) and G2/M (mitosis) transitions. May primarily function in the control of the germline meiotic cell cycle and additionally in the control of mitotic cell cycle in some somatic cells. \{ECO:0000269|PubMed:10022926\}.
Ccnb1	268697	Ccnb1_31979	Human Uniprot function (Human *CCNB1*): Essential for the control of the cell cycle at the G2/M (mitosis) transition. \{ECO:0000269|PubMed:17495531,ECO:0000269|PubMed:17495533\}.

Gene Symbol	Entrez Gene IDs	Probe IDs[b]	Definition
Cdc20	107995	Cdc20_30847	Human Uniprot function (Human *CDC20*): Required for full ubiquitin ligase activity of the anaphase promoting complex/cyclosome (APC/C) and may confer substrate specificity upon the complex. Is regulated by the MAD2L1: in metaphase the MAD2L1-CDC20-APC/C ternary complex is inactive and in anaphase the CDC20-APC/C binary complex is active in degrading substrates. The CDC20-APC/C complex positively regulates formation of synaptic vesicle clustering at active zone to the presynaptic membrane in postmitotic neurons. CDC20-APC/C-induced degradation of NEUROD2 induces presynaptic differentiation. \{ECO:0000269|PubMed:9637688, ECO:0000269|PubMed:9734353, ECO:0000269|PubMed:9811605\}.
Cdk1	12534	Cdk1_31242	Human Uniprot function (Human *CDK1*): Plays a key role in the control of the eukaryotic cell cycle by modulating the centrosome cycle as well as mitotic onset; promotes G2-M transition, and regulates G1 progress and G1-S transition via association with multiple interphase cyclins. Required in higher cells for entry into S-phase and mitosis. Phosphorylates PARVA/actopaxin, APC, AMPH, APC, BARD1, Bcl-xL/ BCL2L1, BRCA2, CALD1, CASP8, CDC7, CDC20, CDC25A, CDC25C, CC2D1A, CENPA, CSNK2 proteins/CKII, FZR1/CDH1, CDK7, CEBPB, CHAMP1, DMD/dystrophin, EEF1 proteins/EF-1, EZH2, KIF11/ EG5, EGFR, FANCG, FOS, GFAP, GOLGA2/GM130, GRASP1, UBE2A/hHR6A, HIST1H1 proteins/histone H1, HMGA1, HIVEP3/KRC, LMNA, LMNB, LMNC, LBR, LATS1, MAP1B, MAP4, MARCKS, MCM2, MCM4, MKLP1, MYB, NEFH, NFIC, NPC/nuclear pore complex, PITPNM1/NIR2, NPM1, NCL, NUCKS1, NPM1/numatrin, ORC1, PRKAR2A, EEF1E1/p18, EIF3F/p47, p53/TP53, NONO/p54NRB, PAPOLA, PLEC/plectin, RB1, TPPP, UL40/R2, RAB4A, RAP1GAP, RCC1, RPS6KB1/S6K1, KHDRBS1/SAM68, ESPL1, SKI, BIRC5/survivin, STIP1, TEX14, beta-tubulins, MAPT/TAU, NEDD1, VIM/vimentin, TK1, FOXO1, RUNX1/AML1, SAMHD1, SIRT2 and RUNX2. CDK1/CDC2-cyclin-B controls pronuclear union in interphase fertilized eggs. Essential for early stages of embryonic development. During G2 and early mitosis, CDC25A/B/C-mediated dephosphorylation activates CDK1/cyclin complexes which phosphorylate several substrates that trigger at least centrosome separation, Golgi dynamics, nuclear envelope breakdown and chromosome condensation. Once chromosomes are condensed and aligned at the metaphase plate, CDK1 activity is switched off by WEE1- and PKMYT1-mediated phosphorylation to allow sister chromatid separation, chromosome decondensation, reformation of the nuclear envelope and cytokinesis. Inactivated by PKR/EIF2AK2- and WEE1-mediated phosphorylation upon DNA damage to stop cell cycle and genome replication at the G2 checkpoint thus facilitating DNA repair. Reactivated after successful DNA repair through WIP1-dependent signaling leading to CDC25A/B/C-mediated dephosphorylation and restoring cell cycle progression. In proliferating cells, CDK1-mediated FOXO1 phosphorylation at the G2-M phase represses FOXO1 interaction with 14-3-3 proteins and thereby promotes FOXO1 nuclear accumulation and transcription factor activity, leading to cell death of postmitotic neurons. The phosphorylation of beta-tubulins regulates microtubule dynamics during mitosis. NEDD1 phosphorylation promotes PLK1-mediated NEDD1 phosphorylation and subsequent targeting of the gamma-tubulin ring complex (gTuRC) to the centrosome, an important step for spindle formation. In addition, CC2D1A phosphorylation regulates CC2D1A spindle pole localization and association with SCC1/RAD21 and centriole cohesion during mitosis. The phosphorylation of Bcl-xL/BCL2L1 after prolongated G2 arrest upon DNA damage triggers apoptosis. In contrast, CASP8 phosphorylation during mitosis prevents its activation by proteolysis and subsequent apoptosis. This phosphorylation occurs in cancer cell lines, as well as in primary breast tissues and lymphocytes. EZH2 phosphorylation promotes H3K27me3 maintenance and epigenetic gene silencing. CALD1 phosphorylation promotes Schwann cell migration during peripheral nerve regeneration. CDK1-cyclin-B complex phosphorylates NCKAP5L and mediates its dissociation from

Gene Symbol	Entrez Gene IDs	Probe IDs[b]	Definition
			centrosomes during mitosis (PubMed:26549230). Regulates the amplitude of the cyclic expression of the core clock gene ARNTL/BMAL1 by phosphorylating its transcriptional repressor NR1D1, and this phosphorylation is necessary for SCF(FBXW7)-mediated ubiquitination and proteasomal degradation of NR1D1 (PubMed:27238018). \{ECO:0000269|PubMed:16371510, ECO:0000269|PubMed:16407259, ECO:0000269|PubMed:16933150, ECO:0000269|PubMed:17459720, ECO:0000269|PubMed:18356527, ECO:0000269|PubMed:18480403, ECO:0000269|PubMed:19509060, ECO:0000269|PubMed:19917720, ECO:0000269|PubMed:20171170, ECO:0000269|PubMed:20360007, ECO:0000269|PubMed:20395957, ECO:0000269|PubMed:20935635, ECO:0000269|PubMed:20937773, ECO:0000269|PubMed:21063390, ECO:0000269|PubMed:23355470, ECO:0000269|PubMed:23601106, ECO:0000269|PubMed:23602554, ECO:0000269|PubMed:25556658, ECO:0000269|PubMed:26549230, ECO:0000269|PubMed:27238018\}.; FUNCTION: (Microbial infection) Acts as a receptor for hepatitis C virus (HCV) in hepatocytes and facilitates its cell entry. {ECO:0000269|PubMed:21516087\}.
Ces1d	104158	Ces1d_31073	Human Uniprot function (Human *CES1*): Involved in the detoxification of xenobiotics and in the activation of ester and amide prodrugs (PubMed:7980644, PubMed:9169443, PubMed:9490062, PubMed:18762277). Hydrolyzes aromatic and aliphatic esters, but has no catalytic activity toward amides or a fatty acyl-CoA ester (PubMed:7980644, PubMed:9169443, PubMed:9490062, PubMed:18762277). Hydrolyzes the methyl ester group of cocaine to form benzoylecgonine (PubMed:7980644). Catalyzes the transesterification of cocaine to form cocaethylene (PubMed:7980644). Displays fatty acid ethyl ester synthase activity, catalyzing the ethyl esterification of oleic acid to ethyloleate (PubMed:7980644). Converts monoacylglycerides to free fatty acids and glycerol. Hydrolyzes of 2-arachidonoylglycerol and prostaglandins (PubMed:21049984). Hydrolyzes cellular cholesteryl esters to free cholesterols and promotes reverse cholesterol transport (RCT) by facilitating both the initial and final steps in the process (PubMed:18762277, PubMed:16024911, PubMed:11015575, PubMed:16971496). First of all, allows free cholesterol efflux from macrophages to extracellular cholesterol acceptors and secondly, releases free cholesterol from lipoprotein-delivered cholesteryl esters in the liver for bile acid synthesis or direct secretion into the bile (PubMed:18762277, PubMed:18599737, PubMed:16971496). \{ECO:0000269|PubMed:11015575, ECO:0000269|PubMed:16024911, ECO:0000269|PubMed:16971496, ECO:0000269|PubMed:18599737, ECO:0000269|PubMed:18762277, ECO:0000269|PubMed:21049984, ECO:0000269|PubMed:7980644, ECO:0000269|PubMed:9169443, ECO:0000269|PubMed:9490062\}.
Ces1g	12623	Ces1g_30475	No description available.
Chn1	108699	Chn1_30496	Human Uniprot function (Human *CHN1*): GTPase-activating protein for p21-rac and a phorbol ester receptor. Involved in the assembly of neuronal locomotor circuits as a direct effector of EPHA4 in axon guidance.
Clu	12759	Clu_30840	Human Uniprot function (Human *CLU*): [Isoform 1]: Functions as extracellular chaperone that prevents aggregation of non-native proteins (PubMed:11123922, PubMed:19535339). Prevents stress-induced aggregation of blood plasma proteins (PubMed:11123922, PubMed:12176985, PubMed:17260971, PubMed:19996109). Inhibits formation of amyloid fibrils by APP, APOC2, B2M, CALCA, CSN3, SNCA and aggregation-prone LYZ variants (in vitro) (PubMed:12047389, PubMed:17412999, PubMed:17407782). Does not require ATP (PubMed:11123922). Maintains partially unfolded proteins in a state appropriate for subsequent refolding by other chaperones, such as HSPA8/HSC70 (PubMed:11123922). Does not refold proteins by itself (PubMed:11123922). Binding to cell surface receptors triggers internalization of the

Gene Symbol	Entrez Gene IDs	Probe IDs[b]	Definition
			chaperone-client complex and subsequent lysosomal or proteasomal degradation (PubMed:21505792). Protects cells against apoptosis and against cytolysis by complement(PubMed:2780565). Intracellular forms interact with ubiquitin and SCF (SKP1-CUL1-F-box protein) E3 ubiquitin-protein ligase complexes and promote the ubiquitination and subsequent proteasomal degradation of target proteins (PubMed:20068069). Promotes proteasomal degradation of COMMD1 and IKBKB (PubMed:20068069). Modulates NF-kappa-B transcriptional activity (PubMed:12882985). A mitochondrial form suppresses BAX-dependent release of cytochrome c into the cytoplasm and inhibit apoptosis (PubMed:16113678, PubMed:17689225). Plays a role in the regulation of cell proliferation (PubMed:19137541). An intracellular form suppresses stress-induced apoptosis by stabilizing mitochondrial membrane integrity through interaction with HSPA5 (PubMed:22689054). Secreted form does not affect caspase or BAX-mediated intrinsic apoptosis and TNF-induced NF-kappa-B-activity (PubMed:24073260). Secreted form act as an important modulator during neuronal differentiation through interaction with STMN3 (By similarity). Plays a role in the clearance of immune complexes that arise during cell injury (By similarity). \{ECO:0000250|UniProtKB:P05371, ECO:0000250|UniProtKB:Q06890, ECO:0000269|PubMed:11123922, ECO:0000269|PubMed:12047389, ECO:0000269|PubMed:12176985, ECO:0000269|PubMed:12882985,ECO:0000269|PubMed:16113678, ECO:0000269|PubMed:17260971, ECO:0000269|PubMed:17407782, ECO:0000269|PubMed:17412999, ECO:0000269|PubMed:17689225, ECO:0000269|PubMed:19137541, ECO:0000269|PubMed:19535339, ECO:0000269|PubMed:19996109, ECO:0000269|PubMed:20068069, ECO:0000269|PubMed:21505792, ECO:0000269|PubMed:22689054, ECO:0000269|PubMed:24073260, ECO:0000269|PubMed:2780565\}.; FUNCTION: [Isoform 6]: Does not affect caspase or BAX-mediated intrinsic apoptosis and TNF-induced NF-kappa-B-activity. \{ECO:0000269|PubMed:24073260\}.; FUNCTION: [Isoform 4]: Does not affect caspase or BAX-mediated intrinsic apoptosis and TNF-induced NF-kappa-B-activity (PubMed:24073260). Promotes cell death through interaction with BCL2L1 that releases and activates BAX (PubMed:21567405). \{ECO:0000269|PubMed:21567405, ECO:0000269|PubMed:24073260\}.
Cpsf4l	52670	Cpsf4l_31365	No description available.
Cyp2a4	13086	Cyp2a4_30021	Mouse Uniprot function (Mouse *Cyp2a4*): Highly active in the 15-alpha-hydroxylation of testosterone. Also active in the 15-alpha-hydroxylation of progesterone and androstenedione. Little or no activity on corticosterone, pregnenolone, dehydroepiandrosterone, estradiol or estriol.
Cyp2a5	13087	Cyp2a5_31713	Mouse Uniprot function (Mouse *Cyp2a5*): Exhibits a high coumarin 7-hydroxylase activity.
Cyp2c29	13095	Cyp2c29_31205	Mouse Uniprot function (Mouse *Cyp2c29*): A cytochrome P450 monooxygenase that selectively catalyzes the epoxidation of 14,15 double bond of (5Z,8Z,11Z,14Z)-eicosatetraenoic acid (arachidonate) forming 14,15-epoxyeicosatrienoic acid (14,15-EET) regioisomer. Mechanistically, uses molecular oxygen inserting one oxygen atom into a substrate, and reducing the second into a water molecule, with two electrons provided by NADPH via cytochrome P450 reductase (CPR; NADPH--hemoprotein reductase).
Dbp	13170	Dbp_31391	Human Uniprot function (Human *DBP*): This transcriptional activator recognizes and binds to the sequence 5'-RTTAYGTAAY-3' found in the promoter of genes such as albumin, *CYP2A4* and *CYP2A5*. It is not essential for circadian rhythm generation, but modulates important clock output genes. May be a direct target for regulation by the circadian pacemaker component clock. May affect circadian period and sleep regulation.

Gene Symbol	Entrez Gene IDs	Probe IDs[b]	Definition
Ddit4	74747	Ddit4_29434	Human Uniprot function (Human *DDIT4*): Regulates cell growth, proliferation and survival via inhibition of the activity of the mammalian target of rapamycin complex 1 (mTORC1). Inhibition of mTORC1 is mediated by a pathway that involves DDIT4/REDD1, AKT1, the TSC1-TSC2 complex and the GTPase RHEB. Plays an important role in responses to cellular energy levels and cellular stress, including responses to hypoxia and DNA damage. Regulates p53/TP53-mediated apoptosis in response to DNA damage via its effect on mTORC1 activity. Its role in the response to hypoxia depends on the cell type; it mediates mTORC1 inhibition in fibroblasts and thymocytes, but not in hepatocytes (By similarity). Required for mTORC1-mediated defense against viral protein synthesis and virus replication (By similarity). Inhibits neuronal differentiation and neurite outgrowth mediated by NGF via its effect on mTORC1 activity. Required for normal neuron migration during embryonic brain development. Plays a role in neuronal cell death. \{ECO:0000250, ECO:0000269|PubMed:15545625, ECO:0000269|PubMed:15632201, ECO:0000269|PubMed:15988001, ECO:0000269|PubMed:17005863, ECO:0000269|PubMed:17379067, ECO:0000269|PubMed:19557001, ECO:0000269|PubMed:20166753, ECO:0000269|PubMed:21460850\}.
Dtl	76843	Dtl_29371	Human Uniprot function (Human *DTL*): Substrate-specific adapter of a DCX (DDB1-CUL4-X-box) E3 ubiquitin-protein ligase complex required for cell cycle control, DNA damage response and translesion DNA synthesis. The DCX(DTL) complex, also named CRL4(CDT2) complex, mediates the polyubiquitination and subsequent degradation of CDT1, CDKN1A/p21(CIP1), FBH1, KMT5A and (PubMed:16861906, PubMed:16949367, PubMed:16964240, PubMed:17085480, PubMed:18703516, PubMed:18794347, PubMed:18794348, PubMed:19332548, PubMed:20129063, PubMed:23478441 PubMed:23478445, PubMed:23677613, PubMed:27906959). CDT1 degradation in response to DNA damage is necessary to ensure proper cell cycle regulation of DNA replication (PubMed:16861906 PubMed:16949367, PubMed:17085480). CDKN1A/p21(CIP1) degradation during S phase or following UV irradiation is essential to control replication licensing (PubMed:18794348, PubMed:19332548). KMT5A degradation is also important for a proper regulation of mechanisms such as TGF-beta signaling, cell cycle progression, DNA repair and cell migration (PubMed:23478445). Most substrates require their interaction with PCNA for their polyubiquitination: substrates interact with PCNA via their PIP-box, and those containing the "K+4' motif in the PIP box, recruit the DCX(DTL) complex, leading to their degradation. In undamaged proliferating cells, the DCX(DTL) complex also promotes the "Lys-164' monoubiquitination of PCNA, thereby being involved in PCNA-dependent translesion DNA (PubMed:20129063, PubMed:23478441, PubMed:23478445, PubMed:23677613). The DDB1-CUL4A-DTL E3 ligase complex regulates the circadian clock function by mediating the ubiquitination and degradation of CRY1 (PubMed:26431207). \{ECO:0000269|PubMed:16861906, ECO:0000269|PubMed:16949367, ECO:0000269|PubMed:16964240 ECO:0000269|PubMed:17085480, ECO:0000269|PubMed:18703516, ECO:0000269|PubMed:18794347, ECO:0000269|PubMed:18794348 ECO:0000269|PubMed:19332548, ECO:0000269|PubMed:20129063, ECO:0000269|PubMed:23478441, ECO:0000269|PubMed:23478445 ECO:0000269|PubMed:23677613, ECO:0000269|PubMed:26431207, ECO:0000269|PubMed:27906959\}.
Ephx1	13849	Ephx1_29453	Human Uniprot function (Human *EPHX1*): Biotransformation enzyme that catalyzes the hydrolysis of arene and aliphatic epoxides to less reactive and more water soluble dihydrodiols by the trans addition of water (By similarity). Plays a role in the metabolism of endogenous lipids such as epoxide-containing fatty acids (PubMed:22798687). Metabolizes the abundant endocannabinoid 2-arachidonoylglycerol (2-AG) to free arachidonic acid (AA) and glycerol (PubMed:24958911). \{ECO:0000250|UniProtKB:P07687, ECO:0000269|PubMed:22798687, ECO:0000269|PubMed:24958911\}.

Gene Symbol	Entrez Gene IDs	Probe IDs[b]	Definition
Gdf7	238057	Gdf7_29562	Human Uniprot function (Human *GDF7*): May play an active role in the motor area of the primate neocortex. \{ECO:0000250\}.
Gins2	272551	Gins2_84152	Human Uniprot function (Human *GINS2*): The GINS complex plays an essential role in the initiation of DNA replication, and progression of DNA replication forks. GINS complex seems to bind preferentially to single-stranded DNA. \{ECO:0000269|PubMed:17417653\}.
Gsta13	100042295	Gsta1_31374	No description available.
Gstp2	14869	Gstp1_30795	Mouse Uniprot function (Mouse *Gstp2*): Conjugation of reduced glutathione to a wide number of exogenous and endogenous hydrophobic electrophiles. Cannot metabolize 1-chloro-2,4-dinitrobenzene.
H2-q6	110557	H2-q6_31131	No description available.
Hlf	217082	Hlf_30768	Human Entrez Gene Summary (Human *HLF*): This gene encodes a member of the proline and acidic-rich (PAR) protein family, a subset of the bZIP transcription factors. The encoded protein forms homodimers or heterodimers with other PAR family members and binds sequence-specific promoter elements to activate transcription. Chromosomal translocations fusing portions of this gene with the E2A gene cause a subset of childhood B-lineage acute lymphoid leukemias. Alternatively spliced transcript variants have been described, but their biological validity has not been determined. [provided by RefSeq, Jul 2008]
Hmgcs2	15360	Hmgcs2_29615	Human Uniprot function (Human *HMGCS2*): Catalyzes the first irreversible step in ketogenesis, condensing acetyl-CoA to acetoacetyl-CoA to form HMG-CoA, which is converted by HMG-CoA reductase (HMGCR) into mevalonate. \{ECO:0000269|PubMed:11228257, ECO:0000269|PubMed:23751782, ECO:0000269|PubMed:29597274\}.
Hoxa10	15395	Hoxa10_31922	Human Uniprot function (Human *HOXA10*): Sequence-specific transcription factor which is part of a developmental regulatory system that provides cells with specific positional identities on the anterior-posterior axis. Binds to the DNA sequence 5'-AA[AT]TTTTATTAC-3'.
Ifi44	99899	Ifi44_29813	Human Uniprot function (Human *IFI44*): This protein aggregates to form microtubular structures. \{ECO:0000250\}.
Krt18	16668	Krt18_29525	Human Uniprot function (Human *KRT18*): Involved in the uptake of thrombin-antithrombin complexes by hepatic cells (By similarity). When phosphorylated, plays a role in filament reorganization. Involved in the delivery of mutated CFTR to the plasma membrane. Together with KRT8, is involved in interleukin-6 (IL-6)-mediated barrier protection. \{ECO:0000250, ECO:0000269|PubMed:15529338, ECO:0000269|PubMed:16424149, ECO:0000269|PubMed:17213200, ECO:0000269|PubMed:7523419, ECO:0000269|PubMed:8522591, ECO:0000269|PubMed:9298992, ECO:0000269|PubMed:9524113\}.
Lcn2	16819	Lcn2_30771	Human Uniprot function (Human *LCN2*): Iron-trafficking protein involved in multiple processes such as apoptosis, innate immunity and renal development (PubMed:12453413, PubMed:27780864, PubMed:20581821). Binds iron through association with 2,5-dihydroxybenzoic acid (2,5-DHBA), a siderophore that shares structural similarities with bacterial enterobactin, and delivers or removes iron from the cell, depending on the context. Iron-bound form (holo-24p3) is internalized following binding to the SLC22A17 (24p3R) receptor, leading to release of iron and subsequent increase of intracellular iron concentration. In contrast, association of the iron-free form (apo-24p3) with the SLC22A17 (24p3R) receptor is followed by association with an intracellular siderophore, iron chelation and iron transfer to the

Gene Symbol	Entrez Gene IDs	Probe IDs[b]	Definition
			extracellular medium, thereby reducing intracellular iron concentration. Involved in apoptosis due to interleukin-3 (IL3) deprivation: iron-loaded form increases intracellular iron concentration without promoting apoptosis, while iron-free form decreases intracellular iron levels, inducing expression of the proapoptotic protein BCL2L11/BIM, resulting in apoptosis (By similarity). Involved in innate immunity; limits bacterial proliferation by sequestering iron bound to microbial siderophores, such as enterobactin (PubMed:27780864). Can also bind siderophores from M.tuberculosis (PubMed:15642259, PubMed:21978368). \{ECO:0000250|UniProtKB:P11672, ECO:0000269|PubMed:12453413, ECO:0000269|PubMed:15642259, ECO:0000269|PubMed:20581821, ECO:0000269|PubMed:21978368, ECO:0000269|PubMed:27780864\}.
Mest	17294	Mest_29181	Human Entrez Gene Summary (Human *MEST*): This gene encodes a member of the alpha/beta hydrolase superfamily. It is imprinted, exhibiting preferential expression from the paternal allele in fetal tissues, and isoform-specific imprinting in lymphocytes. The loss of imprinting of this gene has been linked to certain types of cancer and may be due to promotor switching. The encoded protein may play a role in development. Alternatively spliced transcript variants encoding multiple isoforms have been identified for this gene. Pseudogenes of this gene are located on the short arm of chromosomes 3 and 4, and the long arm of chromosomes 6 and 15. [provided by RefSeq, Dec 2011]
Nfil3	18030	Nfil3_31222	Human Uniprot function (Human *NFIL3*): Acts as a transcriptional regulator that recognizes and binds to the sequence 5'-[GA]TTA[CT]GTAA[CT]-3', a sequence present in many cellular and viral promoters. Represses transcription from promoters with activating transcription factor (ATF) sites. Represses promoter activity in osteoblasts (By similarity). Represses transcriptional activity of PER1 (By similarity). Represses transcriptional activity of PER2 via the B-site on the promoter (By similarity). Activates transcription from the interleukin-3 promoter in T-cells. Competes for the same consensus-binding site with PAR DNA-binding factors (DBP, HLF and TEF) (By similarity). Component of the circadian clock that acts as a negative regulator for the circadian expression of PER2 oscillation in the cell-autonomous core clock (By similarity). Protects pro-B cells from programmed cell death (By similarity). Represses the transcription of CYP2A5 (By similarity). Positively regulates the expression and activity of CES2 by antagonizing the repressive action of NR1D1 on CES2 (By similarity). \{ECO:0000250|UniProtKB:O08750, ECO:0000269|PubMed:1620116, ECO:0000269|PubMed:7565758, ECO:0000269|PubMed:8836190\}.
Pole	18973	Pole_31952	Human Uniprot function (Human *POLE*): Catalytic component of the DNA polymerase epsilon complex (PubMed:10801849). Participates in chromosomal DNA replication (By similarity). Required during synthesis of the leading DNA strands at the replication fork, binds at/or near replication origins and moves along DNA with the replication fork (By similarity). Has 3'-5' proofreading exonuclease activity that corrects errors arising during DNA replication (By similarity). Involved in DNA synthesis during DNA repair (PubMed:20227374, PubMed:27573199). Along with DNA polymerase POLD1 and DNA polymerase POLK, has a role in excision repair (NER) synthesis following UV irradiation (PubMed:20227374). \{ECO:0000250|UniProtKB:P21951, ECO:0000269|PubMed:10801849, ECO:0000269|PubMed:20227374, ECO:0000269|PubMed:27573199\}.
Rnf125	67664	Rnf125_32252, C730049O14RIK_31254	Human Uniprot function (Human *RNF125*): E3 ubiquitin-protein ligase that mediates ubiquitination and subsequent proteasomal degradation of target proteins, such as DDX58/RIG-I, MAVS/IPS1, IFIH1/MDA5, JAK1 and p53/TP53 (PubMed:15843525, PubMed:17460044, PubMed:17643463, PubMed:26027934, PubMed:26471729, PubMed:25591766, PubMed:27411375). Acts as a negative regulator of type I interferon

Gene Symbol	Entrez Gene IDs	Probe IDs[b]	Definition
			production by mediating ubiquitination of DDX58/RIG-I at 'Lys-181', leading to DDX58/RIG-I degradation (PubMed:17460044, PubMed:26471729). Mediates ubiquitination and subsequent degradation of p53/TP53 (PubMed:25591766). Mediates ubiquitination and subsequent degradation of JAK1 (PubMed:26027934). Acts as a positive regulator of T-cell activation (PubMed:15843525). \{ECO:0000269|PubMed:15843525, ECO:0000269|PubMed:17460044, ECO:0000269|PubMed:17643463, ECO:0000269|PubMed:25591766, ECO:0000269|PubMed:26027934, ECO:0000269|PubMed:26471729, ECO:0000269|PubMed:27411375\}.
S100a4	20198	S100a4_30373	Human Entrez Gene Summary (Human *S100A4*): The protein encoded by this gene is a member of the S100 family of proteins containing 2 EF-hand calcium-binding motifs. S100 proteins are localized in the cytoplasm and/ or nucleus of a wide range of cells, and involved in the regulation of a number of cellular processes such as cell cycle progression and differentiation. S100 genes include at least 13 members which are located as a cluster on chromosome 1q21. This protein may function in motility, invasion, and tubulin polymerization. Chromosomal rearrangements and altered expression of this gene have been implicated in tumor metastasis. Multiple alternatively spliced variants, encoding the same protein, have been identified. [provided by RefSeq, Jul 2008]
Slc51a	106407	Slc51a_29138	Human Uniprot function (Human *SLC51A*): Essential component of the Ost-alpha/Ost-beta complex, a heterodimer that acts as the intestinal basolateral transporter responsible for bile acid export from enterocytes into portal blood. Efficiently transports the major species of bile acids. \{ECO:0000269|PubMed:16317684\}.
Star	20845	Star_29723	Human Uniprot function (Human *STAR*): Plays a key role in steroid hormone synthesis by enhancing the metabolism of cholesterol into pregnenolone. Mediates the transfer of cholesterol from the outer mitochondrial membrane to the inner mitochondrial membrane where it is cleaved to pregnenolone. \{ECO:0000269|PubMed:7761400, ECO:0000269|PubMed:7892608, ECO:0000269|PubMed:8948562\}.
Tuba4a	22145	Tuba4a_29527	Human Uniprot function (Human *TUBA4A*): Tubulin is the major constituent of microtubules. It binds two moles of GTP, one at an exchangeable site on the beta chain and one at a non-exchangeable site on the alpha chain.
Ube2c	68612	Ube2c_31522	Human Uniprot function (Human *UBE2C*): Accepts ubiquitin from the E1 complex and catalyzes its covalent attachment to other proteins. In vitro catalyzes 'Lys-11'- and 'Lys-48'-linked polyubiquitination. Acts as an essential factor of the anaphase promoting complex/cyclosome (APC/C), a cell cycle-regulated ubiquitin ligase that controls progression through mitosis. Acts by initiating 'Lys-11'-linked polyubiquitin chains on APC/C substrates, leading to the degradation of APC/C substrates by the proteasome and promoting mitotic exit. \{ECO:0000269|PubMed:15558010, ECO:0000269|PubMed:18485873, ECO:0000269|PubMed:19820702, ECO:0000269|PubMed:19822757, ECO:0000269|PubMed:20061386, ECO:0000269|PubMed:27259151\}.
Ube2t	67196	Ube2t_30503	Human Uniprot function (Human *UBE2T*): Accepts ubiquitin from the E1 complex and catalyzes its covalent attachment to other proteins. Catalyzes monoubiquitination. Involved in mitomycin-C (MMC)-induced DNA repair. Acts as a specific E2 ubiquitin-conjugating enzyme for the Fanconi anemia complex by associating with E3 ubiquitin-protein ligase FANCL and catalyzing monoubiquitination of FANCD2, a key step in the DNA damage pathway (PubMed:16916645, PubMed:17938197, PubMed:19111657, PubMed:19589784, PubMed:28437106). Also mediates monoubiquitination of FANCL and FANCI (PubMed:16916645, PubMed:17938197, PubMed:19111657, PubMed:19589784). May contribute to ubiquitination and degradation of BRCA1 (PubMed:19887602). In vitro able to promote polyubiquitination using all 7 ubiquitin

Gene Symbol	Entrez Gene IDs	Probe IDs[b]	Definition
			Lys residues, but may prefer 'Lys-11'-, 'Lys-27'-, 'Lys-48'- and 'Lys-63'-linked polyubiquitination (PubMed:20061386). \{ECO:0000269|PubMed:16916645, ECO:0000269|PubMed:17938197, ECO:0000269|PubMed:19111657, ECO:0000269|PubMed:19589784, ECO:0000269|PubMed:19887602, ECO:0000269|PubMed:20061386, ECO:0000269|PubMed:28437106\}.
Ugt1a6a	94284	Ugt1a7c_29171	No description available.
Ugt1a6b	394435	Ugt1a6a_29170	No description available.
Uhrf1	18140	Uhrf1_30587	Human Uniprot function (Human *UHRF1*): Multidomain protein that acts as a key epigenetic regulator by bridging DNA methylation and chromatin modification. Specifically recognizes and binds hemimethylated DNA at replication forks via its YDG domain and recruits DNMT1 methyltransferase to ensure faithful propagation of the DNA methylation patterns through DNA replication. In addition to its role in maintenance of DNA methylation, also plays a key role in chromatin modification: through its tudor-like regions and PHD-type zinc fingers, specifically recognizes and binds histone H3 trimethylated at 'Lys-9' (H3K9me3) and unmethylated at 'Arg-2' (H3R2me0), respectively, and recruits chromatin proteins. Enriched in pericentric heterochromatin where it recruits different chromatin modifiers required for this chromatin replication. Also localizes to euchromatic regions where it negatively regulates transcription possibly by impacting DNA methylation and histone modifications. Has E3 ubiquitin-protein ligase activity by mediating the ubiquitination of target proteins such as histone H3 and PML. It is still unclear how E3 ubiquitin-protein ligase activity is related to its role in chromatin in vivo. May be involved in DNA repair. \{ECO:0000269|PubMed:10646863, ECO:0000269|PubMed:15009091, ECO:0000269|PubMed:15361834, ECO:0000269|PubMed:17673620, ECO:0000269|PubMed:17967883, ECO:0000269|PubMed:19056828, ECO:0000269|PubMed:21745816, ECO:0000269|PubMed:21777816, ECO:0000269|PubMed:22945642\}.

[a]Descriptions of orthologous human genes are shown due to the increased detail available in public resources such as UniprotKB[35] and Entrez Gene.[36] Gene definitions adapted from Human UniprotKB were used as the primary resource due to the greater breadth of annotation and depth of functional detail provided. Gene definitions adapted from Mouse UniprotKB were used as the secondary resource if the primary source did not provide a detailed description of function. Human Entrez Gene was used as the third resource. Mouse Entrez Gene was used as the fourth resource.
[b]In some cases, a probe may map to more than one gene, resulting in duplicate reporting of that probe mapped to different genes.
Gene definition version and retrieval dates: https://doi.org/10.22427/NTP-DATA-002-00600-0002-000-0.

Appendix F. Organ Weight Descriptions

Table of Contents

F.1. Organ Weight Descriptions

Heart: The heart drives the circulatory system, supplying oxygen and essential macro- and micronutrients to the tissues. Increased heart weight in subacute studies would indicate severe cardiotoxicity, compensatory myocardial hypertrophy, and/or pulmonary injury. Decreased heart weight in subacute studies is often of unknown toxicological significance; however, it may be caused by decreased load on the heart from dehydration or modulation of contractility.

Kidney: The kidneys remove waste products and xenobiotics from the body, balance blood electrolytes, regulate blood pressure through the release of hormones, synthesize the active form of vitamin D, and control the production of erythropoiesis. In subacute studies, changes in kidney weight may reflect renal toxicity (particularly if accompanied by increases in other markers of kidney toxicity, e.g., increased Kim-1) and/or tubular hypertrophy. Decreased kidney weights in subacute studies are typically of unknown toxicological significance.

Liver: The liver carries out biotransformation and excretion of endogenous and xenobiotic substances, regulation of blood sugar, enzymatic transformation of essential nutrients, generation of blood proteins involved in fluid balance and clotting, and bile production for digestion and absorption of fats. Liver weight changes can be an indication of chemical-induced stress. Specifically, in subacute studies, increases in liver weight in response to low doses of toxicants typically stem from increases in xenobiotic metabolizing enzymes and associated hepatocyte hypertrophy or peroxisome proliferation. Increased liver weight, particularly when accompanied by evidence of leakage of liver-specific enzymes into blood, likely reflects hemodynamic changes related to severe hepatotoxicity. Higher liver weight relative to body weight may also occur at any dose level that causes a slowed rate of body growth and does not necessarily indicate liver toxicity. Decreased liver weight in subacute studies is typically of unknown toxicological significance but in rare cases may be related to glycogen depletion.

Lung: The lung is the main respiratory organ and is primarily responsible for gas exchange but also aids in regulating blood pH and protecting the body from pathogens. An increase in lung weight following short-term exposure is a sensitive indicator of direct pulmonary toxicity. This change is typically driven by an acute inflammatory response, characterized by edema (fluid accumulation) and the infiltration of immune cells like neutrophils and macrophages. It is considered an adverse finding that signals local irritation and cellular injury. While the magnitude of the weight increase often correlates with the dose, a definitive interpretation of the nature and severity of the damage requires correlation with histopathological examination of the lung tissue. Conversely, a decrease in absolute lung weight is less common and usually points to significant systemic toxicity rather than a direct lung effect. The primary cause is often severe body weight loss (inanition), which leads to a proportional, catabolic reduction in the mass of most organs. In this scenario, the toxicological interpretation hinges on the relative lung-to-body-weight ratio, as an increase in this ratio can unmask a direct pulmonary effect that is otherwise obscured by the animal's poor overall condition.

Ovary: The ovary is the female gamete-producing organ and produces and releases essential sex hormones. Changes in ovarian weight are a key indicator of reproductive toxicity, often resulting from hormonal disruption. A decrease in weight is the more frequent and concerning finding, typically signaling an adverse impact on fertility. This can be caused by a direct toxic effect on ovarian cells, leading to follicular atresia, or by disruption of the Hypothalamic-Pituitary-

Gonadal (HPG) axis. It may also occur as a secondary consequence of severe systemic toxicity and body weight loss, which suppresses reproductive function. An increase in ovarian weight is less common but also indicates significant reproductive perturbation, possibly from hormonal overstimulation, inflammation, or cysts. For any change in weight, the interpretation is critically dependent on context. The animal's estrous cycle stage must be considered, as weight fluctuates naturally. Ultimately, a definitive conclusion about the cause and severity of the effect (either increased or decreased weight) is not possible without histopathological correlation to examine the underlying microscopic structure of the ovary.

Appendix G. Supplemental Data

The following supplemental files are available at https://doi.org/10.22427/NIEHS-DATA-NIEHS-13.

G.1. Materials and Methods

Materials and Methods
Materials_and_Methods.pdf

G.2. Theoretical Inhaled Dose

Theoretical Inhaled Dose
Theoretical_Inhaled_Dose.pdf

G.3. Rats

G.3.1. Apical Benchmark Dose Analysis

BMD, NOEL and LOEL Summary for Apical Endpoints
108020004_BMD_NOEL_and_LOEL_Summary_for_Apical_Endpoints.pdf

BMDExpress Project File Rat Apical (bm2 Format)
108020004_4D_Rat_NonGenomic.bm2

Clinical Chemistry Summary
108020004_Clinical_Chemistry_Summary.pdf

Hematology Summary
108020004_Hematology_Summary.pdf

Mean Body Weights Summary
108020004_Body_Weights_Summary.pdf

Organ Weights Summary
108020004_OrganWeights_Summary.pdf

G.3.2. Genomic Benchmark Dose Analysis

GEO/SRA: https://www.ncbi.nlm.nih.gov/bioproject/1304578

All Organ Principal Components Analysis Files
108020004_All_Organ_Principal_Components_Analysis_Files.zip

Animal and Fastaq Metadata
108020004_Animal_and_Fastaq_Metadata.pdf

Attenuation-adjusted Raw Read Counts Rat Study
108020004_Attenuation-adjustedRawReadCountsRatStudy.zip

Benchmark Dose Analysis Rat Heart
108020004_Benchmark_Dose_Analysis_Rat_Heart.txt

Benchmark Dose Analysis Rat Kidney
108020004_Benchmark_Dose_Analysis_Rat_Kidney.txt

Benchmark Dose Analysis Rat Liver
108020004_Benchmark_Dose_Analysis_Rat_Liver.txt

Benchmark Dose Analysis Rat Lung
108020004_Benchmark_Dose_Analysis_Rat_Lung.txt

Benchmark Dose Analysis Rat Ovary
108020004_Benchmark_Dose_Analysis_Rat_Ovary.txt

BMDExpress Expression Data Heart
108020004_BMDExpress_Expression_Data_Heart.txt

BMDExpress Expression Data Kidney
108020004_BMDExpress_Expression_Data_Kidney.txt

BMDExpress Expression Data Liver
108020004_BMDExpress_Expression_Data_Liver.txt

BMDExpress Expression Data Lung
108020004_BMDExpress_Expression_Data_Lung.txt

BMDExpress Expression Data Ovary
108020004_BMDExpress_Expression_Data_Ovary.txt

BMDExpress GO Biological Process BMD Results Rat Heart
108020004_BMDExpress_GO_Biological_Process_BMD_Results_Rat_Heart.txt

BMDExpress GO Biological Process BMD Results Rat Kidney
108020004_BMDExpress_GO_Biological_Process_BMD_Results_Rat_Kidney.txt

BMDExpress GO Biological Process BMD Results Rat Liver
108020004_BMDExpress_GO_Biological_Process_BMD_Results_Rat_Liver.txt

BMDExpress GO Biological Process BMD Results Rat Lung
108020004_BMDExpress_GO_Biological_Process_BMD_Results_Rat_Lung.txt

BMDExpress GO Biological Process BMD Results Rat Ovary
108020004_BMDExpress_GO_Biological_Process_BMD_Results_Rat_Ovary.txt

BMDExpress Individual Gene BMD Results Rat Heart
108020004_BMDExpress_Individual_Gene_BMD_Results_Rat_Heart.txt

BMDExpress Individual Gene BMD Results Rat Kidney
108020004_BMDExpress_Individual_Gene_BMD_Results_Rat_Kidney.txt

BMDExpress Individual Gene BMD Results Rat Liver
108020004_BMDExpress_Individual_Gene_BMD_Results_Rat_Liver.txt

BMDExpress Individual Gene BMD Results Rat Lung
108020004_BMDExpress_Individual_Gene_BMD_Results_Rat_Lung.txt

BMDExpress Individual Gene BMD Results Rat Ovary
108020004_BMDExpress_Individual_Gene_BMD_Results_Rat_Ovary.txt

BMDExpress Project File Rat Genomic (bm2 Format)
108020004_4D_Rat_Genomic.bm2

BMDExpress Project File Rat Genomic (JSON Format)
108020004_4D_Rat_Genomic.json

Curve Fit Rat Heart
108020004_Curve_Fit_Rat_Heart.txt

Curve Fit Rat Kidney
108020004_Curve_Fit_Rat_Kidney.txt

Curve Fit Rat Liver
108020004_Curve_Fit_Rat_Liver.txt

Curve Fit Rat Lung
108020004_Curve_Fit_Rat_Lung.txt

Curve Fit Rat Ovary
108020004_Curve_Fit_Rat_Ovary.txt

Most Potent GO Biological Process in Each Tissue
108020004_Most_Potent_GO_Biological_Process_In_Each_Tissue.pdf

One-way ANOVA Rat Heart
108020004_One-way_ANOVA_Rat_Heart.txt

One-way ANOVA Rat Kidney
108020004_One-way_ANOVA_Rat_Kidney.txt

One-way ANOVA Rat Liver
108020004_One-way_ANOVA_Rat_Liver.txt

One-way ANOVA Rat Lung
108020004_One-way_ANOVA_Rat_Lung.txt

One-way ANOVA Rat Ovary
108020004_One-way_ANOVA_Rat_Ovary.txt

Rat DCB eFDR Synthetic Null Analysis
108020004_Rat_DCB_eFDR_Synthetic_Null_Analysis.zip

TempO-Seq S1500v1.2 Full Manifest Rattus Norvegicus
108020004_TempO-SeqS1500v1.2FullManifestRattusNorvegicus.csv

Top 10 Genes Ranked by Potency of Perturbation Heart
108020004_Top_10_Genes_Ranked_by_Potency_of_Perturbation_Heart.pdf

Top 10 Genes Ranked by Potency of Perturbation Kidney
108020004_Top_10_Genes_Ranked_by_Potency_of_Perturbation_Kidney.pdf

Top 10 Genes Ranked by Potency of Perturbation Liver
108020004_Top_10_Genes_Ranked_by_Potency_of_Perturbation_Liver.pdf

Top 10 Genes Ranked by Potency of Perturbation Lung
108020004_Top_10_Genes_Ranked_by_Potency_of_Perturbation_Lung.pdf

Top 10 Genes Ranked by Potency of Perturbation Ovary
108020004_Top_10_Genes_Ranked_by_Potency_of_Perturbation_Ovary.pdf

Top 10 GO Biological Process Gene Sets Heart
108020004_Top_10_GO_Biological_Process_Gene_Sets_Heart.pdf

Top 10 GO Biological Process Gene Sets Kidney
108020004_Top_10_GO_Biological_Process_Gene_Sets_Kidney.pdf

Top 10 GO Biological Process Gene Sets Liver
108020004_Top_10_GO_Biological_Process_Gene_Sets_Liver.pdf

Top 10 GO Biological Process Gene Sets Lung
108020004_Top_10_GO_Biological_Process_Gene_Sets_Lung.pdf

Top 10 GO Biological Process Gene Sets Ovary
108020004_Top_10_GO_Biological_Process_Gene_Sets_Ovary.pdf

Transcriptomics Data QC Report
108020004_TranscriptomicsDataQCReport.zip

G.3.3. Study Tables

I01 – Animal Removal Summary
108020004_I01_Animal_Removal_Summary.pdf

I02 – Animal Removals
108020004_I02_Animal_Removals.pdf

I04 – Mean Body Weights and Survival
108020004_I04_Mean_Body_Weights_and_Survival.pdf

I04G – Mean Body Weight Gain
108020004_I04G_Mean_Body_Weight_Gain.pdf

I05 – Clinical Observations Summary
108020004_I05_Clinical_Observations_Summary.pdf

PA06 – Organ Weights Summary
108020004_PA06_Organ_Weights_Summary.pdf

PA41 – Clinical Chemistry Summary
108020004_PA41_Clinical_Chemistry_Summary.pdf

PA43 – Hematology Summary
108020004_PA43_Hematology_Summary.pdf

PA48 – Blood and Tissue Concentration
108020004_Blood_and_Tissue_Concentration.pdf

G.3.4. Individual Animal Data

Individual Animal Blood and Tissue Concentration Data

108020004_Individual_Animal_Blood_and_Tissue_Concentration_Data.xlsx

Individual Animal Body Weight Data
108020004_Individual_Animal_Body_Weight_Data.xlsx

Individual Animal Clinical Chemistry Data
108020004_Individual_Animal_Clinical_Chemistry_Data.xlsx

Individual Animal Clinical Observations Data
108020004_Individual_Animal_Clinical_Observations_Data.xlsx

Individual Animal Hematology Data
108020004_Individual_Animal_Hematology_Data.xlsx

Individual Animal Organ Weight Data
108020004_Individual_Animal_Organ_Weight_Data.xlsx

Individual Animal Removal Reasons Data
108020004_Individual_Animal_Removal_Reasons_Data.xlsx

G.4. Mice

G.4.1. Apical Benchmark Dose Analysis

BMD, NOEL and LOEL Summary for Apical Endpoints
108020005_BMD_NOEL_and_LOEL_Summary_for_Apical_Endpoints_Mouse.pdf

BMDExpress Project File Mouse Apical (bm2 Format)
108020005_4D_NonGenomic_Mouse.bm2

Clinical Chemistry Summary
108020005_Clinical_Chemistry_Summary.pdf

Mean Body Weights Summary
108020005_Mean_Body_Weights_Summary.pdf

Organ Weights Summary
108020005_Organ_Weights_Summary.pdf

G.4.2. Genomic Benchmark Dose Analysis

GEO/SRA: https://www.ncbi.nlm.nih.gov/bioproject/1304935

All Organ Principal Components Analysis Files
108020005_All_Organ_Principal_Components_Analysis_Files.zip

Animal and Fastaq Metadata
108020005_Animal_and_Fastaq_Metadata.pdf

Attenuation-adjusted Raw Read Counts Mouse Study
108020005_Attenuation-adjustedRawReadCountsMouseStudy.zip

Benchmark Dose Analysis Mouse Heart
108020005_Benchmark_Dose_Analysis_Mouse_Heart.txt

Benchmark Dose Analysis Mouse Kidney
108020005_Benchmark_Dose_Analysis_Mouse_Kidney.txt

Benchmark Dose Analysis Mouse Liver
108020005_Benchmark_Dose_Analysis_Mouse_Liver.txt

Benchmark Dose Analysis Mouse Lung
108020005_Benchmark_Dose_Analysis_Mouse_Lung.txt

Benchmark Dose Analysis Mouse Ovary
108020005_Benchmark_Dose_Analysis_Mouse_Ovary.txt

BMDExpress Expression Data Heart
108020005_BMDExpress_Expression_Data_Heart.txt

BMDExpress Expression Data Kidney
108020005_BMDExpress_Expression_Data_Kidney.txt

BMDExpress Expression Data Liver
108020005_BMDExpress_Expression_Data_Liver.txt

BMDExpress Expression Data Lung
108020005_BMDExpress_Expression_Data_Lung.txt

BMDExpress Expression Data Ovary
108020005_BMDExpress_Expression_Data_Ovary.txt

BMDExpress GO Biological Process BMD Results Mouse Heart
108020005_BMDExpress_GO_Biological_Process_BMD_Results_Mouse_Heart.txt

BMDExpress GO Biological Process BMD Results Mouse Kidney
108020005_BMDExpress_GO_Biological_Process_BMD_Results_Mouse_Kidney.txt

BMDExpress GO Biological Process BMD Results Mouse Liver
108020005_BMDExpress_GO_Biological_Process_BMD_Results_Mouse_Liver.txt

BMDExpress GO Biological Process BMD Results Mouse Lung
108020005_BMDExpress_GO_Biological_Process_BMD_Results_Mouse_Lung.txt

BMDExpress GO Biological Process BMD Results Mouse Ovary
108020005_BMDExpress_GO_Biological_Process_BMD_Results_Mouse_Ovary.txt

BMDExpress Individual Gene BMD Results Mouse Heart
108020005_BMDExpress_Individual_Gene_BMD_Results_Mouse_Heart.txt

BMDExpress Individual Gene BMD Results Mouse Kidney
108020005_BMDExpress_Individual_Gene_BMD_Results_Mouse_Kidney.txt

BMDExpress Individual Gene BMD Results Mouse Liver
108020005_BMDExpress_Individual_Gene_BMD_Results_Mouse_Liver.txt

BMDExpress Individual Gene BMD Results Mouse Lung
108020005_BMDExpress_Individual_Gene_BMD_Results_Mouse_Lung.txt

BMDExpress Individual Gene BMD Results Mouse Ovary
108020005_BMDExpress_Individual_Gene_BMD_Results_Mouse_Ovary.txt

BMDExpress Project File Mouse Genomic (bm2 Format)
108020005_4D_Mouse_Genomic.bm2

BMDExpress Project File Mouse Genomic (JSON Format)
108020005_4D_Mouse_Genomic.json

Curve Fit Mouse Heart
108020005_Curve_Fit_Mouse_Heart.txt

Curve Fit Mouse Kidney
108020005_Curve_Fit_Mouse_Kidney.txt

Curve Fit Mouse Liver
108020005_Curve_Fit_Mouse_Liver.txt

Curve Fit Mouse Lung
108020005_Curve_Fit_Mouse_Lung.txt

Curve Fit Mouse Ovary
108020005_Curve_Fit_Mouse_Ovary.txt

Mouse DCB eFDR Synthetic Null Analysis
108020005_Mouse_DCB_eFDR_Synthetic_Null_Analysis.zip

Most Potent GO Biological Process in Each Tissue
108020005_Most_Potent_GO_Biological_Process_In_Each_Tissue.pdf

One-way ANOVA Mouse Heart
108020005_One-way_ANOVA_Mouse_Heart.txt

One-way ANOVA Mouse Kidney
108020005_One-way_ANOVA_Mouse_Kidney.txt

One-way ANOVA Mouse Liver
108020005_One-way_ANOVA_Mouse_Liver.txt

One-way ANOVA Mouse Lung
108020005_One-way_ANOVA_Mouse_Lung.txt

One-way ANOVA Mouse Ovary
108020005_One-way_ANOVA_Mouse_Ovary.txt

TempO-Seq S1500v1.2 Full Manifest Mus Musculus
108020005_TempO-SeqS1500v1.2FullManifestMusMusculus.csv

Top 10 Genes Ranked by Potency of Perturbation Heart
108020005_Top_10_Genes_Ranked_by_Potency_of_Perturbation_Heart.pdf

Top 10 Genes Ranked by Potency of Perturbation Kidney
108020005_Top_10_Genes_Ranked_by_Potency_of_Perturbation_Kidney.pdf

Top 10 Genes Ranked by Potency of Perturbation Liver
108020005_Top_10_Genes_Ranked_by_Potency_of_Perturbation_Liver.pdf

Top 10 Genes Ranked by Potency of Perturbation Lung
108020005_Top_10_Genes_Ranked_by_Potency_of_Perturbation_Lung.pdf

Top 10 Genes Ranked by Potency of Perturbation Ovary
108020005_Top_10_Genes_Ranked_by_Potency_of_Perturbation_Ovary.pdf

Top 10 GO Biological Process Gene Sets Heart
108020005_Top_10_GO_Biological_Process_Gene_Sets_Heart.pdf

Top 10 GO Biological Process Gene Sets Kidney
108020005_Top_10_GO_Biological_Process_Gene_Sets_Kidney.pdf

Top 10 GO Biological Process Gene Sets Liver
108020005_Top_10_GO_Biological_Process_Gene_Sets_Liver.pdf

Top 10 GO Biological Process Gene Sets Lung
108020005_Top_10_GO_Biological_Process_Gene_Sets_Lung.pdf

Top 10 GO Biological Process Gene Sets Ovary
108020005_Top_10_GO_Biological_Process_Gene_Sets_Ovary.pdf

Transcriptomics Data QC Report
108020005_TranscriptomicsDataQCReport.zip

G.4.3. Study Tables

I01 – Animal Removal Summary
108020005_I01_Animal_Removal_Summary.pdf

I02 – Animal Removals
108020005_I02_Animal_Removals.pdf

I04 – Mean Body Weights and Survival
108020005_I04_Mean_Body_Weights_and_Survival.pdf

I04G – Mean Body Weight Gain
108020005_I04G_Mean_Body_Weight_Gain.pdf

I05 – Clinical Observations Summary
108020005_I05_Clinical_Observations_Summary.pdf

PA06 – Organ Weights Summary
108020005_PA06_Organ_Weights_Summary.pdf

PA41 – Clinical Chemistry Summary
108020005_PA41_Clinical_Chemistry_Summary.pdf

PA48 – Blood and Tissue Concentration
108020005_Blood_and_Tissue_Concentration.pdf

G.4.4. Individual Animal Data

Individual Animal Blood and Tissue Concentration Data
108020005_Individual_Animal_Blood_and_Tissue_Concentration_Data.xlsx

Individual Animal Body Weight Data
108020005_Individual_Animal_Body_Weight_Data.xlsx

Individual Animal Clinical Chemistry Data
108020005_Individual_Animal_Clinical_Chemistry_Data.xlsx

Individual Animal Clinical Observations Data
108020005_Individual_Animal_Clinical_Observations_Data.xlsx

Individual Animal Organ Weight Data
108020005_Individual_Animal_Organ_Weight_Data.xlsx

Individual Animal Removal Reasons Data
108020005_Individual_Animal_Removal_Reasons_Data.xlsx

G.5. Software

G.5.1. Analysis Pipeline Evaluation

Analysis Pipeline Evaluation
AnalysisPipelineEvaluation.zip

DTT tBMD Pipeline bm2
DTT_tBMD_Pipelinebm2.zip

EPA tBMD Pipeline bm2
EPA_tBMD_Pipelinebm2.zip

G.5.2. BMDExpress Preview Software

BMDExpress Preview Software
https://github.com/auerbachs/BMDExpress-3/releases/download/3.20.141/BMDExpress3_windows-x64_3_20_0141.exe

National Institute of
Environmental Health Sciences
Division of Translational Toxicology
Office of Policy, Review, and Outreach
P.O. Box 12233
Durham, NC 27709

www.niehs.nih.gov/reports

ISSN 2768-5632